POWER SYSTEM TOPOLOGY CONTROL FOR ENHANCED RESILIENCE OF SMART ELECTRICITY GRIDS

A Dissertation

by

PAYMAN DEHGHANIAN

Submitted to the Office of Graduate and Professional Studies of
Texas A&M University
in partial fulfillment of the requirements for the degree of

DOCTOR OF PHILOSOPHY

Chair of Committee,	Mladen Kezunovic
Committee Members,	Chanan Singh
	Alex Sprintson
	Erick Moreno-Centeno
Head of Department,	Miroslav Begovic

December 2017

Major Subject: Electrical Engineering

ABSTRACT

Disruptive events, whether they are malicious attacks, natural disasters, or human-caused accidents, continually pose a risk to the acceptable electricity grid operations, and lessons learned from some recent catastrophic events have pushed the focus on the concept of "resilience". It is becoming more and more apparent that further considerations beyond the classical reliability-oriented view are needed for enhancing the electricity grid survivability in the face of High Impact Low Probability (HILP) emergencies to keep the lights on at all times. This observation is verified by several major electricity grid outages. From 1980 to 2014, a total of 178 weather/climate caused blackouts occurred in the United States alone (8 of which occurred in 2014) with the overall damages/costs reaching or exceeding US$ 1 trillion. Both the frequency and intensity of such wide area outage events have been trending higher in recent years. With increasing dependence on electricity for most daily activities and vital services (e.g., transportation, commerce, communications, health care, etc.), an urgent need to enhance the resilience of the electricity delivery infrastructure to reduce the impact and risk from natural and human-triggered events is well recognized.

In line with the constant national push to operate the electricity grid in a smarter way by introducing advanced technologies and control mechanisms into grid operations, this dissertation tries to introduce effective decision making support tools to achieve improved efficiency and resilience by a smarter use of the grid existing infrastructure. The

proposed tools are focused on the network topology control through transmission line switching actions and are taking into account several practical considerations that are essential for a successful implementation of this technology in real world scenarios. This dissertation strives to examine harnessing of the transmission assets, in both normal and emergency operating states and under various uncertainty scenarios arisen from the stochastic renewable patterns and load profiles, to reach the improved grid efficiency and resiliency goals. Such considerations, which are employed in the grid operational time frame, make it possible to reach more resilient and efficient use of existing electricity network facilities with minimal additional cost.

DEDICATION

This Ph.D. Dissertation is lovingly dedicated to my parents (Fariba and Jalil), my sister (Paria), and my twin brother (Pooria), without whom my achievements so far could never be accomplished. They are the ones always nursing me with affections and love. Their support, encouragement, and constant love have sustained me throughout my life and especially during the past couple of years living abroad.

ACKNOWLEDGEMENTS

I would like to express my sincere gratitude to my committee chair and advisor, Prof. Mladen Kezunovic, for his understanding, wisdom, patience, encouragements, and for pushing me farther than where I thought I could go. Thanks also to my committee members, Prof. Chanan Singh, Prof. Alex Sprintson, and Prof. Erick Moreno-Centeno, for their time, guidance, and exquisite support throughout the course of this doctoral research.

There are people in everyone's lives who make success both possible and rewarding. Appreciation goes to my friends and colleagues, specifically Bei Zhang, Ashkan Roshanzamir, Mohammad Tasdighi, Tamara Becejac, Qin Yan, Po-Chen Chen, and the department faculty and staff for making my time at Texas A&M University a wonderful experience in a healthy and friendly environment.

Most of all, I am fully indebted to my parents for their terrific supports both on and off water, without which, pursuit of this advanced degree would never have been started and accomplished.

CONTRIBUTORS AND FUNDING SOURCES

Contributors

This work was supervised by a dissertation committee consisting of Professor Mladen Kezunovic [advisor], Professor Chanan Singh and Professor Alex Sprintson of the Department of Electrical and Computer Engineering (ECEN), and Professor Erick Moreno-Centeno of the Department of Industrial and Systems Engineering (ISE) at Texas A&M University.

The data analyzed for Section 6 was provided by Professor Erick Moreno-Centeno. The analyses depicted in Section 6 were conducted in part by his student, Dr. Yaping Wang of the Department of Industrial and Systems Engineering (ISE) in collaboration with me and were published in 2015. All other work conducted for the dissertation was completed by me as the student, independently, but under supervisory of my advisor, Prof. Mladen Kezunovic.

Funding Sources

This work was made possible in part by the Advanced Research Project Agency-Energy (ARPA-E) under the Green Electricity Network Integration (GENI) Project "Robust Adaptive Transmission Control". This graduate study was also supported through several scholarships and fellowships as follows:

- Aggies Commit Fellowships, 2015-2017

- American Public Power Association Research Grant, Demonstration of Energy & Efficiency Developments (DEED), 2016-2017
- Association of Energy Engineers (AEE) Foundation Scholarship, 2016
- Higher Standard Scholarship, National Society of Maintenance and Reliability Professionals (SMRP), 2016
- Sigma Xi Grants-in-Aid of Research, 2016
- Love of Learning Scholarship, Phi Kappa Phi Honor Society, 2015
- Texas A&M Energy Institute Fellowship by ConocoPhillips, 2014

The dissertation's contents are solely the responsibility of the author and do not necessarily represent the official views of the above awarding offices.

NOMENCLATURE

Nomenclature 1: Section 3

A. Sets

$n \in \Omega_B$	Set of system buses.
$d \in \Omega_D$	Set of system load types at different load points.
$g \in \Omega_G$	Set of system generating units.
$h \in \Omega_H$	Set of system probable contingencies.
$k \in \Omega_{K'}$	Set of optimal transmission line switching candidates.
$k \in \Omega_L$	Set of system transmission lines.
$x \in \Omega_X$	Set of failed components in a system contingency state.
$y \in \Omega_Y$	Set of online components in a system contingency state.
$z \in \Omega_Z$	Set of uncertain variables of the system.

B. Variables and Functions

$f_X(.)$	Probability density function of variable X.
$\overline{\mathrm{GC}^t}$	Expected total system generation dispatch cost, probabilistically realized at time *t*.
G_W	Output wind power of a wind turbine (in MW).

$IL_{n,h,k}^{t}$	Interrupted load at bus *n* (MW) due to contingency *h* in the optimal topology *k* at time *t*.
$\mathbf{P_{D_n}}$	Vector of demand (in MW) at load bus *n*.
$\overline{P_{d_n}^{t}}$	Expected active power (in MW) of bus *n* at time *t*.
$\overline{P_{d_n,h}^{t,\text{supplied}}}$	Expected active power (in MW) survived at bus *n* during contingency *h* at time *t*.
$\overline{P_{g_n}^{t}}$	Expected output power of generator *g* at bus *n* at time *t* (in MW).
$P_{g,n}^{Wind}$	Wind generation output at bus *n* (in MW).
P_{h}^{t}	Probability of contingency *h* at time *t*.
P_{knm}^{t}	Power flow through transmission line *k* (connecting bus *n* to *m*) at time *t*.
$P_{z,i}$	Probability of concentration *i* for random variable *k*.
$\lambda_{z,i}$	Skewness of concentration *i* for random variable *k*.
v	Wind speed (m/s).
$\mathbf{X}$	Vectors of random input variables.
$\mathbf{Y}$	Vectors of random output variables.
α_k	Switch action for transmission line *k* (1: no switch, 0: switch).
θ_n	Voltage angle at bus *n*.
τ_h^t	Duration of contingency *h* at time *t*.
$x_{(.),(.)}$	Concentrations of X.
σ_x	Standard deviation value of variable *x*.

μ_x Mean value of variable *x*.

C. Dual Variables

$\boldsymbol{\eta}$ Lagrange multipliers for equality constraints.

$\boldsymbol{\pi}$ Lagrange multipliers for inequality constraints.

D. Parameters

B_k Susceptance of transmission link *k*.

c_{g_n} Linear generation cost of generator *g* at bus *n*.

$E(.)$ Expected value of a given variable.

K, K', K'' Parameters of wind turbines.

M_k Big M-Value for transmission line *k*.

$P_{g_n}^{\min}$ Minimum generation limit of generator *g* at bus *n* (in MW).

$P_{g_n}^{\max}$ Maximum generation limit of generator *g* at bus *n* (in MW).

$P_k^{\min}$ Minimum limit on the power flow of transmission line *k* (in MW).

$P_k^{\max}$ Maximum limit on the power flow of transmission line *k* (in MW).

P_r Rated power of a wind turbine (in MW).

v_i, v_r, v_o Cut-in, rated, and cut-out wind speed (m/s).

VOLL_n Value of lost load at bus *n* (in $/MWh).

r Number of random input variables in the PEM method.

Γ_x Failure rate of component *x* of the system (occ./year).

γ_x Repair rate of component *x* of the system (hr./year).

$\xi_{(.),(.)}$ Location of concentrations.

$\theta_n^{\min}$ Minimum voltage angle at bus *n*.

$\theta_n^{\max}$ Maximum voltage angle at bus *n*.

ψ Shaping coefficient of the Weibull probability distribution.

β Scaling coefficient of the Weibull probability distribution.

χ Maximum number of transmission line switching possibilities.

E. Performance Indices

$\overline{\text{EENS}}_{n,k}^{t}$ Expected energy not supplied (in MWh) at bus *n* when optimal topology plan *k* is adopted at time *t*.

$\overline{\text{RC}}_{TS,k}^{t}$ Expected risk cost of the transmission system accommodated with optimal topology *k* at time *t*.

Nomenclature 2: Section 4

A. Sets

$n \in \Omega_B$	Set of system bus-bars.
$d \in \Omega_D$	Set of demands at a system load point.
$g \in \Omega_G$	Set of system generating units.
$v \in \Omega_\Theta$	Set of system contingency states.
$k \in \Omega_K$	Set of optimal transmission line switching (TLS) plans.
$k \in \Omega_L$	Set of system transmission lines.
$k \in \Omega_O$	Set of system transformer branches.
$\varpi \in \Omega_P$	Set of system OLTC transformers.
$k \in \Omega_Q$	Set of OLTC transformer branches.
$k \in \Omega_T$	Set of non-OLTC transformer branches.
$m \in \Omega_M$	Set of down equipment in a system contingency state.
$n \in \Omega_N$	Set of available equipment in a system contingency state.
$b \in \Omega_{\hat{\lambda}}$	Set of random variables.
$i \in \Re$	Set of objective functions.
$j \in \Im$	Set of all equality constraints.
$k \in \aleph$	Set of all inequality constraints.

B. Variables and Functions

$e_{(.)}$	Real voltage variables at a bus-bar.
$f_{(.)}$	Imaginary voltage variables at a bus-bar.
$\overline{\mathrm{GC}_{TS}^{t}}$	Expected system generation dispatch cost at time *t*.
$\overline{\mathrm{IL}}_{n,v,k}^{t}$	Load outage at bus-bar *n* (in MW) due to contingency *v* when optimal TLS plan *k* is adopted at time *t* (in MW).
$\mathbf{P}_{\mathbf{D_n}}$	Demand vector (MW) at load point *n* (in MW).
$\overline{P_{d_n}^{t}}$	Expected active demand of load point *n* at time *t* (in MW).
$\overline{Q_{d_n}^{t}}$	Expected reactive demand of load point *n* at time *t* (in MVar).
$\overline{P_{d_n,v}^{t,\mathrm{supplied}}}$	Expected value of survived demand power (in MW) at load point *n* during contingency *v* at time *t*.
$\overline{P_{g_n}^{t}}$	Expected active power output of generating unit *g* at bus-bar *n* at time *t* (in MW).
$\overline{Q_{g_n}^{t}}$	Expected reactive power output of generating unit *g* at bus-bar *n* at time *t* (in MVar).
$Q_{C_n}^{t}$	Reactive variable of VAR source equipment at bus-bar *n* at time *t*.
P_{v}^{t}	Probability of contingency state *v* at time *t*.
P_{knm}^{t}	Active power flow through transmission line *k* (between bus *n* and *m*) at time *t* (in MW).

Q^t_{knm}	Reactive power flow through transmission line *k* (between bus *n* and *m*) at time *t* (in MVar).
$\overline{P}^t_{loss,knm}$	Expected active power losses of transmission line *k* at time *t* (in MW).
$\lambda_{b,i}$	Skewness of concentration *i* for random variable *b*.
$P_{b,i}$	Probability of concentration *i* for random variable *b*.
TNVIS^t_k	Total number of voltage-unstable states when optimal TLS plan *k* is implemented at time *t*.
TNTIS^t_k	Total number of transient-unstable states when optimal TLS plan *k* is implemented at time *t*.
U_n	Voltage magnitude at bus-bar *n*.
$\mathbf{X}$	Vectors of random input variables.
$\mathbf{Y}$	Vectors of random output variables.
∂_k	Switch status of transmission line *k* (1: in, 0: out).
θ_n	Voltage angle of bus-bar *n*.
$\xi_{b,i}$	Location of concentration *i* for random variable *b*.
μ_x	Mean value of variable *x*.
σ_x	Standard deviation of variable *x*.
$\mu_{f_i}(.)$	Membership value for the objective function *i*.

C. Parameters

B_k	Susceptance of transmission link *k*.
G_k	Conductance of transmission link *k*.
c_{g_n}	Production cost of generating unit *g* at bus-bar *n*.
$f_i^{\min}$	Minimum value of objective function *i*.
$f_i^{\max}$	Maximum value of objective function *i*.
K_{ϖ}	Turn ratio variable of transformer ϖ.
$K_{\varpi}^{\min}$	Minimum turn ratio for transformer ϖ.
$K_{\varpi}^{\max}$	Maximum turn ratio for transformer ϖ.
M_k	Big M-Value for transmission line *k*.
$P_{g_n}^{\min}$	Minimum limit on the active power generation of generating unit *g* at bus-bar *n* (in MW).
$P_{g_n}^{\max}$	Maximum limit on the active power generation of generating unit *g* at bus-bar *n* (in MW).
$P_k^{\min}$	Minimum limit on the active flow of transmission line *k* (in MW).
$P_k^{\max}$	Maximum limit on the active flow of transmission line *k* (in MW).
$Q_{g_n}^{\min}$	Minimum limit on the reactive power generation generating unit *g* at bus-bar *n* (in MVar).
$Q_{g_n}^{\max}$	Maximum limit on the reactive power generation generating unit *g* at bus-bar *n* (in MVar).

π	Total number of random input variables.
∇_n	Importance (weight) factor for load point *n*.
λ_1, λ_2	User-defined importance factors for voltage and transient probability indicators.
δ	Total number of sampled states in MCS.
σ_m	Repair rate of equipment *m* (hr./year).
φ_m	Failure rate of equipment *m* (occ./year).
$\theta_n^{\min}$	Minimum limit on voltage angle at bus-bar *n*.
$\theta_n^{\max}$	Maximum limit on voltage angle at bus-bar *n*.
χ	Maximum number of transmission line switching possibilities.
μ_{d_i}	Satisfactory membership level for objective *i*.

D. Performance Indices

$\overline{\text{EDNS}}_{TS,k}^{t}$	System expected demand not supplied (in MW) when optimal TLS plan *k* is adopted at time *t*.
EDNS_{TS}^{L}	The minimum desired level of the EDNS index.
$\overline{\text{IR}}_{TS,k}^{t}$	Expected system instability risk when optimal TLS plan *k* is implemented at time *t*.
$\overline{P}_{loss,TS,k}^{t}$	Expected system total active power losses when optimal TLS plan *k* is implemented at time *t*.

$\overline{\text{TIP}}_{TS,k}^{t}$ Expected system transient instability probability when optimal TLS plan *k* is adopted at time *t*.

$\overline{\text{VIP}}_{TS,k}^{t}$ Expected system voltage instability probability when optimal TLS plan *k* is adopted at time *t*.

Nomenclature 3: Section 5

D_i, F_i, M_i	Deterioration state *i*, failed state *i*, and maintenance state *i* in the circuit breaker (CB) deterioration state diagram.
$f_{B_k}^{t_i}(t)$	Probability distribution assigned to the timing parameter *i* of the monitoring signals for the k^{th} CB in the system.
FP_O^{AB}	Failure probability of the AB contacts of the CB in its opening operation.
FP_C^{AB}	Failure probability of the AB contacts of the CB in its closing operation.
FP_C^{CC}	Failure probability of the CB close coil in its closing operation.
FP_O^{TC}	Failure probability of the CB trip coil in its opening operation.
FP_O^{FT}	Failure probability of the CB free traveling time in its opening operation.
FP_C^{FT}	Failure probability of the CB free traveling time in its closing operation.
FP_O^{MT}	Failure probability of the CB mechanism traveling time in its opening operation.
FP_C^{MT}	Failure probability of the CB mechanism traveling time in its closing operation.
FP_{CB}^{O}	The overall CB failure probability in opening operations.
FP_{CB}^{C}	The overall CB failure probability in closing operations.
$P_{B_k}^{t_i, D_j}$	Probability of the timing signal *i* being in the deterioration state D_j for the k^{th} CB in the system.

$P_O^{t_i,D_j}$	Probability of the timing signal *i* being in the deterioration state D_j for the CB opening operation.
$P_{O/C}^{AB,D_i}$	Probability of AB contacts of CB, falling in deterioration state D_i once opening/closing.
P_C^{CC,D_i}	Probability of CB close coil in deterioration state D_i once closing.
P_O^{TC,D_i}	Probability of CB trip coil in deterioration state D_i once opening.
$P_{CB,O/C}^{D_i}$	Probability of the CB, as a component, falling into the deterioration state D_i in its opening/closing operation
t_i	The signal timing parameter *i* of the CB.
$\sigma_k^{\min}$	Minimum threshold for the signal timing parameter *k* to be acceptable.
$\sigma_k^{D_i,\max}$	Maximum threshold for the signal timing parameter *k* to stay in deterioration state D_i.
μ	The mean value of a variable.
σ	The standard deviation value of a variable.

Nomenclature 4: Section 6

A. Sets

$g \in G$	Set of system generating units.
$g \in \dot{G}$	Set of generating units out of service due to a contingency.
$k \in K$	Set of system transmission lines.
$k \in \hat{K}$	Set of transmission lines in service.
$k \in \bar{K}$	Set of transmission lines out of service.
$k \in \dot{K}$	Set of out of service transmission lines due to a contingency.
$n \in N$	Set of system buses.

B. Decision Variables

P_g	Power output of generating unit g (in MW).
P_k	Power flow through transmission line k (in MW).
s_k	Switch action for transmission line k (0: no switch, 1: switch).
θ_n	Bus angle at bus n.
u_n	Unfulfilled demand at bus n (in MW).

C. Parameters

B_k	Susceptance of transmission line k.
$B^t(\mathrm{RD}_i)$	Incremental benefits obtained via generation re-dispatch-only at node i of the switching tree at time t.

$B^t(S_i)$	Incremental benefits obtained through successful implementation of switching transmission line *i* and generation re-dispatch at time *t*.
c_g	Linear generation cost of generating unit *g*.
d_n	Demand (in MW) at bus *n*.
$\mathrm{FP}^t(\mathrm{B}_i)$	Failure probability of the CB *i* at time *t*.
$MB^t(S_i)$	Mean benefits obtained through successful implementation of transmission line switching and generation re-dispatch at node *i* of the decision tree at time *t*.
M_k	Big M-Value for transmission line *k*.
$P^t(S_i)$	Availability index of transmission line *i* at time *t*.
$P_k^{\max}$	Maximum line flow limit for transmission line *k* (in MW).
$P_k^{\min}$	Minimum line flow limit for transmission line *k* (in MW).
$P_g^{\max}$	Maximum generation limit for generator *g* (in MW).
$P_g^{\min}$	Minimum generation limit for generator *g* (in MW).
$\theta^{\max}$	Maximum bus angle difference.
$\theta^{\min}$	Minimum bus angle difference.
τ	Minutes between two switching operations.

TABLE OF CONTENTS

Page

LIST OF FIGURES

Page

LIST OF TABLES

Page

1. INTRODUCTION

1.1 Problem Statement

Bulk electric transmission systems have been traditionally characterized with fixed configuration over time except in the cases of faults and forced outages when the topology changes as a consequence of circuit breakers tripping or scheduled operator intervention. Given a fixed system topology with a certain generation pattern and load profile, the system operator commonly dispatches the committed generating units to optimize the cost while ensuring that the system security and reliability constraints are met. This traditional view does not assume the topology changes during a dispatch calculation interval. However, it is acknowledged that system operators can actually change the grid topology by operating circuit breakers to improve various system conditions and constraints [1]-[3].

Lately, it is becoming more and more apparent that further considerations beyond the classical reliability oriented view are needed for enhancing the grid resilience and keeping the lights on at all times [4]. This is accelerated by several major weather-caused grid outages (see Figure 1). From 1980 to 2014, a total of 178 weather/climate caused blackouts occurred in the United States alone (8 of which occurred in 2014) with the overall damages/costs reaching or exceeding US$ 1 trillion [5]. As an outcome, various industries were halted for hours (if not days) resulting in significant economic loss and also, dozens of people in need of specific health care at homes or nursing facilities lost their lives due to the loss of electricity supply that was essential for their wellbeing, and

the power was not restored for several days [5]-[8]. As an example, during the 2003 blackout in North America, 50 million people were inconvenienced for up to two days, 11 people lost their lives, and $6 billion damages were reported [9]. Similarly during the winter storms in Chenzhou, China, a nearly 2-week blackout resulted in 4.6 million people out of electricity and exceeding 60 people losing their lives including 11 electricians working on power restoration [9]. Figure 1 demonstrates that both the frequency and intensity of such wide area outage events have been trending higher in recent years. With increasing dependence on electricity for most daily activities and vital services (e.g., transportation, commerce, communications, health care, etc.), an urgent need to enhance the resilience of the electricity delivery infrastructure to reduce the impact and risk from natural and human-triggered events is well recognized.

Power system topology control, often called transmission line switching (TLS), offers the system operators an opportunity to harness the flexibility of the transmission system topology by temporarily moving transmission lines in and out of service. By

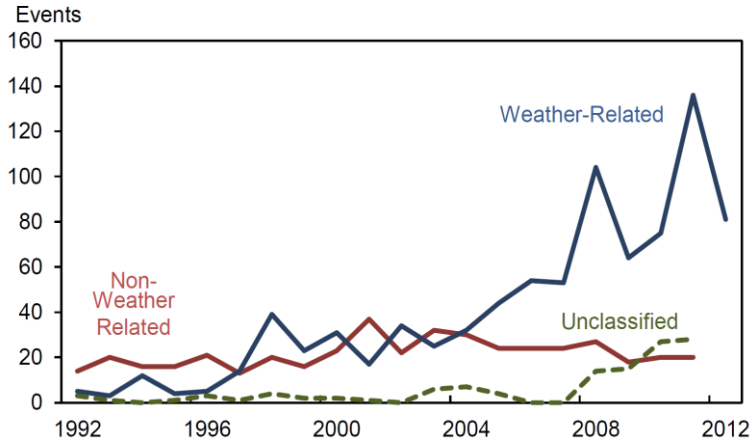

Figure 1. Weather-dependent outages in US between 1992-2012 [6].

changing the way how electric power flows through the system, transmission switching can be employed either in emergency scenarios to alleviate voltage violations, congestions and overloading conditions, and even load outage recovery, or during normal operating conditions for higher economic benefits or loss improvements [1]-[3].

There is a constant national push to operate the grid in a smarter way by introducing advanced technologies and control mechanisms into grid operation [8]-[17]. Disruptive events whether they are malicious attacks, natural disasters, or human-caused accidents continuously pose a risk for the grid operations and lessons learned from some catastrophic events have pushed the focus on the concept of "resilience" [4]-[12]. The ultimate goal is to achieve an improved resilience by the efficient use of the current infrastructure in a smarter way. In order to reach the improved grid efficiency and resiliency goals, this research strives to examine harnessing the transmission line assets, in both normal and emergency states, along with several critical practical considerations (such as circuit breaker reliability and adequacy of relay settings) for flexible and reliable implementation of such technologies. Such considerations, which are employed in the grid operational time frame, make it possible to have more efficient use of existing network facilities with minimal additional costs.

1.2 On the Concept of Resilience

The electricity grid is vulnerable to various threats such as inflexible system operation, aged assets, volatile weather patterns, and cyber physical security. With the rapid deployment of variable renewable generation, increasing demand to deliver higher

quality electricity, and intensified legislative focus and regulatory oversights, there is an urgent need to enhance the resilience of the power delivery infrastructure to reduce the risks. In face of such disruptive events, power systems may reside in different operating states as a result of an external disruption and, thus, it is critically important to define such states to be able to devise the mitigation plans and proactive decisions [4], [18], [19].

The UK Energy Research Center [20] provides a definition for resilience as follows: "*Resilience is the capacity of an energy system to tolerate disturbance and to continue to deliver affordable energy services to consumers. A resilient energy system can speedily recover from shocks and can provide alternative means of satisfying energy service needs in the event of changed external circumstances*."

The National Infrastructure Advisory Council (NIAC), USA provides a similar and more generic definition of resilience that is applicable to any critical infrastructure, and it additionally considers the "*ability to absorb lessons by the disruptive events and adapt the operation and structure of a critical infrastructure to prevent or mitigate the impact of similar events in the future*" [21].

Figure 2 demonstrates the conceptual definition of "resilience", reflecting the states of a power system in face of an extreme emergency (e.g., a severe weather-driven event), the timing sequence of such states, and possible actions that can be triggered at different levels for the main sake of resiliency enhancement. Through the presented trapezoidal model for resilience, various phases of power system operating states are precisely characterized, as follows [22]:

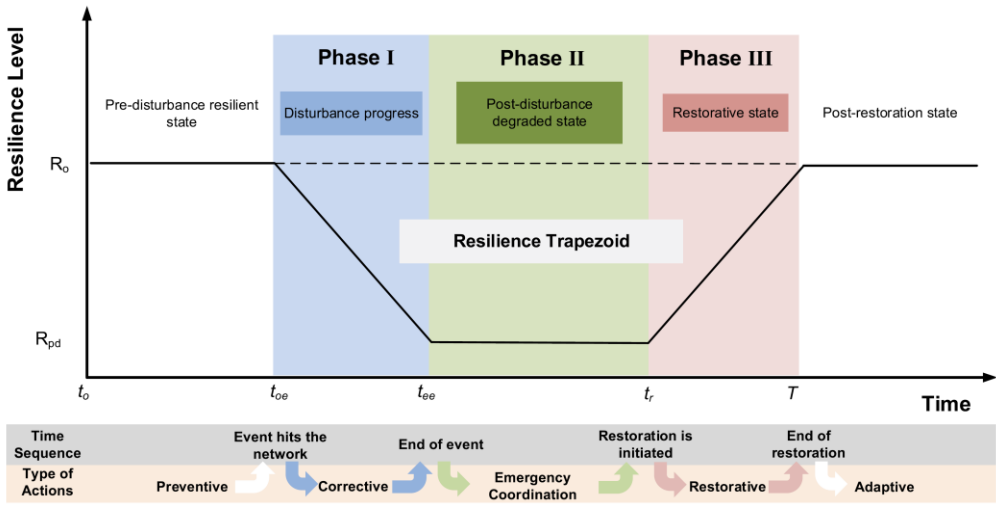

Figure 2. Conceptual definition of resilience associated with an event [22].

- If the time and location of the external shock to the system can be sufficiently predicted, the preventive actions should be triggered by the system operators before an extreme event strikes the network at t_{oe}. Preventive actions, such as preventive generation reschedules, could enhance the pre-disturbance resilience of the electricity grid and its infrastructure during $t \in [t_o , t_{oe}]$ to better withstand the disruption.
- When the disturbance is in progress in Phase I of the trapezoidal chart in Figure 2, $t \in [t_{oe} , t_{ee}]$, the network performance degrades to its minimum. Emergency or corrective actions (such as generation re-dispatch alone or a co-optimized generation re-dispatch and corrective transmission line switching actions) can be called to mitigate the consequences of the external shock on the grid performance and return it back to the normal and desired condition.

- Following the event in Phase II, $t \in [t_{ee}, t_r]$, the system operating state has already migrated to a degraded condition and will reside in the post-disturbance state for a period of time that is desired to be as minimal as possible. If well implemented, suitable and effective emergency coordination and preparedness in Phase II enable a quick commencement of the restoration phase in Phase III, $t \in [t_r, T]$. As shown in Figure 2, T is the time that is needed for the network to fully recover from its minimum performance with post-disturbance resilience level of R_{pd} to its desirable performance with the pre-disturbance resilience level of R_0 or to a desired resilience level different than R_0.
- When the system recovers from the disruptive event in the post-disturbance state, $t > T$, the impacts of the disruptive event on the system performance and resilience need to be assessed and fully analyzed. Such post-disturbance studies of the event allow design and development of adaptive plans that can be taken in order to increase the resilience of the critical infrastructure during similar but unforeseen events that may happen in future.

This conceptual definition in the form of the resilience trapezoid can be applied to any threat, irrespective of its nature, ranging from weather disasters, malicious attacks, etc. Within the broad definition of resilience described above, a resilient power grid should possess the following key features and principles [22]-[25]:

- *Pre-Disturbance Resilient State*: An acceptable prediction and accurate estimation of the event's spatial and temporal characteristics as well as its severity would enable the application of proper preventive actions and fosters the network

topology to appear in a state that would help the system operator to deal effectively with the upcoming disruptive event. They would also enable the prepositioning and allocation of the resources possibly required following the event, e.g., repair and recovery crews, generation reserves, mobile generators, etc. Therefore, accessibility to preventive operational flexibility is very critical for enhancement of the grid resilience in face of disruptive disasters.

- *Phase I (Disturbance Progress)*: A highly robust and resistant network with appropriate level of redundancy would enhance the system survivability and help boost the grid resilience to the initial impacts of the disruptive event and reduce the level of performance degradation, i.e., $R_o – R_{pd}$ (see Figure 2). Furthermore, resourcefulness (supported by smart grid technologies, e.g., advanced monitoring and distributed energy systems) is particularly important as it provides the corrective operational flexibility required for dealing with the prevailing conditions and reducing the slope/speed of the resilience degradation. Also, advanced information systems would help develop high situation awareness allowing the system operators to remain sufficiently informed on the evolving conditions of the power grid.
- *Phase II (Post-Disturbance Degraded State)*: Disaster assessment, priority setting and proper emergency preparedness and coordination would help the system operator to assess the detrimental consequences of the disruptive event, identify the critical components for the faster system recovery to a resilient state, and

initiate as fast as possible the procedures for restoring the damaged infrastructure. This reduces the duration of Phase II, i.e., t_{ee}–t_r (see Figure 2).

- *Phase III (Restorative State)*: Following the implemented actions in Phase II, a resilient system should demonstrate high restorative capabilities in order to first restore the collapsed infrastructure (i.e., infrastructure resilience), and then restore the disconnected customers (i.e., operational resilience). Several actions should take place in this phase, such as reenergizing transmission and distribution lines, repair and restoration of damaged components, generation unit restarting, resynchronization of areas, load restoration, etc. Such actions are aimed to reduce the duration of Phase III, i.e., T–t_r (see Figure 2).
- *Post-Restoration State*: Following the disruptive event and the restoration of the infrastructure to a resilient state, the impact of the event and the performance of the network should be thoroughly analyzed to identify weaknesses or limitations of the network, which could be improved to be better prepared for future (similar or unforeseen) events. Therefore, being adaptive and reflective to the experiences gained through the different events and threats is a key feature of a resilient infrastructure.

If a power system possesses the key resilience features mentioned throughout the different phases of an event, it should be then capable of effectively anticipating the impacts of the upcoming event, rapidly recovering from the degraded to a resilient state, and adapting its operation and structure to reduce the effects of future disruptions.

1.3 Research Motivation

The transmission grid is built to be a redundant network in order to ensure mandatory reliability standards; however, it is well known that such network redundancy can cause dispatch inefficiency [26]-[31]. Consequently, due to the interdependency between network branches (transmission lines), it is possible to temporarily remove a branch during certain operating conditions and improve the network efficiency when it is in its normal operating state, and also help alleviate the severe conditions following an outage (or violation) in the system emergency operating states. Additionally, such flexibility is virtually ignored and is not incorporated into the current dispatch optimization. This shortcoming in today's electricity grid operations needs to be alleviated since it is very unlikely that with all variations in load and generation, there exists solely a single optimal network topology for all periods in the operation time horizon when the system is either in its normal or emergency operating states and/or for all possible electricity market realizations.

The decisions to enforce transmission line switching (TLS) are currently either not frequently adopted in practice by the transmission system operators (TSO) or are made in an ad-hoc manner for some selected planned scenarios. The reasons are multiple: lack of systematic decision-making tools, lack of proper training and, a lack of the mindset that will trust that such rather complex and critical decisions can be automated and systematically applied. For this practice to be frequently realized in every-day operation, there is a need to develop robust tools for the operator decision making taking into account practical implementation concerns associated with various uncertainties originated from

renewable intermittence, variable loads, and other unpredictable grid disruptions. In the meantime, special attention needs to be paid to various competing (inconsistent) performance indicators of the grid following the topology change and other practical considerations (such as circuit breaker reliability and line availability, stability issues, relay settings, etc.) when developing and verifying a decision making framework for the system operator. Robust decision making tool sets need to suggest recovery options by mitigating the disastrous consequences of possible grid violations or an electricity outage. As a result, the electricity grid resilience in the face of such emergencies can be effectively enhanced in a timely manner.

The suggested decision making support tools in this dissertation aim at bridging the gap between the theoretical advancements in transmission line switching (TLS) and the implementation practices. This dissertation tries to tackle the TLS implementation decisions under different network operating conditions taking into account various sources of uncertainties and, yet, providing the operator with more flexibility in decision making.

1.4 Research Objectives

This dissertation focuses on developing decision making support tools for two cases of network topology control: (1) improved economic efficiency of the grid in normal operating conditions and (2) optimized corrective action to improve the grid resilience in face of emergency operating conditions arisen from various sources of disruptions.

Within the former category, a general probabilistic topology control formulation that can efficiently capture major uncertainties in generation/load patterns and incorporate

such probabilistic features in power system topology switching optimization will be proposed. A probabilistic decision making framework to quantify the risks associated with switching transmission lines for economic efficiency under such uncertainties and define, in an automated manner, the optimal number of TLS actions per hour for final implementations will be proposed. This will help verifying the effectiveness of the topology control solutions obtained through traditional deterministic formulations and their validity under many sources of grid uncertainties. A probabilistic multi-objective optimization framework for TLS accommodation in economic scenarios considering several requisite (and contradictory/competing) objectives will be also introduced. The presented framework would help the TSOs to more systematically approach a reliable implementation of TLS in practice while the desired system reliability, limited network losses, tolerable instability risks, and favorable economic gains are ensured.

Within the latter category, this dissertation also tries to bridge the gap between the theoretical advancements in previous literature and practical requirements that the operator will have to deal with. An implementation procedure, to be pursued in day-to-day operation planning scenarios, for realizing TLS in response to probable contingencies will also be proposed. The suggested framework provides several transmission line switching options per contingency, where the operator is presented with a set of AC feasible and stable TLS plans based on a selected optimization criterion such as minimum operation cost or maximum load shed recovery. The operator can use this information, other operating conditions not explicitly considered in the optimization, and his/her own experience to predictively select the most reliable switching actions for implementation to

help in realizing a more economically efficient grid operation or fast recovery from the pre-defined critical outages or violations ensuring the system maximum resilience.

1.5 Dissertation Outline

The remainder of this dissertation is organized as follows. Section 2 reviews the past work and literature on the application of transmission line switching (TLS) in power systems in both economic and emergency scenarios. It also provides a brief review of several recent research efforts on assessment of power system resilience in face of extreme emergencies and the mitigation tools developed for recovering from such extremes.

Section 3 sets forth a probabilistic formulation for a more efficient application of topology control strategies in real world scenarios with anticipated increase in the presence of highly variable renewable generation and uncertain loads. Such uncertainties are modeled via the Point Estimation Method (PEM) embedded into the DC optimal power flow (DCOPF)-based formulations for optimal switching solutions. Hourly and daily advantages of the proposed probabilistic framework, compared to the conventional operations and deterministic formulations, are discussed. As the anticipated economic gains would increase through sequential implementation of several switching actions, a new probabilistic decision making approach to identify the optimal number of switching actions at each hour is also proposed. This decision support tool uses the probabilistic reliability cost/value analytics in which not only the financial benefits, but also the costs of reliability risks are taken into account. The approach is tested through various scenarios

on the modified IEEE 118-bus test system, with and without renewables integration, where the results reveal its applicability and efficiency.

Section 4 first presents the derivation of algorithms and theoretical foundations of a new multi-objective optimization framework for reliable implementation of TLS in power systems. Various critical and sometimes contradictory/competing objectives including economic benefits, power system reliability performance, network losses, AC feasibility concerns and instability risks are all taken into account through the proposed formulations. The probabilistic nature of the involved uncertainties is systematically handled via Monte Carlo Simulations (MCS) in combination with the 2-Point Estimation Method (2-PEM). The proposed multi-objective optimization problem is tackled through a robust technique, the Non-Dominated Sorting Genetic Algorithm II (NSGA-II), followed by a fuzzy decision making approach to account for the operator/decision maker practical preference in selecting the final topology control solution for implementation. Next, two case studies are analyzed: one using the modified IEEE 118-bus test system to confirm the algorithm efficiency, and the other using the Iran 400kV transmission grid, mainly to investigate the algorithm performance in real world applications. The proposed multi-objective decision framework for economic TLS applications is studied in both cases taking into account various uncertainty scenarios. The optimal solutions in Pareto fronts are found in each case study, comprehensively examined, and the final optimal solution for implementation is suggested to the operator using the fuzzy satisfying method. The operator may reliably implement the suggested TLS solutions as the desired system

reliability, limited network losses, tolerable instability risks, and favorable economic gains are ensured.

Life-cycle assessment of power system circuit breakers (CB), if efficiently done, can well lead to an optimal decision on when, where, and how to perform maintenance activities and makes it possible to realize the anticipated benefits from the TLS actions. Section 5 elaborates a new approach on the identification of CB's deterioration/recovery states, i.e., the so called life-cycle assessment, using its control circuit condition monitoring data. Reliability-oriented performance indices, which can assess the condition of different physical parts of a CB in real time, are introduced first. Then, a quantitative methodology to define the probability of the CB falling into each class of deterioration/recovery states i.e., healthy, vulnerable, troubled, and failed is proposed. Using this approach, maintenance decisions can be effectively made, and impact of maintenance can be well quantified, and system-wide maintenance optimization with respect to the condition-based differentiation of CBs all over the system can be made possible. Field CB condition data recorded at different time intervals during the operation of CB is utilized to evaluate the applicability and effectiveness of the proposed approach.

In Section 6, a novel decision making framework for optimal transmission switching satisfying the AC feasibility, stability and circuit breaker (CB) reliability requirements needed for practical implementation is suggested. The proposed framework can be employed as a corrective tool in day to day operation planning scenarios in response to potential contingencies. The switching options are determined using an efficient heuristic algorithm based on DC optimal power flow, and are presented in a multi-branch

tree structure. Then, the AC feasibility and stability checks are conducted and the CB condition monitoring data is employed to perform a CB reliability and line availability assessment. Ultimately, the operator will be offered multiple AC feasible and stable TLS options with associated benefits. The effectiveness of the proposed approach is validated on the IEEE-118 bus test system.

Section 7 provides the research conclusions and summarizes the key findings and the main contributions of this dissertation. Future research directions are also laid out in this Section.

2. LITERATURE SURVEY

2.1 Introduction

Power system topology control, often called transmission line switching (TLS), offers the system operators an opportunity to harness the flexibility of the transmission system topology by temporarily removing transmission lines out from service. By changing the way how electricity flows through the system, TLS can be employed either in emergency scenarios (to alleviate violations, congestions, and overloading conditions), or during normal operating conditions (for higher economic benefits). Such considerations, which are employed in the operational time frame, make it possible to have more efficient use of existing network facilities.

Though being performed for decades on a very limited scale with rather focused aims, transmission switching has recently gained further importance with the increased penetration of renewable energy resources and the growing demand for more reliable and resilient operation of power systems [1]-[3].

2.2 Application of TLS as a Corrective Mechanism in Emergency Scenarios

It has been shown that various operating conditions in the electricity grid can be resolved or mitigated through TLS implementations. In 1980s, TLS first was employed as an effective remedy to improve system reliability and alleviate severe operating conditions such as transmission line overloads, voltage violations, etc. [1]-[3], [32]-[71]. Reference

[1] gives an overview of the use of TLS as a corrective mechanism in response to a contingency, as well as the solution techniques, objectives, etc. It discusses the problem formulation and provides an overview on search techniques to solve such optimization problems. Reference [32] proposes a method to alleviate line overloading due to a contingency by the use of TLS and bus-bar switching as a corrective mechanism. This method is limited since it is a heuristic technique which does not consider all possible TLS solutions and it does not co-optimize the topology with the generation. TLS as a corrective mechanism with a continuous variable formulation for the switching decision as well as with discrete control variables is examined in [33], where integrated coordination of network topology optimization and generation rescheduling for power system security applications was studied. A branch and bound technique is suggested in [34] to solve a similar problem based on a linear approximation of the Optimal Power Flow (OPF) formulation. A research on selection of transmission lines for corrective switching actions is conducted in [35] based on the Z-matrix calculations.

While most of this past research acknowledges certain benefits of harnessing the control of transmission network, the flexibility of the transmission grid to co-optimize the generation along with the network topology switching during steady-state operations was not investigated. Reference [36] further examines TLS in the AC setting to relieve line overloading conditions and voltage violations. The authors solved the problem assuming that the generation dispatch is already known as fixed and, hence, the benefit of co-optimizing the network topology along with the generation was not sufficiently captured. A fast corrective switching algorithm to be used in response to a contingency is proposed

in [37]. The benefit of this algorithm over what was proposed in the past research is that the control over the network topology also takes into consideration the ability to re-dispatch generation whereas other methods would assume that the generation is fixed when trying to determine the appropriate switching actions. Due to the complexity of this problem, this method does not search for the actual optimal topology but rather considers limited switching actions.

Previous research on the use of transmission switching as a corrective mechanism was continued in [38], [39] to relieve transmission line overloads and voltage violations. A new solution technique was proposed in [40] to find the best switching actions employing a sparse inverse technique which involves a fast decoupled power flow in order to reduce the number of required iterations. A binary integer programming technique is used in [41] for the same motivation: to use switching actions as a corrective mechanism to relieve transmission line overloads and voltage violations. In [42], TLS is proposed to minimize the network losses. This paper demonstrates that contrary to general belief, it is possible to reduce electrical losses in the network by temporarily opening a transmission line. A mixed integer linear program (MILP) is proposed in [43] to determine the optimal transmission topology with the main objective to minimize the system losses, but with no regards to co-optimizing the generation dispatch along with the transmission grid topology and configuration.

In 2011, a review of the past research on the applications of topology control optimizations was presented in [44]. Optimal topology control with physical power flow constraints in AC setting with considerations to N-1 contingency criterion to improve the

network losses is studied in [45]. In this work, a semi-definite programming relaxation is formulated to find a lower band to the objective function value of the problem. TLS technology as a congestion management tool is studied in [46] and [47]. In [46], the solution of the resulting large-scale mixed-integer programming (MIP) problem is carried out by both a deterministic branch-and-bound algorithm and a genetic algorithm. In [47], TLS is embedded in an OPF framework with AC constraints solved using Benders Decomposition and a guideline is suggested to the operators to find the order of the TLS actions in order to relieve congestion without voltage security violations.

Application of TLS for load shed recovery in face of critical contingencies is investigated in [48], where a DCOPF-based TLS model is implemented aiming at recovering the load outages in case of critical contingencies and solved using a proposed heuristic on a large-scale real-life power system. Several critical factors that the operator will have to deal with when implementing the TLS solutions in practice, e.g., circuit breaker reliability, relay setting coordination, etc., are suggested and extensively investigated in [49]. The authors in [50] suggested a flexible decision making support tool based on the DCOPF model for TLS that ensures a reliable implementation of TLS solutions majorly for load outage recovery. The suggested framework provides multiple TLS solutions per contingency, all in the form of TLS sequences, satisfying the AC feasibility, system stability, and circuit breaker reliability requirements.

Corrective TLS integrated with N-1 contingency analysis for day-ahead and real-time applications is suggested in [51], where the deliverability of the reserves in response to system contingencies is improved through TLS. In [52], a data mining approach is

suggested for real-time corrective TLS to tackle the computational complexity of such optimization problems by generating the rank list of the candidate transmission lines for switching actions and bypassing the need for solving such complex MIP optimization problems over and over. The line outage distribution factors (LODF) incorporated in TLS formulations are proposed in [53] and [54], where in the former, closed-form analytic expressions are derived for post-contingency network parameters and assessment of LODFs in security applications, and in the latter, a shift factor MIP formulation of TLS is introduced to tackle the intractability of the conventional MILP formulations for TLS. An AC-based real-time contingency analysis (RTCA) package with TLS is introduced in [55] where the scalability concern of the corrective TLS implementation in real-world large-scale networks is addressed using the network data from Pennsylvania-New Jersey-Maryland (PJM), Tennessee Valley Authority (TVA), and Electric Reliability Council of Texas (ERCOT). In order to further address the scalability of the TLS optimization problems for real-world applications, performance of AC and DC based TLS heuristics on large-scale Polish system is investigated in [56].

Impact of corrective TLS on power system reliability is deterministically studied on a TVA test case in [57], where the corrective AC-based N-1 contingency analysis is integrated with TLS mechanism, providing additional means in mitigating the system violations in case of contingencies. Application of robust optimization and probabilistic techniques for corrective TLS accommodation in presence of various uncertainties is extensively explored in [58]. Incorporation of robust optimization in the TLS formulations ensures that the switching solutions are feasible for a range of system operating states. The

TLS solutions found through the application of robust optimizations are obtained considering the worst case uncertainty realization resulting in the most conservative solution. The use of such robust optimization models introduces additional complexities to the topology control optimization as finding approximate models with tractable size is typically not a trivial task when facing real-world practical problems.

Within the same direction, reference [59] employs the robust optimization concept with the corrective topology control to evaluate the system do-not-exceed (DNE) limits, defined for renewable integration in the grid. In this work, day-ahead methods to determine the maximum uncertainty in renewable resources in terms of the DNE limits combined with robust corrective topology control is analyzed. Correspondingly, algorithms to solve such problems considering DNE limits for renewable resources are suggested in [60]. AC feasibility concerns and effective use of out-of-market corrections and uneconomic adjustments for day-ahead accommodation of TLS solutions and approximations of such complex optimization problems are reviewed and thoroughly explored in [61] and [62].

The impact of TLS solutions on system transient stability requirements is discussed in [63], where application of TLS is considered in real-time as one of the last steps before the system collapses. In particular, this paper suggests a dynamic corrective TLS strategy and identifies both the transmission lines to be switched on/off during transients and the time when the corrective actions have to be applied in order to ensure the system stability. Reference [64] investigates the stability issues that might arise when incorporating TLS in practice, specifically taking into account the system security margins

and online stability requirements. A theoretical method based on the decomposition technique is proposed in [65] to solve the optimal reconfiguration of the transmission systems constrained by transient stability restrictions. The role of TLS scenarios on ensuring the N-1 reliability criterion and system stability requirements is numerically investigated in [66]. More specifically, the reliability and stability concerns and issues of the robust corrective topology control formulation and solutions, as a congestion management tool to facilitate the integration of renewable resources, are discussed and extensively studied in [66].

2.3 Application of TLS for Grid Financial Efficiency in Economic Scenarios

Co-optimizing the network topology with the generation dispatch provides the system operators with the ability to select the network topology with the generation dispatch. In this way, the operator not only can select any feasible dispatch given the original topology, but also has the ability to select different additional dispatch solutions that are feasible considering other set of topologies [44]. Such co-optimization may bring about potentials for having feasible generation dispatch solutions corresponding to different new topologies, while such dispatch solutions may not be feasible for the original network topology. The reason lies in the fact that the topology change will modify the power flows in a meshed network (due to Kirchhoff's laws) and the way how electricity flows. As a result, the concept of harnessing the grid topology through TLS actions coupled with generation dispatch optimization was not only used as an efficient corrective action in emergency scenarios but also for the sake of reaching economic benefits as

reported in the literature [44]. This sparked a series of studies in recent years aiming at discussing the impacts of optimal topology control on the grid operation efficiency for economic benefits [67]-[97].

The concept of dispatchable network was first introduced in [67] where the biddable and dispatchable transmission rights were discussed to provide the electricity market with greater efficiency and competition. Subsequently, optimal transmission switching, as a mixed integer programming (MIP) problem, based on the DCOPF formulation through which considerable economic savings may be gained, was introduced in 2008 and was numerically analyzed under different system loading conditions [68]. Extensions on the work in [68] were pursued in [69] through sensitivity analysis and discussing on how the TLS implementation in normal operating scenarios affects the nodal prices, load payments, generation revenues, congestion rents, and flowgate prices. Economic efficiency and market implications of the TLS solutions accompanied by the optimized generation dispatches are additionally investigated in [70]. The N-1 reliable DCOPF-based topology control is investigated in [71], where TLS solutions are found in IEEE 118-bus and the RTS 96 system test cases satisfying the N-1 standards while providing a considerable operation cost savings. Leveraging the grid controllability to make better use of the network existing infrastructure through TLS optimizations is further investigated in [72] through multi-period N-1 reliable unit commitment equipped with TLS technology based on the duality concepts. The concept of smart flexible just-in-time transmission and flowgate bidding is introduced in [73] in which the TLS technology is

utilized to allow the network transmission line flows to exceed its rated capacity for a short period of time for a pre-specified monetary penalty.

While most of the past research on TLS for economic efficiency is formulated based on the DCOPF optimizations, AC formulations for economic TLS have been also approached in a couple of past studies. In [74] and [75], the accuracies of the optimal TLS solutions based on both DC and AC OPF formulations are analyzed and several heuristics are proposed to cope with the complex ACOPF-based TLS optimizations. A novel AC solution method for optimal topology control optimization problem with N-1 reliability criterion through which a global optimal solution is guaranteed is suggested in [76]. In this work, which is also adjusted to be attractive for parallelization and accommodation of the human subject participation, it was concluded that the network real power losses may increase in the new system topology, compared to the base case original network topology, while the system operating cost is considerably reduced.

Considering the fact that iterating between DC-based topology control algorithms and AC power flow validation of TLS solutions may become intractable in large-scale systems, AC-based topology control algorithms are proposed in [77] and implemented on a real-size power system through a PJM historical data case study. In order to improve the operator decision making to select among the economically attractive TLS solutions, impact assessment of power system topology control on system reliability performance is extensively studied in [78] under both AC and DC settings. Furthermore, the application of economic TLS in power systems and how it changes the system operating conditions is analyzed in [79], where it probabilistically evaluates the migration likelihood of the

system accommodated with the TLS actions to the system alert and emergency operating states, further enhancing a reliable decision on which TLS solution to finally implement.

In the literature, some references are devoted to study the TLS approach coupled with the unit commitment and expansion planning problems majorly for the sake of power system security improvement. In [80], the TLS is introduced in security-constrained unit commitment for alleviating transmission violations and improve the economic efficiency of the transmission network. In this work, a two-stage optimization framework is developed where the unit commitment is formulated in a master problem and the TLS optimization follows in a sub-problem. The TLS is incorporated in the transmission and generation capacity expansion problems in [81] where the benefits of harnessing the grid flexibility are analyzed in such optimization problems throughout the planning time horizon. The application of TLS in the security-constrained unit commitment for the day-ahead scheduling is introduced in [82] where the entire problem is formulated and solved in an AC setting considering the voltage and reactive power constraints. A probabilistic security analysis taking into account the socio-economic cost of disruptions and economic benefits of topology control solutions is suggested in [83] where two types of security aspects were studied integrated with the topology control program: cascading failures due to overloaded lines and steady-state voltage instability. A deterministic approximation approach coupled to chance-constrained optimizations in order to investigate the possibility of topology control deployment to accommodate higher utilization of wind generations is suggested in [84].

Additional literature has addressed other concerns related to the TLS practical implementation and impacts of frequent TLS adoption on circuit breaker reliability are studied in [85]-[87]. Scalability concerns and the economic TLS solutions of the large-scale networks are verified in [77], [88], and [89] for PJM transmission system, [90] for European electricity networks, [91] for ISO-New England, and [92] for TVA and ERCOT networks. In [93], a decomposition approach, namely Alternating Direction Method of Multipliers, is presented to solve the scalability problem of the TLS formulations for real-size large-scale power systems through which near-optimal solutions are found at relatively lower computational costs.

Last, but not least, computational complexity of the TLS optimization problems has recently motivated researchers to explore the use of advanced optimization techniques and heuristics. In [94], a tractable dynamic TLS incorporated in the OPF problem based on heuristic control policies is introduced. The computational burden is improved up to four orders of magnitude better than what was reported in the past research. Two heuristics relaying on the transmission line ranking parameters are suggested in [95] to improve the computational complexity of the TLS optimization problems. The first one solves a sequence of LPs removing one transmission line at a time and the other solves a sequence of MIPs removing one transmission line at a time but with fewer numbers of binary variables. Tractable transmission topology control policies which employ the sensitivity information from the economic dispatch optimizations to select a few transmission lines for TLS decisions are proposed in [96]. The application of an iterative linear program approximation to the current ACOPF-based TLS formulations is introduced in [97], where

the TLS solutions are found much faster than the conventional nonlinear ACOPF-based formulations and yet with acceptable accuracy.

2.4 Electricity Grid Resilience to Disruptions: Assessments and Mitigations

In order to ensure the grid integrity under any conditions, the system design, planning, and operation must be not only driven by key reliability principles to cope with known and credible outages, but also by the measures that can be taken in response to the High Impact Low Probability (HILP) events, such as the extreme weather phenomena. In contrast to reliability, the concept of resilience has not been widely employed, and hence, its definition has not been yet in consensus. Several definitions for the resilience have been introduced in [20]-[25], [98]-[101].

Modeling and evaluation of resilience for critical electrical power infrastructure to extreme weather events is approached in [102], where a conceptual framework to quantify the power system resilience in face of weather threats using stochastic techniques is suggested. Fragility modelling, impact assessment and adaptation measures for power system resilience to extreme weather conditions is studied in [24]. Assessment of the resilience of transmission networks to extreme wind events is explored in [103], in which a sequential Monte Carlo based time-series model for evaluating the effect of weather on power system components is utilized, with focus on the wind impact on transmission lines and towers. Risk-based defensive islanding is suggested in [104] to boost the power grid resilience to extreme weather events, where it aims to adaptively mitigate the cascading effects that may occur during weather emergencies. The resilience and flexibility of power

systems to future demand and supply scenarios is studied in [105], where two case studies are reported for Great Britain transmission network and the Cyprus network. The concept of demand-side resiliency through deployment of distributed energy resources (DER) including onsite generating units, batteries, and microgrids to enable electricity consumers to continue electricity use during power outages is investigated in [106]-[110]. Several time-dependent metrics for quantification of operational and infrastructure resilience in power systems are introduced in [23] where additional insights are provided to capture the degradation and recovery features of critical infrastructures in face of weather threats.

Proactive preparedness to cope with extreme weather events through resilience-oriented pre-hurricane resource allocation in power distribution systems is proposed in [111] using a new mixed-integer stochastic non-linear program. A heuristic to obtain the allocation plan by solving a MILP is also suggested and the impacts of resource transportation costs, initial distribution of electric buses, and hurricane severity on the allocation plans are discussed. The concepts, metrics, and a quantitative framework for power system resilience evaluation are suggested in [112], where a load restoration framework based on the smart distribution technologies is proposed. The concept of networked microgrids for enhanced power system resilience against extreme events is introduced in [113], through which an appropriate timely response would be possible in emergency conditions. In this study, metrics of the advanced information and communication technologies (ICTs) in microgrid-based distributed systems to support the power system resilience are proposed.

Technologies for early warning systems for timely prediction of the disastrous weather outages are proposed in [114]-[116] to further enhance the system resilience by the use of effective remedial actions and preparedness in face of the severe weather-driven threats. In order to fulfill an effective emergency planning, reference [117] suggested a stochastic integer program aiming at finding the optimal schedule for inspection, damage evaluation, and repair in post-earthquake restoration of electric power systems with the objective to be minimization of the consumers' outage duration. Approaches for joint damage assessment and restoration of power systems in face of natural disasters are suggested in [118] which include an online stochastic combinatorial optimization algorithm to dynamically update the restoration decisions after visiting each potentially damaged location, a two-stage method to evaluate the damage severity and then pursue the restoration plans, and a hybrid algorithm of both approaches that simultaneously consider both the damage assessment and system restoration plans.

A general multi-objective linear-integer spatial optimization model for arcs and nodes restoration of disrupted networked infrastructure after a disaster is proposed in [119], in which the tradeoff between the problem objectives (e.g., system flow maximization and system cost minimization) could be optimally captured. An integrated network design and scheduling problem for restoration of the interdependent civil infrastructures was proposed in [120] through the integer programming and was implemented on a realistic dataset of power infrastructure corresponding to the Lower Manhattan in New York City and New Hanover County, North Carolina. Reference [121] investigated the challenges on how to schedule and allocate the routes to fleets of repair

crews to recover the damaged power system in a timely manner. Extension of this work was presented in [122] through deployment of a randomized adaptive vehicle decomposition technique in order to improve the scalability of the model for large-scale disaster restoration of power networks with more than 24000 components.

A comprehensive survey of models and algorithms for emergency response logistics in electric distribution systems, including reliability planning with fault considerations and contingency planning models were presented in [123] and [124].

3. POWER SYSTEM TOPOLOGY CONTROL FOR GRID ECONOMIC EFFICIENCY: PROBABILISTIC FORMULATIONS AND DECISION MAKING*

3.1 Introduction

Power system topology control or transmission line switching (TLS) has been acknowledged as an effective enhancement in hour- and day-ahead operations in exploiting the network infrastructure resources for significant operational cost reduction in normal operating state. It is also recognized as a promising corrective action for reliability improvements in face of critical contingencies.

Decisions for TLS are currently either not frequently adopted in practice by the transmission system operators (TSOs) or are made in an ad-hoc manner through a manual operator intervention. The reasons are multiple: lack of systematic decision-making support tools, lack of proper training and, a lack of the mindset that will trust that such rather complex and critical decisions can be automated and systematically applied. For this practice to be frequently realized in every-day operation, attempts need to be made to further develop robust tools for the operator decision making taking into account practical implementation concerns when exposed to various uncertainties originated from renewables, loads, and other unpredictable grid disruptions.

---

* Part of this chapter is reprinted with permission from "Probabilistic Decision Making for the Bulk Power System Optimal Topology Control" by P. Dehghanian and M. Kezunovic, July 2016. *IEEE Transactions on Smart Grid*, vol. 7, no. 4, pp. 2071–2081, ©2016 IEEE, with permission from IEEE.

Most of the past research was focused on deterministic modeling and formulations of the topology control optimizations for day-ahead and hour-ahead TLS decisions in both economic and emergency applications. A recent example is [84] where a deterministic approximation approach coupled to chance-constrained optimizations in order to investigate the possibility of topology control deployment to accommodate higher utilization of wind generations is suggested. Previous attempts have neither modeled nor incorporated the uncertainties into the topology control formulations. Robust optimization for corrective switching decisions in response to system contingencies is employed in [58] where the switching solutions are found considering the worst case uncertainty realization resulting in the most conservative solution. The use of such robust optimization models introduces additional complexities to the topology control optimization as finding approximate models with tractable size is typically not a trivial task when facing real-world practical problems. Day-ahead methods to determine the maximum uncertainty in renewable resources in terms of the do-not-exceed limits combined with robust corrective topology control is suggested in [59], [125], and the algorithms to solve for the do-not-exceed limits of renewable resources are further evaluated in [60]. However, the uncertainties have not been yet inherently incorporated in the topology control optimization formulations.

Different from the past research, a general probabilistic topology control formulation that can efficiently capture major uncertainties in generation/load and incorporate such probabilistic features in power system topology control optimization is suggested in this Section. A probabilistic decision making framework to quantify the risks

associated with switching transmission lines for economic gains under such uncertainties and define, in an automated manner, the optimal number of TLS actions per hour for final implementations will be also presented.

3.2 Probabilistic Optimal Topology Control Framework

3.2.1 General Architecture

Figure 3 depicts a general idea of the proposed framework. We first model the hourly uncertainty in renewable (wind) generation and the variability of the system loads. Random behavior of predicted load as well as the wind speed are modeled using the probability distribution functions. The proposed approach employs a robust probabilistic technique, the Point Estimation Method (PEM), to incorporate the uncertainties into the DC and AC optimal power flow (OPF) formulations. The probabilistic DCOPF-based switching optimization framework is developed to find the day-ahead optimal solutions of network topology and generation dispatch for economic savings. As the topology control optimization based on DCOPF does not take into account the reactive power and voltage constraints, the resulting optimal solutions may or may not be AC feasible. As a result, it is suggested that the AC feasibility be conducted in the next step for each topology control plan obtained earlier through the PEM. If the AC power flow does not converge, different adjustments may be tried (known as *out-of-market corrections*) to aid the convergence with the available reactive sources such as further tuning of shunts, generator voltage set points, transformer tap settings, and so on. If AC feasibility is confirmed with all the adjustments satisfying the generator reactive power constraints or if the optimal topology

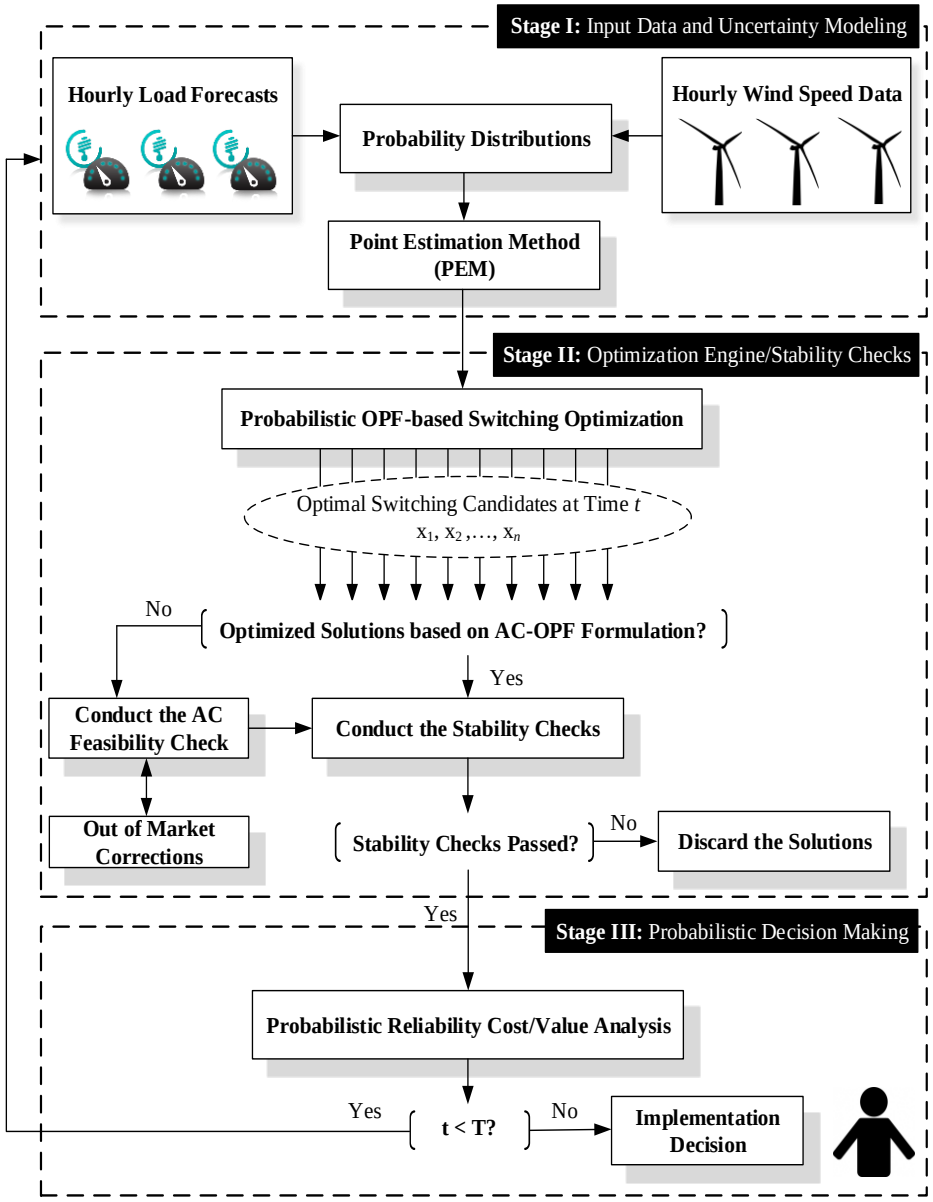

Figure 3. Proposed framework for probabilistic power system topology control: overall architecture [139].

control plans are originally decided using the ACOPF solvers, the system transient stability check is performed using the output of the AC load flow as the initial conditions for the machines. The optimized generation schedules and loading patterns corresponding

to the topology control actions are employed for the system-wide transient stability checks. The switching solutions that cannot pass the AC feasibility and stability checks (even after the out-of-market corrections and with all the reactive power resources at their maximum limits) are considered not viable for implementation and are discarded from the rest of the framework. Those survived sets of AC feasible and stable topology control plans, which may embrace one or several TLS actions, would be entered into the proposed probabilistic decision making module.

Although economically attractive, TLS solutions might have different system-wide impacts as their implementation migrate the system previous topology to new operating states with different levels of risk and reliability performance. The probabilistic reliability cost/value analysis is conducted to evaluate the optimal number of TLS actions per hour for final implementation. The probabilistic decision support tool helps the system operator in deciding whether to adopt (or select among) the economically-attractive TLS plan(s) depending on how the system risk/reliability performance indices are affected in the new network topology.

3.2.2 Renewable Generation and Load Uncertainty Modeling

While different notable approaches are employed in the literature, e.g., time series, artificial neural network, and regression techniques among the others [126]-[130], uncertainties introduced through high penetration of wind generation as well as the variable behavior of loads in the system are characterized here using probability density functions (PDFs) and historical data. In order to account for the chronological

characteristics of the wind velocity and its impact on the output power of wind turbines, wind speed at each hour is statistically modeled via the Weibull probability distribution with the PDF presented in (3.1) [131]. The Weibull distribution is utilized to characterize the wind speed since (1) it is widely proved to provide the best fit to wind speed applications in many countries and (2) its parameters could be easily determined from the observed wind speed summaries [131]-[133].

Employing the curve fitting techniques and maximum likelihood estimations, the PDF parameters are statistically estimated using the historical wind speed data. The output power of the wind generator, which is a function of the wind speed, is probabilistically calculated as formulated in (3.2).

$$f_v(v) = \left(\frac{\psi}{\beta}\right)\left(\frac{v}{\beta}\right)^{\psi-1} e^{-\left(\frac{v}{\beta}\right)^{\psi}} \quad 0 \le v \le \infty \tag{3.1}$$

$$G_W = \begin{cases} 0 & 0 \le v \le v_i, v > v_o \\ \left(K + K' \times v + K'' \times v^2\right) \times P_r & v_i \le v \le v_r \\ P_r & v_r \le v \le v_o \end{cases} \tag{3.2}$$

The other main source of uncertainties in power system operation is the actual load of the system as it fluctuates as a function of time, season, weather condition, electricity price, etc. Similarly, the random variation of loads is statistically modeled via Gaussian distribution with the PDF in (3.3).

$$f_{P_D}(P_D) = \frac{1}{\sqrt{2\pi\sigma_{P_D}^2}} \exp\left[-\frac{\left(P_D - \mu_{P_D}\right)^2}{2\sigma_{P_D}^2}\right] \tag{3.3}$$

3.2.3 Probabilistic Topology Control Optimization

As the deterministic OPF evaluations cannot fully reveal the state of the system, probabilistic analysis is becoming of considerable importance and interest due to the increasing trend of facing many random distortions or uncertainties arisen from measurement errors, forecasting errors, variation of system variables due to adoption of renewable generation resources and load uncertainties. Performing OPF analysis for every possible or probable combination of loads, generation, and network topology is impractical or at least computationally cumbersome. As an analytical tool with tractable computation burden and acceptable level of accuracy, the PEM is suggested to be used for probabilistic formulation of the problem. Using the PEM method for probabilistic OPF analysis, the impact of uncertain input variables and the propagation of such uncertainties over the output parameters would be well captured. The PEM method is selected over the other probabilistic techniques as it is easier to implement and imposes less computational complexities for large-scale scenarios [133]-[138].

Vectors of input and output random variables as well as corresponding nonlinear functions are presented in (3.4)-(3.6), respectively.

$$\mathbf{X} = \left[P_{g,n}^{Wind}, \mathbf{P}_{\mathbf{D_n}} \right] \tag{3.4}$$

$$\mathbf{Y} = h(\mathbf{X}) = h(x_1, x_2) \tag{3.5}$$

$$Y = \left[\eta, \pi, \mathrm{GC}^t \right] \tag{3.6}$$

The probabilistic DCOPF-based optimization for transmission topology control problem is formulated below, where the objective function is introduced in (3.7) subject to system and security constraints in (3.8)-(3.13)* [139].

$$\min \ \overline{\mathrm{GC}^t} = \sum_{\substack{g\in\Omega_G \\ n\in\Omega_B}} c_{g_n} \overline{P_{g_n}^t} \tag{3.7}$$

$$P_{g_n}^{\min} \le \overline{P_{g_n}^t} \le P_{g_n}^{\max} \qquad \forall g \in \Omega_G \tag{3.8}$$

$$P_k^{\min}.\alpha_k \le P_{knm}^t \le P_k^{\max}.\alpha_k \qquad \forall k \in \Omega_L \tag{3.9}$$

$$\sum_{g\in\Omega_G} \overline{P_{g_n}^t} - \sum_{m\in\Omega_B} P_{knm}^t = \sum_{d\in\Omega_D} \overline{P_{d_n}^t} \quad \forall n \in \Omega_B \tag{3.10}$$

$$B_k.(\theta_n - \theta_m) - P_{knm}^t + (1-\alpha_k).\mathrm{M}_k \ge 0 \qquad \forall k \in \Omega_L \tag{3.11}$$

$$B_k.(\theta_n - \theta_m) - P_{knm}^t - (1-\alpha_k).\mathrm{M}_k \le 0 \qquad \forall k \in \Omega_L \tag{3.12}$$

$$\alpha_k \in \{0,1\} \qquad \forall k \in \Omega_L \tag{3.13}$$

The output power of generator *g* at node *n* is limited to its physical capacities in (3.8). Constraint (3.9) limits the power flow across transmission line *k* within the minimum and maximum line capacities. Power balance at each node is enforced by (3.10) and Kirchhoff's laws are incorporated in (3.11) and (3.12). The status of any transmission line *k* of the system is identified via an integer variable in (3.13). Parameter M_k is a user-specified large number greater than or equal to $\left|B_k\left(\theta^{\max} - \theta^{\min}\right)\right|$ which is selected to make the constraints nonbinding and relax those associated with Kirchhoff's laws when a line

* The bar notation over variables show the probabilistic (expected) values.

is removed from service regardless of the difference in the bus angles [68], [69]. Parameter χ introduced in (3.14) limits the number of open transmission lines in the new optimal network reconfiguration.

$$\sum_{k}(1-\alpha_k) \le \chi \; k \in \Omega_L \tag{3.14}$$

The optimization engine is able to provide several sets of optimal solutions for any selection of χ. In doing so, the probabilistic optimization algorithm is first simulated to suggest the best optimal solution for the topology control problem. A Not-To-Switch (NTS) list is designed where the obtained best optimal solution is stored. The optimization engine is simulated again neglecting the solutions previously stored in the NTS box and the process will continue to obtain the second best, third best, etc. optimal switching solution. Such implementation design would not only increase the chance that at least one set of the solutions would survive all the subsequent AC feasibility/stability tests and other operational concerns, but also would provide the operator with more flexibility in final decision making [139].

The two point estimation method (2-PEM) decomposes (3.5) into several sub problems by taking only two deterministic values of each uncertain variable located on the two sides of its mean value. Figure 4 demonstrates a general idea of the 2-PEM application to capture the uncertainties in the probabilistic optimization model. The deterministic topology control optimization (3.7)-(3.13) is then simulated twice for each uncertain variable, one for the value below and the other for the value above the mean,

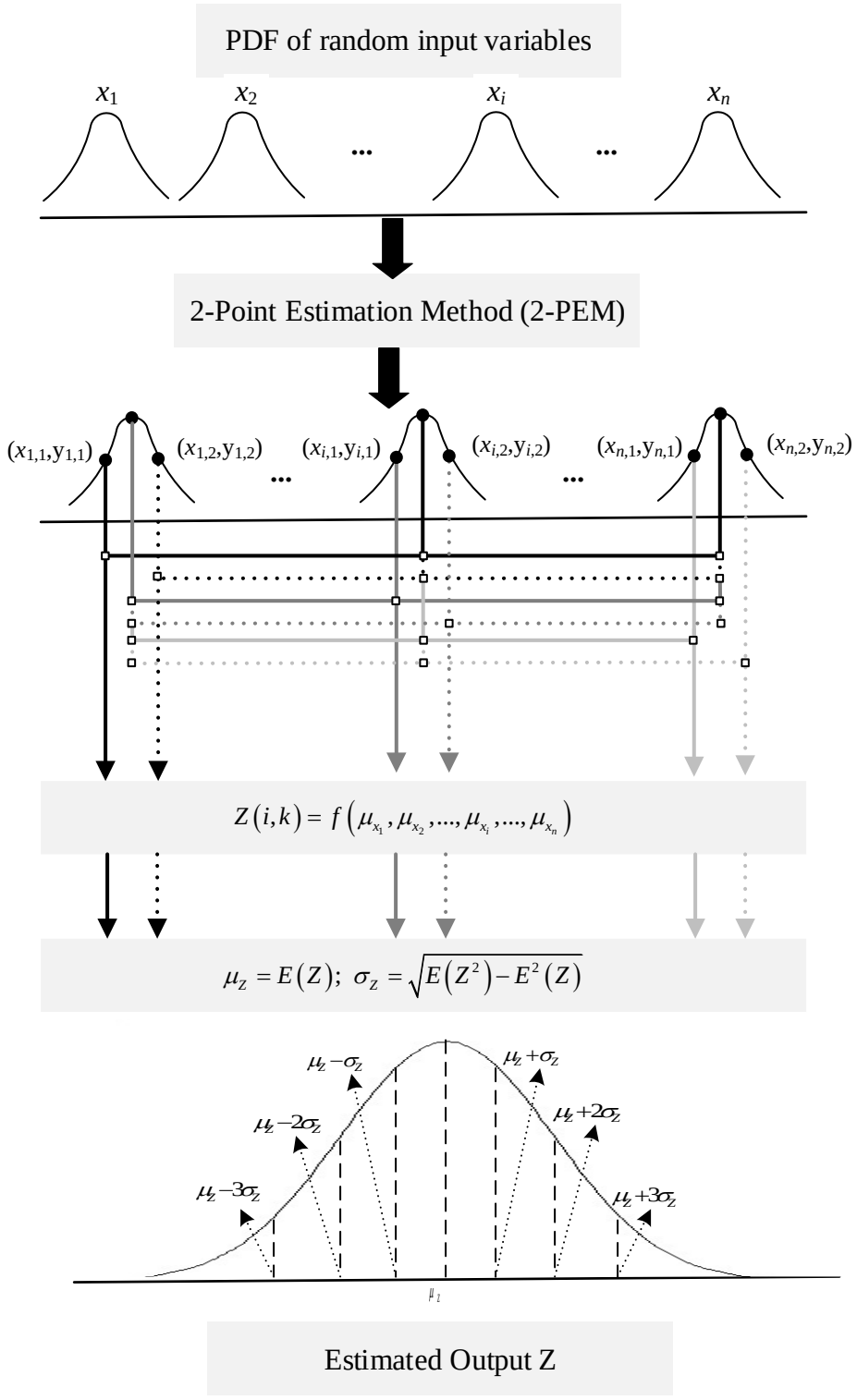

Figure 4. Illustration of the 2-PEM application for capturing the uncertainties.

while keeping the other variables at their mean values. These two pints may or may not be selected symmetrically around the mean of a given variable [138]. As each set of the selected sample points undergoes the optimization problem to obtain the transformed samples, the mean and standard deviation of output variables (e.g., the generation dispatch cost) as well as the status of each line would be calculated at each scenario. The probabilistic optimal topology control formulation would eventually result in the probability distribution function (PDF) of the generation dispatch cost as well as the final status for each transmission line.

Regarding the selection of the final optimal lines to switch, the following procedure is pursued: in each studied scenario, the optimization engine is simulated and the optimal dispatch cost and the optimal switching status of the lines (0 or 1) would be obtained. Having conducted the same process for all the studied probabilistic scenarios (i.e., 2X scenarios for X uncertain factors) for a given generation and load profile at an hour, the final status for each transmission lines would be selected as the "most repeated status" in all the simulated scenarios. For instance, if the status for a given transmission line is 1 in many (more than a threshold) of the studied probabilistic scenarios, the final status of that transmission line would be considered 1.

Note that the transmission line switching embedded in the probabilistic ACOPF formulation can be also approached, if the computational facilities allow, by adding the voltage magnitude and reactive power constraints. Recent advancement in parallel processing and new heuristics to handle such complexities are necessary to make an AC model of the suggested framework work.

3.2.4 The 2-PEM Core Algorithm

The algorithm of the 2-PEM procedure for the above optimization formulation is presented as follows [133], [139]; the requisite variables of the 2-PEM algorithm are initialized in ***Step 1*** using (3.15) and (3.16):

$$E(Y)^{(1)} = 0 \tag{3.15}$$

$$E(Y^2)^{(1)} = 0 \tag{3.16}$$

In ***Step 2***, the locations and probability of concentrations are calculated through (3.17)-(3.20) as follows:

$$\xi_{z,1} = \frac{\lambda_{z,3}}{2} + \sqrt{r + \left(\frac{\lambda_{z,3}}{2}\right)^2} \qquad \forall z \in \Omega_Z \tag{3.17}$$

$$\xi_{z,2} = \frac{\lambda_{z,3}}{2} - \sqrt{r + \left(\frac{\lambda_{z,3}}{2}\right)^2} \qquad \forall z \in \Omega_Z \tag{3.18}$$

$$P_{z,1} = \frac{-\xi_{z,2}}{2r \cdot \sqrt{r + \left(\frac{\lambda_{z,3}}{2}\right)^2}} \qquad \forall z \in \Omega_Z \tag{3.19}$$

$$P_{z,2} = \frac{\xi_{z,1}}{2r \cdot \sqrt{r + \left(\frac{\lambda_{z,3}}{2}\right)^2}} \qquad \forall z \in \Omega_Z \tag{3.20}$$

The two concentrations $x_{z,1}$ and $x_{z,1}$ are determined in ***Step 3*** using the following formulations (3.21) and (3.22):

$$x_{z,1} = \mu_{x,z} + \xi_{z,1} \cdot \sigma_{x,z} \tag{3.21}$$

$$x_{z,2} = \mu_{x,z} + \xi_{z,2} \cdot \sigma_{x,z} \tag{3.22}$$

In ***Step 4***, the deterministic topology control optimization is solved for both concentrations $x_{z,i}$ with respect to vector **X** presented in (3.23).

$$\mathbf{X} = [\mu_{z,1}, \mu_{z,2}, ..., x_{z,i}, ..., \mu_{z,r}] \qquad i = 1,2 \tag{3.23}$$

Equations (3.24) and (3.25) are updated in ***Step 5*** as follows:

$$E(Y)^{(z+1)} \cong E(Y)^{(z)} + \sum_{i=1}^{2} P_{z,i} \cdot h(\mathbf{X}) \tag{3.24}$$

$$E(Y^2)^{(z+1)} \cong E(Y^2)^{(z)} + \sum_{i=1}^{2} P_{z,i} \cdot h^2(\mathbf{X}) \tag{3.25}$$

And eventually in ***Step 6***, the output mean value and the associated standard deviation would be estimated in (3.26) and (3.27), respectively.

$$\mu_Y = E(Y) \tag{3.26}$$

$$\sigma_Y = \sqrt{E(Y^2) - E^2(Y)} \tag{3.27}$$

Detailed background on the mathematical proofs of the 2-PEM technique is provided in Appendix 2.

3.3 Probabilistic Reliability Cost/Value Framework for Optimal Topology Control Decision Making

The output of the above probabilistic topology control optimization engine would be the economically optimal TLS plans that may involve one or several switching actions per hour. Such optimal TLS plans would be different in that: (1) each provides different percentage of economic benefits (denoted as *value*); (2) each would lead to different states with different operational risk and reliability performance (translated as *risk cost*). In order

to identify an efficient selection among the optimal topology control plans, a probabilistic reliability cost/value decision making technique is suggested. This day-ahead support tool would help the operators to (1) decide whether there is any optimal TLS plan at each hour with substantial economic benefits and at the same time high system reliability performance, and (2) if the former condition is confirmed, select the best plan for final implementation among multiple sets of optimal TLS solutions suggested per hour.

The *value* of each topology control plan is considered as the economic benefits realized, compared to the base case condition, via co-optimizing the topology and the generation dispatch. Regarding the *risk cost* associated with each TLS plan, probabilistic analytical state enumeration approach is employed for each optimal TLS solution to assess the reliability of the topologically reconfigured transmission system. Up to the fourth order of contingencies are considered for calculation of reliability indices. The method employs the interrupted load probability for every contingency in each system topology to calculate the expected energy not supplied (EENS) index reflecting the network reliability performance in different scenarios.

Mathematically speaking, the following linear programming optimization problem is run under each contingency scenario. The objective function here is to minimize the system total interrupted load subject to the physical network constrains and security requirements [140].

$$\min_{h\in\Omega_H} \sum_{n\in\Omega_D} \left(\mathrm{IL}^{t}_{n,h,k} = \bar{P}^{t}_{d_n} - \bar{P}^{t,\,\mathrm{supplied}}_{d_n,h} \right) \tag{3.28}$$

$$P^{\min}_{g_n} \le \overline{P^{t}_{g_n}} \le P^{\max}_{g_n} \qquad \forall g \in \Omega_G \tag{3.29}$$

$$\theta_n^{\min} \le \theta_n \le \theta_n^{\max} \qquad \forall n \in \Omega_B \tag{3.30}$$

$$\sum_{g \in \Omega_G} \overline{P_{g_n}^t} - \sum_{m \in \Omega_B} P_{knm}^t = \sum_{d \in \Omega_D} \overline{P_{d_n}^t} - \mathrm{IL}_{n,h,k}^t \quad \forall n \in \Omega_B \tag{3.31}$$

$$P_{knm}^t = 0 \qquad \forall k \in \Omega_{K'} \tag{3.32}$$

$$P_k^{\min} \le P_{knm}^t \le P_k^{\max} \qquad \forall k \notin \Omega_{K'} \tag{3.33}$$

$$0 \le \mathrm{IL}_{n,h,k}^t \le \overline{P}_{d_n}^t \qquad \forall n \in \Omega_B, \forall h \in \Omega_H \tag{3.34}$$

Probabilistically approached, the EENS index of reliability at each bus would be then calculated through (3.35)-(3.37).

$$\overline{\mathrm{EENS}}_{n,k}^t = \sum_{h \in \Omega_H} P_h^t . \tau_h^t . \mathrm{IL}_{n,h,k}^t \qquad \forall n \in \Omega_B \tag{3.35}$$

$$P_h^t = \prod_{x \in \Omega_X} \frac{\Gamma_x}{\left(\gamma_x + \Gamma_x\right)} \times \prod_{y \in \Omega_Y} \frac{\gamma_y}{\left(\gamma_y + \Gamma_y\right)} \tag{3.36}$$

$$\tau_h^t = \left(\sum_{x \in X} \gamma_x + \sum_{y \in Y} \Gamma_y \right)^{-1} \quad \forall h \in \Omega_H \tag{3.37}$$

where, P_h^t is obtained in (3.36) by multiplying the availability of online components and unavailability of the failed ones in a contingency state *h*; and τ_h^t is calculated in (3.37) using the failure rates of online components and repair rates of the failed ones in a given contingency state.

Note that in all the above calculations, the common two-state Markov model for each system component is considered. Taking into account different types of loads and customers at each bus, the system total *risk cost* is assessed in (3.38) for each optimal topology control plan *k* at time *t* based on the corresponding EENS index and the value of

lost load (VOLL) for each type of interrupted demand. The VOLL_n represents the unit interruption costs of different customer sectors served at load point *n* which is directly dependent on the duration of outage and is commonly determined through customer surveys and historical data [141].

$$\overline{\mathrm{RC}}^{t}_{TS,k} = \sum_{n \in \Omega_B} \overline{\mathrm{EENS}}^{t}_{n,k} . \mathrm{VOLL}_n \tag{3.38}$$

In order to determine the final topology control plan with an optimal number of TLS actions involved, the probabilistic cost/value chart is utilized as illustrated in Figure 5. As the number of TLS actions increases, the higher economic benefit is expected. While transmission switching does often degrade the system reliability (and *risk*), there are cases where switching out some transmission lines for economic gains would help improving the system reliability performance. The reason lies in the fact that the suggested framework involves a probabilistic co-optimization of the generation dispatch along with the network topology. Moreover, system reliability may be affected by several other important factors in a given operating state (e.g., available generation capacity, generators' ramping capabilities, etc. in the new topology). Hence, lower/higher reliability performance (i.e., higher/higher *risk*) would be experienced in practice after switching a sequence of transmission lines out.

Figure 5(a) illustrates the case where system reliability degrades (translated to higher *risk cost*) as the number of switching actions increases. As indicated in Figure 5(a), the optimal number of TLS actions is determined when the *risk cost* and economic benefit curves intersect, which assures an efficient compromise between economic gains and

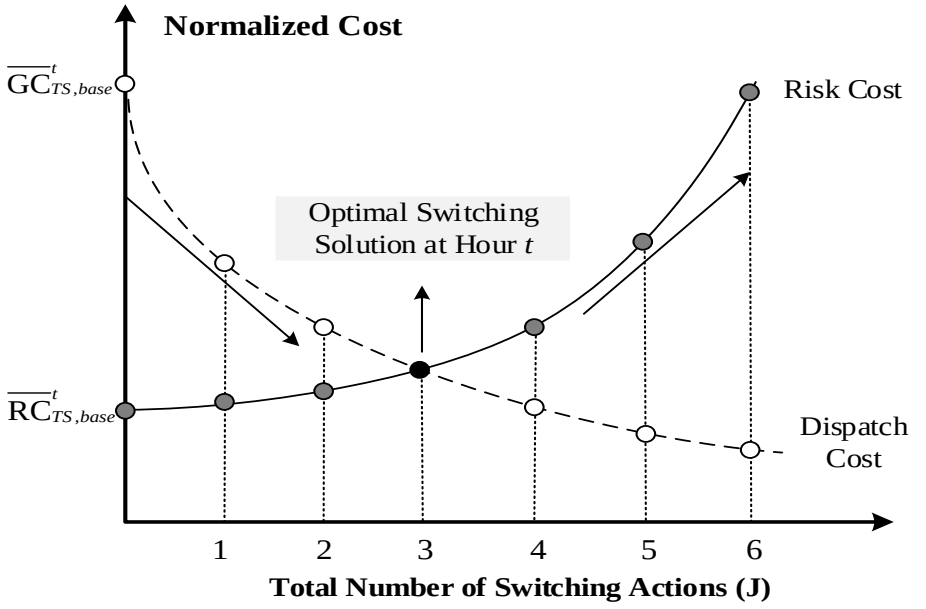

(a)

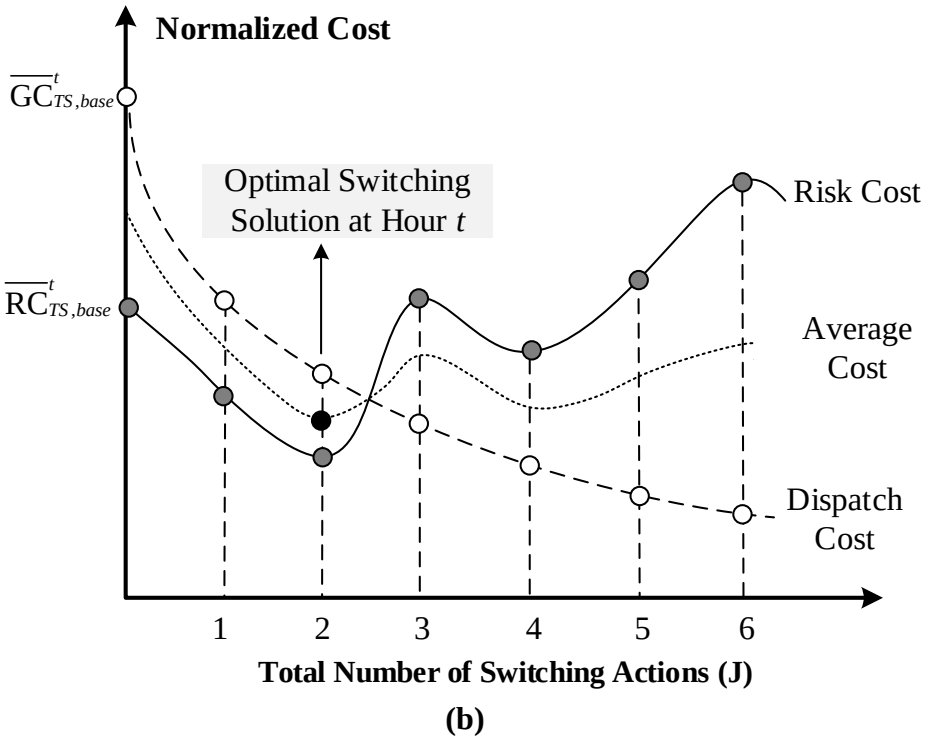

(b)

Figure 5. Probabilistic cost/value framework for optimal topology control decision making at hour *t*: (a) monotonically degrading system reliability with TLS; (b) improved system reliability through TLS.

system reliability and risk performance. Figure 5(b) demonstrates the situation where switching out transmission lines, in some cases, may improve system reliability. In such circumstances, the optimal decision where the average costs are minimized is found.

Note that while the two types of costs (dispatch and risk) may be in different orders of magnitude, such costs are translated into normalized values with regards to the corresponding maximum quantities so that the compromise could be made and a robust optimal number of TLS actions for implementation could be decided.

3.4 Case Study: Modified IEEE 118-Bus Test System

3.4.1 System Descriptions, Data, and Assumptions

The modified IEEE 118-bus test system contains 185 transmission lines and 19 generating units with the installed capacity of 6859.2MW, serving a total demand of 6000 MW at peak load hour [139]. The demands are considered to be of 20% dispatchable load with the interruption cost of 0.2 VOLL and 80% firm load with the interruption cost of 0.8 VOLL. The system one line diagram as well as the required data including hourly generation and load profiles, historical wind data, transmission line parameters, generator variable costs and dynamic settings, and the reliability parameters of the system components and load points is all provided in Appendix 3 [139].

In order to investigate the impacts of different probabilistic scenarios on the performance of the suggested framework, three different numerical studies are conducted. Case 1 is the base case condition with no wind penetration where the conventional generating units are utilized. The modified IEEE 118-bus test system in presence of large-

scale wind farms is studied in Case 2 and Case 3. In Case 2, a large-scale wind farm, comprised of 100 wind turbines with the overall capacity of 300MW, is directly added to bus 90 where the wind energy penetration is expected to be 5% of overall system generation capacities. Similarly in Case 3, two wind farms each of which carrying a capacity of 300MW are directly connected to buses 90 and 91 where the wind penetration is supposed to be 10% of the system entire generation capacities.

3.4.2 Wind Speed Modelling

The random Monte Carlo simulation is hourly implemented to probabilistically simulate the variations of the wind speed. The real hourly wind speed data of two wind farms located in North of Iran (Manjil and Binaloud) in a five-year period of January 1, 2005 to December 31, 2009 are employed as the historical data [139]. The simulation engine is able to accurately capture the chronological and intermittent characteristics of the wind speed over time.

Figure 6 demonstrates the real wind speed data during a day at Manjil wind farm and Figure 7 illustrates how the developed framework can trace the real wind speed diurnal distribution. The wind power generated at time *t* corresponding to a given hourly wind speed distribution is then evaluated using (3.2). The wind farm total generation is the sum of all generations from all the online turbines in the farm. The hourly wind farm generation is fed into the probabilistic topology control optimization as an input random variable.

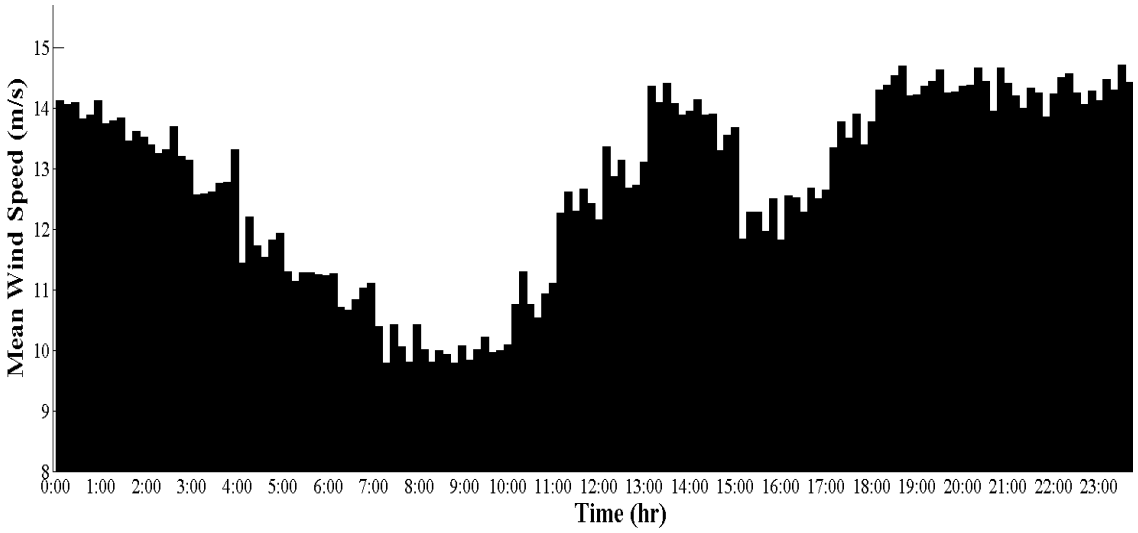

Figure 6. Real diurnal wind speed at Manjil wind farm: October 10, 2008.

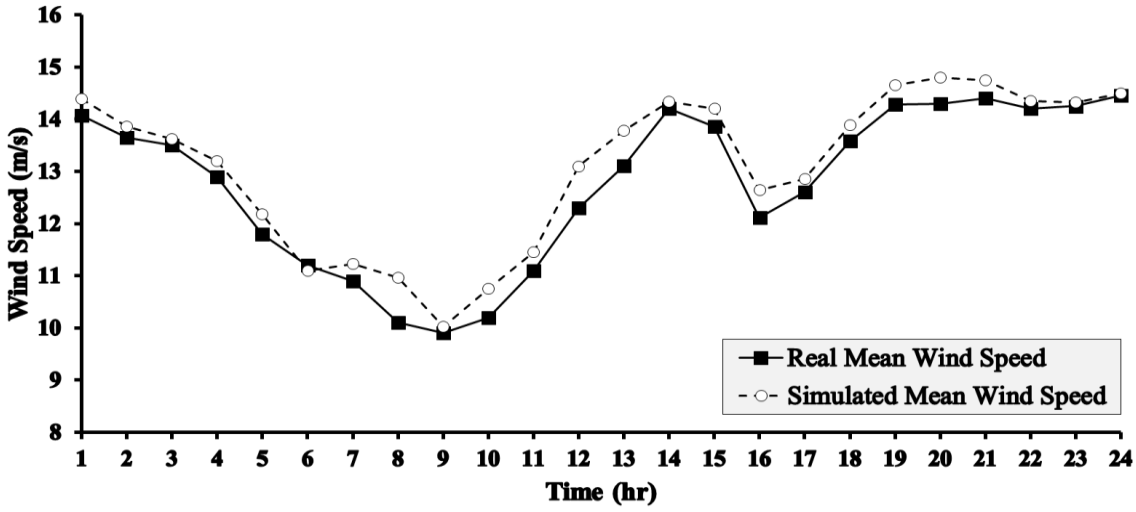

Figure 7. Simulated mean values for the wind speed diurnal distribution at Manjil wind farm: October 10, 2008.

3.4.3 Results and General Discussions: 24-Hour Period (October 10, 2008)

The probabilistic mixed integer linear programing (MILP) optimization formulations in (3.4)-(3.13) are employed in the MATLAB environment applying the MATPOWER operating functions [142] and using the system hourly generation and load

profiles as in [139] (see Appendix 3 for more details). The optimization problem is run on a Dell PowerEdge R815 PC with 4 AMD Opteron 6174 Processors (48 2.2 GHz cores) and 256 GB of Memory running CentOS 5.7.

First, we demonstrate the necessity of employing a probabilistic framework vs. the conventional deterministic formulations for optimal topology control problem. The test results for having just one switching possibility at each hour (on October 10, 2008) are demonstrated in Figure 8 to Figure 10 corresponding to Cases 1-3, respectively. In each case, three scenarios (S) have been studied at each hour: (S1) the system is operated with no topology control program; (S2) the system generation is deterministically dispatched enforced by the topology control; (S3) the suggested probabilistic topology control formulation is applied.

As can be seen in the results of Figure 8 to Figure 10, in all the studied cases and scenarios, the optimal one-line-switch topology control solutions in both deterministic and probabilistic formulations have resulted in considerable economic benefits (lower generation dispatch costs) in almost 91% of the entire 24-hour period compared to the base case condition (where there is no switching actions adopted). However, a main observation is that contrary to the deterministic approach, the probabilistic topology control framework does not always propagate into optimal switching solutions at each hour (day-ahead comparisons). For instance, one can take hour 11 in Case 2 as an example, where the deterministic optimal solution would be switching out line 151 (S2) while in

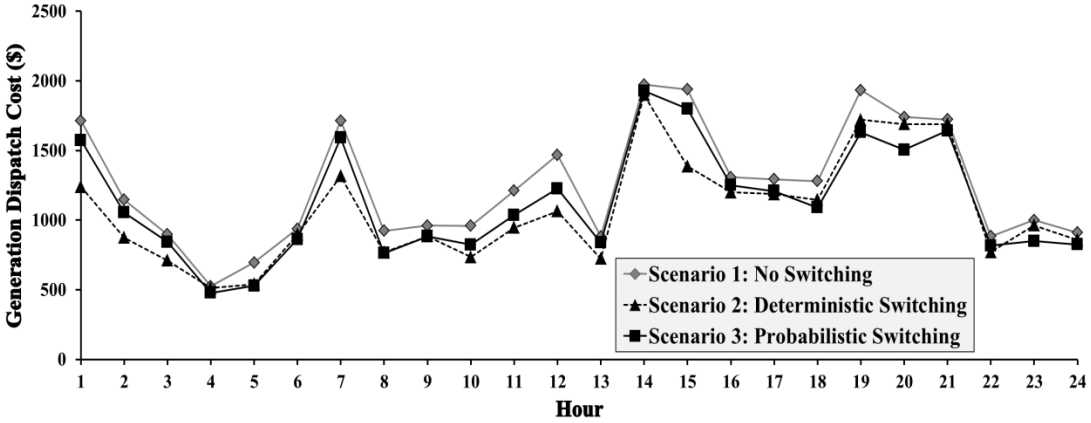

Figure 8. Hourly dispatch costs in the studied scenarios on Oct. 10, 2008: Case 1.

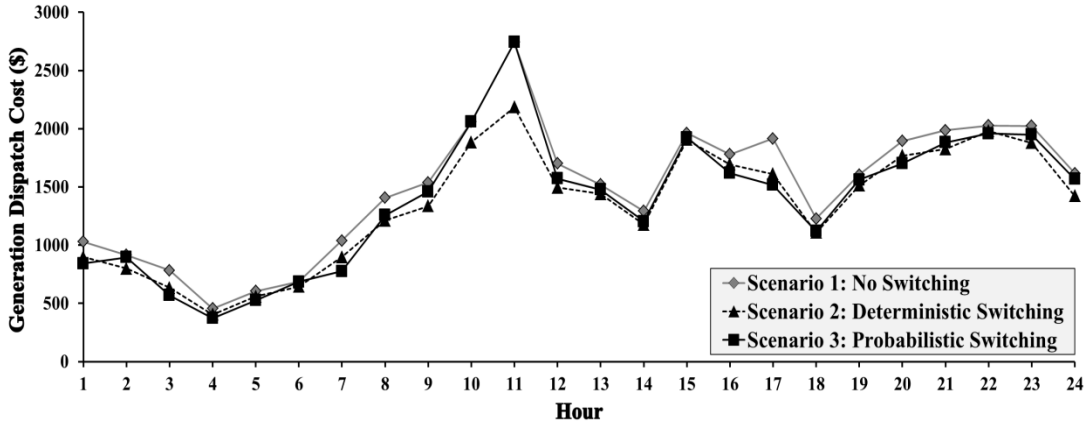

Figure 9. Hourly dispatch costs in the studied scenarios on Oct. 10, 2008: Case 2.

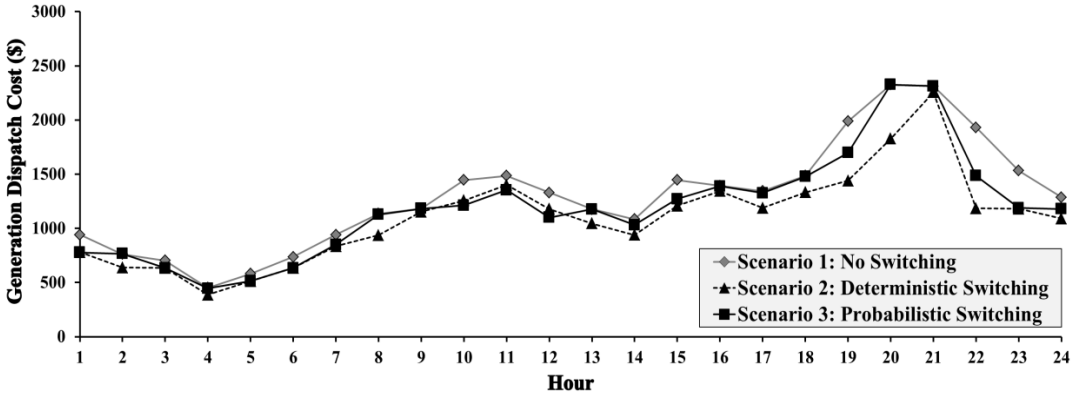

Figure 10. Hourly dispatch costs in the studied scenarios on Oct. 10, 2008: Case 3.

S3, there is no optimal solution found at this hour considering the variable response of load and generation (i.e., the generation dispatch cost is the same as that in S1). The same observation is repeated at hours 6 and 10, too.

The other main observation is that, at most hours (but not all), the optimal hourly topology control plans are different when employing the probabilistic formulation compared to those deterministically found. As a result, the economic benefits through optimal TLS actions obtained using the suggested probabilistic framework for topology control (S3) vary at each hour (either less, equal, or higher) compared to the results from the conventional deterministic methods (S2).

To put a figure on this, take Case 1 as an example. The minimum generation dispatch cost in S2 is $512.74 at hour 4 (corresponding to switching line 85) while in S3, it is $477.5 at hour 4 (corresponding to switching line 155). Table 1 provides further details on the numerical results in various studied cases and scenarios. In Case 1, the total daily generation dispatch cost on Oct. 10, 2008 is $27,052.12 in S3 (+9.91% saving compared to S1) which is 4.89% more than $25,728.91 in S2. Similar observations are valid from the results in Cases 2 and 3. It can be concluded from such day-ahead comparisons that the daily economic savings obtained through application of the probabilistic topology control framework, at least on the studied test system, is generally less than those through conventional deterministic approaches.

Let us now compare the day-ahead probabilistic results (S3) in Case 2 and Case 3 where there is large-scale wind generation included vs. the results in Case 1. The probabilistic topology control approach has resulted in higher economic saving at some

Table 1. Numerical Results on Day-Ahead Topology Control

Cases	Case 1			Case 2			Case 3		
Scenarios	**S1**	**S2**	**S3**	**S1**	**S2**	**S3**	**S1**	**S2**	**S3**
$\min GC^t$ ($)	524.8	512.7	477.5	456.2	403.9	373.2	452.1	386.4	446.2
$\max GC^t$ ($)	1973.4	1900	1927.7	2743.6	2186.3	2743.6	2326.2	2255.2	2326.2
Daily GC ($)	30028	25728.9	27052	35820	32279	33254	31012	26387	28469
Savings* (%)	0	14.32	9.91	0	9.88	7.16	0	14.91	8.20

* Daily Saving

specific hours (e.g., 1, 10, and 11). However, the total daily generation dispatch cost enforced with optimal TLS actions has been increased ($33,254.06 in Case 2 and $28,469.21 in Case 3) compared to Case 1 ($27,052.12), resulting in relatively lower daily economic savings expected from the topology control optimization (9.91%, 7.16%, and 8.20% corresponding to Case 1, Case 2, and Case 3, respectively) compared to the no-switching scenarios. It can be seen that as the stochastic wind generation is increased, the possibility of finding optimal topology control solutions has been decreased in some hours. Taking Case 3 with large scale wind integration into account, the optimization engine could not find any optimal TLS solution at hours 9, 13, 20, and 21 when performing the probabilistic analysis while the optimal topology control plans were found at every hour if deterministically approached.

3.4.4 Topology Control Decision Making: Hour 24 (October 10, 2008)

This Section elaborates on the application of the suggested probabilistic decision making support tool which can identify multiple TLS solutions at each hour that if implemented in a sequence, would offer higher economic gains. Take hour 24 time-frame as an example. Given the probabilistically modeled generation and load profile at this hour, the possibility of at most 5 TLS actions is enforced in the optimization engine. The question would be which optimal plan with how many switching actions involved needs to be selected at this hour for final implementation.

The numerical results for the obtained solutions in Case 1, Case 2, and Case 3 can be found in Table 2 (J is the total number of TLS actions). The solutions obtained using the probabilistic models in S3 are also compared with those of the conventional deterministic approaches (S2). It can be seen that as the number of TLS actions increases at this hour, the higher economic gains are generally obtained in all the studied cases. In order to identify the optimal topology control plan at this hour, the AC feasibility and stability checks are conducted on each solution. The aforementioned checks were successful in all the conducted tests in Case 1 and 77.5% of the tests in Case 2 and Case 3. So, it can be seen that as the probabilistic nature of load and generation is characterized, the possibility of facing unstable TLS solutions would increase. As the optimization engine is able to suggest several sets of optimal TLS plans, the second best optimal sequence of TLS actions at this hour, which is both AC feasible and stable, was replaced (not shown in Table 2). However, the operator might choose to exclude such infeasible solutions from the list and go on with the decision making steps using other available

options. For final decision making, the financial benefits and probabilistic risk costs are calculated for each optimal plan. The probabilistic results for decision making at hour 24

Table 2. Comparison of Multiple Topology Control Solutions at Hour 24

	J	$\overline{GC}_k^{24}$ ($)		Savings (%)		AC Feasibility Check		Stability Check		$\overline{EENS}_{TS,k}^{24}$ (MWh./yr.)		$\overline{RC}_{TS,k}^{24}$ (k$/yr.)	
		S2	S3	S2	S3	S2	S3	S2	S3	S2	S3	S2	S3
Case 1	1	858.39	839.60	5.67	7.72	✓	✓	✓	✓	46.754	48.135	153.34	157.88
	2	803.23	800.09	11.72	12.06	✓	✓	✓	✓	47.856	49.185	160.96	165.42
	3	760.65	741.89	16.39	15.16	✓	✓	✓	✓	49.353	53.923	165.89	250.14
	4	749.99	766.80	17.46	15.72	✓	✓	✓	✓	50.756	55.156	193.43	300.46
	5	730.36	760.99	19.73	16.36	✓	✓	✓	✓	51.755	53.908	345.83	410.23
Case 2	1	1422.63	1769.09	12.06	3.67	✓	✓	✓	✓	46.826	50.965	153.58	167.16
	2	1365.57	1680.53	15.58	8.49	✓	✓	✓	✓	48.112	52.365	161.82	176.12
	3	1356.33	1638.43	16.16	10.79	✓	×	✓	×	50.531	N/A	169.85	N/A
	4	1340.46	1616.25	17.14	11.96	✓	✓	✓	✓	53.546	58.235	204.07	221.94
	5	1330.90	1590.23	17.73	13.41	✓	×	✓	×	59.245	N/A	395.88	N/A
Case 3	1	1129.77	1278.32	12.19	10.00	✓	✓	✓	✓	51.001	56.523	167.27	185.38
	2	1070.93	1242.21	16.76	12.55	✓	✓	✓	✓	54.963	60.489	184.86	203.44
	3	945.63	1221.37	26.49	14.02	✓	×	✓	×	58.147	N/A	195.45	N/A
	4	897.96	1211.79	30.20	14.69	✓	✓	✓	×	60.248	62.859	229.61	N/A
	5	852.63	1192.37	33.73	16.06	✓	✓	×	×	63.453	63.789	N/A	N/A

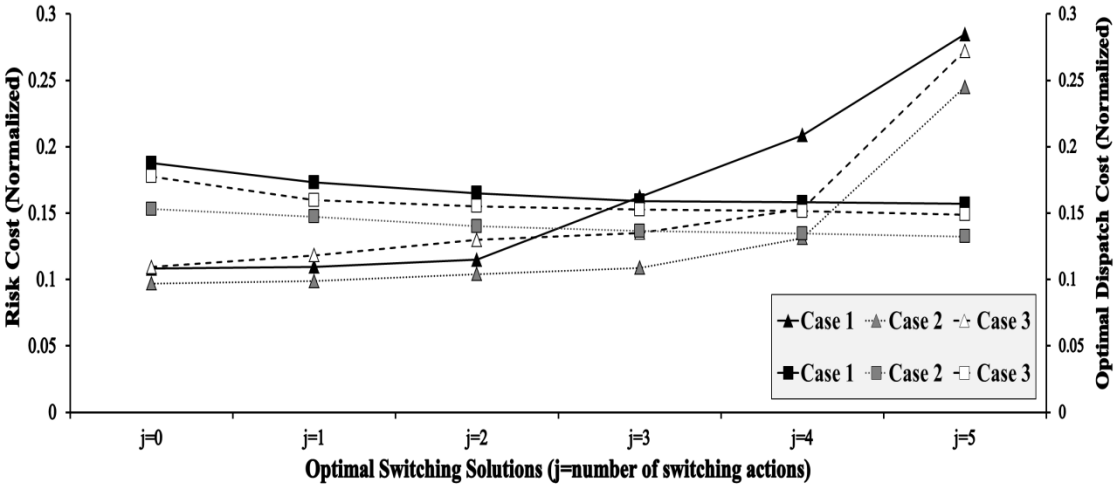

Figure 11. Probabilistic decision making on the optimal number of TLS actions for final implementation.

are illustrated in Figure 11 in all the studied cases in S3. As can be seen in this figure, the optimal dispatch cost and the risk cost curves intersect at different optimal points in different studied cases. In Case 1, it is shown that the optimal number of low-risk switching actions at this hour, which is not only economically attractive but also does not jeopardize the system reliability, is 3 while it is found to be 4 in Case 2 and Case 3. Similar process should be conducted at each hour to decide on the optimal topology control plan for final implementation.

3.5 Discussions

Regarding the computational complexity of the proposed probabilistic framework for topology control, Figure 12 summarizes the computational requirements of implementing various segments of the proposed DCOPF-based probabilistic topology control

optimization on the IEEE 118-bus test system at hour 24. Table 3 also presents a summary of the simulation run time for a complete implementation of the deterministic and the proposed probabilistic topology control decision making on the studied system using the hourly information on October 10, 2008. Note that contrary to Figure 12, the computational results presented in Table 3 include simulation of all modules within the proposed framework for up to 5 TLS actions per hour over the studied 24-hour time frame on October 10, 2008. Rapid advances in both computing hardware and computational performance of modern optimization solvers together with more efficient parallel computation techniques can further expedite the implementation of the proposed framework in large-scale real-world power systems.

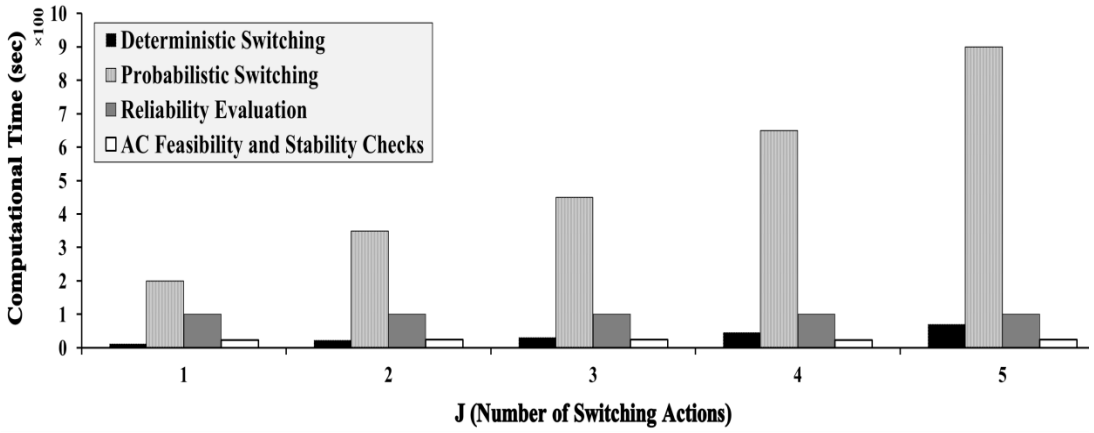

Figure 12. Simulation run time for various modules of the suggested probabilistic decision making framework.

Table 3. Computational Time for Implementation of the Proposed Decision Making Framework: Deterministic vs. Probabilistic Formulations

October 10, 2008	Computational Time (min.)		
	Min	**Max**	**Average**
Deterministic	11.96	13.08	12.33
Probabilistic	42.47	45.39	44.35

3.6 Conclusions

A probabilistic framework for recognizing the day-ahead optimal topology control plans that improve the system economic efficiency was presented in this Section. The existing uncertainties of wind generation and load were statistically modeled, formulated, and incorporated in the probabilistic DCOPF-based topology control optimizations using the PEM technique. Hourly and daily economic analysis performed through various probabilistic cases and scenarios demonstrated the necessity of modeling and incorporating such uncertainties into the conventional transmission switching formulations. Results on the modified IEEE 118-bus test system indicated that contrary to the deterministic approaches, the probabilistic topology control framework does not always propagate into optimal TLS solutions at each hour and the anticipated economic saving may not be as promising as for deterministic solutions.

This Section also addressed the main question: if several topology control actions per hour bring about considerable economic savings, which optimal plan for switching actions should be selected for final implementation. A probabilistic decision making framework to define the optimal number of TLS actions per hour taking into account both

economic gains and risk costs associated with the new system states after the topology change was formulated. Employing the suggested probabilistic framework, the operator will be offered the flexibility in making decisions as he/she is presented with the explicit expected benefits and risks associated with each optimal option.

4 POWER SYSTEM TOPOLOGY CONTROL FOR GRID ECONOMIC EFFICIENCY: A MULTI-OBJECTIVE DECISION MAKING PARADIGM

4.1 Introduction

The network topology control through transmission line switching (TLS) actions is also recognized as an effective approach for improving the grid economic efficiency and realizing higher financial gains [1]. Such practices are currently not frequently adopted due to lack of effective decision support tools and market rules, but are decided in an ad-hoc manner for special planned scenarios. For this technology to be frequently realized in practice, robust operator decision making support tools with special attention to various contradictory/competing performance indicators of the system following the topology change need to be developed and verified.

It has been demonstrated in previous literature that transmission grid topology change, in some cases, may bring about potentials for improving the efficiency of operation by allowing re-dispatch of the cheaper generating units. While economically attractive, the TLS solutions might migrate the current system's operating state to new states with different levels of performance efficiency. Hence, particular attention must be granted to the impact of TLS implementation on power system operating states to ensure that the system reliability and stability in the new migrated operating state is not jeopardized. The necessity of such considerations is further emphasized due to various uncertainties coming from intermittent renewable resources and demand variability.

By bridging the gap between TLS theoretical background and practical requirements, this Section aims at introducing a probabilistic multi-objective optimization framework for TLS accommodation in non-emergency economic scenarios considering several requisite objectives. Various critical and sometimes contradictory/competing objectives including economic benefits, power system reliability performance, network losses, AC feasibility concerns and instability risks are all taken into account through the proposed formulations. The probabilistic nature of the involved uncertainties is systematically handled via Monte Carlo Simulations (MCS) in combination with the 2-Point Estimation Method (2-PEM). The proposed multi-objective optimization problem is tackled through a robust technique, the Non-Dominated Sorting Genetic Algorithm II (NSGA-II), followed by a fuzzy decision making approach to account for the operator/decision maker practical preference in selecting the final topology control solution for implementation.

The presented framework would help the TSOs to more systematically approach a reliable TLS implementation in practice. This Section extensively demonstrates the numerical analysis on the modified IEEE 118-bus test system as well as a real electric network, Iran 400kV Transmission Grid. It presents the effectiveness of the proposed framework for topology control decision making in real world scenarios.

4.2 Problem Statement

In this Section, we suggest several critical and even contradictory/competing objectives to be co-optimized in the proposed multi-objective optimization framework for

TLS implementation decisions in practice. The following four objective functions are suggested to be co-optimized for TLS decision making in economic scenarios.

4.2.1 Economic Efficiency

The probabilistic optimization formulation for non-emergency topology control in DC setting is a mixed integer linear programming (MILP) problem. This optimization seeks to optimize the system generation dispatch costs by enabling the dispatch of lower-cost generators along with harnessing the flexibility of transmission lines. This optimization problem formulation, in which renewable generation resources and uncertain demands are probabilistically incorporated[*], is presented below, with the objective function in (4.1) subject to several system operational constraints in (4.2)-(4.7).

$$\min \ \overline{\mathrm{GC}_{TS}^{t}} = \sum_{\substack{g\in\Omega_G \\ n\in\Omega_B}} c_{g_n} \overline{P_{g_n}^{t}} \tag{4.1}$$

$$P_{g_n}^{\min} \le \overline{P_{g_n}^{t}} \le P_{g_n}^{\max} \qquad \forall g \in \Omega_G \tag{4.2}$$

$$P_{k}^{\min}.\partial_k \le P_{knm}^{t} \le P_{k}^{\max}.\partial_k \qquad \forall k \in \Omega_L \tag{4.3}$$

$$-\sum_{m\in\Omega_B} P_{knm}^{t} + \sum_{g\in\Omega_G} \overline{P_{g_n}^{t}} = \sum_{d\in\Omega_D} \overline{P_{d_n}^{t}} \quad \forall n \in \Omega_B \tag{4.4}$$

$$-P_{knm}^{t} + \left(1-\partial_k\right)\times M_k + B_k.\left(\theta_n - \theta_m\right) \ge 0 \qquad \forall k \in \Omega_L \tag{4.5}$$

[*] The bar notation over variables denotes the probabilistic (expected) values.

$$-P_{knm}^{t}-\left(1-\partial_k\right)\times M_k+B_k.\left(\theta_n-\theta_m\right)\le 0 \qquad \forall k\in\Omega_L \tag{4.6}$$

$$\partial_k\in\{0,1\} \qquad \forall k\in\Omega_L \tag{4.7}$$

The output power of generating units is restricted to their physical capacities in (4.2). The electricity flow of the transmission lines is bounded in (4.3). Constraint (4.4) ensures the power balance at each bus-bar; Kirchhoff's laws are respected in (4.5) and (4.6). An integer variable is introduced in (4.7) identifying the on/off status of any transmission line *k* in the system. Parameter M_k is a large number which is greater than or equal to mod of the line maximum flow. M_k is selected to relax the constraints related to the Kirchhoff's laws when a transmission line is switched out of service. If desired, the restriction on the total number of transmission lines to open can also be enforced in (4.8).

$$\sum_k\left(1-\partial_k\right)\le\chi \qquad \forall k\in\Omega_L \tag{4.8}$$

As can be realized, the probabilistic Direct Current Optimal Power Flow (DCOPF) formulation integrated with TLS is presented here as the main optimization function. The problem can be also formulated based on the ACOPF optimization by including the reactive power constraints and voltage requirements, if the computational burdens are manageable.

4.2.2 System-Wide Reliability Performance

Reliability criterion has been traditionally regarded in power system analysis as a constraint either in deterministic or probabilistic form. Deterministic N-1 criterion is

commonly employed, due to lower computational complexity and easier assessment, mandating the electricity grid to withstand every single component outage. The N-1 standard, however, neglects the possibility of multiple contingencies, which may lead to a cascade and possibly catastrophic blackout. Moreover, such deterministic standards would not be able to capture the probabilistic nature of the component outages in power system where some outages might happen with higher probability and consequences while some others may not. Such strict considerations may lead to inaccurate or conservative operational decisions. On the other hand, new sources of uncertainties are increasingly imposed due to the renewables, demand variability, and sophisticated market implications. Hence, TLS decisions under such probabilistic considerations need to be well thought as its adoption in non-emergency scenarios for economic gains might jeopardize the system reliability performance in the new migrated operating state following its implementation.

Probabilistically approached, the expected demand not supplied (EDNS) index is suggested as an objective for the TLS decision making by the TSOs, reflecting the system reliability performance requirement in the topologically reconfigured state of the system. The objective function to be minimized is formulated in (4.9)-(4.11) [140].

$$\min_{\forall k \in K} \ \overline{\mathrm{EDNS}}^{t}_{TS,k} \tag{4.9}$$

$$\overline{\mathrm{EDNS}}^{t}_{TS,k} = \sum_{n \in \Omega_B} \sum_{v \in \Omega_\Theta} P^{t}_{v} . \overline{\mathrm{IL}}^{t}_{n,v,k} \qquad \forall k \in \Omega_K \tag{4.10}$$

$$P^{t}_{v} = \prod_{m \in \Omega_M} \frac{\varphi_m}{\left(\sigma_m + \varphi_m\right)} \times \prod_{n \in \Omega_N} \frac{\sigma_n}{\left(\sigma_n + \varphi_n\right)} \tag{4.11}$$

The EDNS index of the transmission system following any TLS plan accommodation at time *t* can be calculated through the probabilistic analytical state enumeration method [141]-[144]. The state probabilities of the re-configured system are calculated in (4.11) where the occurrence probability of each system contingency *v* is obtained by multiplying the probability of the failed component by those of the available (i.e., online) ones. The curtailed load at each contingency state *v* at time *t* is calculated by solving the following DC linear programming sub-problem which minimizes the total load outages per contingency.

$$\min_{\forall v \in \Omega_\Theta} \sum_{n \in \Omega_D} \left(\overline{\mathrm{IL}}_{n,v,k}^{t} = \overline{P}_{d_n}^{t} - \overline{P}_{d_n,v}^{t,\,\mathrm{supplied}} \right) \tag{4.12}$$

This objective function is subject to the following constraints:

$$P_{g_n}^{\min} \le \overline{P_{g_n}^{t}} \le P_{g_n}^{\max} \qquad \forall g \in \Omega_G \tag{4.13}$$

$$\theta_n^{\min} \le \theta_n \le \theta_n^{\max} \qquad \forall n \in \Omega_B \tag{4.14}$$

$$-\sum_{m \in \Omega_B} P_{knm}^{t} + \sum_{g \in \Omega_G} \overline{P_{g_n}^{t}} = \sum_{d \in \Omega_D} \overline{P_{d_n}^{t}} - \overline{\mathrm{IL}}_{n,v,k}^{t} \quad \forall n \in \Omega_B \tag{4.15}$$

$$P_k^{\min} \le P_{knm}^{t} \le P_k^{\max} \qquad \forall k \notin \Omega_K \tag{4.16}$$

$$0 \le \overline{\mathrm{IL}}_{n,v,k}^{t} \le \overline{P}_{d_n}^{t} \qquad \forall n \in \Omega_B, \forall v \in \Omega_\Theta \tag{4.17}$$

As it can be seen in (4.12), the load outage at each load point is calculated by taking the difference of the actual demand and the supplied load following the contingency event. In order to reduce the simulation runtime, a risk-based contingency screening strategy is employed that first prioritizes the contingencies based on the product of their occurrence

probability and consequence (i.e., the interrupted load) and then neglects the low-risk contingencies. The 2-PEM method is deployed to account for the uncertainties involved in forecasts of renewable generation and variable loads at different bus-bars of the system, for which the algorithm details were provided before in previous Section and also in Appendix 2.

Constraint (4.18) is eventually enforced to ensure that at least the minimum reliability level of the network for all TLS plans is preserved.

$$\overline{\mathrm{EDNS}}_{TS}^{t} \leq \mathrm{EDNS}_{TS}^{L} \tag{4.18}$$

The presented model is generic enough to be accommodated with any other desired reliability measures, e.g., loss of load probability (LOLP), Loss of Energy Expectation (LOEE), Expected Energy Not Supplied (EENS), etc. [140]-[145].

4.2.3 System Instability Risks

A combination of probabilistic voltage and transient stability criteria is employed in this Section to evaluate the system-wide stability performance of the network accommodated with any TLS plan. Following a change in the system topology, voltage stability analysis for considerable number of system contingency states in the new topology is conducted. The contingency states are randomly selected using the Monte Carlo Simulations (MCS). The optimization formulation and the procedure for calculating the average risk of system voltage instability is described in the following [140]:

1) For any considered contingency, solve the following optimization model in

(4.19) constrained by (4.20)-(4.28).

$$\min_{\forall v \in \Omega_\Theta} \sum_{n \in \Omega_B} \left(\nabla_n \times \overline{\mathrm{IL}}^t_{n,v,k} \right) \tag{4.19}$$

$$\sum_{g \in \Omega_G} \overline{P^t_{g_n}} - \left(\sum_{\substack{m \in \Omega_B \\ k \in \Omega_Q}} P^t_{knm} + \sum_{\substack{m \in \Omega_B \\ k \in \Omega_T}} P^t_{knm} \right) = \sum_{d \in \Omega_D} \overline{P^t_{d_n}} - \overline{\mathrm{IL}}^t_{n,v,k} \qquad \forall n \in \Omega_B \tag{4.20}$$

$$\begin{aligned} &\sum_{g \in \Omega_G} \overline{Q^t_{g_n}} + \sum_{g \in \Omega_G} Q^t_{C_n} - \left(\sum_{\substack{m \in \Omega_B \\ k \in \Omega_Q}} Q^t_{knm} + \sum_{\substack{m \in \Omega_B \\ k \in \Omega_T}} Q^t_{knm} \right) = \\ &\qquad \sum_{d \in \Omega_D} \overline{Q^t_{d_n}} - \overline{\mathrm{IL}}^t_{n,v,k} . \frac{\sum_{g \in \Omega_G} \overline{Q^t_{d_n}}}{\sum_{d \in \Omega_D} \overline{P^t_{d_n}}} \qquad \forall n \in \Omega_B \end{aligned} \tag{4.21}$$

$$e_n = K_\varpi . e_\varpi \qquad \forall n \in \Omega_B, \forall \varpi \in \Omega_P \tag{4.22}$$

$$f_n = K_\varpi . f_\varpi \qquad \forall n \in \Omega_B, \forall \varpi \in \Omega_P \tag{4.23}$$

$$P^{\min}_{g_n} \le \overline{P^t_{g_n}} \le P^{\max}_{g_n} \qquad \forall g \in \Omega_G \tag{4.24}$$

$$Q^{\min}_{g_n} \le \overline{Q^t_{g_n}} \le Q^{\max}_{g_n} \qquad \forall g \in \Omega_G \tag{4.25}$$

$$Q^{\min}_{C_n} \le Q^t_{C_n} \le Q^{\max}_{C_n} \qquad \forall n \in \Omega_B \tag{4.26}$$

$$K^{\min}_\varpi \le K_\varpi \le K^{\max}_\varpi \qquad \forall \varpi \in \Omega_O \tag{4.27}$$

$$0 \le \overline{\mathrm{IL}}^t_{n,v,k} \le \overline{P}^t_{d_n} \qquad \forall n \in \Omega_B \tag{4.28}$$

2) The network is deemed to reach the voltage collapse point if the problem solution mandates any load shedding.

3) If the problem solution does not mandate any load shedding, all bus-bar voltages would be investigated. The system voltage stability at the solution point is confirmed if they are all within the desirable limits. If there is at least one bus-bar with the post-contingency voltage level lower than the desirable limit, eigenvalues of the reduced Jacobean matrix, $\mathbf{J_R}$, at the solution point are evaluated and the system voltage stability condition is decided: system voltage stability is confirmed if the minimum eigenvalue is greater than a certain positive threshold (i.e.,~0). Otherwise, the system voltage is concluded unstable if at least one eigenvalue is smaller than the threshold.

The MCS technique is utilized again to evaluate the voltage instability risk index as introduced in (4.29). The calculated risk index in (4.29) represents the average possibility of voltage instability considering various contingencies in any new topology of the system following a TLS implementation.

$$\overline{\mathrm{VIP}}^{t}_{TS,k} = \frac{\mathrm{TNVIS}^{t}_{k}}{\delta} \qquad \forall k \in \Omega_K \tag{4.29}$$

Similarly, in order to evaluate the system transient instability risk when system topology changes, MCS is utilized to identify the numerous random fault events and time-domain transient stability simulations are performed at each random outage scenario. The transient stability risk index is defined in (4.30) as the probability of transient instability occurrence.

$$\overline{\mathrm{TIP}}^{t}_{TS,k} = \frac{\mathrm{TNTIS}^{t}_{k}}{\delta} \qquad \forall k \in \Omega_K \tag{4.30}$$

The suggested index in (4.30) actually demonstrates the average possibility of the topologically-reconfigured system losing transient stability which is indicative of system dynamic performance following to TLS implementation. An integrative probability of system instability risk is eventually proposed in (4.31), (4.32) by the union of the voltage and transient instability risks [see (4.29)-(4.30)] as the objective function to be minimized for the economic TLS decision making. Any other system stability performance measure can also be used instead.

$$\min_{\forall k \in K} \ \overline{\mathrm{IR}}^{t}_{TS,k} \tag{4.31}$$

$$\begin{aligned} \overline{\mathrm{IR}}^{t}_{TS,k} = \lambda_1 \overline{\mathrm{VIP}}^{t}_{TS,k} + \lambda_2 \overline{\mathrm{TIP}}^{t}_{TS,k} \\ - \lambda_1 \lambda_2 \overline{\mathrm{VIP}}^{t}_{TS,k} . \overline{\mathrm{TIP}}^{t}_{TS,k} \qquad \forall k \in \Omega_K \end{aligned} \tag{4.32}$$

4.2.4 Transmission Network Losses

Transmission losses play an important role in economic operation of electric power systems. Although it is often assumed that taking a transmission line out of service would result in higher network losses (as the path impedance increases), it is possible to reduce the total losses via topology control. TLS, if well formulated and coupled to generation dispatch optimization, can modify the network topology with fewer transmission lines in service and lower losses at the same time. The real power flow through the sending and receiving ends of a given transmission line *k* is expressed in (4.33) and (4.34), respectively.

$$\overline{P}^{t}_{loss,knm} = U_n^2 G_k - U_n U_m \times \left[G_k \cos\left(\theta_n - \theta_m\right) + B_k \sin\left(\theta_n - \theta_m\right) \right] \tag{4.33}$$

$$\overline{P}^{t}_{loss,kmn} = U_m^2 G_k - U_m U_n \times \left[G_k \cos\left(\theta_m - \theta_n\right) + B_k \sin\left(\theta_m - \theta_n\right) \right] \tag{4.34}$$

The objective function is formulated in (4.35)-(4.36) in order to minimize the network total losses:

$$\min_{\forall k \in K} \ \overline{P}^{t}_{loss,TS,k} \tag{4.35}$$

$$\overline{P}^{t}_{loss,TS,k} = \overline{P}^{t}_{loss,knm} + \overline{P}^{t}_{loss,kmn} = \sum_{n \in \Omega_B} U_n \sum_{m \in \Omega_B} U_m G_k \cos\left(\theta_n - \theta_m\right) \qquad \forall k \in \Omega_K \tag{4.36}$$

4.3 Multi-Objective Optimization Modeling

4.3.1 General Concept and Fundamental Background

Multi-objective optimization mechanism is an efficient tool in handling various contradictory/competing, supportive, or mathematically-unrelated objective functions [146], which can be generally described as in below:

$$\begin{aligned} &\min\left[h_i\left(y\right) \right] \qquad i \in \Re \\ &s.t. \end{aligned} \tag{4.37}$$

$$p_j(y) = 0 \qquad j \in \Im \tag{4.38}$$

$$q_k(y) \le 0 \qquad k \in \aleph \tag{4.39}$$

In fact, reaching to one single optimal solution for such optimization problems is inaccurate and a set of solutions can be typically achieved respecting all objective functions. A couple of techniques have been proposed in the literature to handle such type

of problems: A few of them transform a multi-objective optimization problem into a single-objective optimization (e.g., weighted sum and goal programming methods, etc.), which in turn requires adequate and precise knowledge of the problem [147]-[154]. Other methods suggest an effective solution using the non-dominancy concept with respect to all objective functions. Amongst, the Non-Dominated Sorting Genetic Algorithm II (NSGA-II) has demonstrated robustness and efficiency in dealing with non-convex and MILP problems in various fields of engineering [146], [147]. Handling a multi-objective optimization problem through such methods results into a set of non-dominant solutions, called Pareto optimal sets, which are non-dominant with respect to each other for all objective functions [147], [155].

4.3.2 Optimization Method: NSGA-II

In the process of NSGA-II application, the first population for the objective functions is initialized and sorted, based on the non-dominancy concept, into several Pareto fronts. Based on their non-dominancy stand, all Pareto fronts and their individuals are attributed a rank. The parent populations are designated through binary tournament algorithm on the basis of the less non-dominancy rank. Classic crossover and mutation operators are then followed to generate the offspring populations from parents [146]. Populations of parents and offsprings are finally mixed to build a collection among which the next generation is selected. The same process goes on for next generations until a termination criterion is met [147]. In this Section, probabilistic factors, i.e., the expected values of fitness functions are compared through NSGA-II application.

4.3.3 Uncertainty Modeling

One imperative factor, which generally intensifies the risk associated with any decision making, is uncertainty. TLS implementation is also a critical decision to be made by the TSOs and may be affected by prevailing uncertainties, e.g., demand variability, intermittent renewable generation, market regulation, etc. Hence, such system-wide analysis needs to be handled with robust methods to efficiently manage numerous uncertainties in electric power systems.

Random characteristics of the forecasted demand, which is commonly a function of time and is governed by seasons of the year, weather conditions, and electricity price, is statistically modeled using the Gaussian probability distribution function (PDF). In order to consider the chronological features of wind velocity over time and its impact on the wind turbines output power, the hourly wind speed is statistically modeled through the Weibull PDF. The PDF parameters are projected by employing the maximum likelihood estimations and curve fitting techniques and using the historical wind speed data. Such random input variables are used in a developed PEM procedure and the moments of the random quantities would be then calculated. The major advantages of the 2-PEM over the other probabilistic approaches are: (1) it is easy to implement and (2) it requires lower computational burden. One more benefit of using the PEM is the fact that while the PDF of random input variables may be unknown, the moments of output variables can be still calculated. Vector of random input variables that are considered in this study is presented in (4.40).

$$\mathbf{X} = \left[\mathbf{P}_{g,n}^{Wind}, \mathbf{P}_{\mathbf{D_n}} \right] \tag{4.40}$$

The PEM technique is employed to evaluate the moments of the random output variables **Y**, which are actually functions of *n* random input variables **X**. That is,

$$\mathbf{Y} = h(\mathbf{X}) = h(x_1, x_1, ..., x_n) \tag{4.41}$$

where, the random output variables corresponding to any topology control plan can be represented as:

$$\mathbf{Y} = \left[\mathrm{GC}_{TS}^{t}, \mathrm{EDNS}_{TS}^{t}, \mathrm{IR}_{TS}^{t}, \mathrm{P}_{loss,TS}^{t} \right] \tag{4.42}$$

K number of points, called concentrations, is located in the first three moments of the uncertain variables to which the statistical information of each input random variable is mapped. The total number of concentrations distinguishes variations of the PEM method, called K-PEM [138]. Due to required accuracy and computational burden, the 2-PEM is employed. The 2-PEM decomposes (4.41) into a number of sub problems taking into account only two deterministic values of each random variable. These two points are located on two sides of the mean value for a given variable. They may or may not be selected symmetrically around the mean value. The deterministic problem for each objective function is then solved twice for each individual random variable: for the values below and above the mean while keeping all other variables constant at the mean. As such, the transformed samples as well as the mean and standard deviation of all desired output variables at each scenario are estimated [see (4.42)]. The probabilistic formulation of the suggested objectives would eventually result in the PDFs of the output variables. The 2-

PEM procedural algorithm was presented in Section 3 and additional details are provided in Appendix 2.

4.3.4 Proposed Multi-Objective Optimization Framework

Figure 13 illustrates a general idea of the proposed multi-objective optimization framework. As shown, the main probabilistic DCOPF-based TLS optimization is solved first in ***Stage 1*** with a restriction of at most 5 TLS actions. Solving this optimization problem may require an interaction between the ISO and TSOs in order to update the system topology fed into the TLS optimization (transmission lines which are not available for switching or TSOs' other practical constraints would be excluded). Solving this optimization problem in ***Stage 1*** will lead to a total number of economically-attractive TLS actions with the associated dispatch costs as the optimal candidates for final implementation [see (4.1)-(4.8)]. AC feasibility and transient stability checks are then performed and AC infeasible (out-of-market corrections may be needed) and unstable solutions would be discarded. The remaining solutions are then fed into the ***Stage 2***, where the objective functions are probabilistically evaluated for each TLS solution. Applying the NSGA-II, the first population is created. State enumeration method is employed to estimate the probabilistic system reliability criterion [using (4.9)-(4.18)]. Stability performance analysis is conducted on each optimal candidate selected in the first generation through (4.19)-(4.32). Network losses are calculated using the probabilistic OPF [see (4.33)-(4.36)]. Having completed ***Stage 2***, the NSGA-II evaluates the solutions in ***Stage 3*** taking into account the non-dominancy concept and sorts them into the Pareto

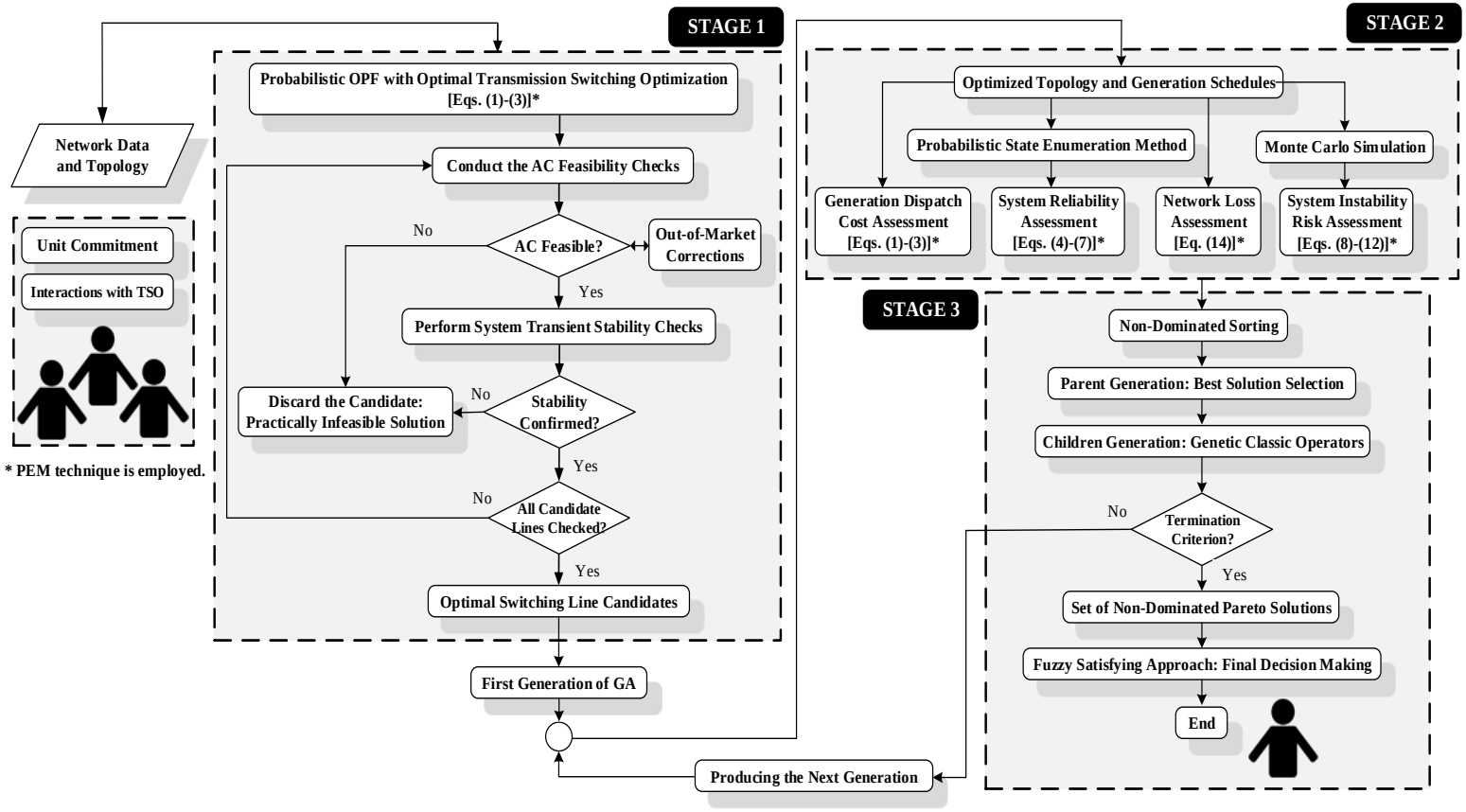

Figure 13. General demonstration of the proposed multi-objective optimization framework for power system topology control decision making.

fronts. In case the termination criterion (which may be either the number of individuals in the first Pareto front or a pre-specified number of iterations) is met, the decision making approach, i.e., the fuzzy satisfying method, is triggered to make the decision among all the optimal Pareto solutions. Otherwise, the traditional GA operands are followed to engender the next generation and the same process goes on.

4.3.5 Final Decision Making Approach: Fuzzy Satisfying Method

Employing a posterior method based on the non-dominancy concept over the entire population to solve a multi-objective optimization problem would result into a set of Pareto-optimal solutions. Eventually, a realistic and promising solution needs to be discovered within the Pareto-optimal front to make a compromise between different objectives. The decision maker's (here the TSO's) preferences play a key role in selecting the final solution. Imprecise nature of the decision maker's thinking necessitates employing a mathematical expression tool to represent human judgments. Fuzzy approach seems to be an effective tool to model this judgement [156].

A fuzzy satisfying method, designated as the Distance Metric, is employed where the decision maker defines his/her imprecise targets for every objective, called satisfaction level. Then, the final solution is found among all the Pareto-optimal solutions that are obtained through the multi-objective optimization module. The step-by-step procedure of the fuzzy decision making via Distance Metric is as follows [155], [156]:

1) A membership function (MSF), which is a continuous monotonically declining set, is attributed to each objective function. The MSF signifies how a solution

contributes to the objective function fulfillment, with the values between zero and one: zero indicating the incompliance and one meaning full compliance with the decision maker's priorities and preferences. Assuming a minimization problem, the MSF is zero at the summit point of the objective and is equal to one at its minimum point. The linear MSF, as expressed in (4.43), is employed in this work:

$$\mu_{f_i}(X) = \begin{cases} 0 & f_i(X) > f_i^{\max} \\ \dfrac{f_i^{\max} - f_i(X)}{f_i^{\max} - f_i^{\min}} & f_i^{\min} \le f_i(X) \le f_i^{\max} \\ 1 & f_i(X) < f_i^{\min} \end{cases} \tag{4.43}$$

2) For each MSF assigned per objective, the final solution can be found by solving the optimization (4.44) considering the satisfaction levels designated by the decision maker:

$$\min_{X \in \text{Solution Set}} \left\{ \sum_{i \in \Re} \left| \mu_{d_i} - \mu_{f_i}(X) \right|^{\tau} \right\} \qquad \tau \in [1, \infty] \tag{4.44}$$

As can be realized, the optimization (4.44) strives to minimize the τ-norm deviations from satisfaction levels considering the MSF of all solutions. Note that the expression (4.44) is less sensitive to the satisfaction levels for bigger values of τ.

4.4 Case Study 1: Modified IEEE 118-Bus Test System

4.4.1 System Characteristics, Assumptions, and Data

The studied network, the modified IEEE 118-bus test system, consists of 185 transmission lines and 19 generating units with the installed capacity of 5859.2MW and a total demand of 4519MW. The demands are assumed to be composed of 80% firm and 20% dispatchable loads, with the interruption cost of 0.8 and 0.2 Value of Lost Load (VOLL), respectively. The system one-line diagram as well as the requisite data including transmission line parameters, generating units' costs and dynamic settings, wind data, and the reliability characteristics of the system equipment are all provided in Appendix 3.

4.4.2 TLS Optimization Results and Discussion–DC Scenario

In the system base case condition, in which no transmission line is switched, the system generation dispatch cost obtained from the DC optimal power flow (DCOPF) is \$2074/h. The mixed integer linear programing (MILP) optimization problem, i.e., the master problem with the objective of minimizing the generation dispatch cost, is solved in the MATLAB environment [142] using DCOPF-based formulations (4.1)-(4.8). The optimization engine is simulated on a PC with an Intel(R) Xeon(R) 3.2 GHz processor and 16 GB of RAM and allows the switching status of each line to be determined.

If there is no restriction on the number of TLS actions for a given generation pattern and load profile, a total of 2^{185} TLS options are theoretically possible. Here, the possibility of at most 5 TLS actions per hour is enforced (implementation of more than 5

TLS actions in an hour may not be practically realistic). With this assumption, the total possibilities for switching implementation at time *t* (Ψ_{TLS}^{t}) would be the statistical combination of 185 distinct TLS actions that will take at most 5 transmission lines out at any given time:

$$\Psi_{TLS}^{t} = C\binom{185}{1} + C\binom{185}{2} + C\binom{185}{3} + C\binom{185}{4} + C\binom{185}{5}$$

Ψ_{TLS}^{t} actually builds the search space for the proposed probabilistic TLS optimization engine. For demonstration purposes, 240 optimal solutions involving at most 5 TLS actions that bring about highest potentials for economic savings are demonstrated in Figure 14 (***Stage 1***). It can be observed that:

- Switching relatively few transmission lines out of service has a significant contribution to the overall cost savings.
- Considering a given value of χ, there are several options available for TLS implementation with different levels of economic efficiency. For instance, if switching only one transmission line out is allowed ($\chi = 1$), around 40 number of different TLS candidates are found with the highest economic saving of 13.62% over the base case. Similarly, in the case of two and three TLS actions, the highest economic saving of 22.78% and 32.35% will be achieved, respectively.
- The optimization framework would provide higher economic savings when the number of subsequent TLS actions increases.

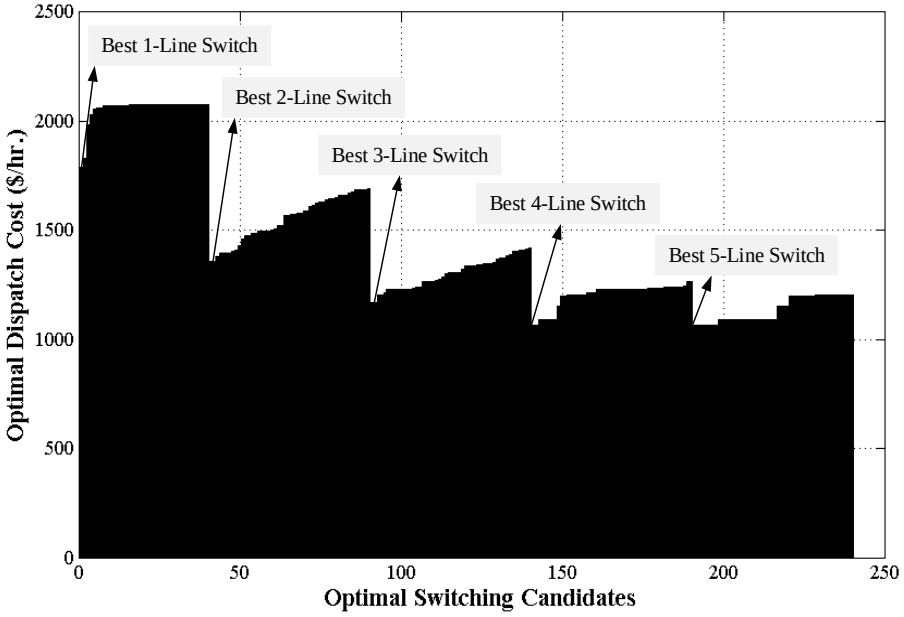

Figure 14. Optimal DCOPF-based TLS scenarios and the associated cost savings.

Although such suggested TLS candidates more or less offer attractive economic savings, the system performance, critical for safe and secure operation, need to be also ensured. Equations (4.9)-(4.36) proposed in Section 4.2 are employed to quantify such aspects of system operation following the adoption of various TLS candidates. Simulations are conducted applying the MATPOWER operation functions in the MATLAB environment [142]. The results in Figure 15 to Figure 18 demonstrate the system instability risk (IR), system-wide reliability risk [represented through the Expected Demand Not Supplied (EDNS) and Loss of Load Probability (LOLP) indices], and network losses after TLS implementations, respectively. The above indices of interests corresponding to the system base case condition are evaluated and tabulated in Table 4.

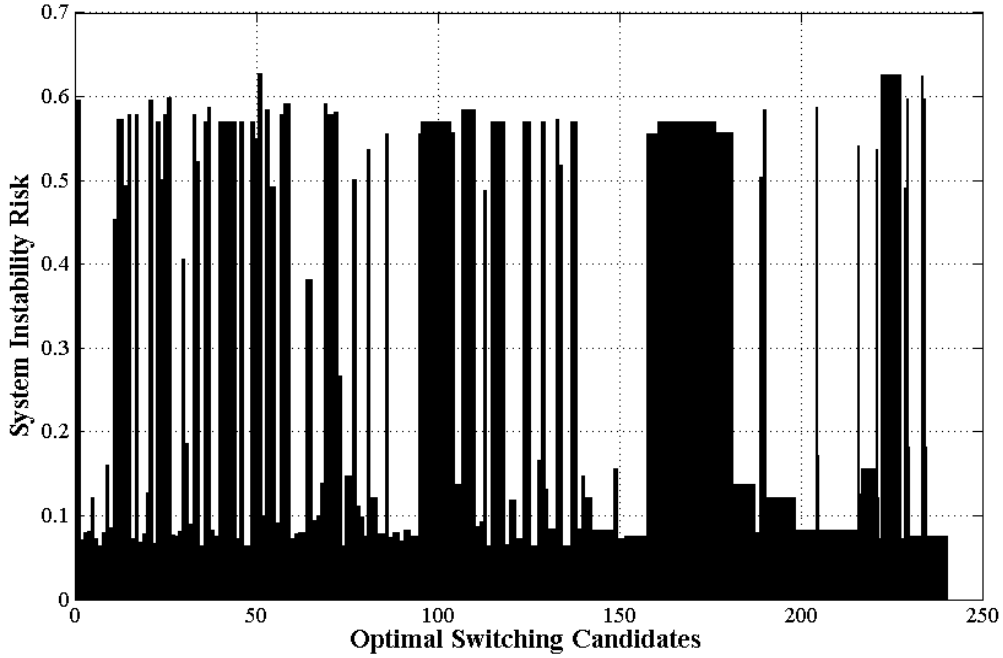

Figure 15. System instability risk after implementation of DCOPF-based TLS candidates

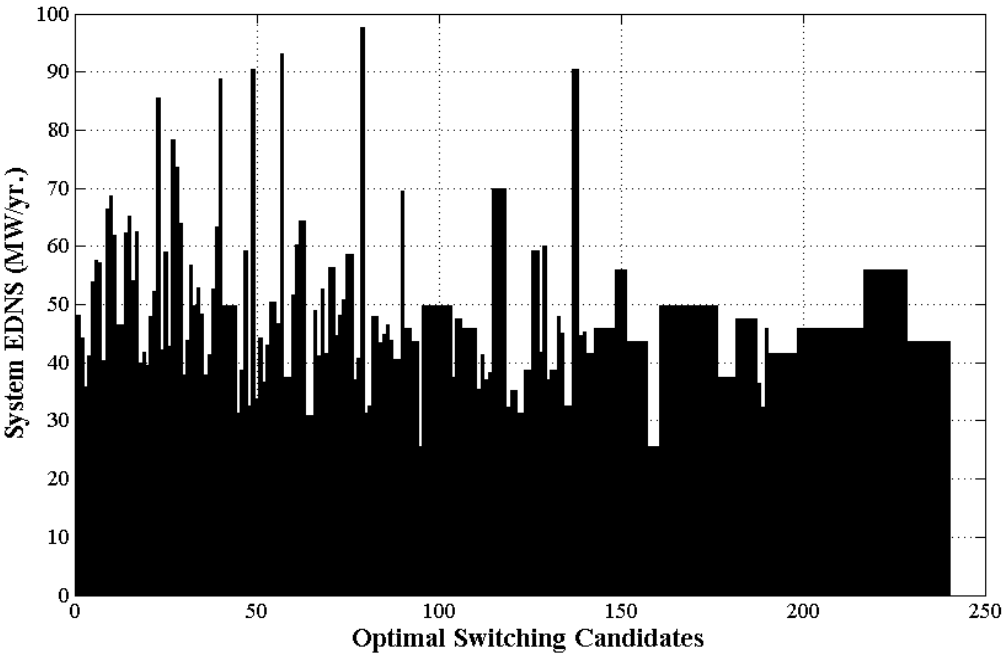

Figure 16. System EDNS index of reliability after implementation of the DCOPF-based TLS candidates.

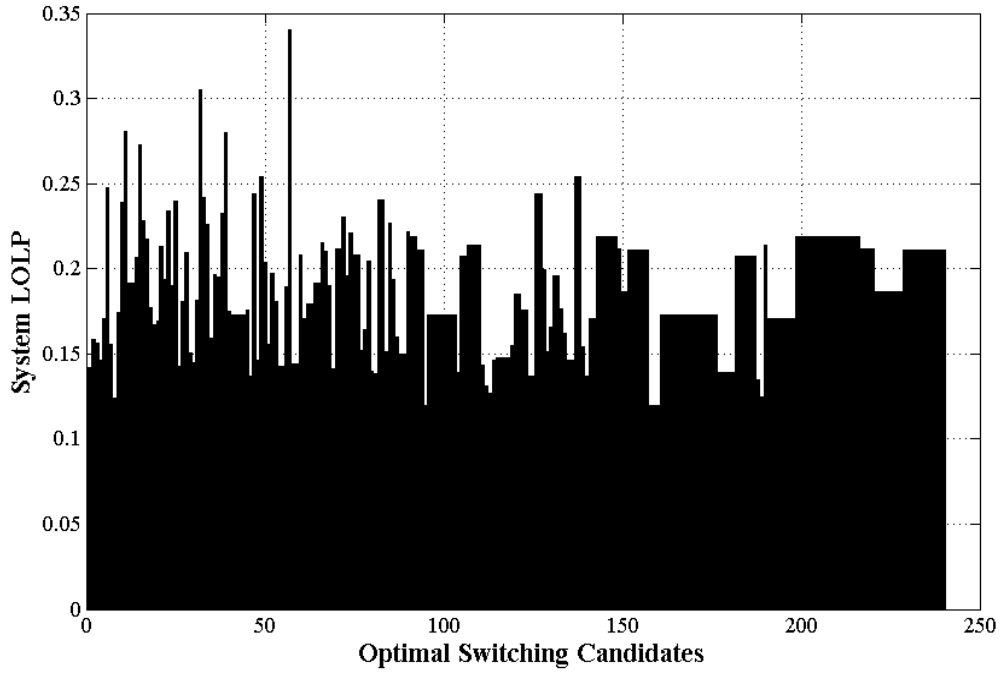

Figure 17. System LOLP index of reliability after implementation of the DCOPF-based TLS candidates.

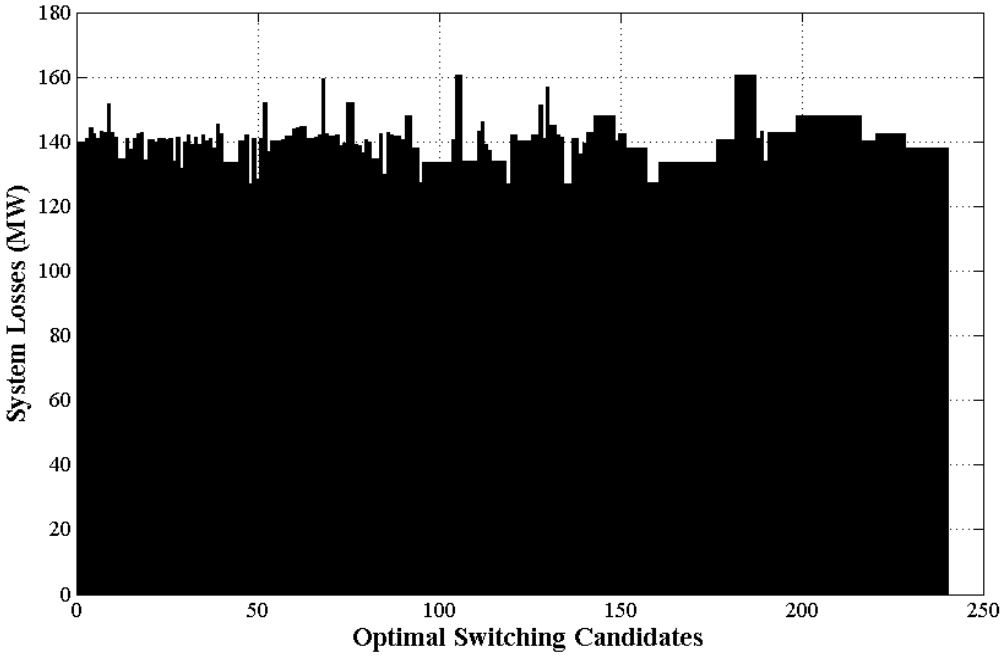

Figure 18. Network losses after implementation of the DCOPF-based TLS candidates.

Table 4. System Performance Indices in the Base Case

$\overline{IR}_{TS}^{base}$ (%)	$\overline{LOLP}_{TS}^{base}$ (%)	$\overline{EDNS}_{TS}^{base}$ (MW./yr.)	$\overline{P}_{loss,TS}^{base}$ (MW)
16.97	15.80	48.1271	140.787

From Figure 15, it can be seen that the system instability risk varies between 0.06 and 0.63 over the studied TLS candidates while it is calculated as 0.1697 for the system base case condition (see Table 4). Observations reveal that there are always some TLS candidates (irrespective of the number of TLS actions involved) which provide a fairly acceptable instability risk (less than 0.1). It can be also seen that some of the most economically-attractive TLS actions may cause the system condition with relatively higher instability risk compared to the base case condition and other candidates. For instance, the instability risk calculated for the best 1-line TLS candidate (with the overall cost saving of 13.62%) is 0.59 while for the second best 1-line switch candidate (with the cost saving of 11.81%) is calculated as 0.07. Note that the suggested instability risk index corresponding to a TLS solution inherently reflects the AC feasibility and voltage/transient stability requirements in many sampled states at the new system configuration after successful implementation of a TLS plan. The AC feasibility and stability checks are still required to make sure a safe and secure operating state immediately following the DCOPF-based TLS adoptions. Those plans passing the aforementioned checks can be regarded as the candidates for final implementation.

Figure 16 and Figure 17, respectively, illustrate the EDNS and LOLP indices reflecting system reliability after implementation of TLS candidates. It can be seen that

switching some transmission lines out of service will drastically degrade the system reliability performance. Take the best 2-line switch action as an example. Implementation of this topology change would degrade the system EDNS index for 15.3% and LOLP index for 9% (while it reflects the economic efficiency of 22.78% over the base case condition in Table 4). On the other hand, there are TLS candidates that can improve the system reliability performance while at the same time guaranteeing the expected economic efficiency. As an example, the third best 1-line TLS action enhances the system EDNS index for 16.7%, LOLP index for 2.026%, and ensures an economic efficiency of 4.417% over the base case topology. This suggests that there is room for improving the system operational reliability by switching some transmission lines out of service in some specific periods of time. In fact, the reason for such an observation is that the topology control optimization engine developed in this Section tries to co-optimize the generation dispatch together with the network topology, which in some cases improves the system reliability performance in the new operating state.

Figure 18 also demonstrates the network losses after implementation of the optimal TLS candidates.

4.4.3 TLS Optimization Results and Discussion–AC Scenario

The system base case generation dispatch cost obtained from the AC optimal power flow (ACOPF) is $354860/h. The economically-attractive topology control results taking into account the TLS formulations in AC setting (considering voltage and reactive

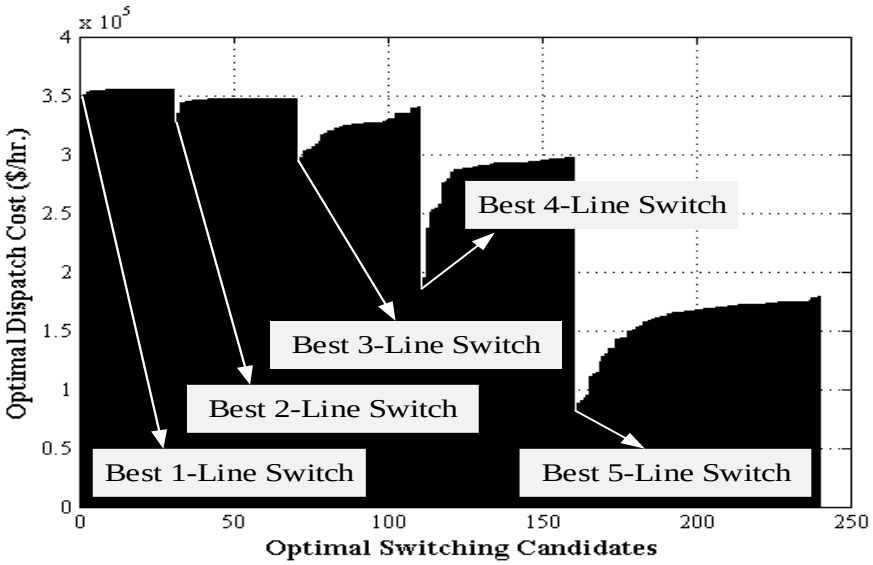

Figure 19. Optimal ACOPF-based TLS scenarios and the associated cost savings.

power constraints) are presented in Figure 19 (***Stage 1***). The best 1-line switch, 2-line switch and 3-line switch candidates suggested in the AC scenario provide, respectively, 2.1%, 8.1%, and 17.4% cost saving compared to the base case condition. The cost savings obtained from the topology changes in AC scenarios are considerably lower than that in the corresponding DCOPF-based switching scenarios (13.62%, 22.78%, 32.35%) [see Figure 14].

Similar analyses as the ones presented in Figure 15 to Figure 18 are conducted for the ACOPF-based TLS candidates and the obtained results are statistically compared with those of the DCOPF-based solutions in Table 5. The statistical analysis in Table 5 shows that the average economic benefits gained through the DCOPF-based TLS candidates is 31% while that of the ACOPF-based candidates is 25%. In contrast to instability risk, the system average LOLP and EDNS indices in the new topologies are higher in the AC

Table 5. Statistical Comparison of the System Performance Indices after Implementation of the DCOPF-Based and ACOPF-Based TLS Candidates

Performance Index	$\overline{GC}_{TS}^{t}$ ($/hr.)		$\overline{IR}_{TS,k}^{t}$ (%)		$\overline{LOLP}_{k}^{t}$ (%)		$\overline{EDNS}_{TS,k}^{t}$ (MW/yr.)		$\overline{P}_{loss,TS,k}^{t}$ (MW)	
	DC	**AC**	**DC**	**AC**	**DC**	**AC**	**DC**	**AC**	**DC**	**AC**
Min.	1065.97	95400.55	6	5	0.1197	0.1215	25.613	23.446	127.08	112.96
Max.	2065.66	354859.5	63	41	0.3403	0.5924	97.683	137.91	160.59	158.91
Mean	1420.05	267226.2	27	23	0.1892	0.2229	48.171	58.867	140.87	131.52
Std.	326.87	83127.95	23	13	0.0351	0.0714	11.622	17.902	6.54	10.44

setting compared to those in DC scenarios. In other words, the TLS solutions proposed by the ACOPF-based formulations could provide more secure, but less reliable, performance conditions compared to the DCOPF-based ones.

Although the aforementioned general conclusions may or may not be valid for other networks, such observations highlight the fact that the assessment using a robust decision making toolset, such as the proposed multi-objective optimization framework, is needed when selecting the most impactful TLS actions.

4.4.4 Multi-Objective Decision Making via NSGA-II

In this subsection, application of the NSGA-II optimization technique is first demonstrated on the DCOPF-based TLS candidates (which are all economically attractive). AC feasibility and stability checks are steered on each of the optimal TLS candidates for which the sample results of the stability checks are demonstrated in Figure 20. As one can see, implementation of the 3-line switch L181-L162-L158 would lead to

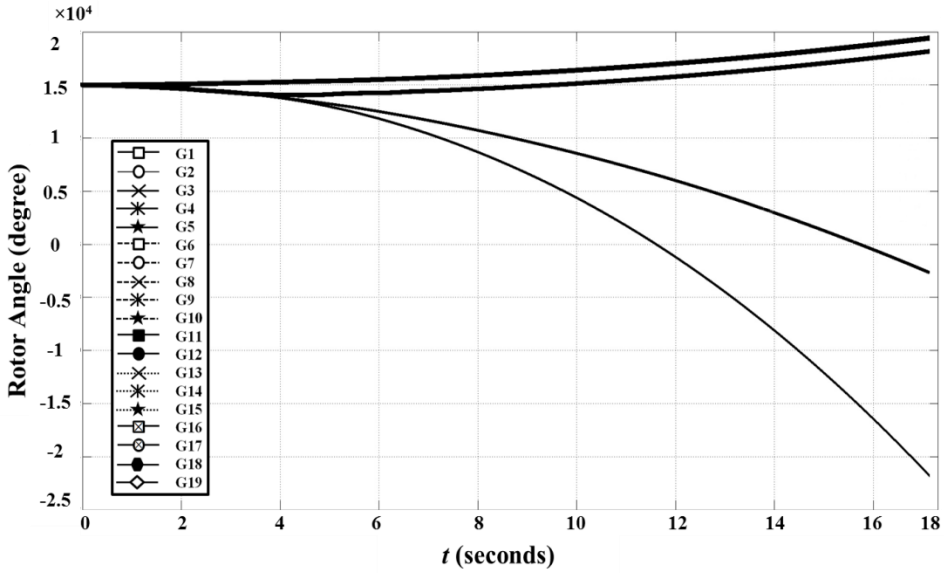

Figure 20. Rotor angle trajectory of system generators after implementation of an unstable TLS plan (L181-L162-L158).

system transient instability and, as a result, is not a feasible TLS candidate solution and would be discarded. Those survived TLS candidate sets that pass the initial AC feasibility and stability checks after implementation would construct the valid search space and feed the multi-objective optimization framework for further evaluations (***Stage 2***). In each iteration of the NSGA-II algorithm, a solution population is sorted into a set of non-dominant fronts where the initial front contains a set of non-dominant solutions in the entire population while the next front contains a set of non-dominant solutions ignoring those in the first one, and so on, until the entire population is classified into *k* levels. Based on its level of non-dominancy, each solution is then attributed a fitness. The solutions of the first level are assigned the highest fitness and so on. The reproduction of populations

is achieved through classical crossover and mutation process. Since all previous solutions are also included in the process, elitism is guaranteed [157].

The proposed multi-objective optimization algorithm is applied with the population size of 80. Having 200 iterations performed, 50 non-dominant solutions are found by the NSGA-II (***Stage 3***). The results of implementing the proposed multi-objective approach on this system analyzing the DCOPF-based TLS candidates are depicted in Figure 21 to Figure 24, which demonstrates the trade-off between various objectives of interest. As it is hard in effectively displaying a non-dominant set in a multi-dimensional space, the projections of different Pareto sets are demonstrated through four trade-off planes. It is important to note that the solutions which appear to be dominant in each of these graphs are, indeed, non-dominant with respect to the other objectives not demonstrated in that graph.

The following observations are made from the results in Figure 21 to Figure 24:

- As demonstrated in Figure 21, while it cannot be generalized to other systems, there is a conflicting relationship between the generation dispatch cost and system instability risk. The range of generation dispatch cost for the optimal plans is between $1195.02 (42.4% economic saving) and $1673.76 (19.3% economic saving) which is corresponding to the system instability risk level ranging between 0.05 and 0.24. It can be inferred, from the optimal Pareto fronts in Figure 21 that as the generation dispatch cost decreases by opening more transmission lines, the instability risk index would generally increase. It can also be shown that the level of instability risk for the solutions selected in the optimal Pareto front would not

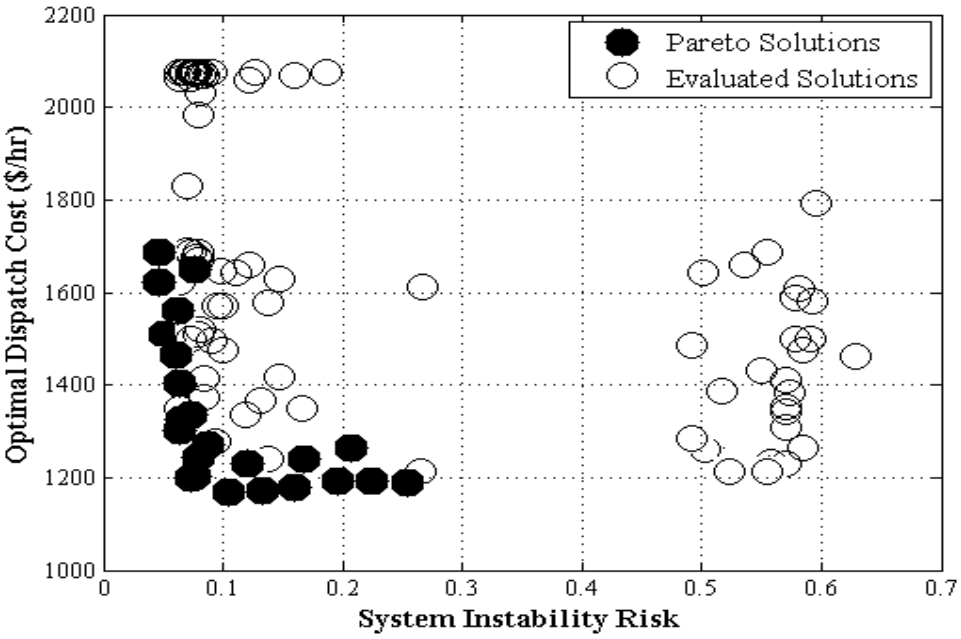

Figure 21. Non-dominant DCOPF-based solutions of the multi-objective problem: Trade-off between the generation dispatch cost and system instability risk.

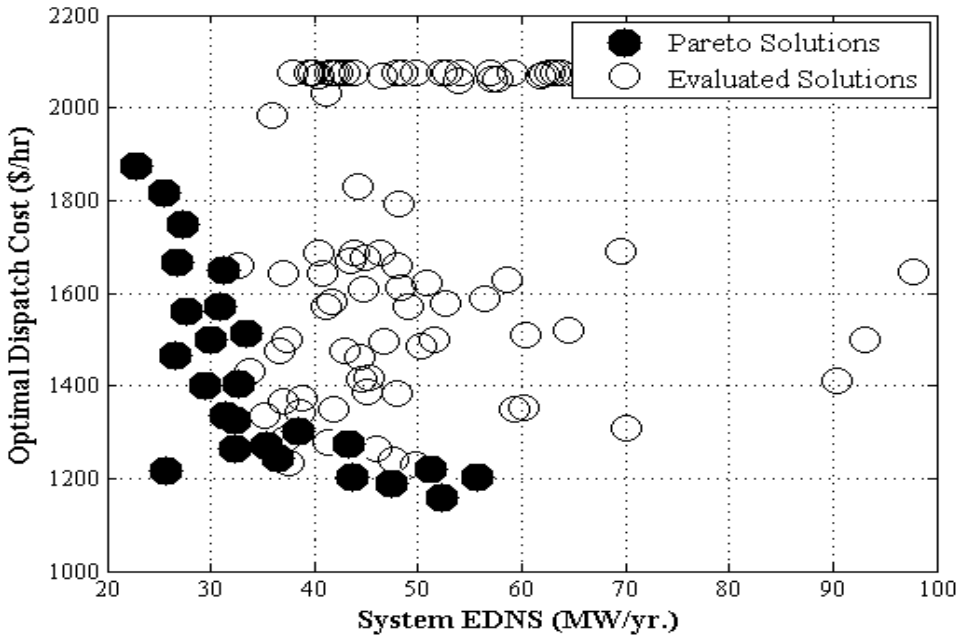

Figure 22. Non-dominant DCOPF-based solutions of the multi-objective problem: Trade-off between the generation dispatch cost and system EDNS.

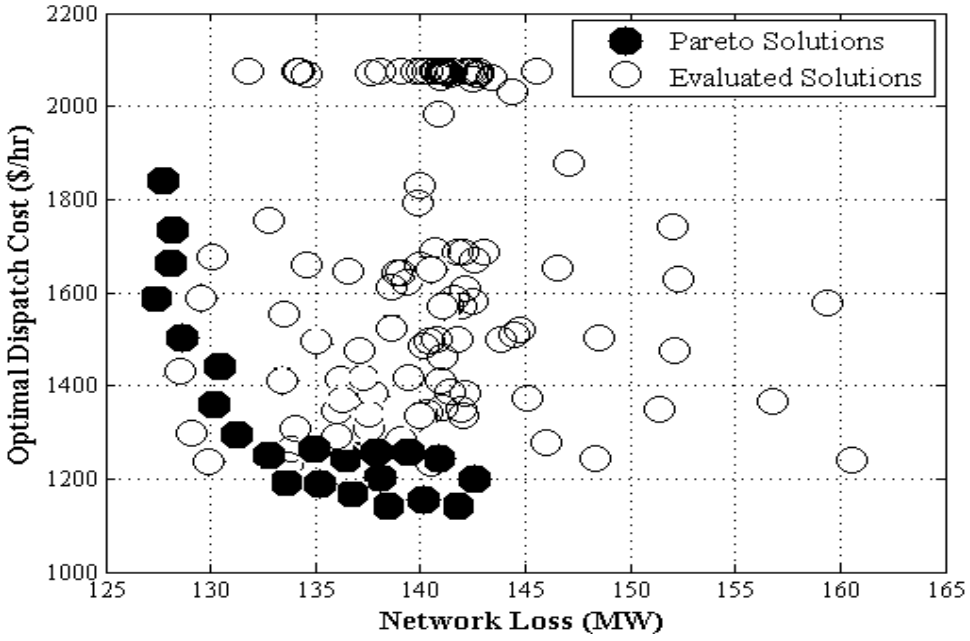

Figure 23. Non-dominant DCOPF-based solutions of the multi-objective problem: Trade-off between the generation dispatch cost and network losses.

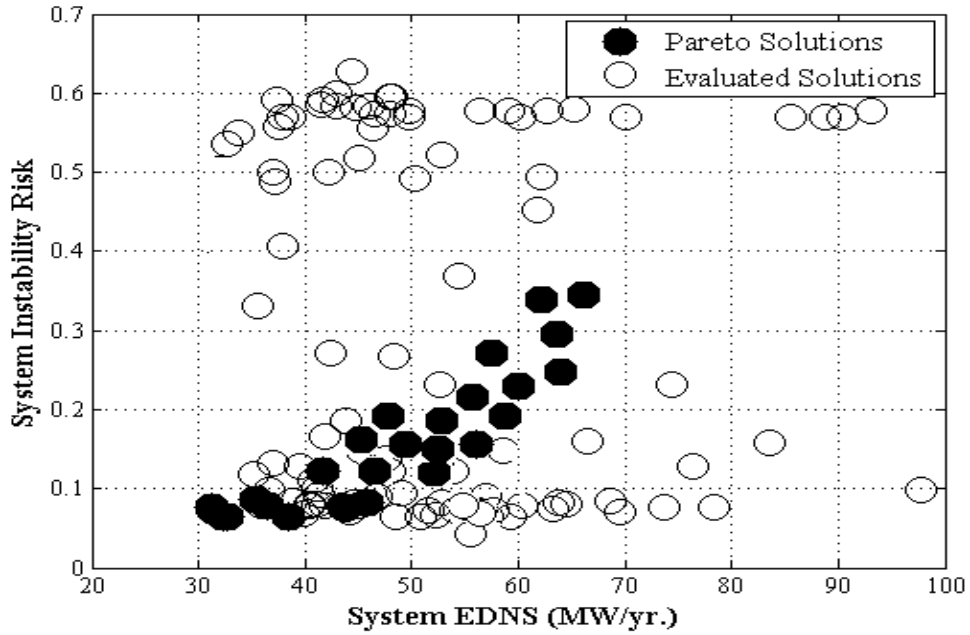

Figure 24. Non-dominant DCOPF-based solutions of the multi-objective problem: Trade-off between the system instability risk and EDNS.

increase anymore once the value of 0.24 is reached meaning that the process is no longer sensitive to the number of optimal TLS actions in this optimal front.

- According to Figure 22, the system EDNS index of reliability associated with the optimal TLS plans varies from 25.613 MW/yr. to 56.72 MW/yr., corresponding to the system generation dispatch cost ranging from $1155.02 to $1853.22. With the increase in the cost saving (i.e., lower generation dispatch cost as a result of switching out more transmission lines), the system reliability is generally observed in this front to degrade, which is reflected through higher EDNS values. Note that similar observations can be made when LOLP index of reliability is tracked in the presented Pareto fronts.
- Trade-off between the system generation dispatch cost and network losses is demonstrated in Figure 23. The range of network losses for the optimal TLS solutions mainly varies between 127.07 MW to 143.07 MW corresponding to the system generation cost ranging from $1182.11 to $1814.41. While the network losses would increase as the generation dispatch cost decreases, the variations of the network losses for the recognized optimal TLS solutions are mainly limited to between 135 MW to 143 MW, reflecting a low sensitivity of this objective to variations of the dispatch costs lower than $1620.
- The trade-off between the system instability risk and the system EDNS objectives is plotted in Figure 24. The results demonstrate the fact that as the system EDNS increases due to adoption of TLS candidates, the system instability risk index also grows accordingly.

4.4.5 Optimal TLS Selection via Fuzzy Satisfying Method

As the solution of the multi-objective problems is not unique, some sort of subjective judgment needs to be embedded in order to identify a flexible and practically viable solution. Among many methods and approaches for selection of a compromised solution within a set of optimal Pareto solutions, a fuzzy technique is of significant interest mainly because of the simplicity as well as similarity to human reasoning (***Stage 3***). Fuzzy satisfying approach is utilized to differentiate the TLS plans in the optimal Pareto front.

For the fuzzy satisfying method to be applied, the decision maker should determine the desirable levels (reference values) for each objective function. The trade-offs depicted in Figure 21 to Figure 24 assists the decision maker to select reasonable reference MSF values. For instance, if the decision maker relaxes a little bit the range of the desired objectives, the reference values would decrease and if he/she is strict regarding the final selection, the higher reference value would be selected.

The final results when the fuzzy satisfying method is applied on the obtained DCOPF-based optimal solutions for different satisfaction levels are demonstrated in Table 6. As it can be numerically inferred, the final optimal solution depends heavily on the satisfaction levels [$\mu_{di} (i = 1, 2, 3, 4)$] selected for each objective function by the decision maker. For example, if the generation dispatch cost has to be lower than \$1300, μ_{d1} needs to be selected higher than 0.65. It can be observed, from the third and fourth rows in Table 6, that once μ_{d1} varies from 0.6 to 1, the generation dispatch savings increase while imposing relatively lower system reliability index (38.38 MW/yr. vs. 40.63 MW/yr.).

Table 6. Operator Satisfaction Levels and Final Optimal DCOPF-based TLS Solutions: IEEE 118-Bus Test System

Satisfaction Levels				**Objective Function Value**				**Final TLS Solution**
μ_{d1}	μ_{d2}	μ_{d3}	μ_{d4}	f_1 ($/hr.)	f_2 (%)	f_3 (MW/yr.)	f_4 (MW)	
0.8	0.8	0.8	1	1254.36	12.1	32.26	127.12	66-112-179
1	0.8	0.6	0.8	1190.54	12.9	37.72	133.06	135-169-67
0.6	0.8	0.6	0.6	1406.28	12.6	38.38	142.36	62-164
1	1	0.6	0.6	1202.78	10.9	40.63	139.44	73-135-5-51-126
0.6	0.6	0.4	0.6	1355.54	14.2	42.05	138.56	181-162-120

Also the system reliability performance criterion would drastically increase when the μ_{d3} increases from 0.4 to 0.8 (see the first and fifth rows). It can be revealed, by comparing the first and second rows in Table 6, that if μ_{d1} value varies from 0.8 to 1, the generation dispatch cost would be decreasing imposing a relatively higher instability risk. In summary, the final results are significantly sensitive to the value of μ_{d1} among the others and this would have a great impact on the final selection of the optimal TLS plan for implementation.

Table 7 demonstrates the final ACOPF-based optimal TLS actions where the fuzzy satisfying method is applied on the Pareto optimal solutions. Comparing the second and fourth row of the table, one can conclude that with an increase in μ_{d2}, while μ_{d1} remains constant, the dispatch cost would increase as the operator mandates a higher satisfaction level for the instability risk. The 4-line TLS solution selected in the first row in Table 7 reflects a more efficient performance of the system, from the perspective of all the

Table 7. Operator Satisfaction Levels and Final Optimal ACOPF-based TLS Solutions: IEEE 118-Bus Test System

Satisfaction Levels				Objective Function Value				Final Switching Solution
μ_{d1}	μ_{d2}	μ_{d3}	μ_{d4}	f_1 (k$/hr.)	f_2 (%)	f_3 (MW/yr.)	f_4 (MW)	
0.8	0.8	0.8	1	196.843	14.95	38.446	116.332	109-128-89-140
1	0.6	0.6	0.8	154.479	33.14	52.623	137.081	45-109-140-100-128
0.6	0.8	0.6	0.6	294.129	21.77	50.967	131.550	167-128-29
1	1	0.6	0.6	173.992	13.83	57.815	138.100	109-128-6-140-77
0.6	1	1	0.6	304.156	13.14	32.623	137.081	90-128-49

objective functions, compared to that of the base case condition.

The selected optimal solutions in AC setting introduced a relatively higher instability risk and higher reliability index compared to those obtained in DC setting [see Table 6]. As the selection of the final solution for implementation is highly dependent on the choices of satisfaction level for each objective function, the suggested framework would empower the operator to effectively involve his/her experience and other operational requirements in the TLS decision making.

4.5 Case Study 2: IRAN 400kV Transmission Grid

4.5.1 System Characteristics, Assumptions, and Data

The Iran 400kV transmission grid is being operated by the Iran Grid Management Company (IGMC) as an independent system operator (ISO) established in 2003. The high-voltage grid is comprised of two voltage levels: 230kV and 400kV, in which the 400kV is mainly related to long distance transmission lines. The simplified network diagram

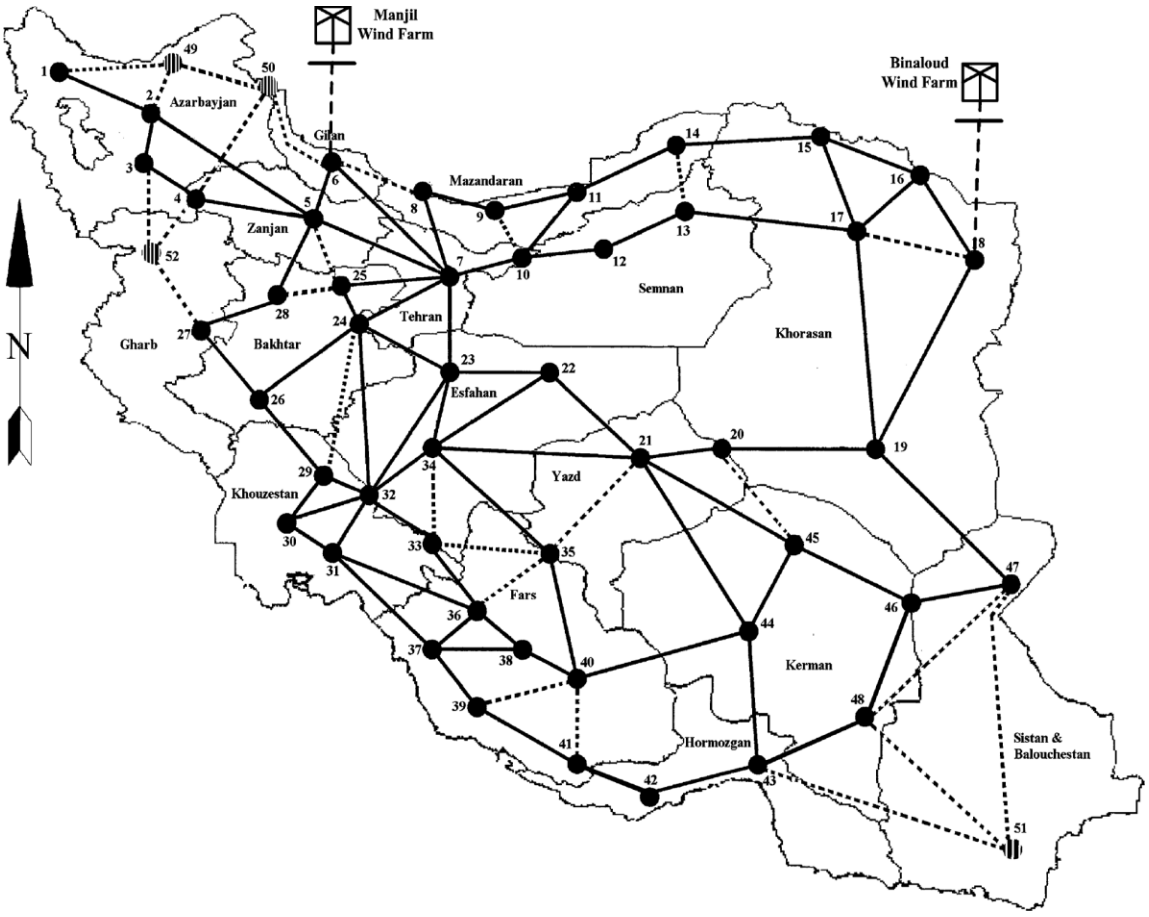

Figure 25. Simplified illustration of the Iran 400kV transmission grid.

depicted in Figure 25 has 52 buses and 101 transmission lines with the overall installed capacity of 33830 MW serving a total demand of 32870 MW. Detailed information on the characteristics of the network and the associated data can be found in [157]-[159]. Two wind farms are located in north of Iran, Manjil in the northwest and Binaloud in the northeast, with the wind data provided in Appendix 3.

Probability density functions (PDF) are used to model the uncertainties and random behavior of the predicted load and wind speed. In order to model the wind speed

variations at the two wind farms, the actual hourly wind speed for five years (Jan. 1, 2005-Dec. 31, 2009) are utilized and the simulation engine can capture the intermittent wind speed characteristics over time fairly accurate. The hourly wind generation feeds the probabilistic topology control optimization engine, introduced in Section 3 of this dissertation with input random variables.

4.5.2 Results and Discussions – AC Scenario

This test case is focused on studying the performance of the developed decision making framework in the AC scenarios. For demonstration purposes, the probabilistic ACOPF-based optimization problem is solved with inclusion of the predicted wind and load data at hour 20. Similar to previous case study, the possibility of at most 5 TLS actions in an hour is assumed. A total of 80 optimal solutions are obtained each of which would differently impact the objectives [see Figure 26 - Figure 29] (***Stage 1***).

Figure 26 to Figure 29 illustrates how the optimal TLS candidates for economic gains would affect the other objectives. According to Figure 26, as the number of optimal TLS actions increases, the higher percentage of economic saving would be realized. The minimum and maximum cost saving would be in the amount of k$43.376 and k$958.982, respectively, in case of 1-line and 5-line TLS actions. Figure 27 demonstrates that the system instability risk may improve up to 61.53% compared to the base case for a 3-line switch candidate while it degrades the most up to -218.01% for a 5-line TLS option. Among all the optimal topology control candidates found, the maximum improvement in network losses and system EDNS index would be 30.7% and 200.29%, respectively [see

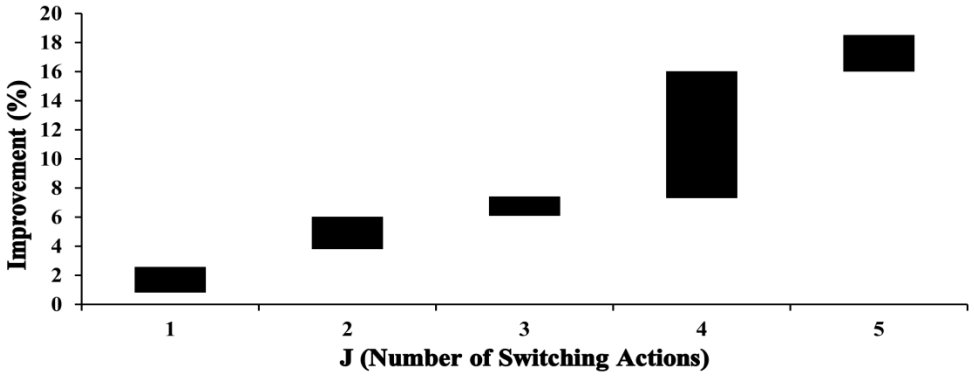

Figure 26. Impact of ACOPF-based optimal TLS candidates on system dispatch cost.

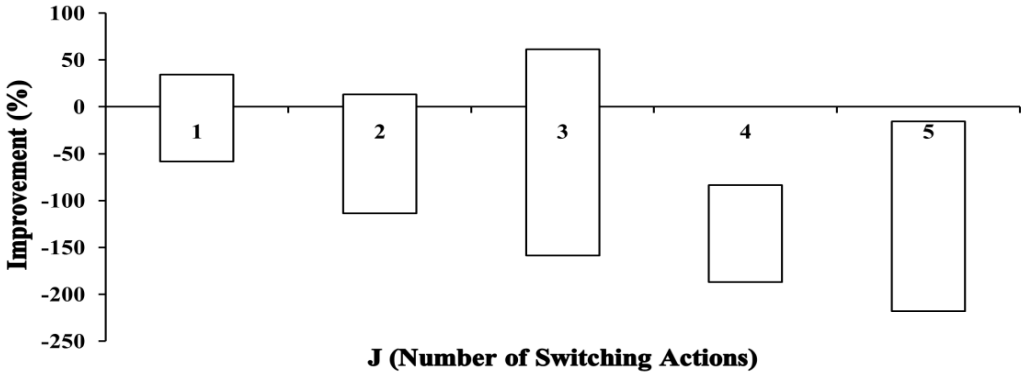

Figure 27. Impact of ACOPF-based optimal TLS candidates on system instability risk.

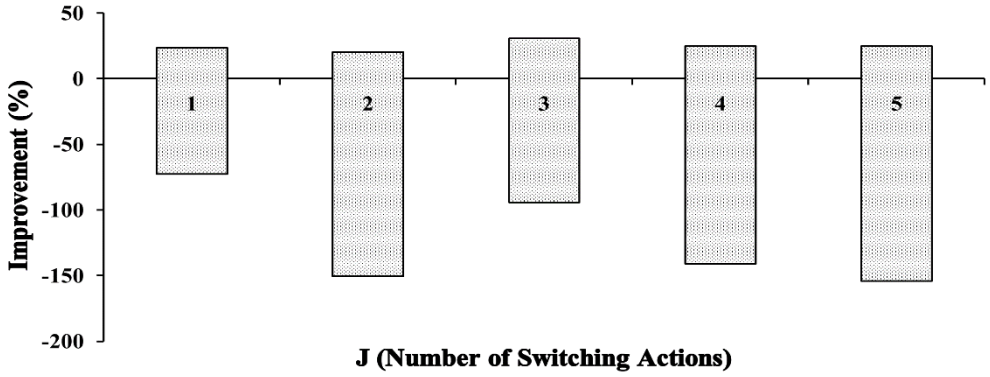

Figure 28. Impact of ACOPF-based optimal TLS candidates on network losses.

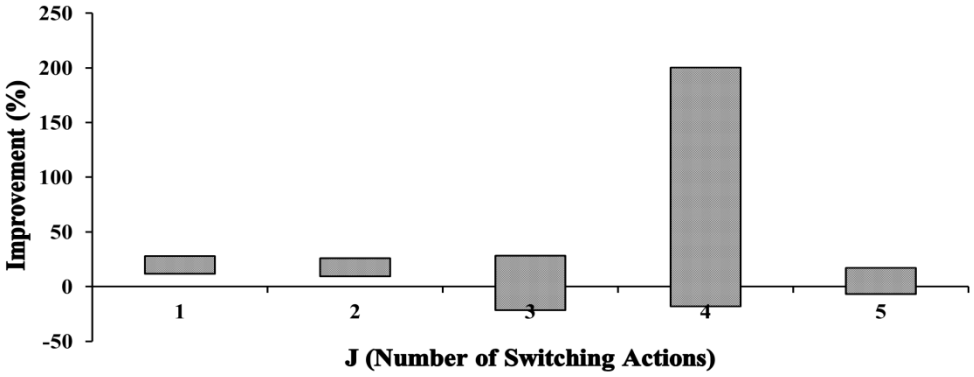

Figure 29. Impact of ACOPF-based optimal TLS candidates on system EDNS – IRAN 400kV Transmission Grid.

Figure 28 and Figure 29]. However, the resulting optimal TLS candidates may adversely affect these two system performance indicators up to -153.99% and -21.48%, for a 5-line and 3-line TLS actions, respectively. All the 80 TLS candidates are then screened in the developed AC feasibility check platform (while assumed to be stable due to the lack of dynamic data). The search space for the developed multi-objective decision making framework contains the survived 74 optimal TLS plans among which the final solution would be selected for implementation. The optimal Pareto fronts, demonstrative of the compromise between various objectives of interest for the non-dominant solutions, are obtained through NSGA-II application with 100 iterations and the results are demonstrated in Figure 30 -Figure 33.

The range of the optimal dispatch cost (corresponding to the optimal TLS candidates in the Pareto fronts) varies between M$4.221 and M$5.137 reflecting a total of 17.4% and 1.18% cost savings respectively (***Stage 2***). Similarly, the selected non-

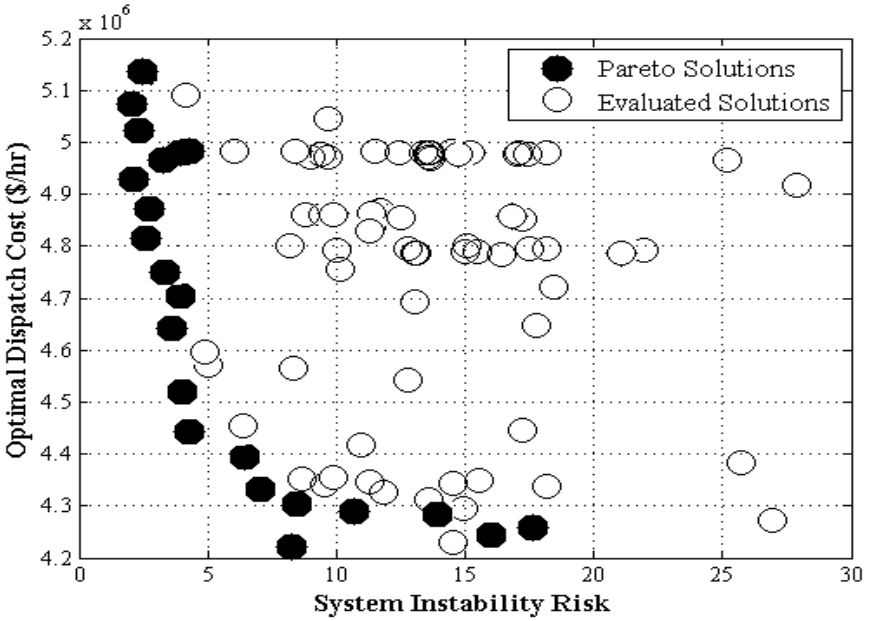

Figure 30. Non-dominant ACOPF-based solutions of the multi-objective problem: Trade-off between the generation dispatch cost and system instability risk.

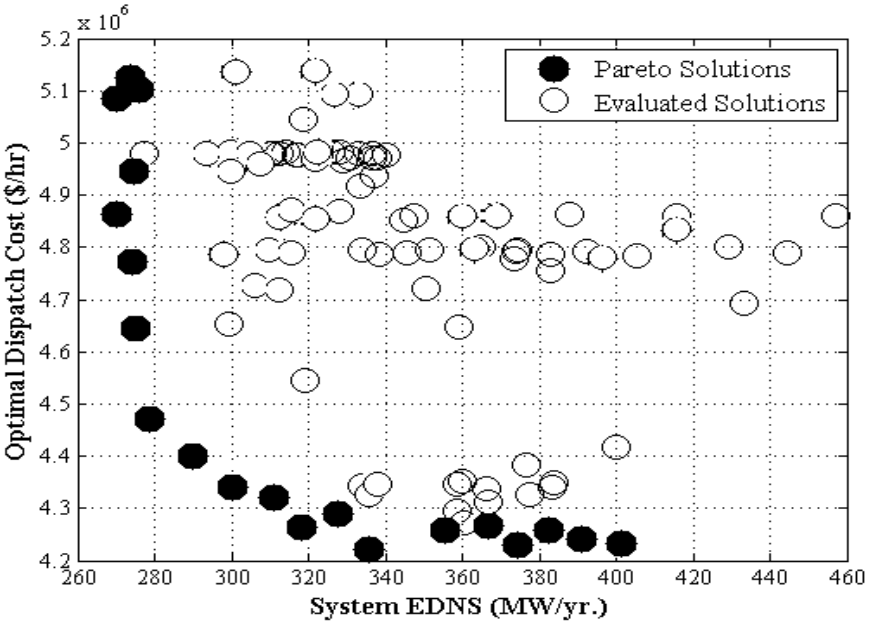

Figure 31. Non-dominant ACOPF-based solutions of the multi-objective problem: Trade-off between the generation dispatch cost and system EDNS.

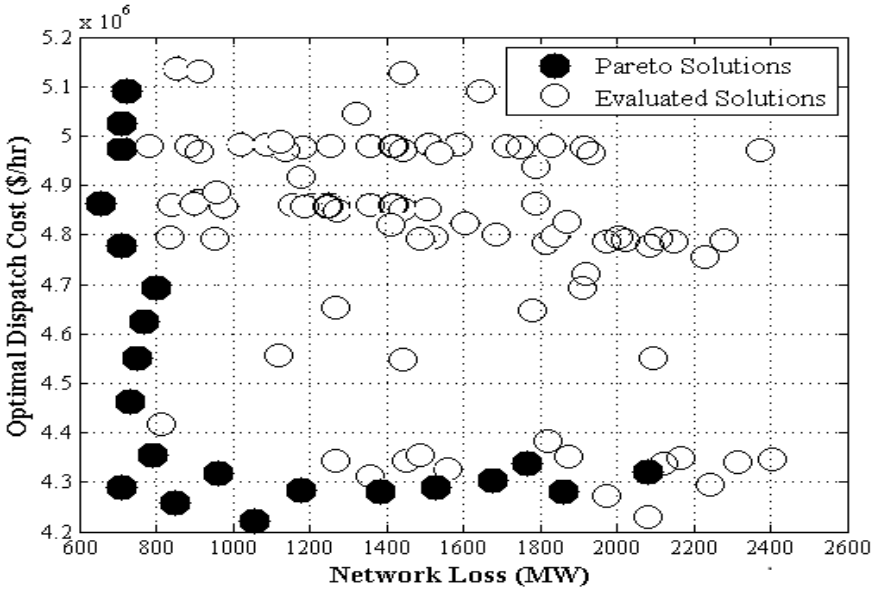

Figure 32. Non-dominant ACOPF-based solutions of the multi-objective problem: Trade-off between the generation dispatch cost and network losses.

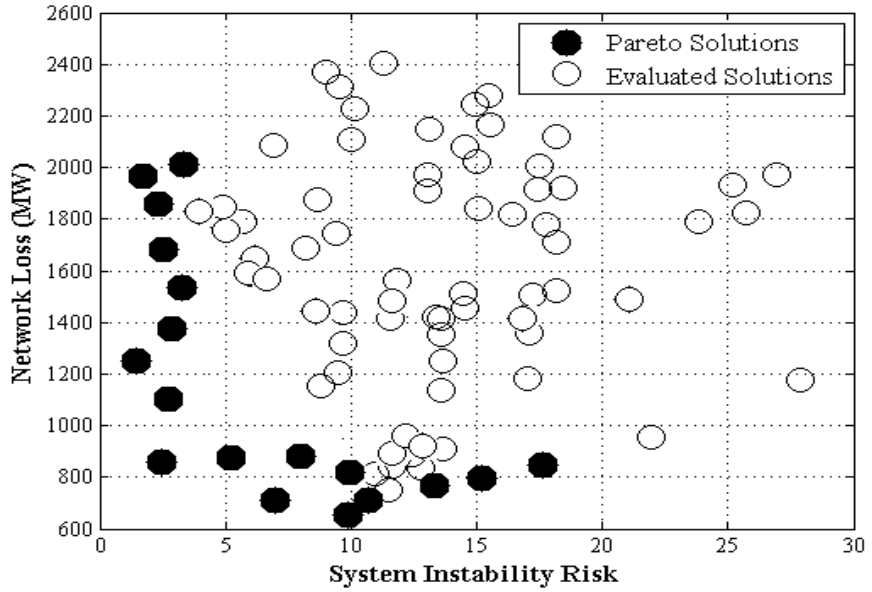

Figure 33. Non-dominant ACOPF-based solutions of the multi-objective problem: Trade-off between the network losses and system instability risk.

dominant solutions in the Pareto fronts would lead to improvements in the system EDNS reliability index ranging from 265MW/yr. to 407MW/yr.

The fuzzy satisfying method is applied on the non-dominant solutions and the results for various satisfaction levels (corresponding to various objectives reflecting the operator expertise and judgments) are tabulated in Table 8 (***Stage 3***). The final decisions for implementing the optimal TLS candidates can be made for various selections of satisfaction levels for each objective (see Table 8). For instance, one can compare the first and second rows of the table, where an increase in μ_{d3} is realized. As a result, the final solution for TLS implementation has been changed from a 2-line TLS plan with M$4.97 dispatch cost (and higher reliability) to another involving 3-line TLS actions with an overall economic value of M$4.89 (and a lower reliability performance), all compared to the system base case condition.

Table 8. Operator Satisfaction Levels and Final Optimal ACOPF-based TLS Solutions: IRAN 400kV Transmission Grid

Satisfaction Levels				**Objective Function Value**				**Final Switching Solution**
μ_{d1}	μ_{d2}	μ_{d3}	μ_{d4}	f_1 (M$/hr.)	f_2 (%)	f_3 (MW/yr.)	f_4 (MW)	
0.8	0.8	1	0.6	4.97	6.33	295.72	892.23	20-17
0.8	0.8	0.6	0.6	4.89	6.26	365.57	1056.54	8-12-17
1	1	0.6	0.6	4.56	5.89	359.92	997.49	16-17-71
1	0.8	0.8	0.8	4.22	7.02	322.41	789.51	17-4

4.6 Conclusions

This Section offers the following contributions:

- New multi-objective optimization decision making paradigm for adoption of network topology control in economic scenarios is proposed.
- Several critical and contradictory/competing objectives for TLS implementation taking into account both ISO's and TSO's requirements are incorporated and quantified.
- Probabilistic nature of the involved uncertainties (e.g., renewable generation and variable loads) is efficiently modeled through the 2-PEM technique.
- The proposed probabilistic multi-objective decision making framework is handled via a robust elicits optimization technique, i.e., NSGA-II, following by the fuzzy satisfying method to account for the TSO's preference and practical experiences.
- The impact of optimal transmission line switching (TLS) on power system requisite performance measures (e.g., generation dispatch cost, network losses, system LOLP and EDNS reliability indicators, as well as the instability risk) is numerically demonstrated. As hypostatized before, different TLS solutions may migrate the grid to new operating conditions with different levels of mentioned performance characteristics. This, hence, verified the need for the proposed all-inclusive decision support tool for TLS implementation decision making.

- The performance of the suggested multi-objective optimization framework for topology control decision making is thoroughly investigated through two case studies where uncertainties of load and renewables are probabilistically handled.
- While several DCOPF- or ACOPF-based topology control plans (involving one or multiple TLS actions) may be suggested at a given hour for economic gains, it is demonstrated that the proposed decision making framework can efficiently recognize the final plan for reliable implementation.

The presented framework provides the TSOs with the tradeoffs between various objectives (system reliability, system stability, network loss, and system economics) when deciding on TLS adoption in bulk power grids. This suggested decision support tool will further help the decision makers to more reliably select the optimal TLS plans for final implementation.

5 CIRCUIT BREAKER HEALTH ASSESSMENT: THE KEY TO RELIABLE TRANSMISSION LINE SWITCHING

5.1 Introduction

Circuit Breakers (CBs) are defined as "*mechanical switching devices, capable of making, carrying, and breaking currents under normal circuit conditions and also making, carrying for a specified time and breaking currents under specified abnormal circuit conditions, such as those of short circuit*" [160]. Moreover, in contrast to fuses and other fault current limiting devices, CBs are the only switching devices that can interrupt (break) fault currents up to the highest short-circuit current levels and even after clearing the fault, CBs should be ready for service again [161].

The electric power grid is subject to interruptions ranging from cascading faults caused by extreme operating conditions, malicious external attacks, and intermittent electricity generation from renewable energy sources. As discussed in the earlier Sections, transmission lines, although traditionally regarded as static assets in power systems, are recently approached as the flexible means of system dynamic reconfiguration and topology. In this context, transmission line switching (TLS) technology can be employed in the utility day-to-day practical operations for the sake of reliability or economic gains.

Reliability of the CBs needs to be ensured at all times since if CBs do not operate as expected, faults cannot be isolated causing potentially catastrophic technical and economic consequences. Moreover, line availability is regarded one of the main concerns

in the switching and reconfiguration schemes. The performance of the CBs to reliably open and close when needed is crucial for successful implementation of switching actions. With the expected role of the topology control in future smart grid applications, high voltage CBs are expected to operate more frequently than ever before, which could accelerate their deterioration and wear/tear. If CB fails, it may lead to unsafe conditions for the field personnel working with the equipment. The maintenance management of the CBs is the key operational procedure that needs to be planned and scheduled, which emphasizes the need to use the advance monitoring technologies available in the market.

Several projects supported by the US Department of Energy (DOE) under the Green Electricity Network Integration (GENI) program have investigated the topology control solutions in power systems. An example project is the Robust Adaptive Topology Control (RATC) for grid operation [162]. This project explored the reliability of CB operation for the TLS applications at length for the first time.

5.2 System Architecture for Power System Topology Control Equipped with Automated Circuit Breaker Reliability Assessment Tools

System architecture for the future topology control solution is illustrated in Figure 34. The suggested solution consists of various analytic components, which can be divided into two main groups [162]:

- Topology Control Optimization, including various optimization algorithms that suggest the optimal topology and the associated transmission line switching plan.

- Support Data Analytics, which mainly employ processing of the substation data to evaluate the performance and condition of CBs, support identification of cascading events due to relay miss-operation, and relay setting coordination evaluation under the proposed topology switching.

As shown in Figure 34, the components of the system require data from various data sources: modeling data tools, market/planning tools, EMS tools (topology processor and state estimator), and substation event-triggered data. The data analytics provide support functions for the use of optimal topology algorithms. In the day-to-day practice, several worthwhile considerations have to be incorporated into the solution design and implementation [162]:

- Data integration and historical data archival for later use,
- Topology processor/state estimator outputs and substation based analysis,
- Security and reliability constraints under the switching optimization framework,
- AC feasibility and stability check on the proposed switching plans,
- Relay settings coordination evaluation to account for the relay setting changes due to the topology modification
- Eventually applying the switching decisions using the associated CBs.

Figure 35 illustrates a UML sequence diagram for a look-ahead economic benefit use case of the suggested solution for topology control. CB reliability evaluation component continuously assesses the CB condition and updates the corresponding line availability information, i.e. transmission the lines with less CBs should not be switched.

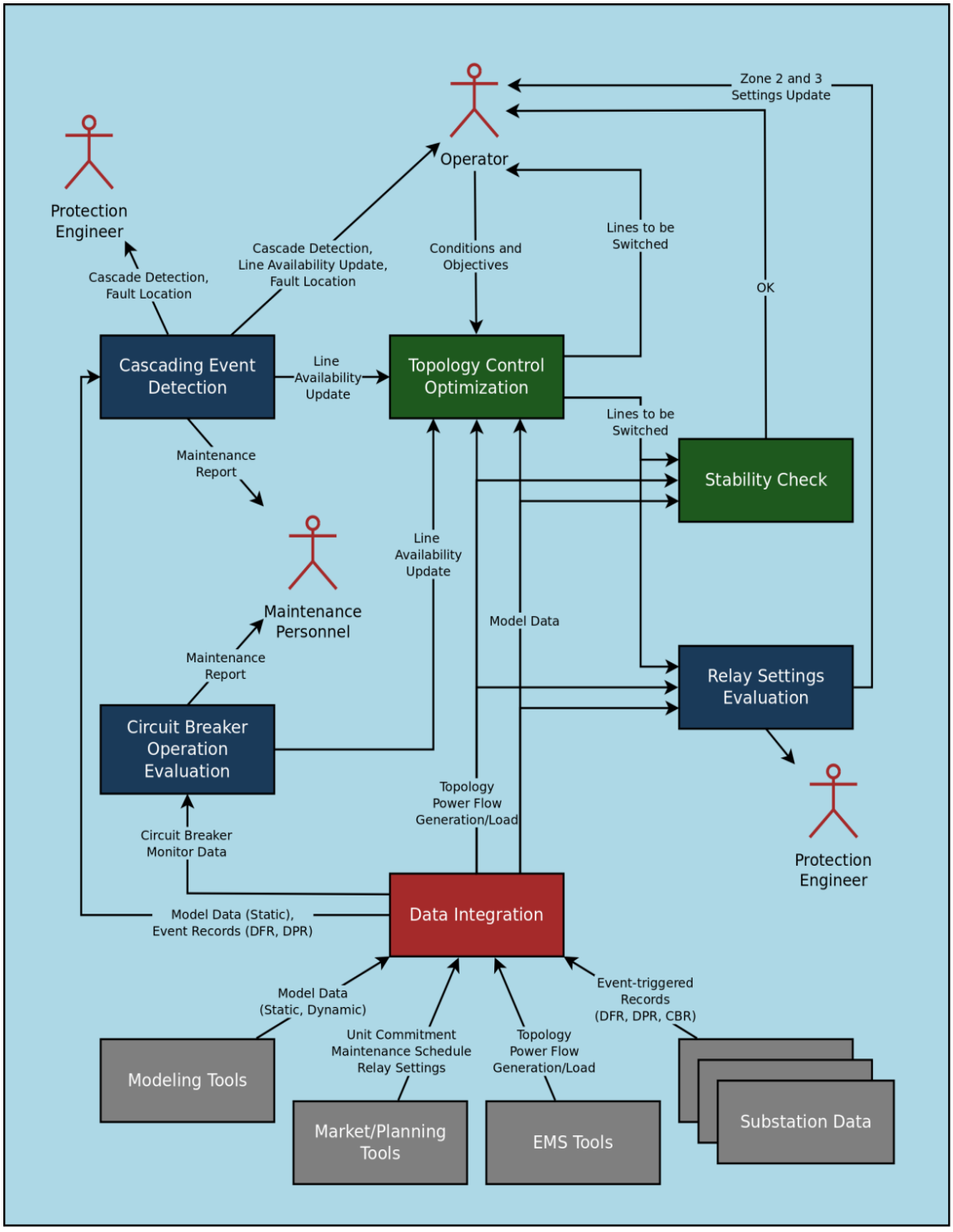

Figure 34. System architecture for the future application of topology control.

The operator initiates the topology control optimization and sets the objectives. The proposed line switching is evaluated for stability, and if the check is passed, the Relay Coordination Check component is activated. Based on the CB reliability status and other practical requirements, the operator then decides (selects among) the reliable switching sequence(s) for final implementation.

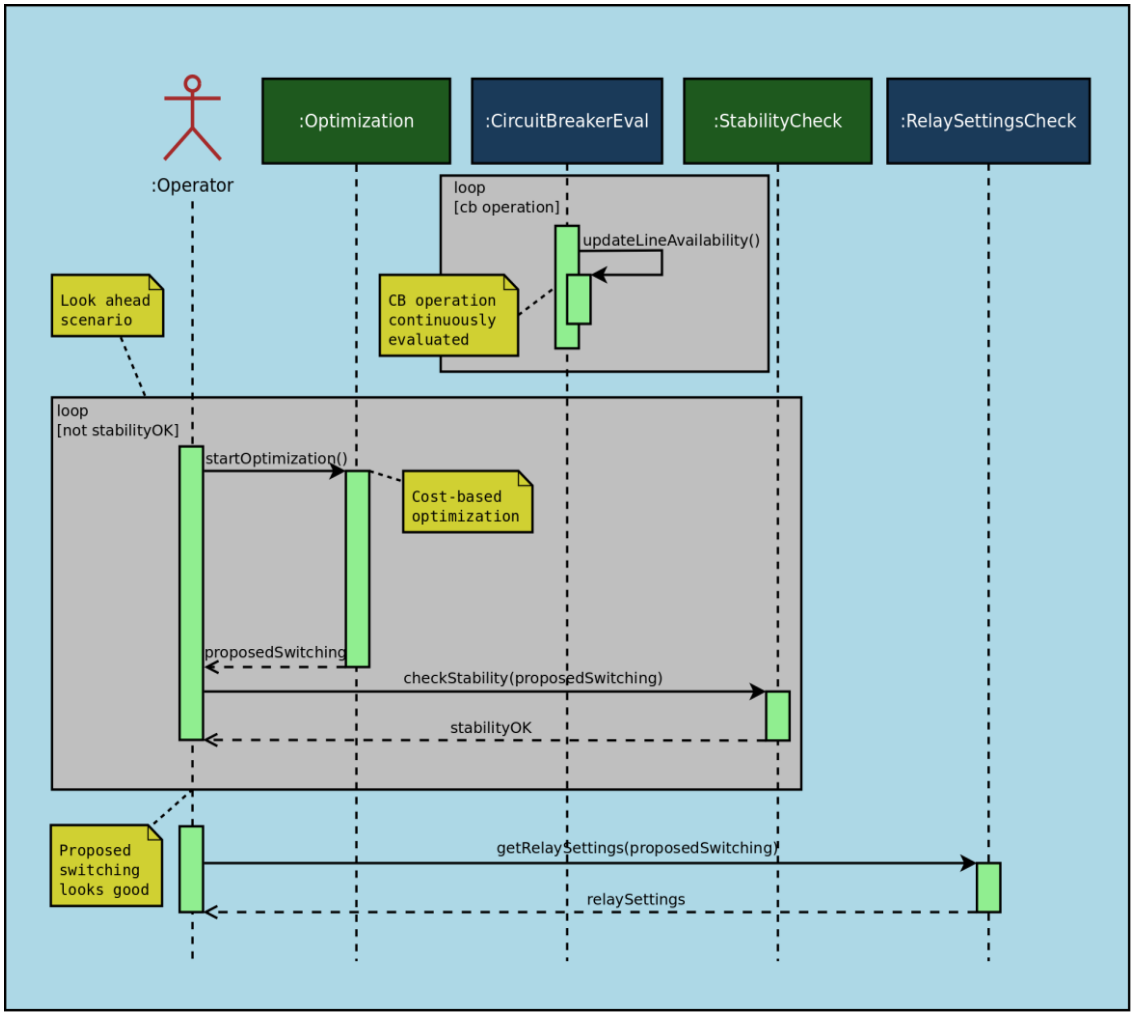

Figure 35. Continuous assessment of CB reliability to support the topology control.

CB reliability can be evaluated using the continuous monitoring and on-line condition-based projection of the failure probability. The monitoring covers variety of signals obtained within the CB control circuit and other subassemblies. In the next Section, the approach suggested for the automated reliability assessment of CBs is presented. Such information may be employed for determining the transmission lines available for implementation of the switching actions.

5.3 Quantitative Assessment of Circuit Breaker Health and Reliability for TLS

5.3.1 Background

In a classical model, the failure-repair process of a deteriorating device is commonly represented by a sequence of states of increasing wear and tear, i.e., D_1, D_2, and so on, finally leading to the equipment failure (F) as depicted in Figure 36.a [163]-[169]. Deterioration is, however, a continuous process in time which is usually demonstrated in discrete steps solely for the purposes of easier modeling. Depending on the sequence of maintenance actions, the stages do not just have to be showing deterioration, but also recovery, i.e. if the CB is repaired/ replaced, the state may go from failed to working/healthy states again. Maintenance effect can be also incorporated as demonstrated in the deterioration/recovery model in Figure 36.b for a 3-state deteriorating component, from which it is obvious that maintenance effect is to improve the component condition to that of the previous or healthy state through a replacement process. Further details on the topic are available in [163]-[169].

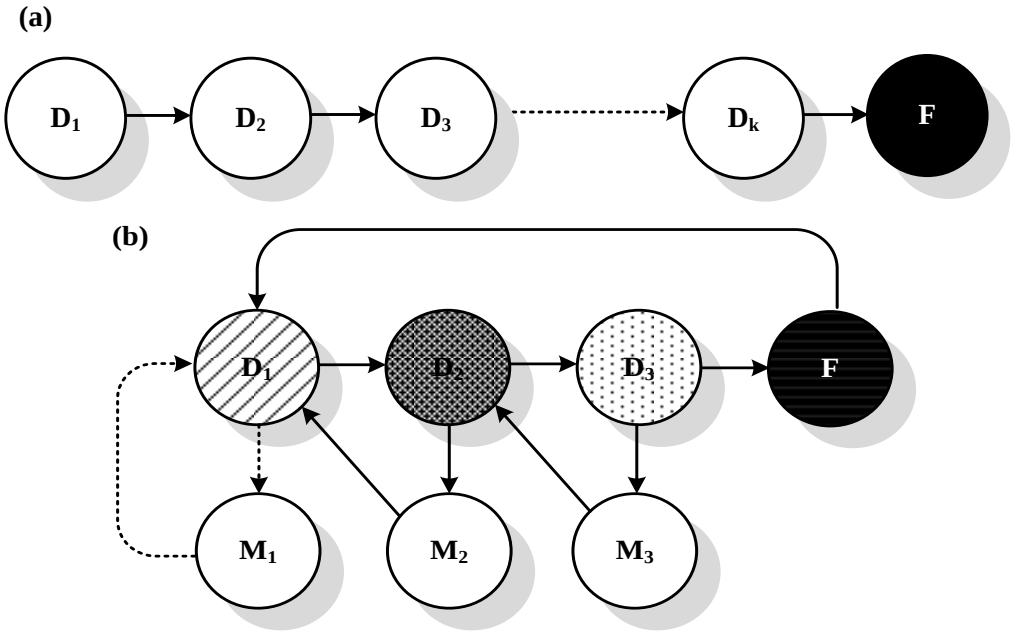

Figure 36. (a) Classic state diagram for a deteriorating component over time; (b) 3-state deterioration/recovery state diagram with maintenance effects [163].

Once knowing the component deterioration/recovery state as time elapses, one can not only differentiate various components of the same type in terms of maintenance consideration, but also can assign the proper preventive maintenance strategy based on the component condition. This could create considerable savings since maintenance can be done as needed, when and where necessary. The common way to identify the deterioration/recovery state for a component (CB in this dissertation) is by taking the past duration of its operation into account, e.g. the second state is reached, on average, in three years of the component being installed and operated, the third in six, and so on. The problem with this approach is that the mean time of the CB falling in each deterioration/recovery state is usually obtained from a large amount of historical data from

many of the CBs working under different operation environments, e.g., temperature, humidity, operation frequency, different voltage levels etc. The deviation among different CBs may impede the fair determination of the deterioration/recovery states. Moreover, the mean transition times between the states are generally uneven, may follow different distributions, and are commonly selected from the historical experiences or expert's judgment [163]-[172], which creates the possibility of making wrong or inaccurate decisions.

The operation count of the CBs starting from its installation time may also be employed to decide on their replacement and inspection requirements as time elapses; however, it cannot be used to assess the deterioration/recovery status of the CBs. It also gives no hints on the exact repair issue with the CB and hence, does not assign any real-time criticality to different CBs system-wide. In response, this dissertation approaches the problem with the main focus on the monitoring signals of the CB control circuit. The goal is to find a linkage between the monitoring signals, deterioration/recovery states of various CBs, and maintenance state distinction, accordingly.

5.3.2 Problem Description

Under a predictive maintenance model, the first question of concern is differentiating the CBs maintenance need in the overall system based on their deterioration/recovery levels and aging mechanisms. The need for maintenance is established through condition monitoring, which is based on the on-going inspection and surveillance of the CB operation to ensure its proper performance and to detect any

abnormalities, indication of an approaching failed state. References [173], [174] have proposed a methodology utilizing the CB control circuit electrical signals to define several performance indices. The proposed method employs the timing instants captured when CB operates (either opening or closing) to reflect the condition of CB's subassemblies, e.g., trip coil, close coil, auxiliary contacts, etc. Although the approach has formulated the general framework, it has not been yet explored in the context of CB practical life-cycle assessments where the deterioration/recovery states of CBs come to play. This ignores the possibility of different types of maintenance practices in different time intervals on various CBs in the system.

In response, this dissertation further sets the specified tolerance of timing instances, determined from the monitoring signals coming out of CB control circuit, into three bands each reflecting a different deterioration/recovery state. This gives a clearer definition of the healthy, vulnerable, and troubled states for a CB. The identification of the deterioration/recovery states, thus, can be achieved through continuously checking whether one or more of timing signals have violated the accepted limits. The index of reliability, i.e., deterioration/recovery state probability, can be then calculated and updated as new monitoring data comes in. While the methodology proposed in this Section is not the Markov process conventionally used in maintenance analysis of system components, similar structure which gives the user a hint for Markov analysis is employed. The presented approach helps identifying the probability of each CB experiencing various deterioration stages, which is helpful in trying to more realistically find the optimum

transition rates (e.g., inspection rate or maintenance rate) facilitated by using the Markov modeling and reliability analysis on that basis.

5.3.3 Circuit Breaker Condition Monitoring and Data Requirements

According to a survey conducted by CIGRE Working Group, CB failures are mostly found to be caused by an malfunction of operating mechanism and control circuit, and in that order compared to other CB subassemblies [175]-[178]. Aging, wear, and corrosion are also reported as the most common cause of major failures in CBs. As a result, the control circuit part of the CB is selected for the condition assessment using the associated monitoring signals. There are portable monitoring devices, available on the market, and sensors of various types that can be installed on different sub-assemblies of CBs, which are able to gather and display the control circuit signals, i.e., both analog and/or digital waveforms [179]-[181].

A CB monitoring (CBM) infrastructure for the main sake of acquisition and automated analysis of the condition monitoring data is introduced in [182]. Once triggered via the operator action in the control house, a relay, or a control device, an initiate signal is sent to CB control circuit to start its operation either opening or closing. The initiate signals are then referred to the trip or close coil through the auxiliary contacts and control relays to energize the coils. This, in turn, creates a coil current. The coil current is measured across a shunt that is placed in series with the coils. In fact, monitoring of coil currents provides insights into the condition of both the coil and operating mechanism. The coil current activates a plunger leading to movement of the operating mechanism. The

stored energy is used then to move all the CB mechanical parts and open/close the main interrupting contacts. As the CB opens/closes its main contacts, the CB auxiliary (52a) and (52b) contacts change the state. The A and B contact signals (52a and 52b), indicating the voltage across auxiliary switches, are monitored which signify the CB status either opening or closing.

Any observed inconsistency may indicate a wrong cable connection or a problem with the operating mechanism. Y coils (52Y) are used to prevent multiple-close attempts in a close operation [182]. Trip and close coil (TC or CC) current as well as the A and B contact (52a and 52b) voltage signals are the most important signals under monitoring employed in the analysis of this Section to investigate the aging and deterioration level of CBs. Usually abnormal behavior of signal waveforms implies an existing problem or developing failure. Since the difference between transitions of auxiliary contacts indicates the relative speed of CB operation, any changes of the signals may sense a deteriorated contact, a binding between the contacts leading to a slow CB operation, etc. [182]. The excessive noise during the contact transition indicates a dirty auxiliary contact; the excessive voltage drop of DC voltage indicates a battery problem and so on. Signal processing modules are developed to extract the timing of the close operation. These timing instants should occur within the manufacture specified tolerance bands to ensure that the CB is functioning properly.

The events representing the change in the signals need to occur in a specific order for a proper CB operation. An example in the case of CB close operation is demonstrated in Figure 37 and the associated timing parameters describing the sequence of breaker

operation are introduced in Table 9. Based on the preliminary research in [173] and [174], only timing parameters t_2–t_6 are selected for analysis in this Section, as tabulated in Table 9. The mal-functions in CBs may result from various parts such as interrupters, dampers and so on. Due to criticality of control circuit in CB proper operation according to [175]-[178], the proposed method has considered control signals for condition assessment of CBs since they are the only major source of monitoring data available in the utilities.

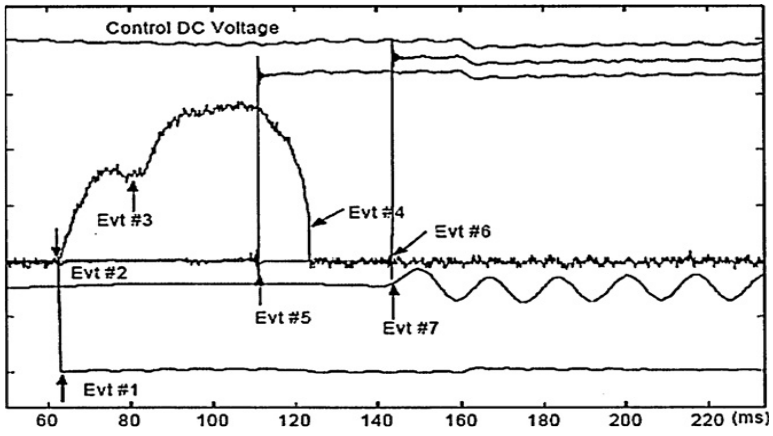

Figure 37. Monitored coil current waveform during the CB close operation [182].

Table 9. CB Events and the Corresponding Signal Timing Parameters

Event	Event Description	Signal Parameter
1	Trip or close operation is initiated	t_1
2	Trip coil current picks up	t_2
3	Trip coil current dips after saturation	t_3
4	Trip coil current drops off	t_4
5	“b” contact breaks or makes (a change of status from low to high or vice vresa)	t_5
6	“a” contact breaks or makes	t_6
7	Phase current breaks or makes	t_7

This methodology helps in extracting the most relevant information out of the control circuit raw monitoring data, useful for the operator and maintenance personnel.

To serve as an example, a group of monitored signals covering both analog and digital ones is illustrated in Figure 38 for the CB opening and closing operations. In the conventional use of the technology, the CB operation parameters are collected over time, but are not used until the breaker is operated and files are downloaded. The monitored data is then analyzed and a specific maintenance action is decided in response. This view is mostly based on the corrective maintenance concept. This approach does not give a clue about the overall health and reliability of the CB over time, which can be helpful in investment decisions about the replacement or repair plans. The solution suggested in this research provides a quantitative approach to evaluate the health and reliability of the CBs separately for opening and closing operations. Such indices of reliability could support other operational decisions in power systems including the reliable implementation of transmission line switching and topology control scenarios as explained earlier.

More information on the importance of CB monitoring and maintenance management, specifically the suggested approach based on the CB control circuit monitoring signals is provided in Appendix 4.

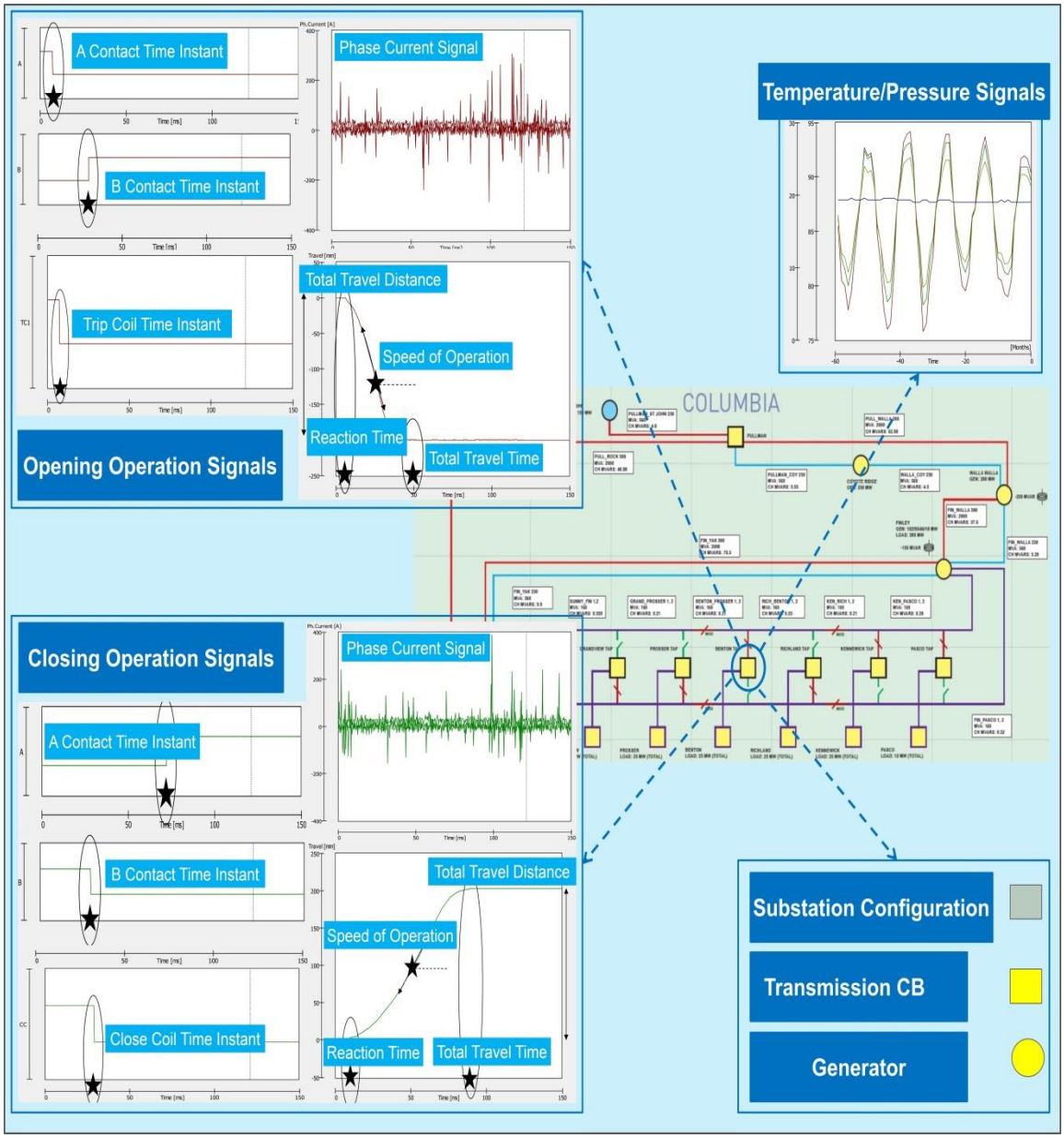

Figure 38. Monitoring CB operations at the substation level to assess its reliability.

5.3.4 Proposed Formulation

5.3.4.1 Probabilistic Treatment of the CB Signal Measurement

CB reliability analysis is approached in this Section in terms of failure probability. A practical approach is devised to assign the failure probabilities considering the monitoring signal parameters. In sub-Section 5.3.4.1, a procedure for assigning the probability distribution to each timing signal parameter is proposed. Sub-Section 5.3.4.2 deals with the condition assessment of CB and the associated subassemblies based on the assigned probabilities. And finally comes the methodology on how to set a correlation between the probabilities and the CB life-cycle deterioration/recovery states in sub-Section 5.3.4.3 and 5.3.4.4.

Conducting some on-line measurements via the CB monitoring devices, both for CB opening and closing operations, a set of data for each signal timing parameter can be recorded. A probability distribution can then be assigned to these timing measurements. According to the Central Limit Theorem (CLT), with the increase in the sample size (sufficiently large), the distribution of the random variables approaches the normal distribution irrespective of the shape of the original distribution [183]. Due to the fact that monitoring data is accumulated with time and that sample size will be large enough, normal distribution can be reasonably adopted in such studies. Besides, it is mathematically easier to deal with normal distribution. Hence, normal distribution is assumed in this work for all signal parameters listed in Table 9, as illustrated in Figure 39 for parameter t_2. The proposed approach is, however, generic enough to be adopted with different types of probability distributions as data may dictate in various applications. Note

that in many practical cases, the methods developed using normal theory work quite well even when the distribution is not normal.

To proceed with the methodology, three bands for every timing parameter are proposed each reflecting different deterioration/recovery levels of a CB, i.e., healthy, vulnerable, and troubled states. If one new value of t_i falls in the health margin, then it indicates a proper operation of the breaker, reflected by that time instant t_i. Similarly, one new value of t_i may fall in the second band meaning that the associated parts of CB respond with some delays and may be in the vulnerable deterioration state or may require maintenance. One new value of t_i could fall in the third margin span suggesting that the associated CB parts and subassemblies cannot respond correctly in time and may be in the troubled state; hence in a vital need of maintenance. If t_i falls out of the entire proposed

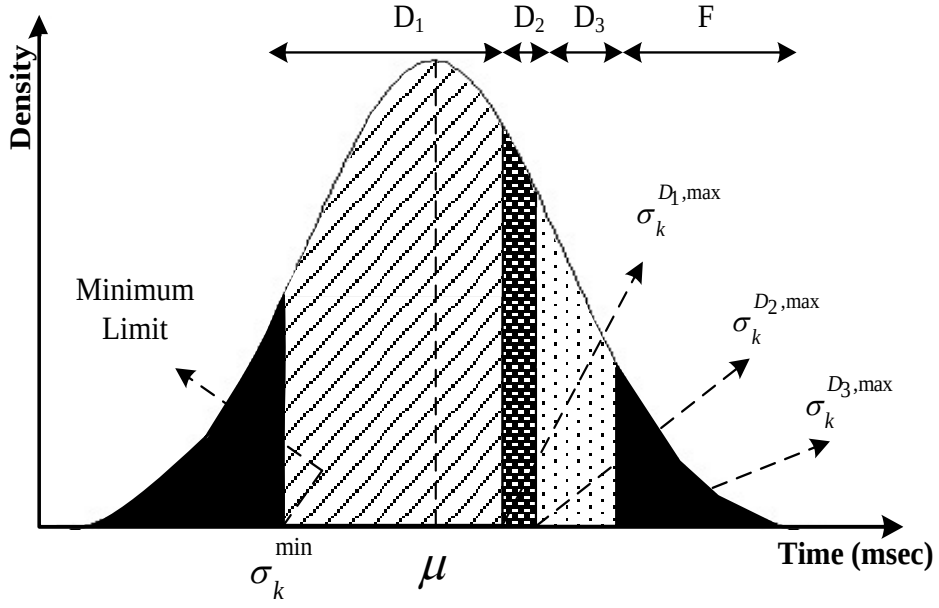

Figure 39. Probability distribution and the bands assigned to timing parameter t_2.

margin spans, it can be concluded that there is something wrong going on associated with the close coil operation of the CB which is an indicative of the failed state. These limits may be different for different types of CBs, but are the same for the CBs of the same type in a substation.

With the accumulation of monitoring data from the CBs of the same type in a substation with certain operational practices and geographical/operation conditions, these boundaries can be determined as the benchmark based on the historical data on the CB operation over time, operator expertise, expert systems and data mining approaches [180], [181]. Interestingly enough, similar limits for CB timing parameters can be automatically set around the values measured during the commissioning process and are, nowadays, being taken into account and supported by some monitoring devices of different vendors, in real world practices [177]. For instance, in the case of the ABB CBS monitoring device, the set up begins by selecting the ABB breaker type followed by the mechanism type. By doing so, breaker specific default settings are recalled. The timing settings are defined through test operations while the CBS is in a special learning mode. The tool also allows the user to modify the default settings depending on the conditions of the CB. These boundaries are selected as the threshold sets for each type of CB in a substation and can help in determining the wear condition of the CB when passes the desired thresholds [177].

In general, and according to the probability distribution assigned, the probability of a CB falling into each deterioration/recovery state margin with respect to the timing parameter t_i can be calculated in (5.1)-(5.4), respectively for the healthy, vulnerable, troubled, and failed states.

$$P_{B_k}^{t_i,D_1} = \int_{t=\sigma_k^{\min}}^{t=\sigma_k^{D_1,\max}} f_{B_k}^{t_i}(t)dt \tag{5.1}$$

$$P_{B_k}^{t_i,D_2} = \int_{t=\sigma_k^{D_1,\max}}^{t=\sigma_k^{D_2,\max}} f_{B_k}^{t_i}(t)dt \tag{5.2}$$

$$P_{B_k}^{t_i,D_3} = \int_{t=\sigma_k^{D_2,\max}}^{t=\sigma_k^{D_3,\max}} f_{B_k}^{t_i}(t)dt \tag{5.3}$$

$$P_{B_k}^{t_i,F} = 1 - \sum_{j=1}^{3} P_{B_k}^{t_i,D_j} \tag{5.4}$$

These probabilities are used in the rest of the Section analysis to define some performance indices for various subassemblies of a CB. Noteworthy is that the proposed approach can be employed in dealing with both the opening and closing operation of the CB when assessing the condition.

5.3.4.2 Reliability Performance of CB Subassemblies

Some CB subassemblies are to be monitored continuously (each time breaker operates) using the monitoring signals.

- **Performance of CB Trip Coil**

As can be traced in Figure 40.a, a sample representation of the trip coil current is demonstrated. The trip coil current signal, in general, should be fairly smooth except for a dip at the beginning and abrupt change at the moment the tail end of the waveform starts decaying. Once the trip initiate input is active, the coil current makes a gradual transition

to a nonzero value at time "t_2". The time instant "t_3" corresponds to the time at which the operating mechanism starts moving using the trip coil energy. The coil current starts dropping down to zero at time "t_4". Possible abnormalities regarding the trip coil can be pointed out as the pickup delayed, dip delayed, drop-off delayed, etc. In the worst case, the aforementioned abnormalities may result in the CB not opening when it is supposed to. These abnormalities can be addressed by the probabilities $P_{B_k}^{t_2}$, $P_{B_k}^{t_3}$, and $P_{B_k}^{t_4}$ reflecting the timing parameters "t_2", "t_3", and "t_4". These time instants should be always kept within

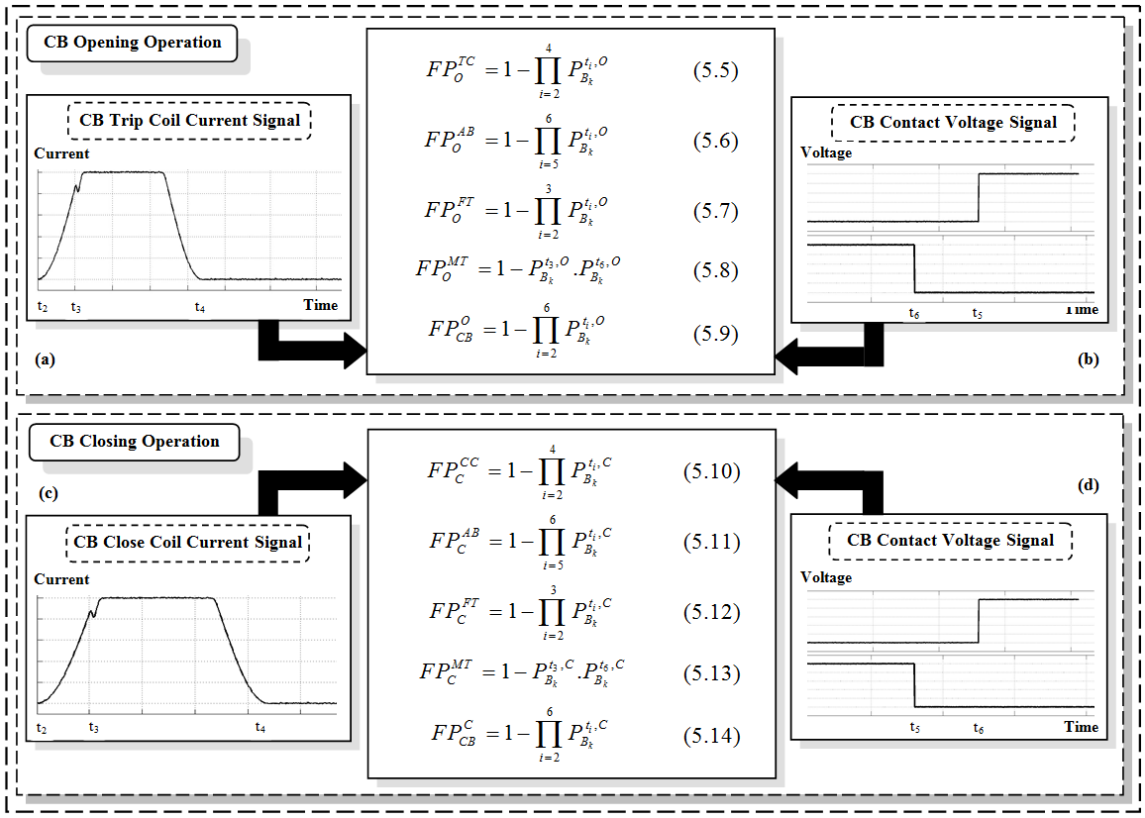

$$FP_O^{TC} = 1 - \prod_{i=2}^{4} P_{B_k}^{t_i,O} \quad (5.5)$$

$$FP_O^{AB} = 1 - \prod_{i=5}^{6} P_{B_k}^{t_i,O} \quad (5.6)$$

$$FP_O^{FT} = 1 - \prod_{i=2}^{3} P_{B_k}^{t_i,O} \quad (5.7)$$

$$FP_O^{MT} = 1 - P_{B_k}^{t_3,O}.P_{B_k}^{t_6,O} \quad (5.8)$$

$$FP_{CB}^{O} = 1 - \prod_{i=2}^{6} P_{B_k}^{t_i,O} \quad (5.9)$$

$$FP_C^{CC} = 1 - \prod_{i=2}^{4} P_{B_k}^{t_i,C} \quad (5.10)$$

$$FP_C^{AB} = 1 - \prod_{i=5}^{6} P_{B_k}^{t_i,C} \quad (5.11)$$

$$FP_C^{FT} = 1 - \prod_{i=2}^{3} P_{B_k}^{t_i,C} \quad (5.12)$$

$$FP_C^{MT} = 1 - P_{B_k}^{t_3,C}.P_{B_k}^{t_6,C} \quad (5.13)$$

$$FP_{CB}^{C} = 1 - \prod_{i=2}^{6} P_{B_k}^{t_i,C} \quad (5.14)$$

Figure 40. General formulations for the failure probability estimation of CB subassemblies in both opening and closing operations.

the margins to assure the proper operation of the trip coils. As a result, the performance index associated with the trip coil is defined as the probability that it will fail to operate properly, as demonstrated in (5.5).

- **Performance of CB Auxiliary Contacts**

As the CB opens its main contacts, the status of the auxiliary "a" and "b" contacts is also changed as can be seen in Figure 40.b. Some possible abnormalities regarding the operation of "a" and "b" contacts can be considered including the delay in transition, premature transition, unstable contacts, noise, and contacts bounce. The auxiliary contacts can properly operate only if the timings "t_5" and "t_6" fall within their tolerance span. The performance index reflecting the auxiliary contacts operation can be defined as the probability that the auxiliary contacts fail to operate properly, as introduced in (5.6).

- **Performance of CB Operating Mechanism**

The time period between the instant at which the trip coil current (TC) rises, i.e., "t_2", and the instant at which the dip occurs, i.e., "t_3", is called the free travel time which reflects the performance of the trip latch mechanism. So, the timing parameters need to fall in the tolerance limits for the CB to exhibit a normal free travel time. The corresponding performance index is defined as the probability that free travel time is abnormal, as introduced in (5.7) in Figure 40.

The coil current also needs to correlate with the event of change of "a" or "b" contact. The time period between the dip and the change of the "a" contact for open operation is the mechanism travel time whose normal value is ensured once the timings "t_3" and "t_6" fall in their corresponding tolerance limits. Any notable violation in these

timings can be reported as the CB abnormal operation. So, the corresponding performance index is defined as the probability that the mechanism traveling time is abnormal, as formulated in (5.8) in Figure 40.

- **CB Total Performance**

In addition to the performance evaluation of the CB different subassemblies, an index to evaluate the CB overall performance is proposed. If none of the timing parameters, i.e., "t_2" to "t_6", which are extracted out of the control circuit monitoring signals via the signal processing techniques, is violated, one can conclude the CB operation in either opening or closing is proper. In other words, if any of these timings fall out of the corresponding tolerance limits, one can conclude there is a failure. In response, the CB failure probability, i.e., the probability that the CB does not open properly, is estimated in (5.9) in Figure 40. Similar discussions can be made for the CB closing operation whose derivations are formulated through (5.10)-(5.14) in Figure 40.

5.3.4.3 CB Deterioration/Recovery Model

According to equations (5.5)-(5.14) describing the failure probability assessment of CB subassemblies, an approach to derive the life-cycle deterioration/recovery state probabilities of each CB subassembly is proposed next. The three CB subassemblies under study, i.e., CB trip coil, close coil, and contacts, are taken into consideration here. The performance indices associated with the CB opening/closing operation are elaborated in detail.

- **CB Trip Coil Deterioration/Recovery Level**

The probability of a CB trip coil subassembly falling into the failed, troubled, vulnerable, and healthy states can be reached through (5.15)-(5.18), respectively.

$$P_O^{TC,F} = 1 - \prod_{i=2}^{4} \left(1 - P_O^{t_i,F}\right) \tag{5.15}$$

$$P_O^{TC,D_3} = 1 - \left(P_O^{TC,F} + \prod_{i=2}^{4} \left(\sum_{j=1}^{2} P_O^{t_i,D_j} \right) \right) \tag{5.16}$$

$$P_O^{TC,D_2} = 1 - \left(P_O^{TC,F} + P_O^{TC,D_3} \right) - \prod_{i=2}^{4} P_O^{t_i,D_1} \tag{5.17}$$

$$P_O^{TC,D_1} = \prod_{i=2}^{4} P_O^{t_i,D_1} \tag{5.18}$$

- **CB Auxiliary Contacts Deterioration/Recovery Level**

Similarly, the probability of a CB auxiliary contacts falling into the failed, troubled, vulnerable, and healthy states can be reached through (5.19)-(5.22), respectively.

$$P_{O/C}^{AB,F} = 1 - \prod_{i=5}^{6} \left(1 - P_{O/C}^{t_i,F}\right) \tag{5.19}$$

$$P_{O/C}^{AB,D_3} = 1 - \left(P_{O/C}^{AB,F} + \prod_{i=5}^{6} \left(\sum_{j=1}^{2} P_{O/C}^{t_i,D_j} \right) \right) \tag{5.20}$$

$$P_{O/C}^{AB,D_2} = 1 - \left(P_{O/C}^{AB,F} + P_{O/C}^{AB,D_3} \right) - \prod_{i=5}^{6} P_{O/C}^{t_i,D_1} \tag{5.21}$$

$$P_{O/C}^{AB,D_1} = \prod_{i=5}^{6} P_{O/C}^{t_i,D_1} \tag{5.22}$$

- **CB Close Coil Deterioration/Recovery Level**

Probability of a CB close coil reaching the failed, troubled, vulnerable and healthy states can be calculated through (5.23)-(5.26), respectively.

$$P_C^{CC,F} = 1 - \prod_{i=2}^{4} \left(1 - P_C^{t_i,F}\right) \tag{5.23}$$

$$P_C^{CC,D_3} = 1 - \left(P_C^{CC,F} + \prod_{i=2}^{4} \left(\sum_{j=1}^{2} P_C^{t_i,D_j} \right) \right) \tag{5.24}$$

$$P_C^{CC,D_2} = 1 - \left(P_C^{CC,F} + P_C^{CC,D_3} \right) - \prod_{i=2}^{4} P_C^{t_i,D_1} \tag{5.25}$$

$$P_C^{CC,D_1} = \prod_{i=2}^{4} P_C^{t_i,D_1} \tag{5.26}$$

5.3.4.4 CB Deterioration/Recovery State Probability

Similar to the previous analysis, the probability of a CB, in general, transitioning into the failed, troubled, vulnerable, and healthy states can be calculated through (5.27)-(5.30), respectively. As a consequence, one can differentiate the CBs in the system from the life-cycle viewpoint, since different CBs can have different probability distributions for each deterioration/recovery state.

$$P_{CB,O/C}^{F} = 1 - \prod_{i=2}^{6} \left(1 - \sum_{j=1}^{3} P_{O/C}^{t_i,D_j} \right) \tag{5.27}$$

$$P_{CB,O/C}^{D_3} = 1 - \left(P_{CB,O/C}^{F} + \prod_{i=2}^{4} \left(\sum_{j=1}^{2} P_{O/C}^{t_i,D_j} \right) \cdot \prod_{i=5}^{6} \left(1 - P_{O/C}^{t_i,F}\right) \right) \tag{5.28}$$

$$P_{CB,O/C}^{D_2} = 1 - \left(P_{CB,O/C}^{F} + P_{CB,O/C}^{D_3} + \prod_{i=2}^{6} P_{O/C}^{t_i,D_1} \right) \tag{5.29}$$

$$P_{CB,O/C}^{D_1} = \prod_{i=2}^{6} P_{O/C}^{t_i,D_1} \tag{5.30}$$

The CBs possessing higher probabilities associated with the troubled state would call for a major maintenance action and those of higher failure probability would be essentially in need of prompt part replacements. The proposed methodology can be applied for any other subassemblies of CBs. The proposed algorithm can be updated during time. Once the new monitoring data scan arrives, the associated timing values can be extracted employing the signal processing module. Then, the new probability distributions are assigned and the updated probabilistic indices can be calculated through (5.15)-(5.30).

5.4 Numerical Analysis

5.4.1 Algorithm Uses of Recorded Monitoring Data

To illustrate the applicability of the proposed methodology in real world practice, history of the signals coming from the control circuit of a 38 KV SF6 CB, i.e., a GE VIB-15.5-20000-2 manufacturer type one, containing 18 number of samples for opening operation is documented and the associated timing parameters are extracted employing the signal processing tool previously developed in [182].

Detailed description of data sets and how the measurements are done can be found in [182]. The tolerance limits for the signal timing parameters reflecting the deterioration/recovery level decisive thresholds are devised as demonstrated in Table 10.

5.4.2 Application Considerations

We decided to use normal distribution as the assigned probability distribution to the extracted timing parameters. The method is generic enough to be adopted with different type of probability distributions as data dictates in various applications. Due to the space limit, only the signals for the CB opening operation have been taken into account in this Section for the sake of demonstration. Employing equations (5.15)-(5.18) and according to the limits and thresholds in Table 10, the deterioration assessment is done for

Table 10. CB Deterioration Level Thresholds for Signal Timing Parameters

Event	$\sigma_k^{\min}$	$\sigma_k^{D_1,\max}$	$\sigma_k^{D_2,\max}$	$\sigma_k^{D_3,\max}$
t_1	0.00	1.00	1.50	2.00
t_2	13.6	16.1	17.4	18.6
t_3	26.4	30.9	33.2	35.4
t_4	28.7	33.7	36.2	38.7
t_5	22.4	27.4	29.9	32.4

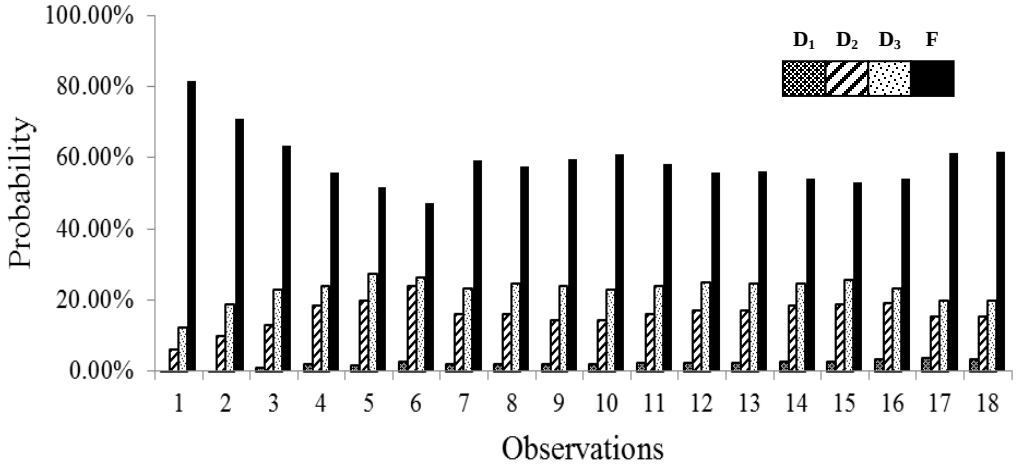

Figure 41. Probability of the CB trip coil staying in each deterioration state.

The CB trip coil, as illustrated in Figure 41. As it can be observed in this figure, the CB trip coil is mostly in its failed state of deterioration since the associated failure probability is far more than that of the other deterioration/recovery states in all the observations done during the time period under study. It reflects the fact that the CB trip coil is in a critical need to be repaired or replaced.

Similar procedure can be pursued for the “a” and “b” contacts of the CB using equations (5.19)-(5.22). As demonstrated in Figure 42, it can be concluded that the auxiliary contacts have been performing quite well during the first observations but are in the troubled state since the probability of this state overweighs the rest in the first few observations. It can also be traced that the probability of vulnerable state has gone ahead of that of the troubled state after a while, which reflects some maintenance practices done on the “a” and “b” contacts during the studied time interval. As a consequence, one may conclude that the CB contacts may call for minor maintenance activities to maintain their proper functionality.

One can likewise evaluate an overall deterioration/recovery level of a CB as a stand-alone component with the aid of the proposed approach using equations (5.27)-(5.30). As can be seen in Figure 43, the results obtained for the CB under study demonstrate that the CB is constantly on the edge of failed state due to the abnormal operation of different subassemblies and high failure probability assigned. A major maintenance is in urgent need in response. Based on these performance probabilities, one can easily get to a conclusion regarding the overall deterioration/recovery status of the CB, as tabulated in the classical life cycle model in Table 11.

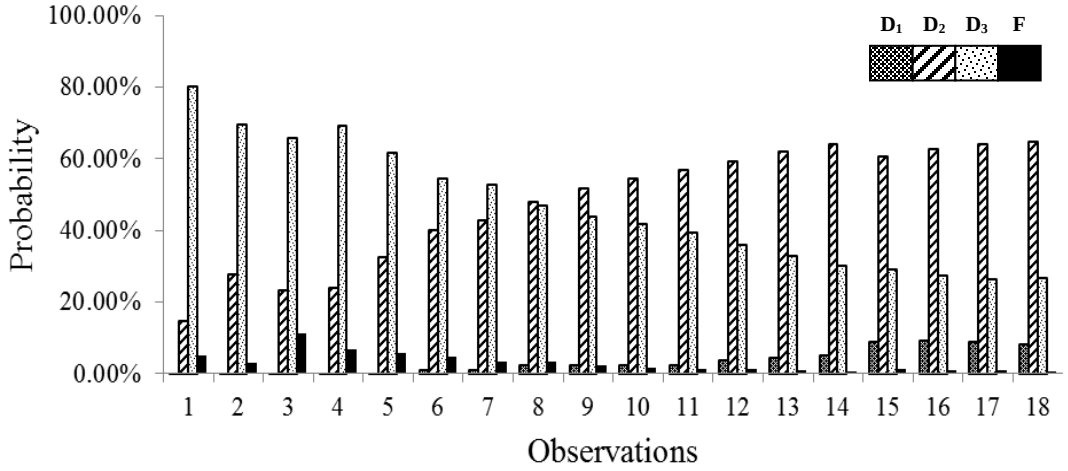

Figure 42. Probability of the CB AB contacts staying in each deterioration state.

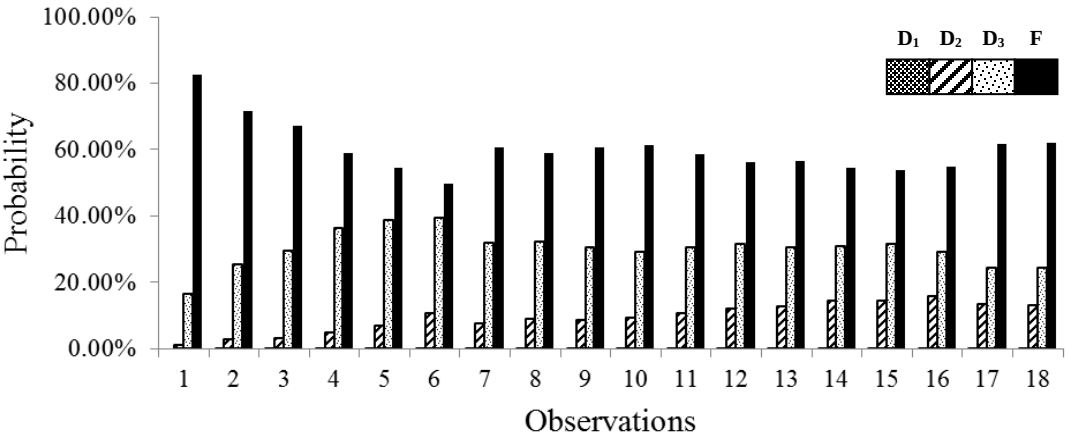

Figure 43. Probability of the CB, as a component, in each deterioration state.

Table 11. CB Deterioration Level Thresholds for Signal Timing Parameters

Deterioration/Recovery State	**D1**	**D2**	**D3**	**D4**
$P_{CB,O}^{D_i}$	0.28%	13.21%	24.40%	62.11%

5.4.3 Discussion on the Impacts of Maintenance

Maintenance is of considerable impact on the deterioration/recovery behavior of a component in terms of condition improvements. Consequently, one may be interested in investigating the effects of maintenance on the CB deterioration/recovery status implementing the proposed methodology. In this regard, the following considerations are made [163]-[169], [181]:

- CB, as a component, is assumed to have four deterioration/recovery states, introduced earlier, where in the vulnerable state, the CB will still work properly. The objective is to keep the CB at least working in vulnerable state, and look for timely maintenance.
- In the troubled state, the CB could still work but on the edge of failure. In the failed state, the CB may or may not work as expected; the open/close operation is not reliable at all and a large breaker operation delay may exist.
- There are three types of maintenance states assigned: minor for vulnerable condition, major for troubled condition, as well as failure repair (replacement) for failed condition. Take into account that these are all among the preventive maintenance considerations and not the corrective maintenance actions, which are commonly done on the CB after it fails.
- Maintenance should not turn the CB into a worse state, i.e., maintenance activities are assumed to be judiciously applied with no drawbacks. So, the states can be recovered/ improved via maintenance/repair.

- Minor maintenance will only bring the CB into the prior deterioration/recovery state; for instance, troubled state to vulnerable state, but will not lead to the healthy state directly from the troubled deterioration state. A major maintenance action can bring CB to healthy state.
- Minor and major repair actions have very small impact in turning the failed CB into a healthy state since a replacement has to be considered if aiming so.

Taking the above introduced assumptions into account and assuming the data presented in [166] and [169], the effect of different maintenance policies on the CB in different deterioration/recovery states can be quantified as demonstrated in two case studies in Table 12 and Table 13. It is obvious that the probability of successfully bringing the CB into a better working state following major maintenance is larger than following the minor maintenance [184], [185].

As noted earlier, maintenance attempts are devoted to keep the CB being at least in the vulnerable state (i.e., the sum of probability of the D_1 and D_2 larger than 85% after maintenance) before any action is taken. In the first case in Table 12, the analysis shows that the CB is very likely to be in a faulted situation. Even after a major maintenance, the total probability of D_1 and D_2 is 42.61% which implies that a repair is in an urgent need. In the second case, the analysis results demonstrate that the CB is in its pretty good working state with a very small possibility of having damages. A minor maintenance could bring the CB into a state with a 90.5%, as the total probability of D_1 and D_2. However, a major maintenance, as a means of preventive action, which may cost more than ten times of the minor one, will only improve the overall reliability performance a bit better [166].

Table 12. Effects of Maintenance on the CB Deterioration/Recovery: Case I

	Deterioration/Recovery State Probability			
	D_1 (%)	**D_2 (%)**	**D_3 (%)**	**F (%)**
Before maintenance	0.28	13.21	24.40	62.11
Minor maintenance	9.53	21.04	10.43	59.00
Major maintenance	35.99	6.62	7.41	49.98
Failure repair	99.00	0.91	0.08	0.01

Table 13. Effects of Maintenance on the CB Deterioration/Recovery: Case II

	Deterioration/Recovery State Probability			
	D_1 (%)	**D_2 (%)**	**D_3 (%)**	**F (%)**
Before maintenance	20	60	15	5
Minor maintenance	62.00	28.50	4.75	4.75
Major maintenance	88.00	7.85	2.00	2.15
Failure repair	99.20	0.78	0.02	0

Thus, one could make a conclusion that the proposed model will not only identify the cause of deterioration in a timely manner, but it could also give an optimized economic maintenance solution.

The following points are worthy to note regarding the observations made:

- The calculated failure probability of the CB (more than 50%) reflects that some parts of the CB under study responsible for the trip operation are not reliable enough and need maintenance. The failure probability index calculated here in real-time is different from the failure rate index (number of failures per year) commonly used in system reliability studies. Failure probability used here reflects

the CB condition at any given time. As a result, the two indices are different in unit and order of magnitude (failure rate is usually a very small value).

- Historical records are initially used to get an estimate of the CB reliability index as proposed in this Section. Such data may be acquired during time and with the operation of the CB by the monitoring devices. The probability distribution will then be updated as new data arrives. This gives a dynamic update of failure probability of CB in real time as time passes.
- The proposed approach considers the CB failures mainly related to the breaker timing parameters that can be recognized by the control circuit monitoring signals. Some mechanical failures in the release and operating mechanisms as well as contact overheating, dielectric breakdowns, nozzle damages, incorrect assembly after maintenance, etc. may also affect the timing of the switching operation. Moreover, sudden mechanical breakdowns, corrosion, leaks, and a wide variety of different wear and tear processes may be very difficult to detect. The research presented in this Section of the dissertation helps where the control circuit signals are the only or major source of monitoring data available in utilities, which is not rare in practice today. This also highlights the need for more comprehensive research on predictive asset maintenance management.
- Conducting the same procedure for every CB in a substation would lead to a reasonable differentiation of CBs maintenance scheduling and asset management practices. Making such a distinction between different CBs throughout a power system would definitely open new opportunities for the cost-effective asset

management decisions. It may be of interest to conduct a cost/benefit analysis to assess the economic aspect of putting the proposed approach in practice in the future. The gained economic benefits of the proposed monitoring scheme should outweigh the costs of device replacement and installation, fault detection, and assessment of CB condition monitoring over time.

5.5 Conclusions

The followings are some advantages of contributions elaborated in this Section:

- A quantitative approach to assess the reliability status of individual CBs and its subassemblies in real time is proposed.
- The proposed methodology uses the field monitoring signals from CB control circuit, which takes the advantage of increasing deployment of smart sensors and monitoring devices in the system.
- The presented approach allows a quantitative assessment of CB status leading to the classification into different deterioration/recovery states in real time.
- The real-time deterioration/recovery states differentiate the status of all the CBs in the system, which in general, is a helpful and reliable criterion as time elapses.
- Deterioration-based distinction helps in improving the system-wide maintenance scheduling and asset management practices to answer where, when, and how to perform the maintenance tasks on the system CBs.

- While only monitoring of CBs is considered in this research work, the same concept can be extended to other power system assemblies, e.g., transformers, insulators, etc. [186], [187].
- Since the most critical prerequisite for reliability and maintenance analyses is the past historical records, benefiting from a data gathering structure is an imperative. This, indeed, is in line with the increasing trend in system-wide application of monitoring devices.
- This CB monitoring approach helps a more reliable and informed decision making for TLS implementation in practice as it unfolds the reliability of the associated CBs and, correspondingly, the availability of the transmission lines selected for optimal TLS implementations.

6 POWER SYSTEM TOPOLOGY CONTROL DECISION MAKING SUPPORT TOOL FOR CORRECTIVE RECOVERY AND ENHANCED RESILIENCE*

6.1 Introduction

Bulk electric transmission systems have been traditionally characterized with static assets and fixed configuration over time except in the cases of faults and forced outages. Power system topology control, often called transmission switching (TLS), offers the system operators an opportunity to harness the flexibility of the transmission system topology by temporarily removing transmission lines out of the system. By changing the way how electricity flows through the system, TLS can be employed in emergency scenarios to alleviate violations, congestions, and overloading conditions. Such considerations, which are employed in the operational time frame, make it possible to have more efficient use of the existent network facilities.

Though being performed for decades on a very limited scale with rather focused aims, transmission switching has recently gained further importance with the increased penetration of renewable energy resources and the growing demand for more reliable operation of power systems. It has been shown that various operating conditions can be resolved through transmission switching; amongst, one can mention voltage violations and

* Part of this chapter is reprinted with permission from "Flexible Implementation of Power System Corrective Topology Control" by P. Dehghanian, Y. Wang, G. Gurrala, E. Moreno-Centeno, and M. Kezunovic, Nov. 2015. *Electric Power System Research*, vol. 128, pp. 79-89, ©2015 Elsevier.

overloading conditions as a result of possible contingencies, network losses and congestion management, security enhancement, reliability improvements, and also cost reduction for economic benefits [50].

Many of the past research works on corrective TLS have suggested optimization procedures that provide one switching sequence and involves repetitive solution of transmission switching optimization until a valid switching plan satisfying the AC feasibility and stability is found. However, if the selected transmission lines are not switchable due to the associated circuit breaker (CB) failures, the switching process stops and the operator may need to re-run the optimization engine to obtain a new switching sequence. In practice, transmission line switching implementation involves several operational procedures and clearances at various levels of the utility organizations which are commonly time consuming. So, transmission system operators (TSOs) need to be provided with switching plans with high probability of success to minimize the involved time and labor. To the best of the author's knowledge, none of the existing topology control algorithms address such practical considerations.

Trying to bridge the gap between the theoretical advancements in previous literature and the practical requirements that the operator will have to deal with, this Section proposes an implementation procedure for realizing TLS in practice. The main objective of this Section is to demonstrate how such technologies can empower the operator not only to obtain feasible switching actions, but also allow the operator to use his/her experience and personal judgment to decide which feasible set of actions to implement. The proposed framework, to be used in day to day operation planning

scenarios in response to probable contingencies, provides several switching options per contingency in a tree-like structure. At each level of the switching tree, the framework suggests the operator a set of AC feasible and stable TLS plans based on a selected optimization criterion such as maximum load shed recovery (LSR) or minimum generation cost, etc.

This Section also proposes a decision making support tool based on a CB reliability assessment technique using condition monitoring data. A mean benefit index is proposed to quantify the impacts of failed CBs associated with switching of a transmission line in any substation configuration. The operator can use this information, other operating conditions not explicitly considered in the optimization, and his/her own experience to select the most reliable TLS actions at each level of the tree for implementation. It is important to mention that the suggested switching actions will be a temporary solution to recover from the critical contingencies in a timely manner and the switched transmission lines would be returned back to service when the contingency is permanently mitigated.

6.2 Problem Description and the Proposed Framework

This Section elaborates the proposed switching implementation framework containing four main modules: (1) the Binary Switching Tree (BST) algorithm, (2) AC feasibility check, (3) system stability check, and (4) the CB reliability and transmission line availability assessment. The framework is illustrated in Figure 44 and the details come in the following.

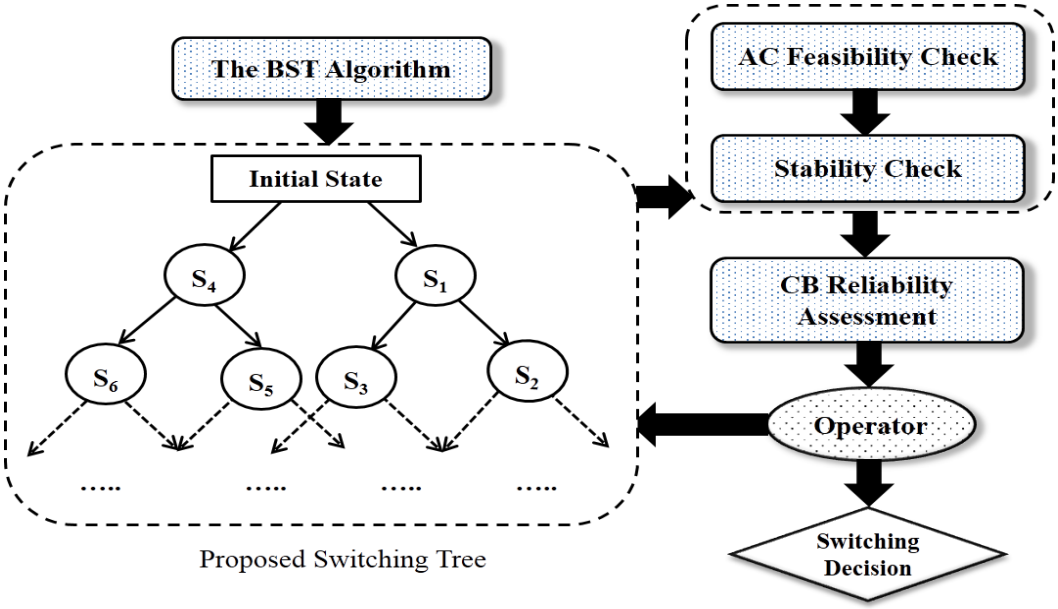

Figure 44. The overall framework proposed for transmission line switching.

6.2.1 BST Algorithm

The proposed BST algorithm is an extended version of the MIP-H algorithm previously suggested in [48]. The MIP-H finds one TLS operation and corresponding re-dispatch action per level to iteratively increase the LSR. In contrast, the proposed BST algorithm provides multiple TLS actions at each level for further AC feasibility, stability, and CB reliability checks. This sub-Section presents the BST algorithm in terms of the maximum LSR objective but the idea is valid for any other objective function.

In this context, the BST algorithm can be triggered by the operator for a forecasted contingency. The TLS actions proposed by the BST algorithm are given in a binary tree structure, that is, each path from the root node to a leaf node represents a viable TLS sequence and the corresponding intermediate system states. The root node denotes the

system state immediately following the contingency. Each non-root node represents an updated system state over its parent node; specifically, the system update from a parent to a child node consists of one transmission line switch and a time-constrained generation re-dispatch. The generation re-dispatch of the child node must be attainable from the parent node's generation re-dispatch by ramping up/down the generating units at most in τ minutes (in this work τ =10). The BST has two properties: (1) each non-leaf node has two child nodes, the left (right) child is obtained by choosing the one-line switch and generation re-dispatch that combined achieve the largest (second largest) amount of LSR over its parent's state; we refer to this transmission line switch as the line switch *leading to* this left (right) child; (2) given any non-root node, the line switch leading to this node is different from every transmission line switch leading to any sibling of this node's ancestors; this guarantees the diversity of the TLS options.

First, an overview of the BST algorithm is presented here. Without loss of generality, we henceforth assume that all the lines are initially closed; however, the BST algorithm can be easily adapted to a more general setting. The BST is built in a breadth-first-search (BFS) order, creating each level from left to right. At each node, say node v, if the stopping criteria have not been met, the BST algorithm will create node v's two child nodes. The left child is created by solving an optimization model to find a transmission line switch and generator re-dispatch that combined recover the most potential load shed. The inputs for this optimization model are: (1) the generation re-dispatch of node v; (2) the line status sets $\hat{K}$ and $\bar{K}$ at node v (the sets of closed and open transmission lines, respectively); and (3) the *Not-to-Switch* (NTS) list which includes all

transmission line switches leading to the sibling nodes of node v's ancestors. The right child is created by solving the same model, except that the NTS list also includes the transmission line switch leading to its (left) sibling node. In practice, the operator may not want to switch some specific transmission lines. The proposed BST algorithm can include those transmission lines in the aforementioned NTS list to assure that they will not be switched nor included in the outcome switching tree.

Next, the BST algorithm is described in detail. The BST algorithm takes the following inputs: all DCOPF inputs, the contingency set $\dot{G} \cup \dot{K}$, the potential amount of load shed* that may be shed following a contingency, denoted by $LS_{\dot{G} \cup \dot{K}}$, the time interval between two consecutive line switches, τ, the minimum desired improvement in LSR percentage between a child node and its parent, δ (say 0.01%), and the maximum number of levels in the BST, H. The BST algorithm comprises three procedures: (1) $LS_{\dot{G} \cup \dot{K}}$ calculation (as described in [48]); (2) initialization procedure to create the root node and place it in the BFS queue; and (3) the main procedure at every node after it is taken out of the BFS queue.

- ***Initialization Procedure***

First, create the root node by setting its BST level as 0 and its current generator levels, denoted by P_g^{Root}, as the generator dispatch in effect at the time that the contingency

* Instead of using the less tractable load shedding dynamically triggered by relays, the load shed in our paper is defined as the difference between the total demand during normal system state and the amount of demand still fulfilled following the contingency set $\dot{G} \cup \dot{K}$.

set $\dot{G} \bigcup \dot{K}$ occurs. Then, initialize $\bar{K}$ to include all transmission lines that are currently open and available to be closed, and initialize $\hat{K}$ to include all other transmission lines. Then, set NTS list as empty. Last, push the root node into the BFS queue.

- ***Main Procedure***

Step 1: *Check the BFS Queue:* If the BFS queue is empty, then stop and output the BST. Otherwise, pick the first node in the BFS queue, say node v, and continue to the next step, ***Step 2***.

Step 2: *Determine if Node v is a Leaf Node:* Node v is a leaf node (meaning it is the end of a switching sequence) if any of the following criteria is met: there is no load shed at node v, i.e. $LS_{\dot{G} \cup \dot{K}}$ is fully recovered; node v's tree level is equal to H; node v's LSR percentage improvement over its parent node is less than δ; If node v is a leaf node, go back to ***Step 1***. Otherwise, continue to ***Step 3***.

Step 3: *Create the Left Child of Node* v: To create the left child of node v, say node v_L, we need to find the τ-minute constrained generation re-dispatch and single line switch starting from node v's system state (specified by node v's generator dispatch, P_g^v, and transmission line status, $\hat{K}$ and $\bar{K}$) that combined recover the most load shed. This is done as follows:

Step 3(a): *Create the NTS List:* Form the node NTS list, denoted by T, by appending the transmission line switch leading to the sibling node of node v to the NTS list used to create node v.

Step 3(b): *Solve the Following Optimization Problem*

Maximize $$LS_{\dot{G}\cup\dot{K}} - \sum_{\forall n\in N} u_n \tag{6.1}$$

Subject to:

$$\theta^{\min} \le \theta_n - \theta_m \le \theta^{\max} \qquad \forall k(m,n) \in K \tag{6.2}$$

$$\sum_{\forall k(n,..)} P_k - \sum_{\forall k(..,n)} P_k + \sum_{\forall g(n)} P_g = d_n - u_n \qquad \forall n \in N \tag{6.3}$$

$$P_k^{\min}(1-s_k) \le P_k \le P_k^{\max}(1-s_k) \qquad \forall k \in \hat{K} \tag{6.4}$$

$$B_k(\theta_n - \theta_m) - P_k + s_k.M_k \ge 0 \qquad \forall k \in \hat{K} \tag{6.5}$$

$$B_k(\theta_n - \theta_m) - P_k - s_k.M_k \le 0 \qquad \forall k \in \hat{K} \tag{6.6}$$

$$P_k^{\min}.s_k \le P_k \le P_k^{\max}.s_k \qquad \forall k \in \bar{K} \tag{6.7}$$

$$B_k(\theta_n - \theta_m) - P_k + (1-s_k).M_k \ge 0 \qquad \forall k \in \bar{K} \tag{6.8}$$

$$B_k(\theta_n - \theta_m) - P_k - (1-s_k).M_k \le 0 \qquad \forall k \in \bar{K} \tag{6.9}$$

$$\max\left\{P_g^{\min}, P_g^{v} - \tau r_g\right\} \le P_g \le \min\left\{P_g^{\max}, P_g^{v} + \tau r_g\right\} \qquad \forall g \in G\backslash\dot{G} \tag{6.10}$$

$$0 \le u_n \le d_n \qquad \forall n \in N \tag{6.11}$$

$$P_k = 0 \qquad k \in \dot{K} \tag{6.12}$$

$$P_g = 0 \qquad g \in \dot{G} \tag{6.13}$$

$$s_i = 0 \qquad \forall i \in T \tag{6.14}$$

$$\sum_{\forall k \in K \setminus \dot{K}} s_k = 1 \tag{6.15}$$

$$s_k \in \{0,1\} \qquad \forall k \in K \setminus \dot{K} \tag{6.16}$$

The main decision variables in this optimization model are s_k and u_n, where s_k determines the switching action of transmission line k and u_n denotes the unfulfilled demand at node n. The objective (6.1) is to maximize the LSR associated with the contingency set $\dot{G} \cup \dot{K}$; constraint (6.2) sets the range for the difference between the angles of adjacent buses. The node balance constraints (6.3) are analogous to those in the DCOPF model, but are modified to allow for partial demand fulfillment. Constraints (6.4)-(6.6) and (6.7)-(6.9) reflects the set of closed and open transmission lines, respectively; Constraints (6.4) and (6.7) set the transmission line thermal limits, while constraints (6.5), (6.6), (6.8), and (6.9) determine the transmission line power flow. The reachable re-dispatch limits for the online generating units are set by constraints (6.10), where P_g^v denotes the generator dispatch at node v. Constraints (6.11) set the bound for the unmet demand at each node. The transmission line and generating unit outages are reflected in constraints (6.12) and (6.13), respectively. Constraints (6.14) force not to switch the transmission lines resided in the NST list. Constraint (6.15) allows only one transmission line switch (which significantly accelerates the computations).

Step 3(c): *Record the System State for Node* v_L: Save the transmission line switch, generation dispatch $P_g^{v_L}$ and update the transmission line status sets $\hat{K}$ and $\bar{K}$; then record the LSR.

Step 3(d): *Set the Tree Level*: Set the level of the node v_L as node v's level plus 1.

Step 3(e): *Update the BST Queue:* Append node v_L to the end of BST queue.

Step 4: *Create the Right Child of Node* v: This step is identical to ***Step 3*** except that the NTS list to create node v's right child, say node v_R, also contains the transmission line switch leading to node v_L.

Step 5**:** *Compute & Record the LSR for Time-constrained Re-dispatch-only Option Starting from Node* v: Specifically, we need to find the τ-minute constrained generation re-dispatch starting from node v's system state that recovers the most potential load shed. This is done by solving the optimization model in ***Step 3(b)*** with two modifications: removing constraint (6.15) and setting the values of all switching variables, s_k, to zero (note that by doing so, the model in ***Step (3b)*** is reduced to a simple LP problem).

Note: The re-dispatch-only LSR at each non-leaf node in the BST is provided for two main purposes: 1) as a benchmark to allow the operator evaluate the effectiveness of the suggested TLS actions leading to that node's child nodes; 2) to give the operator the re-dispatch-only option in case he/she prefers it over the proposed TLS options or uses it as a fallback option in case of CB failure or other restricting conditions for TLS implementation.

Step 6: Go to ***Step 1***

As mentioned earlier, the BST algorithm can be modified to find the TLS plans with different objectives. For instance, if one wants to minimize the system generation cost, three minor changes are needed: (1) replace the objective function to minimize the total generation cost, (2) remove the u_n variables and (3) keep track of total generation cost at each node of the BST architecture.

6.2.2 AC Feasibility and Stability Check

The output of the proposed BST algorithm is an H-level BST and the corresponding optimized generation schedules and loading profile. Since the DCOPF always assumes flat voltage profile of 1 per unit for the generators, it does not consider the reactive power and voltage constraints and as a consequence, the resulting solutions may or may not be AC feasible. AC feasibility, hence, needs to be assessed for each proposed TLS option.

For AC power flow, the original network data excluding the opened transmission lines with the generation schedules and loading patterns suggested by the BST algorithm is used. If the AC power flow does not converge, different adjustments may be tried to aid the convergence with the available reactive power sources, e.g., shunts, generator voltage set points, transformer tap settings etc. If AC feasibility is achieved with all the adjustments satisfying the generating units' reactive power constraints, then the transient stability is performed using the output of the AC load flow as the initial conditions for the machines. If the AC power flow is not feasible even with all the reactive power resources at their maximum limits, then the solutions are concluded infeasible. In practice, utilities

commonly do some adjustments to the DC solution for AC feasibility. Even after all the possible adjustments, if the AC solution is not feasible, then the DCOPF solution needs to be rethought.

Transmission line switching is a large disturbance in the system. Transient stability simulations, if simulated for longer time, will help in tracking both the initial impact of switching and the oscillatory behavior after the TLS is implemented. It is assumed here that the time between consecutive switching operations is sufficient for damping of the electromechanical oscillations. For the transient stability simulations, the generation schedules and loading patterns corresponding to the previous TLS actions are taken as the initial condition for the current switching action. The analysis has to be conducted at each level of the switching tree. This will eventually lead to various sets of AC feasible and stable TLS actions which can be safely implemented.

6.2.3 CB Reliability Assessment

Switching or de-energizing a transmission line requires isolation of the sources feeding the transmission line, which involve operating several CBs. Mal-operation of any of these CBs is an impediment to the successful execution of switching operation. It is, hence, important to take the CB reliability into account while using the topology control in day to day operations. Inspired by the wide deployment of smart sensors in the system in recent years, CB condition and reliability assessment using condition monitoring data has become popular. In this Section, a dynamic procedure employing the CB control circuit monitoring data proposed in Section 5 is employed to find the CB's failure

probability index, which is regarded as its reliability measure. There are several other methodologies in the literature that can be employed individually or collectively for assessing the CB reliability [see Section 5]. The failure probability index employed in this research can be dynamically updated as and when new monitoring data arrives, providing a continuous quantitative measure of CB reliability over time.

6.2.4 Approach for Identifying the Reliable Switching Options

A new decision framework is proposed in this Section which offers the system operator not only a set of TLS actions, as introduced earlier through the BST algorithm, but also the mean benefit index associated with each TLS action taking the CB reliability and transmission line availability conditions into account. At each level of the tree, the operator can select the TLS option with the highest mean benefit index. However, the operator can use his/her own experience and other criteria to select the best TLS option at every level of the tree. The main step in evaluating the mean benefit index associated with each TLS action is to determine the transmission line availability index (probability of switching success) and also the incremental benefits from the successful implementation of each TLS action.

Here, the availability index of a transmission line for successful switching is calculated according to the substation configuration. This is illustrated using a line switching example having a breaker-and-a-half substation configuration as shown in Figure 45. There are four CBs involved in switching this transmission line. The current practice in line switching for transmission voltages higher than 138kV mandates opening

the CBs at one end of the line, one at a time, followed by opening the CBs at the other end within a couple of minutes. Open ended transmission lines at such high voltages are prone to the Ferranti effect (rise of voltage on the open end) which may result in insulation damages and unsafe conditions. As a result, in such high voltage levels, if only one side was successfully opened, the operators would reclose it to avoid unsafe conditions. For switching implementation of transmission lines at 138kV or lower voltage levels, or shorter transmission lines, opening one end of the line may be sufficient. So, equations (6.17) and (6.18) are introduced accordingly to evaluate the availability of transmission lines considering the associated CB reliability and health conditions.

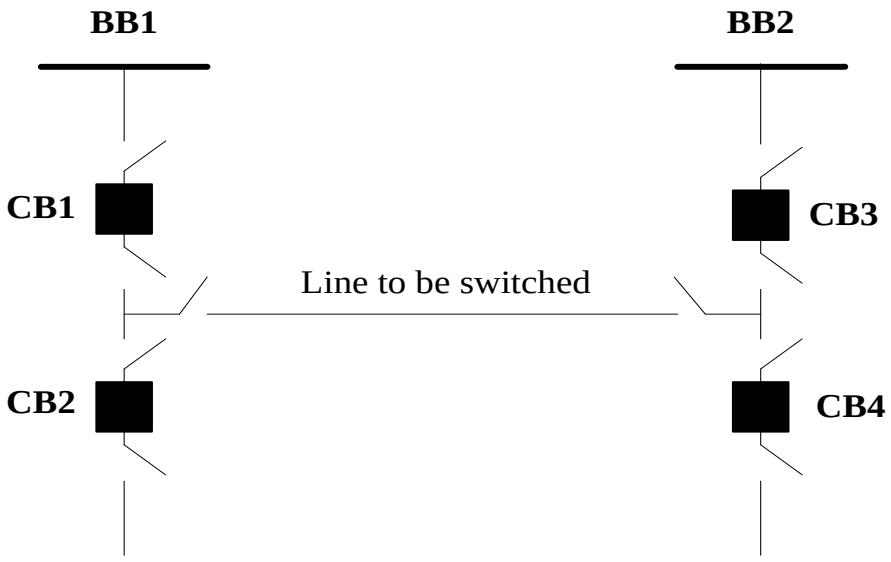

Figure 45. A sample line for switching obtained by the BST algorithm in a breaker-and-a-half substation configuration.

$$P^t(S_i) = \prod_{i=1}^{4}\left(1\text{-}\mathrm{FP}^t(\mathrm{B}_i)\right) \qquad \forall \mathrm{V} > 138 \text{ kV} \qquad (6.17)$$

$$P^t(S_i) = \prod_{i=1}^{2}\left(1\text{-}\mathrm{FP}^t(\mathrm{B}_i)\right) + \prod_{i=3}^{4}\left(1\text{-}\mathrm{FP}^t(\mathrm{B}_i)\right) - \prod_{i=1}^{4}\left(1\text{-}\mathrm{FP}^t(\mathrm{B}_i)\right) \quad \forall \mathrm{V} \leq 138 \text{ kV} \qquad (6.18)$$

where in (6.17), all the four CBs associated with the transmission line need to be reliable to make the switching action successfully implemented, while in (6.18), one pair of the CBs at either end of the transmission line needs to be reliable for successful switching implementation.

The procedure continues with the evaluation of incremental benefits gained from each TLS action. Every TLS option in the switching tree is expected to provide some benefits to the system operator depending on the objective function utilized in the optimization algorithm. For example, if minimization of generation cost is the objective, an obtained cost saving can be treated as the benefit. Similarly, if the objective function is the LSR, then the amount of load shed recovered due to each TLS option is the benefit gained. If the CB fails to operate, then the TLS action cannot be realized and the switching benefits will be lost. However, in such cases of CB failure, the operators may obtain the benefits by implementing the re-dispatch-only solution.

Hence, a mean benefit index is proposed here for each switching action at every level of the switching tree taking into account the following factors: (a) probability of successful switching implementation in terms of the associated CB reliability; (b) the incremental benefits (here, the benefit is in terms of MW load shed recovered) from each single TLS action and the corresponding generation re-dispatch compared to the previous state; (c) probability of switching implementation failure due to the unavailability or

failure of the associated CBs; (d) the benefits (here, the benefit is in terms of MW load shed recovered) from the generation re-dispatch-only practice (when the TLS action cannot be implemented successfully) compared to the previous state.

The proposed mean benefit index for each TLS action is calculated as:

$$MB^t\left(S_i\right)=P^t\left(S_i\right).B^t\left(S_i\right)+\left(1-P^t\left(S_i\right)\right).B^t\left(\mathrm{RD}_i\right) \tag{6.19}$$

The mean benefit index is calculated at each node considering only the incremental benefits from the previous state to the next immediate state. At each level of the tree, each TLS option provided to the operator will be accompanied by its mean benefit index. Having one end of the transmission line switched, the remaining end will experience less stress because of the no load switching; the possibility of failure can be, hence, less in this case. To aid the operator in deciding which end of the transmission line to start the switching process with, the availability index is also calculated for both ends of the line separately using (6.18). The operator can then select to begin switching the end of the transmission line with higher index of reliability. It implies that the reliable CBs are always triggered first to start the switching process.

Figure 46 illustrates the proposed framework's entire process. Note that if either of the aforementioned checks fails at any level of the tree, the proposed BST algorithm could be called again to start at that level to propose an alternative TLS option (to do this, the only change to the BST algorithm, in ***Step 3(b)***, is to add them to the NTS list). However, this decision can be made by the operator looking at the entire tree. If the switching tree does not result in at least one implementable switching path i.e. at least one path which satisfies the AC feasibility and stability checks with reliable CBs for switching

or any other practical concerns apart from these, then the operator may choose to re-run the BST algorithm to get new sets of acceptable results.

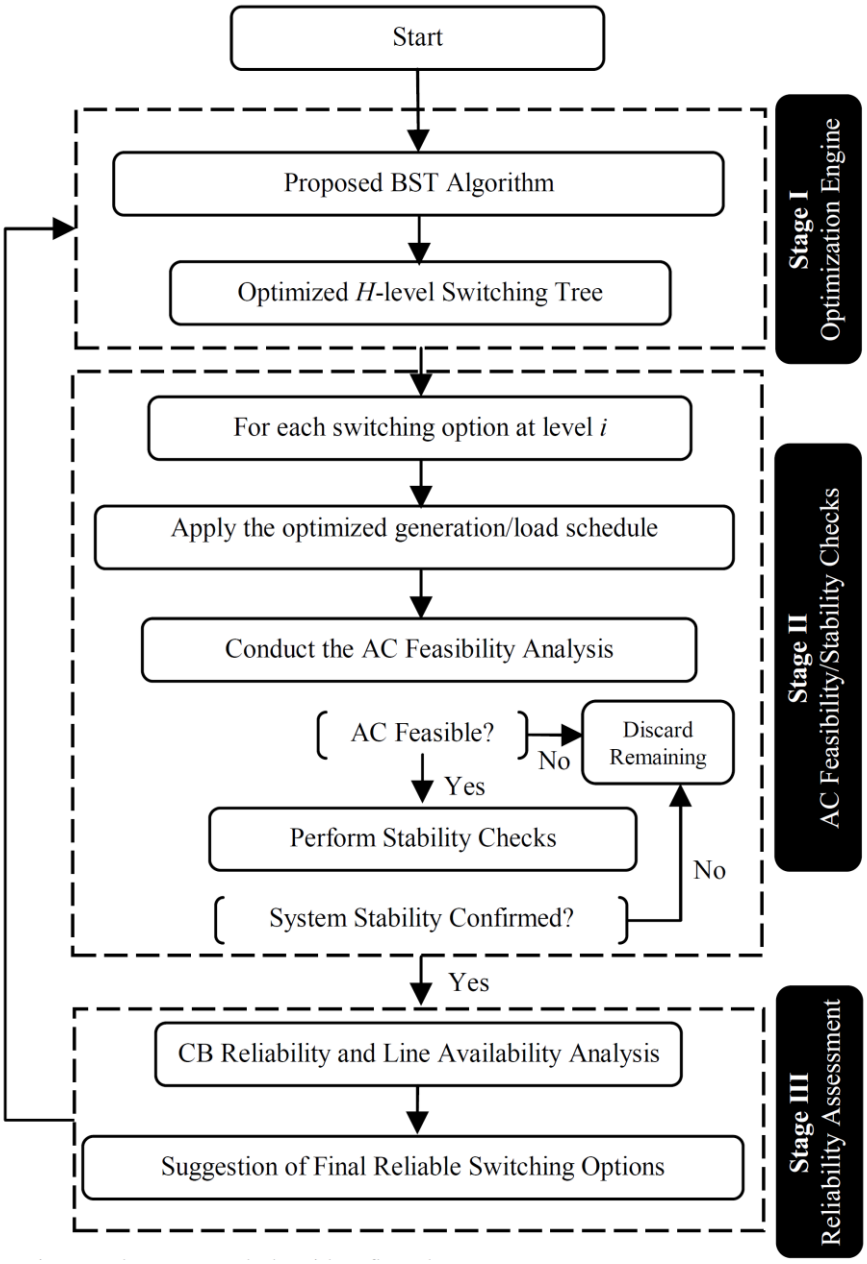

Figure 46. The proposed algorithm flowchart.

6.3 Case Studies: IEEE 118-Bus Test System

In this Section, the proposed framework is applied on the IEEE 118-bus test system which contains 186 transmission lines and 19 generators with the installed capacity of 5859.2MW serving a total demand of 4519MW [188], [189]. The one-line diagram of the studied network is illustrated in Appendix 3. The results are presented for contingency planning scenarios where maximizing LSR is regarded as the optimization objective function. The proposed framework here is used to plan for the non-trivial contingencies, i.e. those whose impacts on the system cannot be mitigated by a time-unconstrained generation re-dispatch alone. These non-trivial test cases were run on a desktop machine with12 GB RAM and two 2.40 GHz Intel Xeon processors. It took at most 18 seconds to execute the BST algorithm for each case study and about 2-3 seconds for the AC feasibility, stability, and CB reliability simulations of each TLS action.

6.3.1 Case Study 1: Single-Order Generator Contingency

One such non-trivial case, the outage of generator 13 (G13), is considered in this Section to demonstrate the effectiveness of the proposed framework. The initial load shed caused by the G13 contingency is 805.2 MW, of which only 584.3 MW (72.6% of the system total load shed) can be recovered through the time-unconstrained re-dispatch. Reconfiguration is needed in this scenario to recover the load shed. Figure 47 illustrates the TLS actions obtained from the BST algorithm.

In this figure, each node/box denotes a system state (the LSR on each node is given both in percentage and MW). The numbers on top of each solid-line arrow represent

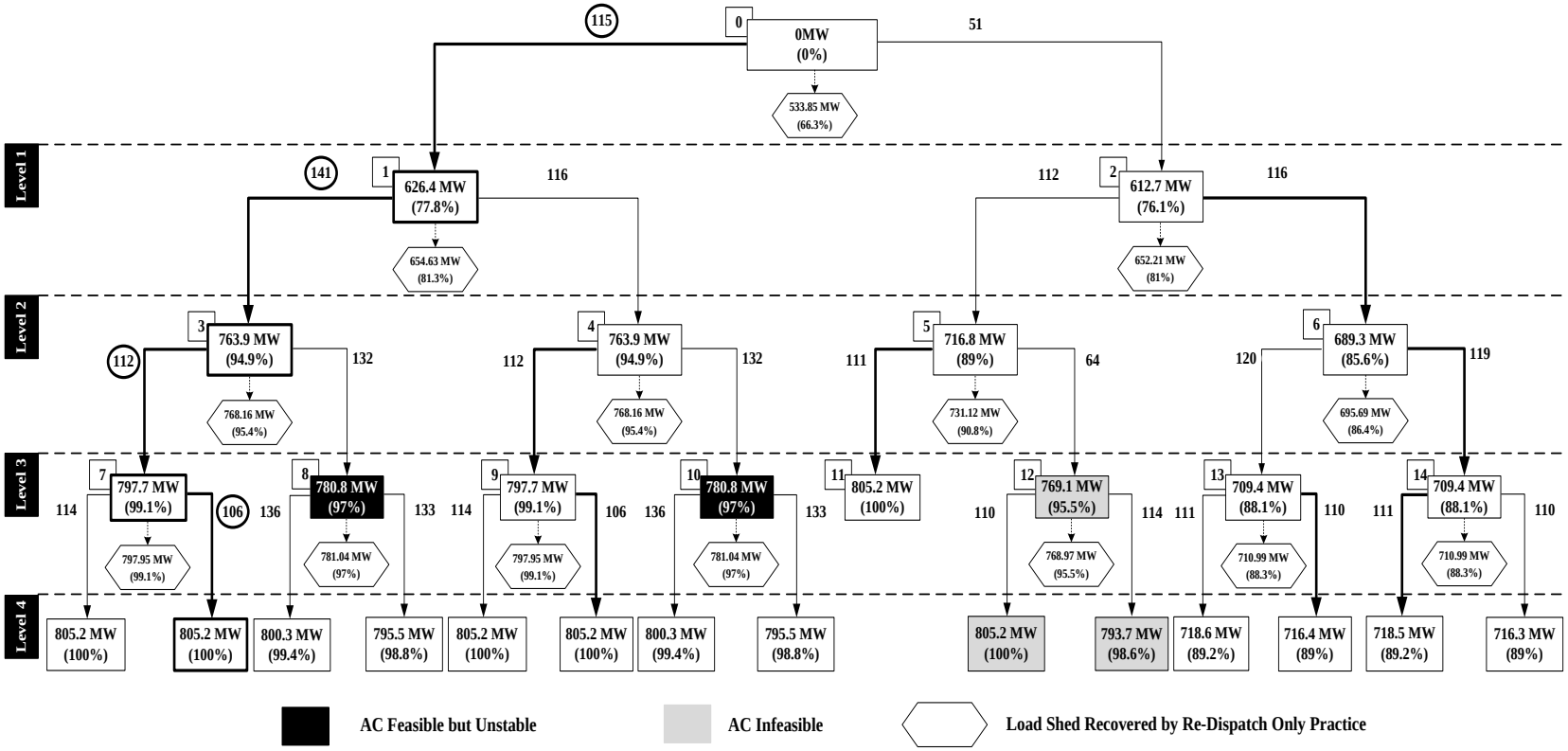

Figure 47. Proposed switching tree in case study 1: G13 single-order contingency.

the transmission line switches leading to the node in the lower level. The number in the boxes located in the upper left-hand side of each node/box represents the node index. The LSR obtained by the re-dispatch only solution is presented in the hexagons below each parent node (each hexagon and corresponding parent node are connected by a dashed arrow).

The figure illustrates that the operator is offered two TLS options (more options can be provided at each level if desired) at each node: the switching leading to its left child and the switching leading to its right child. For example at level 1, transmission line 51 and transmission line 115 can be switched (note that with either switch, the LSR (77.8% or 76.1%) is already greater than that obtained by doing only a 40-minute re-dispatch with LSR of 72.6%). If the operator decides to select transmission line 51 at level 1, he/she has two TLS options, i.e., lines 112 and 116, to implement at level 2.

The optimized generation and load schedules for each TLS option would be the other outputs of the BST algorithm. These changes at each level of the tree are used in an AC power flow solver. AC power flow problems were solved using the Matpower version 4.1 toolbox in MATLAB [142]. The AC infeasible switching solutions, transmission line 64 at level 3 and transmission lines 110 and 114 at level 4, are shown in gray boxes in Figure 47.

Next, transient stability simulations are conducted using the 6^{th} order models for synchronous machines for 20 seconds. First swing, multi swing, and small oscillation instabilities can be detected in such time domain simulations. The solutions which are first swing unstable, e.g., transmission line 132 at level 3, are highlighted in black boxes. These

cases are indeed unstable after the second swing. If the operator chooses to switch the transmission line 141 at level 2, then he/she is left with only one TLS option, i.e., transmission line 112, since switching transmission line 132 is an unstable case. The operator may choose to re-run the optimization starting from level 2 as the base case and get another alternate TLS option excluding the two already considered. This would be faster than running the entire optimization starting from the beginning.

CB reliability assessment is then performed at each level. The results of the proposed benefit assessment framework for decision making at each level are tabulated in Table 14 assuming the associated substation configurations to be breaker-and-a-half scheme and the transmission voltages are higher than 138kV [188]. The CB failure probabilities are simulated based on a set of real condition monitoring data introduced in [173] and the employed values for the proposed switching candidates are demonstrated in Table 15.

The switching level 1 offers two options to maximize LSR in response to the G13 outage. Though both solutions meet AC feasibility and stability requirements, the benefit analysis shows that switching transmission line 115 is of higher mean benefit at this level and is highlighted with a thick arrow. Similarly, at each non-leaf node of the tree in Figure 47, the TLS action with the highest mean benefit is highlighted with thick arrows. Note that the conditions of all the responsible CBs associated with a transmission line have been taken into account for calculating the mean benefit indices.

An example calculation assuming the selection of highest mean benefit index TLS option at each level by the operator is shown in Table 14 (however, recall that the

Table 14. Benefit Assessment of the Switching Tree Concerning the CB Reliability Condition: Case Study 1

Switching Line			$P^t(S_i)$ (%)	$B^t(S_i)$ (MW)	$MB^t(S_i)$
No.	**From**	**To**			
			Switching Level 1 ($B^t(\mathrm{RD}_1)$ = 533.847 MW)		
51	30	38	0.727219	612.7	591.191
115	68	69	0.693979	626.4	**598.077**
			Switching Level 2 ($B^t(\mathrm{RD}_2)$ = 28.182 MW)		
141	81	80	0.678778	137.5	**102.385**
116	68	81	0.614512	137.5	95.359
			Switching Level 3 ($B^t(\mathrm{RD}_3)$ = 4.026 MW)		
112	65	66	0.580683	33.8	**21.3153**
132	77	80	0.655972	16.9	12.4709
			Switching Level 4 ($B^t(\mathrm{RD}_4)$ = 0 MW)		
114	66	67	0.618354	7.5	4.63765
106	62	66	0.698266	7.5	**5.23699**

Table 15. CB Failure Probability Values for the Proposed Switching Candidates: Case Study 1

TLS Option	CB Failure Probability Index				TLS Option	CB Failure Probability Index			
	From End CBs		To End CBs			From End CBs		To End CBs	
51	0.0523	0.0891	0.0478	0.1153	**112**	0.2499	0.0346	0.1689	0.0355
115	0.0894	0.0723	0.0863	0.1009	**132**	0.1239	0.0246	0.1276	0.1201
116	0.1127	0.0756	0.1705	0.0968	**114**	0.1468	0.0673	0.0723	0.1624
141	0.1788	0.0764	0.0699	0.0378	**106**	0.1381	0.1129	0.0408	0.0479

operator may choose to deviate from this sequence due to other considerations; e.g. he/she may choose to switch transmission lines 51, 112 and 111 since this would achieve 100% LSR with the least number of TLS actions). Once the operator selects a transmission line for switching based on the mean benefit index or from his/her own experience, the

operator's concern then might be to select the most reliable switching process. Here, solely the CBs related to the corresponding end-of-line need to be considered. The results for the highlighted sequence in Table 14 are tabulated in Table 16. The proposed approach is generic enough to be applied to various substation configurations. From Table 16 for transmission line 115 at level 1, we conclude that it is more reliable to start with the from-end of the line since it has higher mean benefit index, i.e., 612.035, compared to the other end with the value of 609.880.

The benefit analyses in Table 14 and Table 16 demonstrate that transmission line 141 may be selected at level 2 and, if so, the switching process has to start with the to-end of the transmission line. Similarly, transmission lines 112 and 106 can be selected at switching levels 3 and 4, respectively. Switching these two transmission lines would be started through the to-end of the lines since they are more reliable to start the process. These options 115-141-112-106 are marked in bold.

Note that our method provides several AC feasible, stable, and reliable TLS options. The load shed can be fully/partially recovered via a combination of TLS actions and re-dispatch through the proposed framework. Due to the variety of involved CBs with different reliability indicators, the final sequence may or may not lead to 100% LSR, which is not uncommon in practice.

Here we demonstrate that the benefit (the LSR) obtained by the BST algorithm is due to both, the switching actions and the re-dispatch. Specifically, at every node, if one were to perform only an optimal re-dispatch (with no switching), the LSR would be much

less. This is seen in Figure 47 by comparing, at each non-leaf node, the LSR percentages at both of its child nodes and the re-dispatch only LSR percentage (inside the hexagon).

Remarks: (1) All LSR percentages obtained with transmission line switching are substantially higher than those with re-dispatch only. (2) In only 8 out of 28 nodes, the re-dispatch-only solution achieves 99% or more of the LSR percentage recovered by switching; moreover, at those 8 nodes, the corresponding re-dispatch only results already benefitted from the previous TLS actions that led to their parents. (3) The LSR percentages for 10-, 20-, 30-, and 40-minute re-dispatch-only solutions are 66.3%, 71.3%, 72.6%, and 72.6%, respectively; in contrast, the LSR percentages recovered by the BST algorithm after 10, 20, 30 and 40 minutes (i.e. at levels 1, 2, 3 and 4, resp.) are, on average, 77.0%,

Table 16. Benefit Assessment to Determine which End-of-Line is used to Start the Switching Process: Case Study 1

Selected Line			$P^t(S_i)$ (%)	$B^t(S_i)$ (MW)	$MB^t(S_i)$
No	**From**	**To**			
	68	69	**Switching Level 1** ($B^t(\mathrm{RD}_1)$ = 533.847 MW)		
115	From-end		0.8448	626.4	**612.035**
	To-end		0.8215	626.4	609.880
	81	80	**Switching Level 2** ($B^t(\mathrm{RD}_2)$ = 28.182 MW)		
141	From-end		0.7585	137.5	111.095
	To-end		0.8949	137.5	**126.015**
	65	66	**Switching Level 3** ($B^t(\mathrm{RD}_3)$ = 4.026 MW)		
112	From-end		0.7241	33.8	25.586
	To-end		0.8019	33.8	**27.903**
	62	66	**Switching Level 4** ($B^t(\mathrm{RD}_4)$ = 0 MW)		
106	From-end		0.7646	7.5	5.734
	To-end		0.9132	7.5	**6.849**

91.1%, 95.5%, and 96.5%, respectively; furthermore, the maximum LSR percentage without any TLS is only 72.6%. We conclude that switching is very beneficial to maximize the LSR.

6.3.2 Case Study 2: Second-Order Line-Generator Contingency

Another non-trivial case, the second order contingency involving the outage of generator 17 (G17) and transmission line 119 (L119) is studied to demonstrate the capability of the suggested framework in handling higher-order contingencies. The initial load shed caused by the G17-L119 contingency is 352 MW, of which only 277.38 MW (78.8% of the system total load shed) can be recovered through the time-unconstrained re-dispatch. Figure 48 illustrates the TLS actions obtained from the BST algorithm with the objective of maximizing LSR. The AC feasibility, stability, and CB reliability checks are conducted on the obtained solutions and Figure 48 shows the associated results.

In the suggested switching tree for this contingency, there are several switching sequences that recover 100% of the total load shed. This provides the operator with plenty of flexibility in decision making for practical implementations. Also, there are two AC infeasible TLS actions recognized: transmission line 111 and 107 both located at level 4 of the tree and highlighted in gray. Transient stability checks passed in all the switching solutions except on the AC infeasible ones. Similar to the previous case study, the operator is offered two TLS options at each node: at level 1, transmission line 113 and transmission

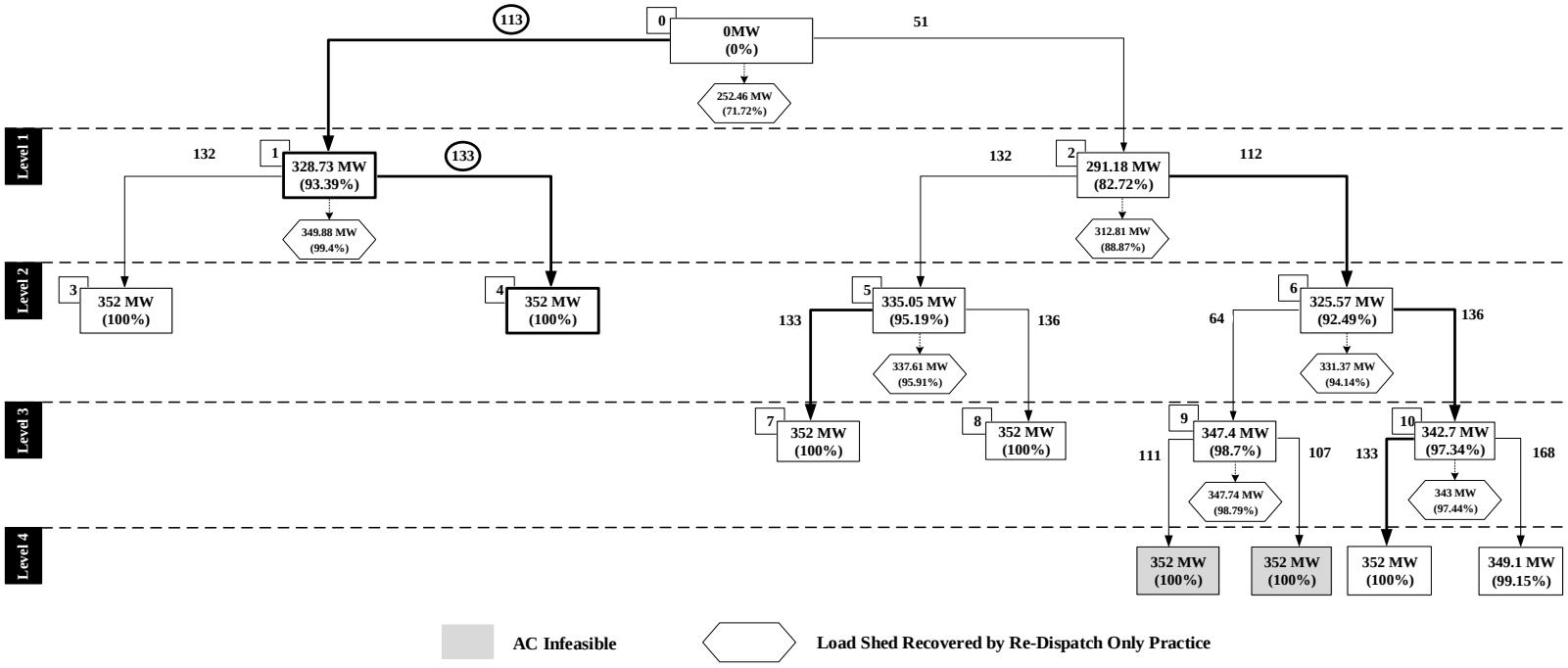

Figure 48. Proposed switching tree in case study 2: G17-L119 contingency.

line 51 can be switched. If the operator decides to select either one, he/she would have two other line switching options at level 2, and so on.

The results of the proposed benefit assessment framework for decision making at each level are tabulated in Table 17 assuming the associated substation configurations to be breaker-and-a-half scheme and the transmission voltages are higher than 138kV. Similar to the previous case study, the TLS action with the highest mean benefit index at each non-leaf node of the tree is highlighted with thick arrows illustrated in Figure 48. The benefit analysis shows that at Level 1, switching transmission line 113 would bring higher mean benefits compared to switching transmission line 51.

An example mean benefit index calculation (assuming that the operator always selects the TLS option with the highest mean benefit index) is demonstrated in Table 17 and the selected TLS actions are also highlighted with thick arrows and circles in Figure 48. However, recall again that the system operator may choose to deviate from this sequence due to other considerations not necessarily incorporated in the optimization engine. The selected switching sequence is able to recover 100% of the total load shed.

Table 18 also demonstrates the CB reliability and transmission line availability analysis which helps the operator decide which end-of-line to switch first. From Table 18, it can be concluded that the selected switching sequence (highlighted in thick arrows with circled numbers on top) would better be implemented starting at the from-end and to-end of the transmission lines 113 and 133, respectively.

Table 17. Benefit Assessment of the Switching Tree Concerning the CB Reliability Condition: Case Study 2

Switching Line			$P^t(S_i)$ (%)	$B^t(S_i)$ (MW)	$MB^t(S_i)$
No.	**From**	**To**			
			Switching Level 1 ($B^t(\mathrm{RD}_1)$ = 252.46 MW)		
51	30	38	0.7235	291.18	280.475
113	65	68	0.6504	328.73	**302.072**
			Switching Level 2 ($B^t(\mathrm{RD}_2)$ = 21.15 MW)		
132	77	80	0.6155	23.27	22.457
133	77	80	0.8085	23.27	**22.865**

Table 18. Benefit Assessment to Determine which End-of-Line is used to Start the Switching Process: Case Study 2

Selected Line			$P^t(S_i)$ (%)	$B^t(S_i)$ (MW)	$MB^t(S_i)$
No	**From**	**To**			
	65	68	**Switching Level 1** ($B^t(\mathrm{RD}_1)$ =252.46 MW)		
113	From-end		0.8390	328.73	**316.450**
	To-end		0.7753	328.73	311.593
	77	80	**Switching Level 2** ($B^t(\mathrm{RD}_2)$ =21.15 MW)		
133	From-end		0.8809	23.27	23.018
	To-end		0.9178	23.27	**23.096**

6.3.3 Case Study 3: Second-Order Line-Line Contingency

The second order contingency involving the outage of transmission lines 11 (L11) and 152 (L152) is selected as the third case study. The initial load shed caused by the L11-L152 contingency is 49.15 MW, of which only 18.09 MW (36.8% of the system total load shed) can be recovered through the time-unconstrained re-dispatch.

Figure 49 illustrates the TLS actions obtained from the BST algorithm in this scenario. In the proposed switching tree for this contingency, there is one AC infeasible and unstable TLS action, (transmission line 120 at level 4) which is shown in gray. Transient stability checks passed in all the other TLS solutions.

The results of the proposed benefit assessment framework for decision making at each level of the tree are tabulated in Table 19. The mean benefit assessment suggests the system operator to select transmission line 154 at level 1 for implementation, through which the total load shed would be completely recovered only through this single TLS action combined with the corresponding generation re-dispatch; however, if for any reasons, the other option, i.e., the transmission line 145, is selected for switching at level 1, the operator would have two TLS options ahead, i.e., transmission lines 134 and 148, to implement at level 2, and so on.

In such cases, an example calculation of a switching sequence decision by the system operator is shown in Table 19. The selected switching sequence (switching transmission lines 145-148-143-136 denoted in Figure 49 by circled numbers on top of their arrows) is able to recover 78.43% of the total load shed.

Table 20 demonstrates the CB reliability and transmission line availability analysis which helps the operator to decide which end-of-line to switch first. It can be concluded, from Table 20, that the selected switching sequence should be implemented starting at the from-end, from-end, from-end and to-end of the transmission lines 145, 148, 143, and 136, respectively.

Table 19. Benefit Assessment of the Switching Tree Concerning the CB Reliability Condition: Case Study 3

Switching Line			$P^t(S_i)$ (%)	$B^t(S_i)$ (MW)	$MB^t(S_i)$
No.	**From**	**To**			
			Switching Level 1 ($B^t(\mathrm{RD}_1)$ = 16.53 MW)		
154	89	92	0.6505	49.153	**37.75**
145	83	85	0.7235	30.227	26.440
			Switching Level 2 ($B^t(\mathrm{RD}_2)$ = 1.194 MW)		
134	77	82	0.5667	8.786	5.496
148	85	88	0.9401	6.243	**5.941**
			Switching Level 3 ($B^t(\mathrm{RD}_3)$ = 0 MW)		
143	82	96	0.6521	0.92	**0.600**
132	77	80	0.5750	0.90	0.518
			Switching Level 4 ($B^t(\mathrm{RD}_4)$ = 0 MW)		
136	79	80	0.6850	1.16	**0.795**
120	69	77	0.6155	1.02	0.628

Table 20. Benefit Assessment to Determine which End-of-Line is used to Start the Switching Process: Case Study 3

Selected Line			$P^t(S_i)$ (%)	$B^t(S_i)$ (MW)	$MB^t(S_i)$
No	**From**	**To**			
	83	85	**Switching Level 1** ($B^t(\mathrm{RD}_1)$ =16.53 MW)		
145	From-end		0.8571	30.227	**28.270**
	To-end		0.8441	30.227	25.515
	85	88	**Switching Level 2** ($B^t(\mathrm{RD}_2)$ = 1.194 MW)		
148	From-end		0.9713	6.243	**6.082**
	To-end		0.9019	6.243	5.748
	82	96	**Switching Level 3** ($B^t(\mathrm{RD}_3)$ = 0 MW)		
143	From-end		0.8516	0.92	**0.783**
	To-end		0.7657	0.92	0.705
	79	80	**Switching Level 4** ($B^t(\mathrm{RD}_4)$ = 0 MW)		
136	From-end		0. 7464	1.16	0.866
	To-end		0. 9178	1.16	**1.065**

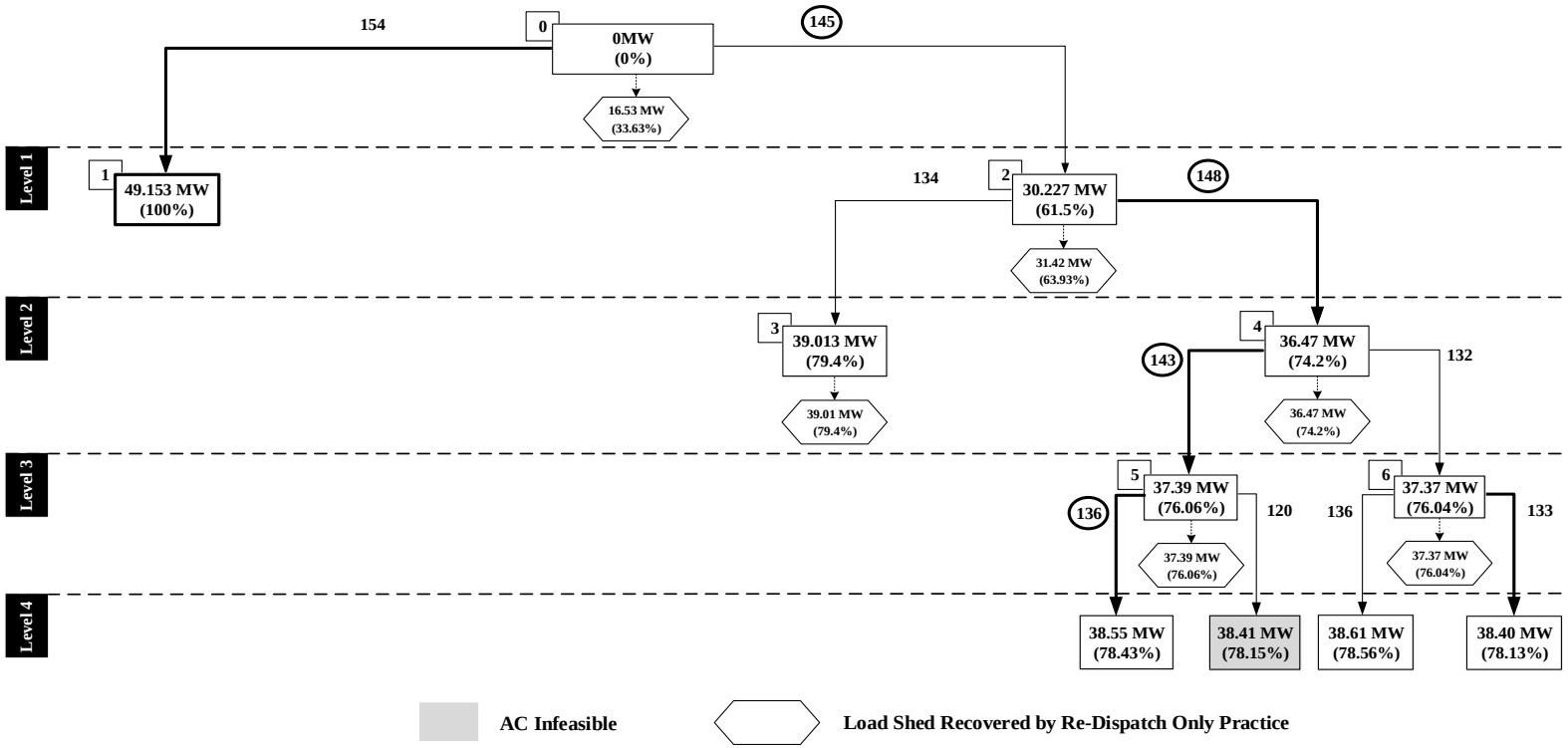

Figure 49. Proposed switching tree in case study 3: L11-L152 contingency.

6.4 Discussions

- In this Section, the bus-branch model is utilized for the switching optimization framework (creating the BST tree), the AC feasibility check and stability analysis. The node-breaker configurations are employed to calculate the mean benefit index based on the CB reliability indicators and to determine the most reliable end-of-line to implement each TLS action. In practice, there is a model-conversion requirement from the bus-branch structure into the node-breaker configuration models. Future research is needed to efficiently incorporate the node-breaker models into switching optimization formulations.
- Regarding the N-k contingency stability checks after TLS implementations, recent literature suggests that the system should still be able to meet the N-1 criterion after TLS implementation [47], [71]. The proposed BST framework here is generic enough to be integrated with such algorithms and, hence, will allow flexible decision making using a switching options tree.
- The operation of CBs for frequent switching implementations is not free. System CBs might need maintenance after several operations which may impose some additional costs. Since the true marginal cost of switching a CB is difficult to quantify at this time, we assumed a zero marginal cost to switch a CB. The reasoning is that the cost of switching a CB is negligible compared to the gained monetary benefits by minimizing the customer outage duration in the cases of contingency mitigation through implementation of the proposed TLS actions. If the suggested solution framework is going to be used in day-to-day operations, the

impact of CB maintenance and degradation due to an increase in the switching frequency need to be investigated and considered in the cost functions.

- Since the suggested framework is intended as a corrective tool in the day to day operational planning scenarios, usually the computational time requirement for the whole framework including the stability/AC feasibility and CB reliability considerations is less than an hour. In reference [48], the computational efficiency of the MIP-H algorithm has been evaluated on a real-life, large-scale test case consisting of 13k buses, 1k generating units, and 19k transmission lines. Since the BST algorithm is an extended version of MIP-H, it is reasonable to conclude that its results will be reached just as efficiently and quickly as those obtained with the MIP-H. Specifically, in [48], the MIP-H algorithm was expected to reach a speed of one-minute computational time per contingency for the above real-life large-scale network within a few years considering the rapid advances in both computing hardware and computational capability of modern optimization solvers. This expected improvement in solving speed can also further be expedited by using a parallelized version of the current program.
- The BST algorithm proposed in this dissertation uses MIP to determine the best lines to switch jointly with the associated best generator re-dispatch (i.e., the suggested algorithm co-optimizes the generation along with the network topology). It should be noted that there are sensitivity-based approaches that are also able to determine appropriate TLS actions. The proposed framework is modular and, thus, can use sensitivity-based approaches instead of MIP to

determine the TLS actions; this change will speed up the algorithm at the cost of losing the benefits expected from the co-optimization process.

6.5 Conclusions

The following remarks are the contributions presented in this Section:

- A new practical decision making paradigm for transmission switching to empower the operator, in an advisory mode, with a diverse set of TLS actions along with their benefits is proposed.
- The proposed framework for implementation of topology control ensures the AC feasibility, stability, and acceptable circuit breaker (CB) reliability.
- Using efficient DCOPF-based optimization, multiple TLS options are determined per contingency and are aimed to be presented to the system operator as a binary decision tree.
- The AC feasibility and stability checks are conducted at each level of the tree to ensure the reliable implementation of the proposed options in practice.
- A CB reliability assessment method using real-time CB condition monitoring signals to assess the availability of CBs for switching implementation is proposed to be included in the framework.
- The presented framework can be integrated as a corrective tool in day to day operation planning scenarios in response to system critical contingencies.

7 CONCLUSIONS

7.1 Contributions

Bulk electric transmission systems have been traditionally characterized with fixed configuration over time except in the cases of faults and forced outages when the topology changes as a consequence of circuit breakers tripping due to breaker operation or scheduled operator intervention. Given a fixed system topology with a certain generation pattern and load profile, the system operator commonly dispatches the committed generating units to optimize the cost while ensuring that the system security and reliability constraints are met. This traditional view does not assume the topology changes during a dispatch calculation interval. However, it is acknowledged that system operators can actually change the grid topology by operating circuit breakers to improve various system conditions and constraints. Lately, it is becoming more and more apparent that further considerations beyond the classical reliability oriented view are needed for enhancing the grid resilience and keeping the lights on at all times. The ultimate goal is to achieve an improved resilience by the efficient use of the existing infrastructure in a smarter way. In order to reach the improved grid efficiency and resiliency goals, this research strived to examine harnessing the transmission line assets, in both normal and emergency states with systematic management of uncertain factors, along with several practical considerations for flexible and reliable implementation of these technologies. Such considerations, which

are employed in the grid operational time frame, make it possible to have more efficient use of existing network facilities with minimal additional costs.

The dissertation contributions are as follows:

- The existing uncertainties of wind generation and electricity demand were stochastically modeled, formulated, and incorporated in the new probabilistic power system topology control optimization framework.
- Hourly and daily economic analysis of the probabilistic topology control optimization was widely explored to demonstrate the necessity of modeling and incorporating the probabilistic factors into the conventional TLS formulations.
- A probabilistic decision making support tool for use in hour-ahead operating time-frame to define optimal number of switching actions per hour taking into account both economic gains and risk costs associated with the new system operating states after switching implementations was formulated.
- A multi-objective optimization decision making support tool for use in day-ahead operating time frame to implement topology switching actions for higher grid economic efficiency was proposed where several critical and contradictory/competing objectives for TLS implementation, taking into account both ISO's and TSO's requirements, were incorporated and quantified. The presented framework provides the TSO operators with the tradeoffs between various objectives which will further help them to more reliably select an optimal TLS plan for final implementation.

- A practical paradigm for corrective TLS decision making to enhance the system resilience in face of extreme operating conditions (faults or violations) and empower the operator, in an advisory mode, with a diverse set of TLS actions along with their benefits was proposed. The proposed framework for implementation of topology control in response to critical contingencies ensures AC feasibility, stability, and acceptable circuit breaker reliability concerns.
- Automated analytics based on continuous monitoring of circuit breaker data collected in power substations were proposed to assess the reliability and health status of individual circuit breakers over time. The suggested approach allows a quantitative assessment of circuit breaker maintenance status leading to the classification into different deterioration/recovery states in real time.

7.2 Impact

In this dissertation, probabilistic decision making framework for implementation of power system topology control through transmission line switching (TLS) actions in face of various system operating conditions is proposed. The suggested implementation techniques provide *robust* topology control solutions to manage continuous uncertainties in the grid such as intermittent renewable generation and stochastic load. In practice, TLS implementation involves several operational procedures and clearances at various levels of the utility organizations, which are commonly time consuming. The transmission operators need to be provided with promising switching plans with high probability of

success to minimize the involved time and labor. Trying to bridge the gap between the theoretical advancements in previous literature and the practical requirements that the operators will have to deal with, this dissertation uniquely proposes implementation procedures for realizing transmission switching in practice. The main objective of this dissertation is to demonstrate how such technologies can empower the operator not only to obtain feasible switching actions with high confidentiality to several system performance requisites, but also how it will allow the operators to use their experience to decide which feasible set of actions to implement. The presented framework also provides the TSOs with the tradeoffs between various objectives which will further help the decision makers to more reliably select the optimal TLS plan for final implementation.

7.3 Suggestions for Future Research

Ongoing and future work includes investigating the scalability and tractability of the proposed probabilistic framework as well as other efficient probabilistic techniques in large-scale real-world transmission systems. Another extension of the work may be focused on modifications of the DCOPF-based topology control optimizations with inclusions of realistic factors such as losses and nomogram constraints.

Future work may also include the practical mechanisms for selection of an optimal switching sequence which is very critical as far as the system stability is concerned. The procedure on how to return the switched transmission lines back into service should be elaborated.

In this dissertation, the bus-branch model is utilized for the switching optimization frameworks. In practice, there is a model-conversion requirement from the bus-branch structure into the node-breaker configuration model. Future research is needed to efficiently incorporate the node-breaker model into switching optimization formulations.

REFERENCES

[1] H. Glavitsch, "State of the art review: switching as means of control in the power system," *International Journal of Electric Power and Energy Systems*, vol. 7, no. 2, pp. 92–100, Apr.1985.

[2] A. A. Mazi, B. F. Wollenberg, and M. H. Hesse, "Corrective control of power system flows by line and bus-bar switching," *IEEE Transactions on Power Systems*, vol. 1, no. 3, pp. 258–264, 1986.

[3] C. P. Barrows, "*Flexible network topologies and the smart grid in electric power systems*," Doctor of Philosophy Dissertation, Penn State University, November 2012.

[4] "Enhancing the resilience of the nation's electricity systems," *The National Academies Series (NAS) consensus study report*, July 2017.

[5] R. J. Campbell, "Weather-related power outages and electric system resiliency," *Congressional Research Service*, Library of Congress, 2012.

[6] "Economic benefits of increasing electric grid resilience to weather outages," *Executive Office of President Report*, August 2013.

[7] "A methodology for cost-risk analysis in the statistical validation of simulation models," *National Climatic Data Center*, 2012.

[8] "State of Reliability 2015," *North American Reliability Council (NERC) Report*, May 2015.

[9] R. Cormier, "The 12 Biggest Blackouts in History," Nov. 2015. [Online] Available at: http://mentalfloss.com/article/57769/12-biggest-electrical-blackouts-history.

[10] P. Dehghanian and S. Aslan, "Enhancing electric safety by improving system resiliency in face of extreme emergencies," *IEEE Industry Applications Society (IAS) Electrical Safety Workshop (ESW)*, pp. 1, 2017, Reno, NV, USA.

[11] P. Dehghanian, S. Aslan, and P. Dehghanian, "Quantifying power system resiliency improvement using network reconfiguration," *IEEE 60th International Midwest Symposium on Circuit and Systems (MWSCAS)*, pp. 1364-1367, Aug. 2017, Boston, MA, USA.

[12] P. Dehghanian, "Quantifying power system resilience improvement through network reconfiguration in cases of extreme emergencies," *Master of Science Thesis*, Texas State University, 2017. [Online] Available: https://digital.library.txstate.edu/handle/10877/6780.

[13] A. Rouhani and A. Abur, "Real-time dynamic parameter estimation for an exponential dynamic load model," *IEEE Transactions on Smart Grid*, vol. 7, no. 3, pp. 1530-1536, July 2015.

[14] A. Rouhani and A. Abur, "Linear phasor assisted dynamic state estimator," *IEEE Transactions on Smart Grid*, early access, March 2016.

[15] A. Rouhani and A. Abur, "Observability analysis for dynamic state estimation of synchronous machines," *IEEE Transactions on Power Systems*, vol. 32, no. 4, pp. 3168-3175, July 2017.

[16] A. Rouhani, “Robust dynamic state estimation in power systems,” *Doctor of Philosophy Dissertation*, Northeastern University, May 2017.

[17] A. Rouhani, “Robust dynamic state estimator accounting for load changes,” *Master of Science Thesis*, Northeastern University, 2014.

[18] Z. Bie, Y. Lin, G. Li, and F. Li, “Battling the extreme: A study on the power system resilience,” in *Proceedings of the IEEE*, in press, pp.1–14, 2017.

[19] A. Gholami, F. Aminifar, and M. Shahidehpour, “Front lines against the darkness: enhancing the resilience of the electricity grid through microgrid facilities,” in *IEEE Electrification Magazine*, vol. 4, no. 1, pp. 18–24, March 2016.

[20] M. Chaudry, P. Ekins, K. Ramachandran, A. Shakoor, J. Skea, G. Strbac, X. Wang, and J. Whitaker, *Building a Resilient UK Energy System*. London, U.K.: UK Energy Research Center (UKERC), Apr. 14, 2011.

[21] “A Framework for Establishing Critical Infrastructure Resilience Goals,” *National Infrastructure Advisory Council (NIAC)*, Washington, DC, USA, Oct. 2010.

[22] M. Panteli, D. N. Trakas, P. Mancarella, N. D. Hatziargyriou, “Power systems resilience assessment: hardening and smart operational enhancement strategies,” in *Proceedings of the IEEE*, vol. 105, no. 7, pp. 1202–1213, 2017.

[23] M. Panteli, P. Mancarella, D. Trakas, E. Kyriakides, and N. Hatziargyriou, “Metrics and quantification of operational and infrastructure resilience in power systems,” *IEEE Transactions on Power Systems*, vol. 32, no. 6, pp. 4732–4742, 2017.

[24] M. Panteli, C. Pickering, S. Wilkinson, R. Dawson, and P. Mancarella, “Power system resilience to extreme weather: fragility modelling, probabilistic impact

assessment, and adaptation measures," *IEEE Transactions on Power Systems*, vol. 32, no. 5, pp. 3747–3757, 2017.

[25] D. N. Trakas, N. D. Hatziargyriou, M. Panteli and P. Mancarella, "A severity risk index for high impact low probability events in transmission systems due to extreme weather," *2016 IEEE Power and Energy Society (PES) Innovative Smart Grid Technologies Conference Europe (ISGT-Europe)*, pp. 1–6, 2016, Ljubljana, Slovenia.

[26] M. Moeini-Aghtaie, P. Dehghanian, M. Fotuhi-Firuzabad, and A. Abbaspour, "Multi-agent genetic algorithm: An online probabilistic view on economic dispatch of energy hubs constrained by wind availability," *IEEE Transactions on Sustainable Energy*, vol. 5, no. 2, pp. 699-708, April 2014.

[27] R. Ghorani, M. Fotuhi-Firuzabad, P. Dehghanian, and W. Li, "Identifying critical component for reliability centered maintenance management of deregulated power systems," *IET Generation, Transmission, and Distribution*, vol. 9, no. 9, pp. 828-837, June 2015.

[28] M. Asghari Gharakheili, M. Fotuhi-Firuzabad, and P. Dehghanian, "A new multi-attribute support tool for identifying critical components in power transmission systems," *IEEE Systems Journal*, in press, November 2015.

[29] F. Pourahmadi, M. Fotuhi-Firuzabad, and P. Dehghanian, "Identification of critical generating units for maintenance: A game theory approach," *IET Generation, Transmission & Distribution*, vol. 10, no. 12, pp. 2942-2952, 2016.

[30] R. Azizpanah-Abarghooee, P. Dehghanian, and V. Terzija, “A practical multi-area bi-objective environmental economic dispatch equipped with a hybrid gradient search method and improved Jaya algorithm,” *IET Generation, Transmission & Distribution*, vol. 10, no. 14, pp. 3580-3596, 2016.

[31] F. Pourahmadi, M. Fotuhi-Firuzabad, and P. Dehghanian, “Application of game theory in reliability centered maintenance of electric power systems,” *IEEE Transactions on Industry Applications*, vol. 53, no. 2, pp. 936-946, March-April 2017.

[32] A. A. Mazi, B. F. Wollenberg, and M. H. Hesse, “Corrective control of power system flows by line and bus-bar switching,” *IEEE Transactions on Power Systems*, vol. 1, no. 3, pp. 258–264, Aug. 1986.

[33] B. G. Gorenstin, L. A. Terry, M. V. F. Pereira, and L. M. V. G. Pinto, “Integrated network topology optimization and generation rescheduling for power system security applications,” *International Symposium on High Technology in the Power Industry*, pp. 110–114, 1986, Bozeman, MT, USA.

[34] A. G. Bakirtzis and A. P. (Sakis) Meliopoulos, “Incorporation of switching operations in power system corrective control computations,” *IEEE Transactions on Power Systems*, vol. 2, no. 3, pp. 669–675, Aug. 1987.

[35] E. B. Makram, K. P. Thornton, and H. E. Brown, “Selection of lines to be switched to eliminate overloaded lines using a Z-matrix method,” *IEEE Transactions on Power Systems*, vol. 4, no. 2, pp. 653-661, May 1989.

[36] R. Bacher and H. Glavitsch, “Network topology optimization with security constraints,” *IEEE Transactions on Power Systems,* vol. 1, no. 4, pp. 103–111, 1986.

[37] G. Schnyder and H. Glavitsch, “Integrated security control using an optimal power flow and switching concepts,” *IEEE Transactions on Power Systems,* vol. 3, no. 2, pp. 782–790, May 1988.

[38] A. G. Bakirtzis and A. P. S. Meliopoulos, “Incorporation of switching operations in power system corrective control computations,” *IEEE Transactions on Power Systems,* vol. 2, no. 3, pp. 669–675, Aug. 1987.

[39] G. Schnyder and H. Glavitsch, “Security enhancement using an optimal switching power flow,” *IEEE Transactions on Power Systems*, vol. 5, no. 2, pp. 674–681, May 1990.

[40] W. Shao and V. Vittal, “A new algorithm for relieving overloads and voltage violations by transmission line and bus-bar switching,” *IEEE Power and Energy Society (PES) Power Systems Conference and Exposition,* pp. 322–327, 2004, New York, USA.

[41] W. Shao and V. Vittal, “Corrective switching algorithm for relieving overloads and voltage violations,” *IEEE Transactions on Power Systems*, vol. 20, no. 4, pp. 1877–1885, November 2005.

[42] R. Bacher and H. Glavitsch, “Loss reduction by network switching,” *IEEE Transactions on Power Systems,* vol. 3, no. 2, pp. 447–454, May 1988.

[43] S. Fliscounakis, F. Zaoui, G. Simeant, and R. Gonzalez, "Topology influence on loss reduction as a mixed integer linear programming problem," in *IEEE Power Tech Conference*, pp. 1987–1990, July 2007, Lausanne, Switzerland.

[44] K. W. Hedman, S. S. Oren, and R. P. O'Neill, "A review of transmission switching and network topology optimization," in *Proc. IEEE Power and Energy Society (PES) General Meeting*, pp. 1–7, July 2011, Detroit, MI, USA.

[45] G. Poyrazoglu and O. HyungSeon, "Optimal topology control with physical power flow constraints and N-1 contingency criterion," *IEEE Transactions on Power Systems*, vol. 30, no. 6, pp. 3063–3071, Nov. 2015.

[46] G. Granelli, M. Montagna, F. Zanellini, P. Bresesti, R. Vailati, and M. Innorta, "Optimal network reconfiguration for congestion management by deterministic and genetic algorithms," *Electric Power Systems Research*, vol. 76, no. 6-7, pp. 549–556, Apr. 2006.

[47] M. Khanabadi, H. Ghasemi, and M. Doostizadeh, "Optimal transmission switching considering voltage security and N-1 contingency analysis," *IEEE Transactions on Power Systems*, vol. 28, no. 1, pp. 542–550, Feb. 2013.

[48] A. R. Escobedo, E. Moreno-Centeno, and K. W. Hedman, "Topology control for load shed recovery," *IEEE Transactions on Power Systems*, vol. 29, no. 2, pp. 908–916, March 2014.

[49] M. Kezunovic, T. Popovic, G. Gurrala, P. Dehghanian, A. Esmaeilian, and M. Tasdighi, "Reliable implementation of robust adaptive topology control," in *Proc.*

The 47th Hawaii International Conference on System Sciences (HICSS), 6–9 Jan. 2014, Big Island, USA.

[50] P. Dehghanian, Y. Wang, G. Gurrala, E. Moreno-Centeno, and M. Kezunovic, "Flexible implementation of power system corrective topology control," *Electric Power Systems Research*, vol. 128, pp. 79–89, Nov. 2015.

[51] M. Abdi-Khorsand, K. W. Hedman, "Day-ahead corrective transmission topology control," in *Proc. IEEE Power and Energy Society (PES) General Meeting*, pp.1–5, July 2014, Washington DC, USA.

[52] J. Shi, S. S. Oren, "A data mining approach for real-time corrective switching," in *Proc. IEEE Power and Energy Society (PES) General Meeting*, pp. 1–5, July 2015, Denver, USA.

[53] T. Guler, G. Gross, and M. Liu, "Generalized line outage distribution factors," *IEEE Transactions on Power Systems*, vol. 22, no. 2, pp. 879–881, May 2007.

[54] P. A. Ruiz, A. Rudkevich, M. C. Caramanis, E. Goldis, E. Ntakou, and C. R. Philbrick, "Reduced MIP formulation for transmission topology control," in *Proc. 50th Annual Allerton Conference on Communication, Control, and Computing*, 1–5 Oct. 2012, Monticello, IL, USA.

[55] M. Sahraei-Ardakani, X. Li, P. Balasubramanian, K. W. Hedman, and M. Abdi-Khorsand, "Real-time contingency analysis with transmission switching on real power system data," *IEEE Transactions on Power Systems*, vol. 31, no. 3, pp. 2501–2502, May 2016.

[56] M. Sahraei-Ardakani, A. Korad, K. W. Hedman, P. Lipka, and S. Oren, "Performance of AC and DC based transmission switching heuristics on a large-scale polish system," in *Proc. IEEE Power and Energy Society (PES) General Meeting*, pp.1–5, July 2014, National Harbor, MD, USA.

[57] X. Li, P. Balasubramanian, M. Abdi-Khorsand, A. Korad, K. W. Hedman, "Effect of topology control on system reliability: TVA test case," *Cigre US National Committee Grid of the Future Symposium*, Oct. 2014, Houston, Texas, USA.

[58] A. S. Korad and K. W. Hedman, "Robust corrective topology control for system reliability," *IEEE Transactions on Power Systems*, vol. 28, no. 4, pp. 4042–4051, Nov. 2013.

[59] A. S. Korad and K. W. Hedman, "Zonal do-not-exceed limits with robust corrective topology control," *Electric Power Systems Research*, vol. 129, pp. 235–242, Dec. 2015.

[60] S. Zhang, N. G. Singhal, K. W. Hedman, V. Vittal, and J. Zhang, "An evaluation of algorithms to solve for do-not-exceed limits for renewable resources," *48th Hawaii International Conference in System Sciences (HICSS)*, pp. 2567–2576, Jan. 2015, Hawaii, USA.

[61] Y. Al-Abdullah, M. Abdi-Khorsand, K. W. Hedman, "Analyzing the impacts of out-of-market corrections," in *Proc. IREP Symposium in Bulk Power System Dynamics and Control*, pp. 1–10, Aug. 2013, Crete, Greece.

[62] Y. Al-Abdullah, M. Abdi-Khorsand, K. W. Hedman, "The role of out-of-market corrections in day-ahead scheduling," *IEEE Transactions on Power Systems*, vol. 30, no. 4, pp. 1937–1946, July 2015.

[63] S. Bruno, M. D'Aloia, G. D. Carne, and M. La Scala, "Controlling transient stability through line switching," in *Proc. 3rd IEEE Power and Energy Society (PES) Innovative Smart Grid Technologies (ISGT Europe)*, Germany, 2012.

[64] G. M. Huang, W. Wang, and J. An, "Stability issues of smart grid transmission line switching," in *Proc. 19th World Congress of the International Federation of Automatic Control (IFAC)*, Aug. 2014, Cape Town, South Africa.

[65] L. Chen, Y. Tada, H. Okamoto, R. Tanabe, and H. Mitsuma, "Optimal reconfiguration of transmission systems with transient stability constraints," *International Conference on Power System Technology*, vol. 2, pp. 1346–1350, Aug. 1998, Beijing, China.

[66] A. S. Korad and K. W. Hedman, "Reliability and stability analysis of corrective topology control actions," *IEEE Power Tech Conference*, pp.1–6, 2015, Eindhoven, Netherland.

[67] R. P. O'Neill, R. Baldick, U. Helman, M. H. Rothkopf, and W. S. Jr., "Dispatchable transmission in RTO markets," *IEEE Transactions on Power Systems*, vol. 20, no. 1, pp. 171–179, Feb. 2005.

[68] E. B. Fisher, R. P. O'Neill, and M. C. Ferris, "Optimal transmission switching," *IEEE Transactions on Power Systems*, vol. 23, no. 3, pp. 1346–1355, Aug. 2008.

[69] K. W. Hedman, R. P. O'Neill, E. B. Fisher, and S. S. Oren, "Optimal transmission switching—sensitivity analysis and extensions," *IEEE Transactions on Power Systems*, vol. 23, no. 3, pp. 1469–1479, Aug. 2008.

[70] K. W. Hedman, S. S. Oren, and R. P. O'Neill, "Optimal transmission switching: economic efficiency and market implications," *Journal of Regulatory Economics*, vol. 40, no. 2, pp. 111–140, 2011.

[71] K. W. Hedman, R. P. O'Neill, E. B. Fisher, and S. S. Oren, "Optimal transmission switching with contingency analysis," *IEEE Transactions on Power Systems*, vol. 24, no. 3, pp. 1577–1586, Aug. 2009.

[72] R. P. O'Neill, K. W. Hedman, E. A. Krall, A. Papavasiliou, and S. S. Oren, "Economic analysis of the N-1 reliable unit commitment and transmission switching problem using duality concepts," *Energy Systems*, vol. 1, no. 2, pp. 165–195, May 2010.

[73] K. W. Hedman, R. P. O'Neill, E. B. Fisher, and S. S. Oren, "Smart flexible just-in-time transmission and flowgate bidding," *IEEE Transactions on Power Systems*, vol. 26, no. 1, pp. 93–102, Feb. 2011.

[74] M. Soroush, J. D. Fuller, "Accuracies of optimal transmission switching heuristics based on DCOPF and ACOPF," *IEEE Transactions on Power Systems*, vol. 29, no. 2, pp. 924–932, March 2014.

[75] M. Soroush, "Accuracies of optimal transmission switching heuristics based on exact and approximate power flow equations," *Master of Science Thesis*, University of Waterloo, Ontario, Canada, 2013.

[76] G. Poyrazoglu and O. HyungSeon, “Optimal topology control with physical power flow constraints and N-1 contingency criterion,” *IEEE Transactions on Power Systems*, vol. 30, no. 6, pp. 3063–3071, Nov. 2015.

[77] E. A. Goldis, X. Li, M. C. Caramanis, A. M. Rudkevich, and P. A. Ruiz, “AC-based topology control algorithms (TCA)- a PJM historical data case study,” in *Proc. 48th Hawaii International Conference in System Sciences (HICSS)*, pp. 2516–2519, Jan. 2015, Hawaii, USA.

[78] P. Dehghanian and M. Kezunovic, “Impact assessment of power system topology control on system reliability,” *IEEE Conference on Intelligent System Applications to Power Systems* (ISAP), 11–16 Sep. 2015, Porto, Portugal.

[79] P. Dehghanian and M. Kezunovic, “Probabilistic impact of transmission line switching on power system operating states,” *IEEE Power and Energy Society (PES) Transmission and Distribution (T&D) Conference and Exposition*, May 2–5, 2016, Dallas, USA.

[80] A. Khodaei and M. Shahidehpour, “Transmission switching in security-constrained unit commitment,” *IEEE Transactions on Power Systems*, vol. 25, no. 4, pp. 1937–1945, Nov. 2010.

[81] A. Khodaei, M. Shahidehpour and S. Kamalinia, “Transmission switching in expansion planning,” *IEEE Transactions on Power Systems*, vol. 25, no. 3, pp. 1722–1733, Aug. 2010.

[82] A. Khodaei and M. Shahidehpour, "Security-constrained transmission switching with voltage constraints," *International Journal of Electrical Power and Energy Systems*, vol. 35, no. 1, pp. 74–82, Feb. 2012.

[83] P. Henneaux, D. S. Kirschen, "Probabilistic security analysis of optimal transmission switching," *IEEE Transactions on Power Systems*, vol. 31, no. 1, pp. 508–517, Jan. 2016.

[84] Q. Feng and J. Wang, "Chance-constrained transmission switching with guaranteed wind power utilization," *IEEE Transactions on Power Systems*, vol. 30, no. 3, pp. 1270–1278, May 2015.

[85] P. Dehghanian, T. Popovic, and M. Kezunovic, "Assessing the impact of power system topology control on circuit breaker reliability and electric safety," *IEEE Industry Application Society (IAS) Electrical Safety Workshop (ESW)*, 27–30 Jan. 2015, Louisville, Kentucky, USA.

[86] P. Dehghanian, T. Popovic, and M. Kezunovic, "Circuit breaker operational health assessment via condition monitoring data," *46th North American Power Symposium (NAPS)*, pp. 1–6, Sept. 2014, Washington State University, Pullman, Washington, USA.

[87] P. Dehghanian and M. Kezunovic, "Circuit breakers and the impact of their maintenance on electric safety," *IEEE Industrial Application Society (IAS) Electrical Safety Workshop (ESW)*, 4–7 Feb. 2014, San Diego, California, USA.

[88] E. A. Goldis, X. Li, M. C. Caramanis, B. Keshavamurthy, M. Patel, A. M. Rudkevich, and P. Ruiz, "Applicability of topology control algorithms (TCA) to a

real-size power system," in *Proc. 51th Annual Allerton Conference*, Oct. 2013, Illinois, USA.

[89] P. Balasubramanian, M. Sahraei-Ardakani, X. Li and K. W. Hedman, "Towards smart corrective switching: analysis and advancement of PJM's switching solutions," *IET Generation, Transmission & Distribution*, vol. 10, no. 8, pp. 1984–1992, 2016.

[90] J. Han and A. Papavasiliou, "The impacts of transmission topology control on the European electricity network," *IEEE Transactions on Power Systems*, vol. 31, no. 1, pp. 496–507, Jan. 2016.

[91] J. D. Lyon, *et.al*., "Harnessing flexible transmission: corrective transmission switching for ISO-NE," *IEEE Power and Energy Technology Systems Journal*, vol. 3, no. 3, pp. 109–118, Sept. 2016.

[92] M. Sahraei-Ardakani, X. Li, P. Balasubramanian, K. W. Hedman and M. Abdi-Khorsand, "Real-time contingency analysis with transmission switching on real power system data," *IEEE Transactions on Power Systems*, vol. 31, no. 3, pp. 2501–2502, May 2016.

[93] O. Mäkelä, J. Warrington, M. Morari and G. Andersson, "Optimal transmission line switching for large-scale power systems using the Alternating Direction Method of Multipliers," in Proc. *Power Systems Computation Conference*, pp. 1–6, Aug. 2014, Wroclaw, Poland.

[94] P. A. Ruiz, J. M. Foster, A. Rudkevich, and M. C. Caramanis, "On fast transmission topology control heuristics," in *Proc. IEEE Power and Energy Society (PES) General Meeting*, pp. 1–9, July 2011, Detroit, Michigan, USA.

[95] J. D. Fuller, R. Ramasra, and A. Cha, "Fast heuristics for transmission line switching," *IEEE Transactions on Power Systems*, vol. 27, no. 3, pp. 1377–1386, 2012.

[96] P. A. Ruiz, J. M. Foster, A. Rudkevich, and M. C. Caramanis, "Tractable transmission topology control using sensitivity analysis," *IEEE Transactions on Power Systems*, vol. 27, no. 3, pp. 1550–1559, 2012.

[97] P. A. Lipka, R. P. O'Neill, S. S. Oren, A. Castillo, M. Pirnia, and C. Campaigne, "Optimal transmission switching using the IV-ACOPF linearization," *FERC Staff Technical Paper*, Nov. 2013. [Online]. Available: http://www.ferc.gov/industries/electric/indus-act/market-planning/opf-papers/acopf-10.pdf.

[98] T. J. Overbye, V. Vittal, and I. Dobson, *Engineering Resilient Cyber–Physical Systems*. Tempe, AZ, USA: PSERC, May 2012, ser. PSERC Publication 12–16.

[99] Cabinet Office, "Keeping the country running: Natural hazards and infrastructure," London, U.K., Oct. 2011.

[100] M. Keogh and C. Cody, *Resilience in Regulated Utilities*. Washington, DC, USA: The National Association of Regulatory Utility Commissioners (NAURC), Nov. 2013.

[101] U. G. Knight, *Power Systems in Emergencies: From Contingency Planning to Crisis Management*. Hoboken, NJ, USA: Wiley, 2001.

[102] M. Panteli, P. Mancarella, "Modeling and evaluating the resilience of critical electrical power infrastructure to extreme weather events," *IEEE Systems Journal*, in press, pp.1–10, 2017.

[103] M. Panteli, P. Mancarella, S. Wilkinson, R. Dawson and C. Pickering, "Assessment of the resilience of transmission networks to extreme wind events," *IEEE Eindhoven Power Tech*, pp. 1–6, 29 June – 2 July 2015, Eindhoven, Netherland.

[104] M. Panteli, D. N. Trakas, P. Mancarella and N. D. Hatziargyriou, "Boosting the power grid resilience to extreme weather events using defensive islanding," *IEEE Transactions on Smart Grid*, vol. 7, no. 6, pp. 2913–2922, Nov. 2016.

[105] M. Panteli, A. I. Nikolaidis, C. A. Charalambous, Y. Zhou, F. R. Wood, S. Glynn, and P. Mancarella, "Analyzing the resilience and flexibility of power systems to future demand and supply scenarios," *18th Mediterranean Electro-technical Conference (MELECON)*, pp. 1–6, 2016, Limassol, Cyprus.

[106] A. Zibelmen, "REVing up the energy vision in New York: Seizing the opportunity to create a cleaner, more resilient, and affordable energy system," *IEEE Power and Energy Magazine*, vol. 14, no. 3, pp. 18–24, May/Jun. 2016.

[107] D. Manz, R. Walling, N. Miller, B. LaRose, R. D'Aquila, and B. Daryanian, "The grid of the future: Ten trends that will shape the grid over the next decade," *IEEE Power and Energy Magazine*, vol. 12, no. 3, pp. 26–36, May/Jun. 2014.

[108] B. Zhang, P. Dehghanian and M. Kezunovic, "Optimal allocation of PV generation and battery storage for enhanced resilience," *IEEE Transactions on Smart Grid*, in press, 2017

[109] C. Chen, J. Wang, F. Qiu, and D. Zhao, "Resilient distribution system by microgrids formation after natural disasters," *IEEE Transactions on Smart Grid*, vol. 7, no. 2, pp. 958–966, Mar. 2016.

[110] H. Aki, "Demand-side resiliency and electricity continuity: experiences and lessons learned in Japan," in *Proceedings of the IEEE,* in press, pp.1–13, 2017.

[111] H. Gao, Y. Chen, S. Mei, S. Huang, and Y. Xu, "Resilience-oriented pre-hurricane resource allocation in distribution systems considering electric buses," in *Proceedings of the IEEE*, in press, pp.1–20, 2017.

[112] Z. Bie, Y. Lin, G. Li, and F. Li, "Battling the extreme: a study on the power system resilience," in *Proceedings of the IEEE*, in press, pp.1–14, 2017.

[113] Z. Li, M. Shahidehpour, F. Aminifar, A. Alabdulwahab, and Y. Al-Turki, "Networked microgrids for enhancing the power system resilience," in *Proceedings of the IEEE*, in press, pp.1–22, 2017.

[114] M. Yeary, B. L. Cheong, J. M. Kurdzo, T. Y. Yu, and R. Palmer, "A brief overview of weather radar technologies and instrumentation," *IEEE Instrumentation & Measurement Magazine*, vol. 17, no. 5, pp. 10–15, Oct. 2014.

[115] Y. Xie, Y. Xue, H. Wang, T. Xu, Z. Dong, and X. Jin, "Space-time early warning of power grid fault probability by lightning," *Automation of Electric Power Systems*, vol. 37, no.17, pp.44–51, 2013.

[116] A. Arab, A. Khodaei, Z. Han, and S. K. Khator, "Proactive recovery of electric power assets for resiliency enhancement," *IEEE Access*, vol. 3, pp. 99–109, Feb. 2015.

[117] N. Xu, S. D. Guikema, R. A. Davidson, L. K. Nozick, Z. Cagnan, and K. Vaziri, "Optimizing scheduling of post-earthquake electric power restoration tasks," *Earthquake Engineering Structural Dynamics*, vol. 36, no. 2, pp. 265–284, Feb. 2007.

[118] P. Van Hentenryck, N. Gillani, and C. Coffrin, "Joint assessment and restoration of power systems," in *Proc. 20th European Conference on Artificial Intelligence*, pp. 792–797, Aug. 2012, Montpellier, France.

[119] T. C. Matisziw, A. T. Murray, and T. H. Grubesic, "Strategic network restoration," *Networks and Spatial Economics*, vol. 10, no. 3, pp. 345–361, Sep. 2010.

[120] S. G. Nurre, B. Cavdaroglu, J. E. Mitchell, T. C. Sharkey, and W. A. Wallace, "Restoring infrastructure systems: An integrated network design and scheduling (INDS) problem," *European Journal of Operation Research*, vol. 223, no. 3, pp. 794–806, Dec. 2012.

[121] P. Van Hentenryck, C. Coffrin, and R. Bent, "Vehicle routing for the last mile of power system restoration," in *Proc. 17th Power System Computation Conference*, pp. 1–8, Aug. 2011, Stockholm, Sweden.

[122] B. Simon, C. Coffrin, and P. Van Hentenryck, "Randomized adaptive vehicle decomposition for large-scale power restoration," in *Proc. 9th International Conference on Integration of Artificial Intelligence (AI) and Operations Research*

(OR) Techniques in Constraint Programming, pp. 379–394, Jun. 2012, Nantes, France.

[123] N. Perrier, B. Agard, P. Baptiste, J. M. Frayret, A. Langevin, R. Pellerin, D. Riopel, and M. Trepanier, "A survey of models and algorithms for emergency response logistics in electric distribution systems. Part I: Reliability planning with fault considerations," *Computers and Operations Research*, vol. 40, no. 7, pp. 1895–1906, Jul. 2013.

[124] N. Perrier, B. Agard, P. Baptiste, J. M. Frayret, A. Langevin, R. Pellerin, D. Riopel, and M. Trepanier, "A survey of models and algorithms for emergency response logistics in electric distribution systems. Part II: Contingency planning level," *Computers and Operations Research*, vol. 40, no. 7, pp. 1907–1922, Jul. 2013.

[125] A. S. Korad and K. W. Hedman, "Enhancement of do-not-exceed limits with robust corrective topology control," *IEEE Transactions on Power Systems*, vol. 31, no. 3, pp. 1889–1899, May 2016.

[126] R. Billinton, H. Chen, and R. Ghajor, "A sequential simulation technique for adequacy evaluation of generating system including wind energy," *IEEE Transactions on Energy Conversion*, vol. 11, no. 4, pp.728–734, 1996.

[127] B. Zhang, P. Dehghanian and M. Kezunovic, "Spatial-temporal solar power forecast through Gaussian Conditional Random Field," *IEEE Power and Energy Society (PES) General Meeting*, pp. 1-5, July 2016, Boston, MA, USA.

[128] B. Zhang, P. Dehghanian and M. Kezunovic, "Simulation of weather impacts on the wholesale electricity market," *10th International Conference on Deregulated*

Electricity Market Issues in South Eastern Europe (DEMSEE'15), pp. 1-5, Sep. 2015, Budapest, Hungary.

[129] A. Mcre and M. C. Deo, "Forecasting wind with neural network," *Marine Structures*, vol. 16, no. 1, pp. 35–49, Jan.–Feb. 2003.

[130] J. V. Seguro and T. W. Lambert, "Modern estimation of the parameters of the Weibull wind speed distribution for wind energy analysis," *Journal of Wind Engineering and Industrial Aerodynamics*, vol. 85, no. 1, pp. 75–84,March 2000.

[131] A. N. Celik, "A statistical analysis of wind power density based on the Weibull and Rayleigh models at the southern region of Turkey," *Renewable Energy*, vol. 4, no. 29, pp. 593–604, 2004.

[132] E. C. Morgan, M. Lackner, R. M. Vogel, L. G. Baise, "Probability distributions for offshore wind speeds," *Energy Conversion and Management*, vol. 52, no. 1, pp. 15–26, January 2011.

[133] M. Moeini-Aghtaie, A. Abbaspour, and M. Fotuhi-Firuzabad, "Incorporating large-scale distant wind farms in probabilistic transmission expansion planning—part I: theory and algorithm," *IEEE Transactions on Power Systems*, vol. 27, no. 3, pp. 1585–1593, 2012.

[134] P. Dehghanian, S. H. Hosseini, M. Moeini-Aghtaie, and S. Arabali, "Optimal siting of DG units in power systems from a probabilistic multi-objective optimization perspective," *International Journal of Electrical Power and Energy Systems*, vol. 51, pp. 14-26, October 2013.

[135] M. Moeini-Aghtaie, A. Abbaspour, M. Fotuhi-Firuzabad, and P. Dehghanian, "Optimized probabilistic PHEV demand management in the context of energy hubs," *IEEE Transactions on Power Delivery*, vol. 30, no. 2, pp. 996-1006, April 2015.

[136] M. Moeini-Aghtaie, P. Dehghanian, E. Vaezizade, and M. Fotuhi-Firuzabad, "Embedded generation planning in presence of renewable energies using a probabilistic scenario-based multi-objective optimization approach," *The 1st International Conference on Integration of Renewable into Power Distributions Systems*, CIRED-Workshop, May 2012, Lisbon, Portugal.

[137] P. Dehghanian, M. Moeini-Aghtaie, M. Fotuhi-Firuzabad, and A. Abbaspour, "Incorporating probabilistic cost/worth analysis in maintenance prioritization of power distribution components," *12th International Conference on Probabilistic Methods Applied in Power Systems* (PMAPS), June 2012, Istanbul, Turkey.

[138] E. Rosenblueth, "Point estimation for probability moments," *Proceedings of National Academy of Science* USA., vol. 72, no. 10, pp. 3812–3814, Oct. 1975.

[139] P. Dehghanian and M. Kezunovic, "Probabilistic decision making for the bulk power system optimal topology control," *IEEE Transactions on Smart Grid*, vol. 7, no. 4, pp. 2071–2081, June 2016.

[140] W. Li, *Probabilistic Transmission System Planning*. New York: Wiley and IEEE Press, 2011.

[141] R. Bilinton and R.N. Allan, *Reliability Evaluation of Power Systems*. Plenum press, 2nd edition, 1994.

[142] R. D. Zimmerman, C. E. Murillo-Sánchez, and R. J. Thomas, "MATPOWER: Steady-state operations, planning and analysis tools for power systems research and education," *IEEE Transactions on Power Systems*, vol. 26, no. 1, pp. 12–19, Feb. 2011.

[143] T. Dokic, P. Dehghanian, P-C. Chen, M. Kezunovic, Z. Medina-Cetina, J. Stojanovic, and Z. Obradovic, "Risk assessment of a transmission line insulation breakdown due to lightning and severe weather," *The 49th Hawaii International Conference on System Science* (HICSS), Jan. 2016, Big Island, USA.

[144] M. Kezunovic, Z. Obradovic, T. Dokic, B. Zhang, J. Stojanovic, P. Dehghanian, and P. -C. Chen, *Predicting spatiotemporal impacts of weather on power systems using big data science*, Data Science and Big Data: An Environment of Computational Intelligence, Springer International Publishing, vol. 24, pp. 265-299, 2017, ISBN: 978-3-319-53474-9.

[145] P. Dehghanian and M. Fotuhi-Firuzabad, "A Reliability-oriented outlook on the critical components of power distribution systems," *The 9th IET International Conference on Advances in Power System Control, Operation, and Management* (APSCOM), Nov. 2012, Hong Kong.

[146] N. Srinivas and K. Deb, "Multi objective function optimization using non-dominated sorting genetic algorithm," *IEEE Transactions on Evolutionary Computation*, vol. 2, no. 3, pp. 221–248, 1994.

[147] R. T. Marler and J. S. Arora, "Survey of multi-objective optimization methods for engineering," *Structural and Multidisciplinary Optimization*, vol. 26, no. 6, pp. 369–395, Apr. 2004.

[148] P. Dehghanian, M. Fotuhi-Firuzabad, S. Bagheri-Shouraki, and A. A. Razi Kazemi, "Critical component identification in reliability centered asset management of distribution power systems via fuzzy AHP," *IEEE Systems Journal*, vol. 6, no. 4, pp. 593-602, December 2012.

[149] A. A. Razi Kazemi and P. Dehghanian, "A practical approach to optimal RTU placement in power distribution systems incorporating fuzzy sets theory," *International Journal of Electrical Power and Energy Systems*, vol. 37, no. 1, pp. 31-42, May 2012.

[150] P. Dehghanian, A. A. Razi Kazemi, and M. Fotuhi-Firuzabad, "Optimal RTU placement in power distribution systems using a novel method based on analytical hierarchical process (AHP)," *The 10th International IEEE Conference on Environmental and Electrical Engineering* (EEEIC), May 2011, Rome, Italy.

[151] P. Dehghanian, M. Fotuhi-Firuzabad, and A. A. Razi Kazemi, "An approach for critical component identification in reliability-centered maintenance of power distribution systems based on analytical hierarchical process," *The 21st International Conference and Exhibition on Electricity Distribution* (CIRED), June 2011, Frankfurt, Germany.

[152] A. A. Razi Kazemi, P. Dehghanian, and Gh. Karami, "A probabilistic approach for remote terminal unit placement in power distribution systems," *The 33th IEEE*

International Telecommunications Energy Conference (INTELEC), Oct. 2011, Amsterdam, Netherlands.

[153] P. Dehghanian, A. A. Razi Kazemi, and Gh. Karami, "Incorporating experts knowledge in RTU placement procedure using fuzzy sets theory: a practical approach," *The 33th IEEE International Telecommunications Energy Conference* (INTELEC), Oct. 2011, Amsterdam, Netherlands.

[154] M. Shojaie, V. Rastegar-Moghaddam, A. A. Razi Kazemi, P. Dehghanian, and Gh. Karami, "A new look on the automation of medium voltage substations in power distribution systems," *17th Conference on Electric Power Distribution Networks* (EPDC), May 2012, Tehran, Iran.

[155] K. Deb, *Multi-Objective Optimization Using Evolutionary Algorithms*. New York: Wiley, 2003.

[156] S. K. Bath, J. S. Dhillon, and D. P. Kothari, "Fuzzy satisfying stochastic multi-objective generation scheduling by weightage pattern search methods," *Electric Power Systems Research*, vol. 69, no. 2–3, pp. 311–320, 2004.

[157] P. Maghouli, S. H. Hosseini, M. Oloomi Buygi, and M. Shahidehpour, "A multi-objective framework for transmission expansion planning in deregulated environments," *IEEE Transactions on Power Systems*, vol. 24, no. 2, pp. 1051–1061, May 2009.

[158] TAVANIR Annual Generation and Transmission Reports. [Online] Available at: http://www.tavanir.org.ir/.

[159] Market Operation Reports. [Online]. Available: http://www.igmc.ir

[160] IEC 60050–441 International Electro technical Vocabulary–Chapter 441: Switchgear, control gear and fuses, 1984.

[161] R. Smeets, L. van der Sluis, M. Kapetanovic, D. Peelo, and A. Janssen, *Switching in Electrical Transmission and Distribution Systems*, John Wiley and Sons: United Kingdom, 2015.

[162] Robust Adaptive Topology Control (RATC), Texas Engineering Experiment Station (TEES), [Online] Available at: https://arpa-e.energy.gov/?q=slick-sheet-project/automated-grid-disruption-response-system

[163] J. Endrenyi, *et.al*., "The present status of maintenance strategies and the impact of maintenance on reliability," *IEEE Transactions on Power Systems*, vol. 16, no. 4, pp. 638–646, Nov 2001.

[164] P. Dehghanian, M. Fotuhi-Firuzabad, F. Aminifar, and R. Billinton, "A comprehensive scheme for reliability centered maintenance implementation in power distribution systems- Part I: methodology," *IEEE Transactions on Power Delivery*, vol. 28, no. 2, pp. 761-770, April 2013.

[165] P. Dehghanian, M. Fotuhi-Firuzabad, F. Aminifar, and R. Billinton, "A comprehensive scheme for reliability centered maintenance implementation in power distribution systems- Part II: numerical analysis," *IEEE Transactions on Power Delivery*, vol. 28, no. 2, pp. 771-778, April 2013.

[166] L. Tomasevicz, and S. Asgarpoor, "Optimum maintenance policy using semi-Markov decision processes," *Electric Power Systems Research*, no. 79, pp. 1286–1291, 2009.

[167] H. Sabouhi, A. Abbaspour, M. Fotuhi-Firuzabad, and P. Dehghanian, "Reliability modeling and availability analysis of combined cycle power plants," *International Journal of Electrical Power and Energy Systems*, vol. 79, pp. 108-119, July 2016.

[168] H. Sabouhi, M. Fotuhi-Firuzabad, and P. Dehghanian, "Identifying critical components of combined cycle power plants for implementation of reliability centered maintenance," *IEEE CSEE Journal of Power and Energy Systems*, vol. 2, no. 2, pp. 87-97, June 2016.

[169] J. Endrenyi, G. Anders, and A. L. da Silva, "Probabilistic evaluation of the effect of maintenance on reliability—An application," *IEEE Transactions on Power Systems*, vol. 13, no. 2, pp. 576–582, May 1998.

[170] L. Jalili, M. Sadeghi Khomami, M. Fotuhi-Firuzabad, P. Dehghanian, and A. Rajabi-Ghahnavieh, "Designing a financially efficient risk-oriented model for maintenance planning of power systems: A practical perspective," *12th International Conference on Probabilistic Methods Applied in Power Systems* (PMAPS), June 2012, Istanbul, Turkey.

[171] P. Dehghanian, M. Fotuhi-Firuzabad, S. E. Moghimi, and M. Sadeghi-Khomam, "Investigation of the current maintenance experiences in power distribution utilities of Iran," *The 22th International Conference and Exhibition on Electricity Distribution* (CIRED), June 2013, Stockholm, Sweden.

[172] P. Dehghanian, M. Moeini-Aghtaie, M. Fotuhi-Firuzabad, and R. Billinton, "A practical application of the Delphi method in maintenance-targeted resource allocation of distribution utilities," *13th International Conference on Probabilistic*

Methods Applied to Power Systems (PMAPS), July 2014, Durham University, Durham, England.

[173] S. Natti and M. Kezunovic, "Assessing circuit breaker performance using condition-based data and Bayesian approach," *Electric Power Systems Research*, no. 81, pp.1796–1804, 2011.

[174] M. Kezunovic, M. Knezev, and Z. Djekic, "Automated circuit breaker monitoring," US. DOE CERTS Project, Power System Engineering Research Center (PSERC), 2007.

[175] A. Janssen, D. Makareinis, and C. E. Solver, "International surveys on circuit breaker reliability data for substation and system studies," *IEEE Transactions on Power Delivery*, vol. 29, no. 2, pp. 808–814, April 2014.

[176] M. Runde, "Failure frequencies for high-voltage circuit breakers, disconnectors, earthling switches, instrument transformers, and gas-insulated switchgears," *IEEE Transactions on Power Delivery*, vol. 28, no. 1, pp. 529–530, Jan.2013.

[177] "Field experiences with HV breaker condition monitoring," *ABB technical description*, [Online]. Available: http://www.abb.com.

[178] Working Group A3.12, "Failure survey on circuit breaker control systems summary report for Electra," *CIGRE, Electra* no.216, Oct 2004.

[179] L.T. Rumfiled, "Circuit breaker diagnostic response testing using the RTR-84 response time recorder," *Sixty-first Annual International Conference of Doble Clients*, June 1994, Boston, MA, USA.

[180] S. M. Strachan, S. D. J. McArthur, B. Stephen, J. R. McDonald, A. Campbell, "Providing decision support for the condition-based maintenance of circuit breakers through data mining of trip coil current signatures," *IEEE Transactions on Power Delivery*, vol. 22, no. 1, pp. 178–186, Jan. 2007.

[181] B. Stephen, S. M. Strachan, S. D. J. McArthur, J. R. McDonald, K. Hamilton, "Design of trip current monitoring system for circuit breaker condition assessment," *IET Generation, Transmission & Distribution*, vol. 1, no. 1, pp. 89–95, January 2007.

[182] M. Kezunovic, Z. Ren, G. Latisko, D. R. Sevcik, J. S. Lucey, W. E. Cook, E. A. Koch, "Automated monitoring and analysis of circuit breaker operations," *IEEE Transactions on Power Delivery*, vol. 20, no. 3, pp. 1910–1918, July 2005.

[183] H. Fischer, *A history of the central limit Theorem from classical to modern probability theory*. New York, NY, USA: Springer, 2010.

[184] Y. Guan, M. Kezunovic, P. Dehghanian, and G. Gurrala, "Assessing circuit breaker life cycle using condition-based data," *IEEE Power and Energy Society (PES) General Meeting*, July 2013, Vancouver, Canada.

[185] P. Dehghanian, and M. Kezunovic, "Cost/benefit analysis for circuit breaker maintenance planning and scheduling," *The 45th North American Power Symposium* (NAPS), Sep. 2013, Kansas State, USA.

[186] M. Keravand, J. Faiz, M. Soleimani, M. Ghasemi-Bijan, M. Bandar-Abadi and S. M. Â. Cruz, "A fast, precise and low cost stator inter-turn fault diagnosis technique for wound rotor induction motors based on wavelet transform of rotor current,"

IEEE 11th International Symposium on Diagnostics for Electrical Machines, Power Electronics and Drives (SDEMPED), pp. 254-259, Aug.-Sept. 2017, Tinos, Greece.

[187] J. Faiz and M. Soleimani, "Dissolved gas analysis evaluation in electric power transformers using conventional methods: a review," *IEEE Transactions on Dielectrics and Electrical Insulation*, vol. 24, no. 2, pp. 1239-1248, April 2017.

[188] H. B. Puttgen, *Computational cycle time evaluation for steady state power flow calculations, Report Prepared for Thomson-CSF, Division Simulators*, Georgia Institute of Technology, Dec. 1985, [Online]. Available: https://smartech.gatech.edu/jspui/bitstream/1853/35556/2/e-21-75-302129-fr.pdf.

[189] Power System Test Case Archive, Univ. Washington, Dept. Elect. Eng., 2007, [Online]. Available: http://www.ee.washington.edu/research/pstca/ .

[190] ——, "Two-point estimates in probability," *Applied Mathematical Modeling*, vol. 5, no. 5, pp. 329–335, Oct. 1975.

[191] "Energy independence and security act of 2007," Public Law 110–140, 110th Congress of United States of America, Dec. 19, 2007.

[192] D. Huber, Z. Taylor, S. Knudsen, "Environmental impacts of smart grid," Department of Energy (DOE) - National Energy Technology Laboratory (NETL) report, Jan. 2011.

[193] M. Kezunovic, P. Dehghanian, and J. Sztipanovits, "An incremental system-of-systems integration modelling of cyber-physical electric power systems," *Grid of the Future Symposium, CIGRE US National Committee*, Oct.-Nov. 2016, Philadelphia, Pennsylvania, USA.

[194] T. Becejac, P. Dehghanian, and M. Kezunovic, "Impact of PMU errors on the synchrophasor-based fault location algorithms," *48th North American Power Symposium* (NAPS), Sep. 2016, Denver, Colorado, USA.

[195] T. Becejac, P. Dehghanian, and M. Kezunovic, "Probabilistic assessment of PMU integrity for planning of periodic maintenance and testing," *International Conference on Probabilistic Methods Applied to Power Systems* (PMAPS), Oct. 2016, Beijing, China.

[196] T. Becejac, P. Dehghanian, and M. Kezunovic, "Analysis of PMU algorithm errors during fault transients and out-of-step disturbances," *IEEE Power and Energy Society (PES) Transmission & Distribution (T&D) Conference and Exposition Latin America,* Sep. 2016, Morelia, Mexico.

[197] M. Kezunovic, A. Esmaeilian, T. Becejac, P. Dehghanian, and C. Qian, "Life-cycle management tools for synchrophasor systems: why we need them and what they should entail," *The 2016 IFAC CIGRE/CIRED Workshop on Control of Transmission and Distribution Smart Grids,* October 2016, Prague, Czech Republic.

[198] H. K. Høidalen and M. Runde, "Continuous monitoring of circuit breakers using vibration analysis," *IEEE Transactions on Power Delivery,* vol. 20, no. 4, pp. 2458–2465, October 2005.

[199] S. Natti and M. Kezunovic, "A risk-based decision approach for maintenance scheduling strategies for transmission system equipment," *10th Probabilistic Methods Applied to Power Systems* (PMAPS), pp. 1–6, May 2008, Singapore.

[200] P. Dehghanian, M. Kezunovic, G. Gurrala, and Y. Guan, "Security-based circuit breaker maintenance management," *IEEE Power and Energy Society General Meeting*, pp. 1–5, July 2013, Vancouver, Canada.

[201] J. Yong, J. D. McCalley, and T. Van Voorhis, "Risk-based resource optimization for transmission system maintenance," *IEEE Transactions on Power Systems*, vol. 21, no. 3, pp. 1191–1200, Aug. 2006.

[202] A. A. Razi-Kazemi, M. Vakilian, K. Niayesh, and M. Lehtonen, "Priority assessment of online monitoring investment for power system circuit breakers: qualitative-quantitative approach," *IEEE Transactions on Power Delivery*, vol. 28, no. 2, pp. 928–938, April 2013.

[203] A. A. Razi-Kazemi, M. Vakilian, K. Niayesh, and M. Lehtonen, "Priority assessment of online monitoring investment for system circuit breakers. Part II: determination of optimum number," *IEEE Transactions on Power Delivery*, vol. 28, no. 3, pp.1440–1446, July 2013.

[204] M. Runde, G. E. Ottesen, B. Skyberg, and M. Ohlen, "Vibration analysis for diagnostic testing of circuit breakers," *IEEE Transactions on Power Delivery*, vol. 11, no. 4, pp. 1816–1823, 1996.

[205] H. K. Høidalen and M. Runde, "Continuous monitoring of circuit breakers using vibration analysis," *in Proc. Eleventh International Symposium on High Voltage Engineering*, pp. 102–106, Aug. 1999, London, UK.

[206] L. Stanek and K. Frohlich, “Model-aided diagnosis - A new method for online condition assessment of high voltage circuit breakers,” *IEEE Transactions on Power Delivery*, vol. 15, no. 2, pp. 585–591, 2000.

[207] Z. Stanisic, “Method for static and dynamic resistance measurements of HV circuit breaker,” 2*nd IEEE Power and Energy Society (PES) International Conference and Exhibition on Innovative Smart Grid Technologies* (ISGT-Europe), Dec. 2011, Manchester, UK.

[208] B. Rusek, “Digital modeling and simulations of high voltage circuit-breaker failures for optimization of sensor technique,” *Ph.D. Dissertation*, TU Darmstadt, Germany, 2007.

[209] I. Takagi, E. Yajima, T. Sakakibara, M. Akazaki, S. Wakabayashi, K. Uehara, and N. Takahashi, “Application of gas pressure sensor for fault location system in gas insulated substation,” *IEEE Transactions on Power Delivery*, vol. 10, no. 4, pp. 1806–1815, Oct 1995.

[210] D. S. Lee, B. J. Lithgow, R. E. Morrison, “New fault diagnosis of circuit breakers,” *IEEE Transactions on Power Delivery*, vol. 18, no. 2, pp. 454–459, 2003.

[211] I. Oki, T. Haida, S. Wakabayashi, R. Tsuge, T. Sakakibara, H. Murase, “Development of partial discharge monitoring technique using a neural network in a gas insulated substation,” *IEEE Transactions on Power Systems*, vol. 12, no. 2, pp. 1014–1021, May 1997.

[212] K. Masaki, T. Sakakibara, H. Murase, M. Akazaki, K. Uehara, S. Menju, "On-site measurement for the development of on-line partial discharge monitoring system in GIS," *IEEE Transactions on Power Delivery*, vol. 9, no. 2, pp. 805–810, Apr 1994.

[213] J. D. Wu and C. H. Liu, "An expert system for fault diagnosis in internal combustion engines using wavelet packet transform and neural network," *Expert Systems with Applications*, vol. 36, pp. 4278–4286, 2009.

[214] M. Kezunovic, X. Xu, and D. Won, "Improving circuit breaker maintenance management tasks by applying mobile agent software technology," *Asia Pacific. IEEE/Power and Energy Society (PES) Transmission and Distribution Conference and Exhibition*, vol. 2, pp. 782–787, 6–10 Oct. 2002, Yokohama, Japan.

APPENDIX 1

PUBLICATIONS

A. Journal Publications

- **P. Dehghanian** and M. Kezunovic, "Utilizing topology switching for enhancing the resilience of electric power systems," *IEEE Power Engineering Letters*, under review, 2017.
- B. Zhang, **P. Dehghanian**, and M. Kezunovic, "Optimal allocation of PV generation and battery storage for enhanced resilience," *IEEE Transactions on Smart Grid*, Accepted for Publication, in press, 2017.
- **P. Dehghanian**, B. Zhang, T. Dokic, and M. Kezunovic, "Predictive risk analytics for weather-resilient operation of electric power systems," *IEEE Transactions on Sustainable Energy*, under review, 2017.
- **P. Dehghanian** and M. Kezunovic, "Probabilistic decision making for the bulk power system optimal topology control," *IEEE Transactions on Smart Grid*, vol. 7, no. 4, pp. 2071-2081, June 2016.
- **P. Dehghanian**, Y. Wang, G. Gurrala, E. Moreno-Centeno, and M. Kezunovic, "Flexible implementation of power system corrective topology control", *Elect. Power Syst. Res.*, vol. 128, pp. 79-89, Nov. 2015.

B. Conference Publications

- B. Zhang, **P. Dehghanian** and M. Kezunovic, "Spatial-temporal solar power forecast through Gaussian Conditional Random Field", *IEEE Power and Energy Society (PES) General Meeting*, July 17-21, 2016, Boston, MA, USA.
- **P. Dehghanian** and M. Kezunovic, "Probabilistic impact of transmission line switching on power system operating states," *IEEE Power and Energy Society (PES) Transmission and Distribution (T&D) Conference and Exposition*, May 2-5, 2016, Dallas, USA.
- **P. Dehghanian**, B. Zhang, T. Dokic, and M. Kezunovic, "Weather-driven predictive risk assessment of power system operation for electric safety," *IEEE Industry Application Society (IAS) Electrical Safety Workshop (ESW)*, 7-11 March 2016, Jacksonville, Florida, USA.
- T. Dokic, **P. Dehghanian**, P-C. Chen, M. Kezunovic, Z. Medina-Cetina, J. Stojanovic, and Z. Obradovic, "Risk assessment of a transmission line insulation breakdown due to lightning and severe weather," *The 49th Hawaii International Conference on System Science* (HICSS), 5-8 Jan. 2016, Big Island, USA.
- B. Zhang, **P. Dehghanian** and M. Kezunovic, "Simulation of weather impacts on the wholesale electricity market," 10th *International Conference on Deregulated Electricity Market Issues in South Eastern Europe* (DEMSEE'15), Sep. 24-25, 2015, Budapest, Hungary.

- **P. Dehghanian** and M. Kezunovic, "Impact assessment of power system topology control on system reliability," *IEEE Conference on Intelligent System Applications to Power Systems* (ISAP), Sep. 11-16, 2015, Porto, Portugal.
- **P. Dehghanian**, T. Popovic, and M. Kezunovic, "Assessing the impact of power system topology control on circuit breaker reliability and electric safety," *IEEE Industry Application Society (IAS) Electrical Safety Workshop (ESW),* 27-30 Jan. 2015, Louisville, Kentucky, USA.
- **P. Dehghanian**, T. Popovic, and M. Kezunovic, "Circuit breaker operational health assessment via condition monitoring data," *The 46th North American Power Symposium*, (NAPS), Sep. 2014, Washington State University, Pullman, Washington, USA.
- **P. Dehghanian** and M. Kezunovic, "Circuit breakers and the impact of their maintenance on electric safety," *IEEE Industry Application Society (IAS) Electrical Safety Workshop (ESW),* 4-7 Feb. 2014, San Diego, California, USA.
- M. Kezunovic, T. Popovic, G. Gurrala, **P. Dehghanian**, A. Esmaeilian, and M. Tasdighi, "Reliable implementation of robust adaptive topology control," *The 47th Hawaii International Conference on System Science* (HICSS), 6-9 Jan. 2014, Big Island, USA.
- **P. Dehghanian**, and M. Kezunovic, "Cost/benefit analysis for circuit breaker maintenance planning and scheduling," *The 45th North American Power Symposium* (NAPS), 22-24 Sep. 2013, Kansas State University, Manhattan, Kansas, USA.

- **P. Dehghanian**, M. Kezunovic, G. Gurrala, and Y. Guan, "Security-based circuit breaker maintenance management," *IEEE Power and Energy Society* (*PES*) *General Meeting*, July 21-25, 2013, Vancouver, British Columbia, Canada.

APPENDIX 2

FUNDAMENTALS ON THE POINT ESTIMATION METHOD (PEM)

In this appendix, the fundamental concept of the 2-Point Estimate Method (2-PEM) approach is described [138], [190]. Imagine **Y** as a function of an independent random variable **X** as follows:

$$Y = h(X) \tag{A2.1}$$

The main goal is finding the probability distribution function (PDF) of the $Y\left(f_Y(y)\right)$. Through the 2-PEM, it is assumed that the random variable *X* has only two concentrations placed symmetrically or unsymmetrically around the expectation value of the variable. The symmetrical case is described in the following. As an example, a simple function which involves two concentrations of the variable *X* in $X = x_1$ and $X = x_2$ locations is considered in (A2.2):

$$f_X(x) = P_1 \times \delta(x - x_1) + P_2 \times \delta(x - x_2) \qquad k = 1, 2, ..., n \tag{A2.2}$$

in which, $\delta(.)$ is the Dirac's delta function; ν_X and $P_i(i = 1, 2)$ represent the variation coefficient of *X* and the concentration (weight), respectively. A variable ξ_i is defined as in (A2.3) so that the zeroth and the first three central moments of *X* can be calculated in (A2.4)-(A2.7):

$$\xi_i = \frac{x_i - \mu_X}{\sigma_X} \tag{A2.3}$$

$$M_0(X) = 1 = P_1 + P_2 \tag{A2.4}$$

$$M_1(X) = 0 = \sigma_X\left(\xi_1 \times P_1 + \xi_2 \times P_2\right) \tag{A2.5}$$

$$M_2(X) = \sigma_X^2 \times \nu_X = \sigma_X^2\left(\xi_1^2 \times P_1 + \xi_2^2 \times P_2\right) \tag{A2.6}$$

$$M_3(X) = \sigma_X^3 \times \nu_X = \sigma_X^3\left(\xi_1^3 \times P_1 + \xi_2^3 \times P_2\right) \tag{A2.7}$$

By applying the Taylor series of $h(X)$ with respect to μ_X, the mean value of *Y* can be calculated in (A2.8):

$$\mu_Y = E\left(h(X)\right) = h(\mu_X) + \sum_{j=1}^{\infty} \frac{1}{j!} \frac{\partial h^{(j)}(\mu_X)}{\partial x} \times M_j(X) \tag{A2.8}$$

Imagine the following equation (A2.9) denoting the concentration location *i*:

$$x_i = \mu_X + \xi_i \times \sigma_X \qquad\qquad i = 1, 2 \tag{A2.9}$$

Multiplying Taylor series of $h(X)$ by $P_i\,(i = 1, 2)$ and aggregating them would result in (A2.10):

$$\begin{aligned} P_1 \times h(x_1) + P_2 \times h(x_2) = {} & h(\mu_X) \times (P_1 + P_2) + \\ & \sum_{j=1}^{\infty}\left[\frac{1}{j!} \frac{\partial h^{(j)}(\mu_X)}{\partial x} \times \left(\xi_1^j \times P_1 + \xi_2^j \times P_2\right) \times \sigma_X^j\right] \end{aligned} \tag{A2.10}$$

The first four terms of (A2.10) can be then obtained in (A2.11) which would be used in order to properly estimate the mean value of Y:

$$\sum_{j=1}^{2} P_j \xi_j^i = \frac{M_i(X)}{\sigma_X^i} = \lambda_{X,i} \qquad i = 0,1,2,3 \tag{A2.11}$$

The above equations form an equation set with four unknown variables (i.e., ξ_1, ξ_2, P_1, P_2). From (A2.10) and (A2.11), and by using $M_i(X) = \sigma_X^i \times \lambda_{X,i}$, we would have:

$$\begin{aligned} h(\mu_X) + \sum_{j=1}^{3}\left[\frac{1}{j!}\frac{\partial h^{(j)}(\mu_X)}{\partial x} \times \lambda_{X,j} \times \sigma_X^j\right] = P_1 \times h(x_1) + P_2 \times h(x_2) - \\ \sum_{j=4}^{\infty}\left[\frac{1}{j!}\frac{\partial h^{(j)}(\mu_X)}{\partial x} \times \left(\xi_1^j \times P_1 + \xi_2^j \times P_2\right) \times \sigma_X^j\right] \end{aligned} \tag{A2.12}$$

Using (A2.8) and (A2.11), it can be shown that:

$$\begin{aligned} \mu_Y = h(\mu_X) + P_1 \times h(x_1) + P_2 \times h(x_2) + \\ \sum_{j=4}^{\infty}\left[\frac{1}{j!}\frac{\partial h^{(j)}(\mu_X)}{\partial x} \times \left(\lambda_{X,i} - \left(\xi_1^j \times P_1 + \xi_2^j \times P_2\right)\right) \times \sigma_X^j\right] \end{aligned} \tag{A2.13}$$

As a result of (A2.13), the following equation is approximately valid:

$$\mu_Y \approx P_1 \times h(x_1) + P_2 \times h(x_2) \tag{A2.14}$$

Imagine *Y* as a function of *n* independent random variables (*X*) which are as follows:

$$x_{k,i} = \mu_{X,k} + \xi_{k,i} \times \sigma_{X,k} \quad i = 1,2 \quad k = 1,2,...,n \tag{A2.15}$$

Then, *Y* can be expanded in a multivariate Taylor series around the mean values of *X*. The first three moments of X_k can be still matched as follows:

$$\sum_{i=1}^{2} P_{k,i} \times \xi_{k,i}^{j} = \frac{M_j(X)}{\sigma_X^j} = \lambda_{k,j} \quad j = 1,2,3 \quad ; \quad k = 1,2,...,n \tag{A2.16}$$

$$\sum_{k=1}^{n} \sum_{i=1}^{2} P_{k,i} = 1 \tag{A2.17}$$

The following equations are then derived to satisfy the concentrations:

$$\sum_{i=1}^{2} P_{k,i} = \frac{1}{n} \tag{A2.18}$$

$$\xi_{k,i} = \frac{\lambda_{k.3}}{2} + (-1)^{3-i} \sqrt{n + \left(\frac{\lambda_{k.3}}{2}\right)^2} \qquad i = 1,2 \ ; \quad k = 1,2,...,n \tag{A2.19}$$

$$P_{k,i} = \frac{(-1)^i \xi_{k,3-i}}{2n \times \sqrt{n + \left(\frac{\lambda_{k,3}}{2}\right)^2}} \qquad i = 1,2 \ ; \quad k = 1,2,...,n \tag{A2.20}$$

And finally the first two moment of the random variable Y can be achieved in (A2.21) and (A2.22):

$$E(Y) \cong \sum_{k=1}^{n} \sum_{i=1}^{2} \left(P_{k,i} \times h \times \left(\left[\mu_{X,1}, \mu_{X,2}, ..., x_{k,i}, ..., \mu_{X,n-1}, \mu_{X,n} \right] \right) \right) \tag{A2.21}$$

$$E(Y^2) \cong \sum_{k=1}^{n} \sum_{i=1}^{2} \left(P_{k,i} \times h^2 \times \left(\left[\mu_{X,1}, \mu_{X,2}, ..., x_{k,i}, ..., \mu_{X,n-1}, \mu_{X,n} \right] \right) \right) \tag{A2.22}$$

APPENDIX 3

DATA OF THE STUDIED MODIFIED IEEE 118-BUS TEST SYSTEM

Network parameters and general data for the IEEE 118-bus test system are described as follows.

- *Network Configuration*
- *Generator Data*
- *Bus Data*
- *Transmission Line Data*
- *Tap Changing Transformer Data*
- *General Load Data*
- *Hourly Load Data*
- *Future Market Bidding Strategy Data*
- *Dynamic Data*
- *Reliability Data*
- *Wind Data*

A. Network Configuration

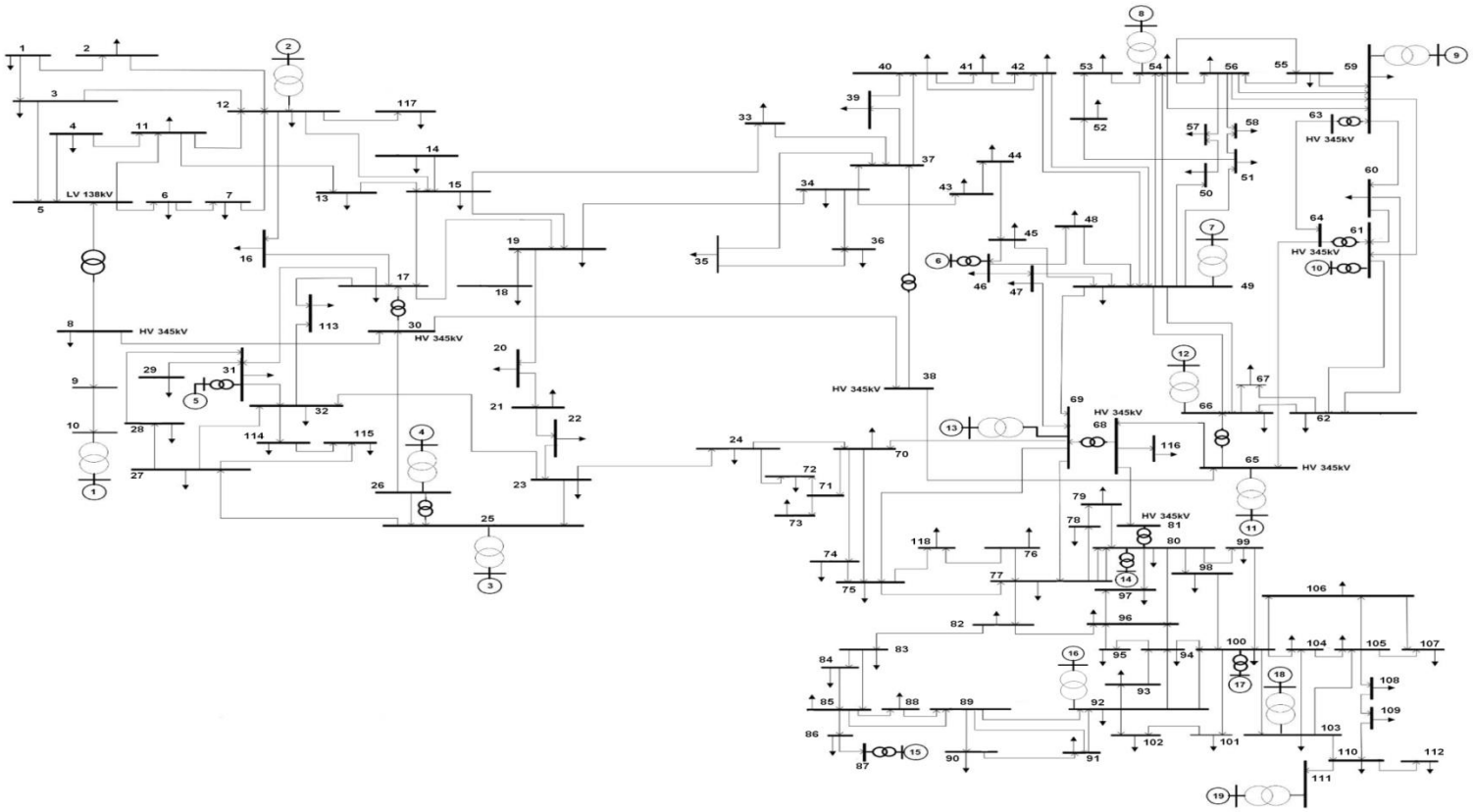

Figure 50. IEEE 118-bus test system one-line diagram.

B. Generator Data

Table 21. IEEE 118-Bus Test System Generator Data

U	Bus No.	P_g (MW)	Q_g (MVar)	Marginal Cost ($/MWh)	P_{max} (MW)	P_{min} (MW)	Q_{max} (MVar)	Q_{min} (MVar)
1	10	450	-5	0.217	550	0	200	-147
2	12	85	91.27	1.052	185	0	120	-35
3	25	220	49.72	0.434	320	0	140	-47
4	26	314	9.89	0.308	414	0	1000	-1000
5	31	7	31.57	5.882	107	0	300	-300
6	46	19	-5.25	3.448	119	0	100	-100
7	49	204	115.63	0.467	304	0	210	-85
8	54	48	3.9	1.724	148	0	300	-300
9	59	155	76.83	0.606	255	0	180	-60
10	61	160	-40.39	0.588	260	0	300	-100
11	65	391	80.76	0.2493	491	0	200	-67
12	66	392	-1.95	0.2487	492	0	200	-67
13	69	513.48	-82.39	0.1897	805.2	0	300	-300
14	80	477	104.9	0.205	577	0	280	-165
15	87	4	11.02	7.142	104	0	1000	-100
16	92	607	0.49	10	1100	0	9	-3
17	100	252	108.87	0.381	352	0	155	-50
18	103	40	41.69	2	140	0	40	-15
19	111	36	-1.84	2.173	136	0	1000	-100

C. Bus Data

Table 22. IEEE 118-Bus Test System Bus Data

Bus No.	Conductance (G) (mhos)	Susceptance (B) (mhos)	Base Voltage (kV)	Voltage-Max (pu)	Voltage-Min (pu)
1	0	0	138	1.06	0.94
2	0	0	138	1.06	0.94
3	0	0	138	1.06	0.94
4	0	0	138	1.06	0.94
5	0	-40	138	1.06	0.94
6	0	0	138	1.06	0.94
7	0	0	138	1.06	0.94
8	0	0	345	1.06	0.94
9	0	0	345	1.06	0.94
10	0	0	345	1.06	0.94
11	0	0	138	1.06	0.94
12	0	0	138	1.06	0.94
13	0	0	138	1.06	0.94
14	0	0	138	1.06	0.94
15	0	0	138	1.06	0.94
16	0	0	138	1.06	0.94
17	0	0	138	1.06	0.94
18	0	0	138	1.06	0.94
19	0	0	138	1.06	0.94
20	0	0	138	1.06	0.94
21	0	0	138	1.06	0.94
22	0	0	138	1.06	0.94
23	0	0	138	1.06	0.94
24	0	0	138	1.06	0.94
25	0	0	138	1.06	0.94
26	0	0	345	1.06	0.94
27	0	0	138	1.06	0.94
28	0	0	138	1.06	0.94
29	0	0	138	1.06	0.94
30	0	0	345	1.06	0.94
31	0	0	138	1.06	0.94
32	0	0	138	1.06	0.94

33	0	0	138	1.06	0.94
34	0	14	138	1.06	0.94
35	0	0	138	1.06	0.94
36	0	0	138	1.06	0.94
37	0	-25	138	1.06	0.94
38	0	0	345	1.06	0.94
39	0	0	138	1.06	0.94
40	0	0	138	1.06	0.94
41	0	0	138	1.06	0.94
42	0	0	138	1.06	0.94
43	0	0	138	1.06	0.94
44	0	10	138	1.06	0.94
45	0	10	138	1.06	0.94
46	0	10	138	1.06	0.94
47	0	0	138	1.06	0.94
48	0	15	138	1.06	0.94
49	0	0	138	1.06	0.94
50	0	0	138	1.06	0.94
51	0	0	138	1.06	0.94
52	0	0	138	1.06	0.94
53	0	0	138	1.06	0.94
54	0	0	138	1.06	0.94
55	0	0	138	1.06	0.94
56	0	0	138	1.06	0.94
57	0	0	138	1.06	0.94
58	0	0	138	1.06	0.94
59	0	0	138	1.06	0.94
60	0	0	138	1.06	0.94
61	0	0	138	1.06	0.94
62	0	0	138	1.06	0.94
63	0	0	345	1.06	0.94
64	0	0	345	1.06	0.94
65	0	0	345	1.06	0.94
66	0	0	138	1.06	0.94
67	0	0	138	1.06	0.94
68	0	0	345	1.06	0.94
69	0	0	138	1.06	0.94
70	0	0	138	1.06	0.94
71	0	0	138	1.06	0.94
72	0	0	138	1.06	0.94

73	0	0	138	1.06	0.94
74	0	12	138	1.06	0.94
75	0	0	138	1.06	0.94
76	0	0	138	1.06	0.94
77	0	0	138	1.06	0.94
78	0	0	138	1.06	0.94
79	0	20	138	1.06	0.94
80	0	0	138	1.06	0.94
81	0	0	345	1.06	0.94
82	0	20	138	1.06	0.94
83	0	10	138	1.06	0.94
84	0	0	138	1.06	0.94
85	0	0	138	1.06	0.94
86	0	0	138	1.06	0.94
87	0	0	161	1.06	0.94
88	0	0	138	1.06	0.94
89	0	0	138	1.06	0.94
90	0	0	138	1.06	0.94
91	0	0	138	1.06	0.94
92	0	0	138	1.06	0.94
93	0	0	138	1.06	0.94
94	0	0	138	1.06	0.94
95	0	0	138	1.06	0.94
96	0	0	138	1.06	0.94
97	0	0	138	1.06	0.94
98	0	0	138	1.06	0.94
99	0	0	138	1.06	0.94
100	0	0	138	1.06	0.94
101	0	0	138	1.06	0.94
102	0	0	138	1.06	0.94
103	0	0	138	1.06	0.94
104	0	0	138	1.06	0.94
105	0	20	138	1.06	0.94
106	0	0	138	1.06	0.94
107	0	6	138	1.06	0.94
108	0	0	138	1.06	0.94
109	0	0	138	1.06	0.94
110	0	6	138	1.06	0.94
111	0	0	138	1.06	0.94
112	0	0	138	1.06	0.94

113	0	0	138	1.06	0.94
114	0	0	138	1.06	0.94
115	0	0	138	1.06	0.94
116	0	0	138	1.06	0.94
117	0	0	138	1.06	0.94
118	0	0	138	1.06	0.94

D. Transmission Line Data

Table 23. IEEE 118-Bus Test System Transmission Line Data

Line No.	From Bus	To Bus	R (pu)	X (pu)	B (pu)	Rate A (MVA)	Rate B (MVA)	Rate C (MVA)
1	1	2	0.0303	0.0999	0.0254	220	230	250
2	1	3	0.0129	0.0424	0.01082	220	230	250
3	2	12	0.0187	0.0616	0.01572	220	230	250
4	3	5	0.0241	0.108	0.0284	220	230	250
5	3	12	0.0484	0.16	0.0406	220	230	250
6	4	5	0.0017	0.00798	0.0021	440	460	500
7	4	11	0.0209	0.0688	0.01748	220	230	250
8	5	6	0.0119	0.054	0.01426	220	230	250
9	5	11	0.0203	0.0682	0.01738	220	230	250
10	6	7	0.0045	0.0208	0.0055	220	230	250
11	7	12	0.0086	0.034	0.00874	220	230	250
12	8	9	0.0024	0.0305	1.1620	1100	1150	1250
13	8	5	0	0.0267	0	880	920	1000
14	8	30	0.0043	0.0504	0.514	220	230	250
15	9	10	0.0025	0.0322	1.230	1100	1150	1250
16	11	12	0.0059	0.0196	0.00502	220	230	250
17	11	13	0.0222	0.0731	0.01876	220	230	250
18	12	15	0.0215	0.0707	0.01816	220	230	250
19	12	17	0.0212	0.0834	0.0214	220	230	250
20	12	117	0.0329	0.14	0.0358	220	230	250
21	13	15	0.0744	0.2444	0.06268	220	230	250
22	14	15	0.0595	0.195	0.0502	220	230	250
23	15	17	0.0132	0.0437	0.0444	440	460	500
24	15	19	0.012	0.0394	0.0101	220	230	250
25	15	33	0.038	0.1244	0.03194	220	230	250
26	16	17	0.0454	0.1801	0.0466	220	230	250
27	17	19	0.0123	0.0505	0.01298	220	230	250
28	17	31	0.0474	0.1563	0.0399	220	230	250
29	17	113	0.0091	0.0301	0.00768	220	230	250
30	18	19	0.0111	0.0493	0.01142	220	230	250
31	19	20	0.0252	0.117	0.0298	220	230	250
32	19	34	0.0752	0.247	0.0632	220	230	250
33	20	21	0.0183	0.0849	0.0216	220	230	250

34	21	22	0.0209	0.097	0.0246	220	230	250
35	22	23	0.0342	0.159	0.0404	220	230	250
36	23	24	0.0135	0.0492	0.0498	220	230	250
37	23	25	0.0156	0.080	0.0864	440	460	500
38	23	32	0.0317	0.1153	0.1173	220	230	250
39	24	70	0.0022	0.4115	0.10198	220	230	250
40	24	72	0.0488	0.196	0.0488	220	230	250
41	25	27	0.0318	0.163	0.1764	440	460	500
42	26	25	0	0.0382	0	220	230	250
43	26	30	0.0079	0.086	0.908	660	690	750
44	27	28	0.0191	0.0855	0.0216	220	230	250
45	27	32	0.0229	0.0755	0.01926	220	230	250
46	27	115	0.0164	0.0741	0.01972	220	230	250
47	28	31	0.0237	0.0943	0.0238	220	230	250
48	29	31	0.0108	0.0331	0.0083	220	230	250
49	30	17	0	0.0388	0	660	690	750
50	30	38	0.0046	0.054	0.422	220	230	250
51	31	32	0.0298	0.0985	0.0251	220	230	250
52	32	113	0.0615	0.203	0.0518	220	230	250
53	32	114	0.0135	0.0612	0.01628	220	230	250
54	33	37	0.0415	0.142	0.0366	220	230	250
55	34	36	0.0087	0.0268	0.00568	220	230	250
56	34	37	0.0025	0.00940	0.00984	440	460	500
57	34	43	0.0413	0.1681	0.04226	220	230	250
58	35	36	0.0022	0.0102	0.00268	220	230	250
59	35	37	0.011	0.0497	0.01318	220	230	250
60	37	39	0.0321	0.106	0.0270	220	230	250
61	37	40	0.0593	0.168	0.0420	220	230	250
62	38	37	0	0.0375	0	660	690	750
63	38	65	0.009	0.0986	1.046	440	460	500
64	39	40	0.0184	0.0605	0.01552	220	230	250
65	40	41	0.0145	0.0487	0.01222	220	230	250
66	40	42	0.0555	0.183	0.0466	220	230	250
67	41	42	0.041	0.135	0.0344	220	230	250
68	42	49	0.0715	0.323	0.0860	220	230	250
69	42	49	0.0715	0.323	0.0860	220	230	250
70	43	44	0.0608	0.2454	0.06068	220	230	250
71	44	45	0.0224	0.0901	0.0224	220	230	250
72	45	46	0.04	0.1356	0.0332	220	230	250
73	45	49	0.0684	0.186	0.0444	220	230	250

74	46	47	0.038	0.127	0.0316	220	230	250
75	46	48	0.0601	0.189	0.0472	220	230	250
76	47	49	0.0191	0.0625	0.01604	220	230	250
77	47	69	0.0844	0.2778	0.07092	220	230	250
78	48	49	0.0179	0.0505	0.01258	220	230	250
79	49	50	0.0267	0.0752	0.01874	220	230	250
80	49	51	0.0486	0.137	0.0342	220	230	250
81	49	54	0.073	0.289	0.0738	220	230	250
82	49	54	0.0869	0.291	0.0730	220	230	250
83	49	66	0.018	0.0919	0.0248	440	460	500
84	49	66	0.018	0.0919	0.0248	440	460	500
85	49	69	0.0985	0.324	0.0828	220	230	250
86	50	57	0.0474	0.134	0.0332	220	230	250
87	51	52	0.0203	0.0588	0.01396	220	230	250
88	51	58	0.0255	0.0719	0.01788	220	230	250
89	52	53	0.0405	0.1635	0.04058	220	230	250
90	53	54	0.0263	0.122	0.0310	220	230	250
91	54	55	0.0169	0.0707	0.0202	220	230	250
92	54	56	0.0027	0.00955	0.00732	220	230	250
93	54	59	0.0503	0.2293	0.0598	220	230	250
94	55	56	0.0048	0.0151	0.00374	220	230	250
95	55	59	0.0473	0.2158	0.05646	220	230	250
96	56	57	0.0343	0.0966	0.0242	220	230	250
97	56	58	0.0343	0.0966	0.0242	220	230	250
98	56	59	0.0825	0.251	0.0569	220	230	250
99	56	59	0.0803	0.239	0.0536	220	230	250
100	59	60	0.0317	0.145	0.0376	220	230	250
101	59	61	0.0328	0.150	0.0388	220	230	250
102	60	61	0.00260	0.0135	0.01456	440	460	500
103	60	62	0.0123	0.0561	0.01468	220	230	250
104	61	62	0.0082	0.0376	0.00980	220	230	250
105	62	66	0.0482	0.218	0.0578	220	230	250
106	62	67	0.0258	0.117	0.031	220	230	250
107	63	59	0	0.0386	0	440	460	500
108	63	64	0.0017	0.0200	0.216	440	460	500
109	64	61	0	0.0268	0	220	230	250
110	64	65	0.0026	0.0302	0.380	440	460	500
111	65	66	0	0.0370	0	220	230	250
112	65	68	0.0013	0.016	0.638	220	230	250
113	66	67	0.0224	0.1015	0.02682	220	230	250

114	68	69	0	0.0370	0	440	460	500
115	68	81	0.0017	0.0202	0.808	220	230	250
116	68	116	0.0003	0.00405	0.164	440	460	500
117	69	70	0.03	0.127	0.122	440	460	500
118	69	75	0.0405	0.122	0.124	440	460	500
119	69	77	0.0309	0.101	0.1038	220	230	250
120	70	71	0.0088	0.0355	0.00878	220	230	250
121	70	74	0.0401	0.1323	0.03368	220	230	250
122	70	75	0.0428	0.141	0.0360	220	230	250
123	71	72	0.0446	0.180	0.04444	220	230	250
124	71	73	0.0086	0.0454	0.01178	220	230	250
125	74	75	0.0123	0.0406	0.01034	220	230	250
126	75	77	0.0601	0.1999	0.04978	220	230	250
127	75	118	0.0145	0.0481	0.01198	220	230	250
128	76	77	0.0444	0.148	0.0368	220	230	250
129	76	118	0.0164	0.0544	0.01356	220	230	250
130	77	78	0.0037	0.0124	0.01264	220	230	250
131	77	80	0.017	0.0485	0.0472	440	460	500
132	77	80	0.0294	0.105	0.0228	220	230	250
133	77	82	0.0298	0.0853	0.08174	220	230	250
134	78	79	0.0054	0.0244	0.00648	220	230	250
135	79	80	0.0156	0.0704	0.0187	220	230	250
136	80	96	0.0356	0.182	0.0494	220	230	250
137	80	97	0.0183	0.0934	0.0254	220	230	250
138	80	98	0.0238	0.108	0.0286	220	230	250
139	80	99	0.0454	0.206	0.0546	220	230	250
140	81	80	0	0.0370	0	220	230	250
141	82	83	0.0112	0.03665	0.03796	220	230	250
142	82	96	0.0162	0.0530	0.0544	220	230	250
143	83	84	0.0625	0.132	0.0258	220	230	250
144	83	85	0.0430	0.148	0.0348	220	230	250
145	84	85	0.0302	0.0641	0.01234	220	230	250
146	85	86	0.0350	0.123	0.0276	220	230	250
147	85	88	0.0200	0.102	0.0276	220	230	250
148	85	89	0.0239	0.173	0.0470	220	230	250
149	86	87	0.0282	0.2074	0.0445	220	230	250
150	88	89	0.0139	0.0712	0.01934	440	460	500
151	89	90	0.0518	0.0320	0.0320	660	230	250
152	89	91	0.00990	0.0320	0.0650	220	220	220
153	89	92	0.00990	0.0505	0.0650	220	690	750

154	90	91	0.0254	0.0505	0.0650	660	230	250
155	91	92	0.0387	0.1272	0.0320	220	230	250
156	92	93	0.0258	0.0320	0.0218	220	230	250
157	92	94	0.0481	0.158	0.0406	220	230	250
158	92	100	0.0648	0.295	0.0472	220	230	250
159	92	102	0.0123	0.0559	0.01464	220	230	250
160	93	94	0.0223	0.0732	0.0187	220	230	250
161	94	95	0.0132	0.0434	0.0111	220	230	250
162	94	96	0.0269	0.0869	0.0230	220	230	250
163	94	100	0.0178	0.0580	0.0604	220	230	250
164	95	96	0.0171	0.0547	0.01474	220	230	250
165	96	97	0.0173	0.0885	0.0240	220	230	250
166	98	100	0.0397	0.179	0.0476	220	230	250
167	99	100	0.0180	0.0813	0.0216	220	230	250
168	100	101	0.0277	0.1262	0.0328	220	230	250
169	100	103	0.0160	0.0525	0.0536	440	460	500
170	100	104	0.0451	0.204	0.0541	220	230	250
171	100	106	0.0605	0.229	0.0620	220	230	250
172	101	102	0.0246	0.112	0.0294	220	230	250
173	103	104	0.0466	0.1584	0.0407	220	230	250
174	103	105	0.0535	0.1625	0.0408	220	230	250
175	103	110	0.0390	0.1813	0.0461	220	230	250
176	104	105	0.00990	0.0378	0.00986	220	230	250
177	105	106	0.0140	0.0547	0.01434	220	230	250
178	105	107	0.0530	0.183	0.0472	220	230	250
179	105	108	0.0261	0.0703	0.01844	220	230	250
180	106	107	0.0530	0.183	0.0472	220	230	250
181	108	109	0.0105	0.0288	0.00760	220	230	250
182	109	110	0.0278	0.0762	0.0202	220	230	250
183	110	111	0.0220	0.0755	0.0200	220	230	250
184	110	112	0.0247	0.0640	0.0620	220	230	250
185	114	115	0.0023	0.0104	0.00276	220	230	250

E. Tap Changing Transformer Data

Table 24. IEEE 118-Bus Test System Tap Changing Transformer Data

Transformer No.	From Bus	To Bus	Circuit ID	Tap Initial	Tap Max	Tap Min	Angle Initial	Angle Max	Angle Min
1	8	5	1	0.985	0	0	0	0	0
2	26	25	1	0.96	0	0	0	0	0
3	30	17	1	0.96	0	0	0	0	0
4	38	37	1	0.935	0	0	0	0	0
5	63	59	1	0.96	0	0	0	0	0
6	64	61	1	0.985	0	0	0	0	0
7	65	66	1	0.935	0	0	0	0	0
8	68	69	1	0.935	0	0	0	0	0
9	81	80	1	0.935	0	0	3.57	-15	15

F. General Load Data

Table 25. IEEE 118-Bus Test System General Load Data

Bus No.	P_d (MW)	Q_d (MVar)	VOLL ($/MWh)
1	51	27	4822.6
2	20	9	5600.331
3	39	10	3144.692
4	39	12	5017.304
6	52	22	4691.259
7	19	2	3715.387
8	28	0	4239.845
11	70	23	4705.575
12	47	10	6647.038
13	34	16	6161.662
14	14	1	3690.068
15	90	30	6320.954
16	25	10	4935.243
17	11	3	4462.167
18	60	34	4928.846
19	45	25	4377.02
20	18	3	4425.513
21	14	8	5393.819
22	10	5	5345.421
23	7	3	5350.315
24	13	0	4902.898
27	71	13	3775.508
28	17	7	4930.343
29	24	4	2478.141
31	43	27	4793.336
32	59	23	5120.816
33	23	9	4936.131
34	59	26	4317.935
35	33	9	4676.323
36	31	17	4027.63
39	27	11	5033.037
40	66	23	3811.758
41	37	10	3858.678
42	96	23	4014.301

43	18	7	2733.43
44	16	8	2363.028
45	53	22	4695.114
46	28	10	4047.043
47	34	0	5322.179
48	20	11	3473.09
49	87	30	4438.655
50	17	4	4355.132
51	17	8	4691.524
52	18	5	4687.715
53	23	11	3981.072
54	113	32	4481.969
55	63	22	4401.073
56	84	18	4876.624
57	12	3	5155.959
58	12	3	5165.564
59	277	113	3981.808
60	78	3	4546.415
62	77	14	3771.53
66	39	18	3831.9
67	28	7	4495.89
70	66	20	5419.578
72	12	0	4038.2
73	6	0	4722.827
74	68	27	2364.649
75	47	11	5170.414
76	68	36	3846.561
77	61	28	2519.534
78	71	26	3831.516
79	39	32	5160.366
80	130	26	5426.527
82	54	27	4551.559
83	20	10	3605.046
84	11	7	4054.619
85	24	15	3863.051
86	21	10	5910.274
88	48	10	4130.639
90	440	42	4948.846
91	10	0	4384.549
92	65	10	5033.166

93	12	7	4041.09
94	30	16	3658.639
95	42	31	3646.574
96	38	15	3792.916
97	15	9	4393.575
98	34	8	4382.368
99	42	0	5351.586
100	37	18	4674.951
101	22	15	4618.687
102	5	3	5452.619
103	23	16	2017.32
104	38	25	4917.975
105	31	26	5001.053
106	43	16	4353.771
107	50	12	2629.402
108	2	1	3800.494
109	8	3	3811.228
110	39	30	4562.925
112	68	13	4933.352
113	6	0	5051.295
114	8	3	4099.866
115	22	7	4612.399
116	184	0	3450.503
117	20	8	1340.186
118	33	15	4236.62

G. Hourly Load Data

Table 26. IEEE 118-Bus Test System Hourly Load Data

Bus No.	**P_d (MW)**																							
Hours	**1**	**2**	**3**	**4**	**5**	**6**	**7**	**8**	**9**	**10**	**11**	**12**	**13**	**14**	**15**	**16**	**17**	**18**	**19**	**20**	**21**	**22**	**23**	**24**
1	47.39	44.69	39.27	27.08	33.85	40.62	47.39	52.81	55.52	59.58	60.26	56.87	54.17	51.46	59.58	60.94	57.55	60.26	63.65	66.35	67.71	60.94	58.91	55.52
2	18.58	17.52	15.40	10.62	13.27	15.93	18.58	20.71	21.77	23.36	23.63	22.30	21.24	20.18	23.36	23.89	22.57	23.63	24.96	26.02	26.55	23.89	23.10	21.77
3	36.24	34.17	30.03	20.71	25.89	31.06	36.24	40.38	42.46	45.56	46.08	43.49	41.42	39.35	45.56	46.60	44.01	46.08	48.67	50.74	51.78	46.60	45.04	42.46
4	36.24	34.17	30.03	20.71	25.89	31.06	36.24	40.38	42.46	45.56	46.08	43.49	41.42	39.35	45.56	46.60	44.01	46.08	48.67	50.74	51.78	46.60	45.04	42.46
6	48.32	45.56	40.04	27.61	34.52	41.42	48.32	53.85	56.61	60.75	61.44	57.99	55.23	52.47	60.75	62.13	58.68	61.44	64.89	67.66	69.04	62.13	60.06	56.61
7	17.65	16.64	14.63	10.09	12.61	15.13	17.65	19.67	20.68	22.19	22.45	21.19	20.18	19.17	22.19	22.70	21.44	22.45	23.71	24.72	25.22	22.70	21.94	20.68
8	26.02	24.53	21.56	14.87	18.58	22.30	26.02	28.99	30.48	32.71	33.08	31.22	29.74	28.25	32.71	33.45	31.59	33.08	34.94	36.43	37.17	33.45	32.34	30.48
11	65.05	61.34	53.90	37.17	46.47	55.76	65.05	72.49	76.21	81.78	82.71	78.07	74.35	70.63	81.78	83.64	78.99	82.71	87.36	91.08	92.94	83.64	80.85	76.21
12	43.68	41.18	36.19	24.96	31.20	37.44	43.68	48.67	51.17	54.91	55.53	52.41	49.92	47.42	54.91	56.16	53.04	55.53	58.65	61.15	62.40	56.16	54.29	51.17
13	31.59	29.79	26.18	18.05	22.57	27.08	31.59	35.21	37.01	39.72	40.17	37.91	36.11	34.30	39.72	40.62	38.37	40.17	42.43	44.23	45.14	40.62	39.27	37.01
14	13.01	12.26	10.78	7.435	9.294	11.15	13.01	14.49	15.24	16.35	16.54	15.61	14.87	14.12	16.35	16.72	15.79	16.54	17.47	18.21	18.58	16.72	16.17	15.24
15	83.64	78.86	69.30	47.79	59.74	71.69	83.64	93.20	97.98	105.1	106.3	100.3	95.59	90.81	105.1	107.5	101.5	106.3	112.3	117.1	119.4	107.5	103.9	97.98
16	23.23	21.90	19.25	13.27	16.59	19.91	23.23	25.89	27.21	29.21	29.54	27.88	26.55	25.22	29.21	29.87	28.21	29.54	31.20	32.52	33.19	29.87	28.87	27.21
17	10.22	9.639	8.470	5.842	7.302	8.763	10.22	11.39	11.97	12.85	12.99	12.26	11.68	11.09	12.85	13.14	12.41	12.99	13.72	14.31	14.60	13.14	12.70	11.97
18	55.76	52.57	46.20	31.86	39.83	47.79	55.76	62.13	65.32	70.10	70.90	66.91	63.73	60.54	70.10	71.69	67.71	70.90	74.88	78.07	79.66	71.69	69.30	65.32
19	41.82	39.43	34.65	23.89	29.87	35.84	41.82	46.60	48.99	52.57	53.17	50.18	47.79	45.40	52.57	53.77	50.78	53.17	56.16	58.55	59.74	53.77	51.98	48.99
20	16.72	15.77	13.86	9.559	11.94	14.33	16.72	18.64	19.59	21.03	21.27	20.07	19.11	18.16	21.03	21.50	20.31	21.27	22.46	23.42	23.89	21.50	20.79	19.59
21	13.01	12.26	10.78	7.435	9.294	11.15	13.01	14.49	15.24	16.35	16.54	15.61	14.87	14.12	16.35	16.72	15.79	16.54	17.47	18.21	18.58	16.72	16.17	15.24
22	9.294	8.763	7.700	5.310	6.638	7.966	9.294	10.35	10.88	11.68	11.81	11.15	10.62	10.09	11.68	11.94	11.28	11.81	12.48	13.01	13.27	11.94	11.55	10.88
23	6.505	6.134	5.390	3.717	4.647	5.576	6.505	7.249	7.621	8.178	8.271	7.807	7.435	7.063	8.178	8.364	7.899	8.271	8.736	9.108	9.294	8.364	8.085	7.621
24	12.08	11.39	10.01	6.904	8.630	10.35	12.08	13.46	14.15	15.18	15.36	14.49	13.80	13.11	15.18	15.53	14.67	15.36	16.22	16.91	17.26	15.53	15.01	14.15
27	65.98	62.21	54.67	37.70	47.13	56.56	65.98	73.52	77.30	82.95	83.89	79.18	75.41	71.64	82.95	84.84	80.12	83.89	88.61	92.38	94.26	84.84	82.01	77.30
28	15.79	14.89	13.09	9.028	11.28	13.54	15.79	17.60	18.50	19.86	20.08	18.95	18.05	17.15	19.86	20.31	19.18	20.08	21.21	22.11	22.57	20.31	19.63	18.50
29	22.30	21.03	18.48	12.74	15.93	19.11	22.30	24.85	26.12	28.04	28.36	26.76	25.49	24.21	28.04	28.67	27.08	28.36	29.95	31.22	31.86	28.67	27.72	26.12

31	39.96	37.68	33.11	22.83	28.54	34.25	39.96	44.53	46.81	50.24	50.81	47.95	45.67	43.39	50.24	51.38	48.52	50.81	53.66	55.95	57.09	51.38	49.67	46.81
32	54.83	51.70	45.43	31.33	39.16	47.00	54.83	61.10	64.23	68.93	69.71	65.80	62.66	59.53	68.93	70.50	66.58	69.71	73.63	76.76	78.33	70.50	68.15	64.23
33	21.37	20.15	17.71	12.21	15.26	18.32	21.37	23.81	25.04	26.87	27.17	25.65	24.43	23.20	26.87	27.48	25.95	27.17	28.70	29.92	30.53	27.48	26.56	25.04
34	54.83	51.70	45.43	31.33	39.16	47.00	54.83	61.10	64.23	68.93	69.71	65.80	62.66	59.53	68.93	70.50	66.58	69.71	73.63	76.76	78.33	70.50	68.15	64.23
35	30.67	28.91	25.41	17.52	21.90	26.28	30.67	34.17	35.92	38.55	38.99	36.80	35.05	33.29	38.55	39.43	37.24	38.99	41.18	42.93	43.81	39.43	38.11	35.92
36	28.81	27.16	23.87	16.46	20.57	24.69	28.81	32.10	33.75	36.22	36.63	34.57	32.92	31.28	36.22	37.04	34.98	36.63	38.68	40.33	41.15	37.04	35.80	33.75
39	25.09	23.66	20.79	14.33	17.92	21.50	25.09	27.96	29.39	31.54	31.90	30.11	28.67	27.24	31.54	32.26	30.47	31.90	33.69	35.13	35.84	32.26	31.18	29.39
40	61.34	57.83	50.82	35.05	43.81	52.57	61.34	68.35	71.85	77.11	77.99	73.60	70.10	66.59	77.11	78.86	74.48	77.99	82.37	85.87	87.63	78.86	76.23	71.85
41	34.38	32.42	28.49	19.65	24.56	29.47	34.38	38.31	40.28	43.23	43.72	41.26	39.30	37.33	43.23	44.21	41.75	43.72	46.17	48.14	49.12	44.21	42.73	40.28
42	89.22	84.12	73.92	50.98	63.73	76.47	89.22	99.42	104.5	112.1	113.4	107.0	101.9	96.87	112.1	114.7	108.3	113.4	119.8	124.9	127.4	114.7	110.8	104.5
43	16.72	15.77	13.86	9.559	11.94	14.33	16.72	18.64	19.59	21.03	21.27	20.07	19.11	18.16	21.03	21.50	20.31	21.27	22.46	23.42	23.89	21.50	20.79	19.59
44	14.87	14.02	12.32	8.497	10.62	12.74	14.87	16.57	17.41	18.69	18.90	17.84	16.99	16.14	18.69	19.11	18.05	18.90	19.96	20.81	21.24	19.11	18.48	17.41
45	49.25	46.44	40.81	28.14	35.18	42.22	49.25	54.88	57.70	61.92	62.62	59.11	56.29	53.48	61.92	63.33	59.81	62.62	66.14	68.96	70.36	63.33	61.22	57.70
46	26.02	24.53	21.56	14.87	18.58	22.30	26.02	28.99	30.48	32.71	33.08	31.22	29.74	28.25	32.71	33.45	31.59	33.08	34.94	36.43	37.17	33.45	32.34	30.48
47	31.59	29.79	26.18	18.05	22.57	27.08	31.59	35.21	37.01	39.72	40.17	37.91	36.11	34.30	39.72	40.62	38.37	40.17	42.43	44.23	45.14	40.62	39.27	37.01
48	18.58	17.52	15.40	10.62	13.27	15.93	18.58	20.71	21.77	23.36	23.63	22.30	21.24	20.18	23.36	23.89	22.57	23.63	24.96	26.02	26.55	23.89	23.10	21.77
49	80.85	76.23	66.99	46.20	57.75	69.30	80.85	90.09	94.72	101.6	102.8	97.03	92.40	87.78	101.6	103.9	98.18	102.8	108.5	113.2	115.5	103.9	100.4	94.72
50	15.79	14.89	13.09	9.028	11.28	13.54	15.79	17.60	18.50	19.86	20.08	18.95	18.05	17.15	19.86	20.31	19.18	20.08	21.21	22.11	22.57	20.31	19.63	18.50
51	15.79	14.89	13.09	9.028	11.28	13.54	15.79	17.60	18.50	19.86	20.08	18.95	18.05	17.15	19.86	20.31	19.18	20.08	21.21	22.11	22.57	20.31	19.63	18.50
52	16.72	15.77	13.86	9.559	11.94	14.33	16.72	18.64	19.59	21.03	21.27	20.07	19.11	18.16	21.03	21.50	20.31	21.27	22.46	23.42	23.89	21.50	20.79	19.59
53	21.37	20.15	17.71	12.21	15.26	18.32	21.37	23.81	25.04	26.87	27.17	25.65	24.43	23.20	26.87	27.48	25.95	27.17	28.70	29.92	30.53	27.48	26.56	25.04
54	105.0	99.02	87.01	60.01	75.01	90.01	105.0	117.0	123.0	132.0	133.5	126.0	120.0	114.0	132.0	135.0	127.5	133.5	141.0	147.0	150.0	135.0	130.5	123.0
55	58.55	55.20	48.51	33.45	41.82	50.18	58.55	65.24	68.59	73.60	74.44	70.26	66.91	63.57	73.60	75.28	71.09	74.44	78.62	81.97	83.64	75.28	72.77	68.59
56	78.07	73.60	64.68	44.61	55.76	66.91	78.07	86.99	91.45	98.14	99.26	93.68	89.22	84.76	98.14	100.3	94.79	99.26	104.8	109.2	111.5	100.3	97.03	91.45
57	11.15	10.51	9.240	6.373	7.966	9.559	11.15	12.42	13.06	14.02	14.18	13.38	12.74	12.10	14.02	14.33	13.54	14.18	14.97	15.61	15.93	14.33	13.86	13.06
58	11.15	10.51	9.240	6.373	7.966	9.559	11.15	12.42	13.06	14.02	14.18	13.38	12.74	12.10	14.02	14.33	13.54	14.18	14.97	15.61	15.93	14.33	13.86	13.06
59	257.4	242.7	213.3	147.1	183.8	220.6	257.4	286.8	301.5	323.6	327.3	308.9	294.2	279.5	323.6	331.0	312.6	327.3	345.7	360.4	367.7	331.0	319.9	301.5
60	72.49	68.35	60.06	41.42	51.78	62.13	72.49	80.77	84.92	91.13	92.17	86.99	82.85	78.70	91.13	93.20	88.02	92.17	97.34	101.4	103.5	93.20	90.09	84.92
62	71.56	67.47	59.29	40.89	51.11	61.34	71.56	79.74	83.83	89.96	90.98	85.87	81.78	77.69	89.96	92.01	86.89	90.98	96.10	100.1	102.2	92.01	88.94	83.83
66	36.24	34.17	30.03	20.71	25.89	31.06	36.24	40.38	42.46	45.56	46.08	43.49	41.42	39.35	45.56	46.60	44.01	46.08	48.67	50.74	51.78	46.60	45.04	42.46
67	26.02	24.53	21.56	14.87	18.58	22.30	26.02	28.99	30.48	32.71	33.08	31.22	29.74	28.25	32.71	33.45	31.59	33.08	34.94	36.43	37.17	33.45	32.34	30.48

70	61.34	57.83	50.82	35.05	43.81	52.57	61.34	68.35	71.85	77.11	77.99	73.60	70.10	66.59	77.11	78.86	74.48	77.99	82.37	85.87	87.63	78.86	76.23	71.85
72	11.15	10.51	9.240	6.373	7.966	9.559	11.15	12.42	13.06	14.02	14.18	13.38	12.74	12.10	14.02	14.33	13.54	14.18	14.97	15.61	15.93	14.33	13.86	13.06
73	5.576	5.257	4.620	3.186	3.983	4.779	5.576	6.213	6.532	7.010	7.090	6.691	6.373	6.054	7.010	7.169	6.771	7.090	7.488	7.807	7.966	7.169	6.930	6.532
74	63.19	59.58	52.36	36.11	45.14	54.17	63.19	70.42	74.03	79.45	80.35	75.83	72.22	68.61	79.45	81.25	76.74	80.35	84.86	88.47	90.28	81.25	78.54	74.03
75	43.68	41.18	36.19	24.96	31.20	37.44	43.68	48.67	51.17	54.91	55.53	52.41	49.92	47.42	54.91	56.16	53.04	55.53	58.65	61.15	62.40	56.16	54.29	51.17
76	63.19	59.58	52.36	36.11	45.14	54.17	63.19	70.42	74.03	79.45	80.35	75.83	72.22	68.61	79.45	81.25	76.74	80.35	84.86	88.47	90.28	81.25	78.54	74.03
77	56.69	53.45	46.97	32.39	40.49	48.59	56.69	63.17	66.41	71.27	72.08	68.03	64.79	61.55	71.27	72.89	68.84	72.08	76.13	79.37	80.99	72.89	70.46	66.41
78	65.98	62.21	54.67	37.70	47.13	56.56	65.98	73.52	77.30	82.95	83.89	79.18	75.41	71.64	82.95	84.84	80.12	83.89	88.61	92.38	94.26	84.84	82.01	77.30
79	36.24	34.17	30.03	20.71	25.89	31.06	36.24	40.38	42.46	45.56	46.08	43.49	41.42	39.35	45.56	46.60	44.01	46.08	48.67	50.74	51.78	46.60	45.04	42.46
80	120.8	113.9	100.1	69.04	86.30	103.5	120.8	134.6	141.5	151.8	153.6	144.9	138.0	131.1	151.8	155.3	146.7	153.6	162.2	169.1	172.6	155.3	150.1	141.5
82	50.18	47.32	41.58	28.67	35.84	43.01	50.18	55.92	58.79	63.09	63.81	60.22	57.35	54.48	63.09	64.52	60.94	63.81	67.39	70.26	71.69	64.52	62.37	58.79
83	18.58	17.52	15.40	10.62	13.27	15.93	18.58	20.71	21.77	23.36	23.63	22.30	21.24	20.18	23.36	23.89	22.57	23.63	24.96	26.02	26.55	23.89	23.10	21.77
84	10.22	9.639	8.470	5.842	7.302	8.763	10.22	11.39	11.97	12.85	12.99	12.26	11.68	11.09	12.85	13.14	12.41	12.99	13.72	14.31	14.60	13.14	12.70	11.97
85	22.30	21.03	18.48	12.74	15.93	19.11	22.30	24.85	26.12	28.04	28.36	26.76	25.49	24.21	28.04	28.67	27.08	28.36	29.95	31.22	31.86	28.67	27.72	26.12
86	19.51	18.40	16.17	11.15	13.94	16.72	19.51	21.74	22.86	24.53	24.81	23.42	22.30	21.19	24.53	25.09	23.69	24.81	26.20	27.32	27.88	25.09	24.25	22.86
88	44.61	42.06	36.96	25.49	31.86	38.23	44.61	49.71	52.25	56.08	56.72	53.53	50.98	48.43	56.08	57.35	54.17	56.72	59.90	62.45	63.73	57.35	55.44	52.25
90	408.9	385.5	338.8	233.6	292.1	350.5	408.9	455.6	479.0	514.0	519.9	490.7	467.3	443.9	514.0	525.7	496.5	519.9	549.1	572.5	584.2	525.7	508.2	479.0
91	9.294	8.763	7.700	5.310	6.638	7.966	9.294	10.35	10.88	11.68	11.81	11.15	10.62	10.09	11.68	11.94	11.28	11.81	12.48	13.01	13.27	11.94	11.55	10.88
92	60.41	56.95	50.05	34.52	43.15	51.78	60.41	67.31	70.76	75.94	76.80	72.49	69.04	65.58	75.94	77.67	73.35	76.80	81.12	84.57	86.30	77.67	75.08	70.76
93	11.15	10.51	9.240	6.373	7.966	9.559	11.15	12.42	13.06	14.02	14.18	13.38	12.74	12.10	14.02	14.33	13.54	14.18	14.97	15.61	15.93	14.33	13.86	13.06
94	27.88	26.28	23.10	15.93	19.91	23.89	27.88	31.06	32.66	35.05	35.45	33.45	31.86	30.27	35.05	35.84	33.85	35.45	37.44	39.03	39.83	35.84	34.65	32.66
95	39.03	36.80	32.34	22.30	27.88	33.45	39.03	43.49	45.72	49.07	49.63	46.84	44.61	42.38	49.07	50.18	47.39	49.63	52.41	54.64	55.76	50.18	48.51	45.72
96	35.31	33.29	29.26	20.18	25.22	30.27	35.31	39.35	41.37	44.39	44.90	42.38	40.36	38.34	44.39	45.40	42.88	44.90	47.42	49.44	50.45	45.40	43.89	41.37
97	13.94	13.14	11.55	7.966	9.957	11.94	13.94	15.53	16.33	17.52	17.72	16.72	15.93	15.13	17.52	17.92	16.92	17.72	18.72	19.51	19.91	17.92	17.32	16.33
98	31.59	29.79	26.18	18.05	22.57	27.08	31.59	35.21	37.01	39.72	40.17	37.91	36.11	34.30	39.72	40.62	38.37	40.17	42.43	44.23	45.14	40.62	39.27	37.01
99	39.03	36.80	32.34	22.30	27.88	33.45	39.03	43.49	45.72	49.07	49.63	46.84	44.61	42.38	49.07	50.18	47.39	49.63	52.41	54.64	55.76	50.18	48.51	45.72
100	34.38	32.42	28.49	19.65	24.56	29.47	34.38	38.31	40.28	43.23	43.72	41.26	39.30	37.33	43.23	44.21	41.75	43.72	46.17	48.14	49.12	44.21	42.73	40.28
101	20.44	19.27	16.94	11.68	14.60	17.52	20.44	22.78	23.95	25.70	25.99	24.53	23.36	22.19	25.70	26.28	24.82	25.99	27.45	28.62	29.21	26.28	25.41	23.95
102	4.647	4.381	3.850	2.655	3.319	3.983	4.647	5.178	5.443	5.842	5.908	5.576	5.310	5.045	5.842	5.974	5.642	5.908	6.240	6.505	6.638	5.974	5.775	5.443
103	21.37	20.15	17.71	12.21	15.26	18.32	21.37	23.81	25.04	26.87	27.17	25.65	24.43	23.20	26.87	27.48	25.95	27.17	28.70	29.92	30.53	27.48	26.56	25.04
104	35.31	33.29	29.26	20.18	25.22	30.27	35.31	39.35	41.37	44.39	44.90	42.38	40.36	38.34	44.39	45.40	42.88	44.90	47.42	49.44	50.45	45.40	43.89	41.37

105	28.81	27.16	23.87	16.46	20.57	24.69	28.81	32.10	33.75	36.22	36.63	34.57	32.92	31.28	36.22	37.04	34.98	36.63	38.68	40.33	41.15	37.04	35.80	33.75
106	39.96	37.68	33.11	22.83	28.54	34.25	39.96	44.53	46.81	50.24	50.81	47.95	45.67	43.39	50.24	51.38	48.52	50.81	53.66	55.95	57.09	51.38	49.67	46.81
107	46.47	43.81	38.50	26.55	33.19	39.83	46.47	51.78	54.43	58.42	59.08	55.76	53.10	50.45	58.42	59.74	56.42	59.08	62.40	65.05	66.38	59.74	57.75	54.43
108	1.858	1.752	1.540	1.062	1.327	1.593	1.858	2.071	2.177	2.336	2.363	2.230	2.124	2.018	2.336	2.389	2.257	2.363	2.496	2.602	2.655	2.389	2.310	2.177
109	7.435	7.010	6.160	4.248	5.310	6.373	7.435	8.285	8.709	9.347	9.453	8.922	8.497	8.072	9.347	9.559	9.028	9.453	9.984	10.40	10.62	9.559	9.240	8.709
110	36.24	34.17	30.03	20.71	25.89	31.06	36.24	40.38	42.46	45.56	46.08	43.49	41.42	39.35	45.56	46.60	44.01	46.08	48.67	50.74	51.78	46.60	45.04	42.46
112	63.19	59.58	52.36	36.11	45.14	54.17	63.19	70.42	74.03	79.45	80.35	75.83	72.22	68.61	79.45	81.25	76.74	80.35	84.86	88.47	90.28	81.25	78.54	74.03
113	5.576	5.257	4.620	3.186	3.983	4.779	5.576	6.213	6.532	7.010	7.090	6.691	6.373	6.054	7.010	7.169	6.771	7.090	7.488	7.807	7.966	7.169	6.930	6.532
114	7.435	7.010	6.160	4.248	5.310	6.373	7.435	8.285	8.709	9.347	9.453	8.922	8.497	8.072	9.347	9.559	9.028	9.453	9.984	10.40	10.62	9.559	9.240	8.709
115	20.44	19.27	16.94	11.68	14.60	17.52	20.44	22.78	23.95	25.70	25.99	24.53	23.36	22.19	25.70	26.28	24.82	25.99	27.45	28.62	29.21	26.28	25.41	23.95
116	171.0	161.2	141.6	97.72	122.1	146.5	171.0	190.5	200.3	214.9	217.4	205.2	195.4	185.6	214.9	219.8	207.6	217.4	229.6	239.4	244.3	219.8	212.5	200.3
117	18.58	17.52	15.40	10.62	13.27	15.93	18.58	20.71	21.77	23.36	23.63	22.30	21.24	20.18	23.36	23.89	22.57	23.63	24.96	26.02	26.55	23.89	23.10	21.77
118	30.67	28.91	25.41	17.52	21.90	26.28	30.67	34.17	35.92	38.55	38.99	36.80	35.05	33.29	38.55	39.43	37.24	38.99	41.18	42.93	43.81	39.43	38.11	35.92

H. Future Market Bidding Strategy Data

Table 27. Disco's Bidding Strategy in Future Market in a Certain Hour

Bus No.	P_d (MW)	X_0	Y_0	X_1	Y_1	X_2	Y_2
1	66.63067	66.63067	249114.6	53.30454	237252	0	0
2	17.41978	17.41978	97406.4	13.93583	92768	0	0
3	48.82983	48.82983	167731.2	39.06386	159744	0	0
4	47.55601	47.55601	182506	38.04481	173815.2	0	0
6	54.34972	54.34972	236396.2	43.47978	225139.2	0	0
7	26.89179	26.89179	64047.48	21.51343	60997.6	0	0
8	33.53308	33.53308	135451.7	26.82647	129001.6	0	0
11	60.96924	60.96924	255309.6	48.77539	243152	0	0
12	45.03014	45.03014	173554.1	36.02411	165289.6	0	0
13	35.16619	35.16619	147826.6	28.13295	140787.2	0	0
14	16.00443	16.00443	55177.92	12.80354	52550.4	0	0
15	117.5835	117.5835	368020.8	94.06683	350496	0	0
16	29.94025	29.94025	117495	23.9522	111900	0	0
17	8.982076	8.982076	55865.04	7.185661	53204.8	0	0
18	58.79177	58.79177	242020.8	47.03341	230496	0	0
19	48.99314	48.99314	201360.6	39.19451	191772	0	0
20	21.55698	21.55698	71986.32	17.24559	68558.4	0	0
21	16.4617	16.4617	61493.04	13.16936	58564.8	0	0
22	12.62934	12.62934	45687.6	10.10347	43512	0	0
23	7.011463	7.011463	25772.04	5.60917	24544.8	0	0
24	12.73822	12.73822	57592.08	10.19057	54849.6	0	0
27	65.70524	65.70524	334043.6	52.5642	318136.8	0	0
28	24.06108	24.06108	72713.76	19.24886	69251.2	0	0
29	28.74264	28.74264	135656.6	22.99411	129196.8	0	0
31	53.83802	53.83802	158602.9	43.07041	151050.4	0	0
32	68.08958	68.08958	211224.7	54.47166	201166.4	0	0
33	25.04094	25.04094	62790	20.03275	59800	0	0
34	61.02368	61.02368	292899.6	48.81894	278952	0	0
35	31.97619	31.97619	162633.2	25.58095	154888.8	0	0
36	28.68821	28.68821	128116.8	22.95056	122016	0	0
39	29.39588	29.39588	133766.6	23.51671	127396.8	0	0
40	73.29374	73.29374	287345.5	58.63499	273662.4	0	0
41	44.31157	44.31157	164413.2	35.44926	156584	0	0
42	137.9647	137.9647	412231.7	110.3717	392601.6	0	0

43	17.8335	17.8335	82237.68	14.2668	78321.6	0	0
44	17.07139	17.07139	68557.44	13.65711	65292.8	0	0
45	49.62461	49.62461	346677.2	39.69969	330168.8	0	0
46	33.53308	33.53308	90152.16	26.82647	85859.2	0	0
47	33.31534	33.31534	89821.2	26.65227	85544	0	0
48	20.68599	20.68599	64831.2	16.54879	61744	0	0
49	87.14247	87.14247	285450.5	69.71397	271857.6	0	0
50	15.17699	15.17699	65202.48	12.14159	62097.6	0	0
51	20.35937	20.35937	68986.68	16.2875	65701.6	0	0
52	22.1449	22.1449	72288.72	17.71592	68846.4	0	0
53	30.54994	30.54994	107052.1	24.43996	101954.4	0	0
54	129.1786	129.1786	511523.9	103.3429	487165.6	0	0
55	68.5904	68.5904	304342.9	54.87232	289850.4	0	0
56	100.5992	100.5992	478255.7	80.4794	455481.6	0	0
57	13.97938	13.97938	62727.84	11.1835	59740.8	0	0
58	15.6778	15.6778	37457.28	12.54224	35673.6	0	0
59	295.5484	295.5484	621488.3	236.4387	591893.6	0	0
60	69.63558	69.63558	386633.5	55.70847	368222.4	0	0
62	51.97628	51.97628	204647.5	41.58102	194902.4	0	0
66	63.69108	63.69108	165962.2	50.95287	158059.2	0	0
67	39.63001	39.63001	118423.2	31.70401	112784	0	0
70	76.168	76.168	400664.9	60.9344	381585.6	0	0
72	13.06484	13.06484	49694.4	10.45187	47328	0	0
73	6.271122	6.271122	22639.68	5.016898	21561.6	0	0
74	63.66931	63.66931	299023.2	50.93545	284784	0	0
75	49.12379	49.12379	207072.6	39.29903	197212	0	0
76	74.03408	74.03408	289598.4	59.22726	275808	0	0
77	71.06183	71.06183	224994.8	56.84946	214280.8	0	0
78	85.03032	85.03032	225260.3	68.02425	214533.6	0	0
79	48.82983	48.82983	174152.2	39.06386	165859.2	0	0
80	168.4275	168.4275	399344.4	134.742	380328	0	0
82	58.20385	58.20385	179943.1	46.56308	171374.4	0	0
83	19.59726	19.59726	106360.8	15.6778	101296	0	0
84	15.56893	15.56893	42328.44	12.45514	40312.8	0	0
85	24.82319	24.82319	97957.44	19.85855	93292.8	0	0
86	22.86347	22.86347	104058.4	18.29077	99103.2	0	0
88	52.25935	52.25935	189463.7	41.80748	180441.6	0	0
90	1	1	2228318	0.8	2122208	0	0
91	1	1	39093.6	0.8	37232	0	0
92	67.22948	67.22948	328255.2	53.78358	312624	0	0

93	12.01965	12.01965	56740.32	9.61572	54038.4	0	0
94	32.66209	32.66209	120607.2	26.12967	114864	0	0
95	45.72693	45.72693	145847.5	36.58154	138902.4	0	0
96	39.71711	39.71711	126275.5	31.77368	120262.4	0	0
97	13.39146	13.39146	59585.4	10.71317	56748	0	0
98	44.42045	44.42045	130262.2	35.53636	124059.2	0	0
99	59.44501	59.44501	161970.5	47.55601	154257.6	0	0
100	46.32574	46.32574	185951.6	37.06059	177096.8	0	0
101	22.03603	22.03603	86892.96	17.62882	82755.2	0	0
102	5.280372	5.280372	25800.6	4.224297	24572	0	0
103	22.53684	22.53684	86321.76	18.02948	82211.2	0	0
104	41.37198	41.37198	190626.2	33.09759	181548.8	0	0
105	37.12591	37.12591	116581.1	29.70073	111029.6	0	0
106	53.83802	53.83802	186957.1	43.07041	178054.4	0	0
107	52.25935	52.25935	250740	41.80748	238800	0	0
108	1.959726	1.959726	7704.48	1.56778	7337.6	0	0
109	8.100199	8.100199	30649.92	6.480159	29190.4	0	0
110	37.79004	37.79004	190499.4	30.23203	181428	0	0
112	77.73578	77.73578	331181.8	62.18863	315411.2	0	0
113	7.512281	7.512281	25804.8	6.009825	24576	0	0
114	8.709892	8.709892	37437.12	6.967913	35654.4	0	0
115	23.9522	23.9522	100013.8	19.16176	95251.2	0	0
116	240.393	240.393	620249.3	192.3144	590713.6	0	0
117	17.41978	17.41978	96751.2	13.93583	92144	0	0
118	34.13189	34.13189	120360.2	27.30551	114628.8	0	0

I. Dynamic Data

Table 28. IEEE 118-Bus Test System Generator Dynamic Data

Parameter	Value	Parameter	Value
X_d (p.u.)	1.8	X_q (p.u.)	1.7
X_d' (p.u.)	0.3	X_q' (p.u.)	0.55
X_d'' (p.u.)	0.25	X_q'' (p.u.)	0.25
T_{do}' (p.u.)	8	T_{qo}' (p.u.)	0.4
T_{do}'' (p.u.)	0.03	T_{qo}'' (p.u.)	0.05
H (sec.)	3.4 for all the generators except for generators at bus#69 and bus#89. 5 & 4 for generators at bus#69 and bus#89, respectively.		

Generator #	Bus #	MVA Ratings (MW)	Minutes to Fully Ramp	Generator Type
1	10	591	30	S*
2	12	300	12	G**
3	25	300	20	CC***
4	26	591	30	S
5	31	192	12	G
6	46	192	12	G
7	49	300	20	CC
8	54	155	12	G
9	59	300	20	CC
10	61	300	20	CC
11	65	591	30	S
12	66	591	30	S
13	69	800	60	S
14	80	591	30	S
15	87	155	12	G
16	89	620	12	G

17	100	400	20	CC
18	103	155	12	G
19	111	155	12	G

* S: Steam Turbine

** G: Gas Turbine

*** CC: Combined-Cycle

J. Reliability Data

Table 29. IEEE 118-Bus Test System Generating Unit Reliability Data

Generator No.	Forced Outage Rate (FOR) (%)
1	0.10
2	0.10
3	0.02
4	0.02
5	0.10
6	0.10
7	0.02
8	0.02
9	0.04
10	0.04
11	0.04
12	0.05
13	0.05
14	0.05
15	0.02
16	0.02
17	0.02
18	0.02
19	0.04

Table 30. IEEE 118-Bus Test System Transmission Line Reliability Data

Line No.	From Bus	To Bus	FOR (%)
1	1	2	0.000438
2	1	3	0.000582
3	2	12	0.000376
4	3	5	0.000445
5	3	12	0.000548
6	4	5	0.000434
7	4	11	0.00175
8	5	6	0.00041
9	5	11	0.000388

10	6	7	0.001317
11	7	12	0.000342
12	8	9	0.000502
13	8	5	0.000502
14	8	30	0.00175
15	9	10	0.00175
16	11	12	0.00175
17	11	13	0.00175
18	12	15	0.000502
19	12	17	0.000489
20	12	117	0.000502
21	13	15	0.000652
22	14	15	0.000615
23	15	17	0.000477
24	15	19	0.000414
25	15	33	0.000514
26	16	17	0.000514
27	17	19	0.000514
28	17	31	0.000439
29	17	113	0.000427
30	18	19	0.000402
31	19	20	0.000678
32	19	34	0.000439
33	20	21	0.000439
34	21	22	0.000477
35	22	23	0.000477
36	23	24	0.000427
37	23	25	0.000427
38	23	32	0.000565
39	24	70	0.000438
40	24	72	0.000582
41	25	27	0.000376
42	26	25	0.000445
43	26	30	0.000548
44	27	28	0.000434
45	27	32	0.00175
46	27	115	0.00041
47	28	31	0.000388
48	29	31	0.001317
49	30	17	0.000342

50	30	38	0.000502
51	31	32	0.000502
52	32	113	0.00175
53	32	114	0.00175
54	33	37	0.00175
55	34	36	0.00175
56	34	37	0.000502
57	34	43	0.000489
58	35	36	0.000502
59	35	37	0.000652
60	37	39	0.000615
61	37	40	0.000477
62	38	37	0.000414
63	38	65	0.000514
64	39	40	0.000514
65	40	41	0.000514
66	40	42	0.000439
67	41	42	0.000427
68	42	49	0.000402
69	42	49	0.000678
70	43	44	0.000439
71	44	45	0.000439
72	45	46	0.000477
73	45	49	0.000477
74	46	47	0.000427
75	46	48	0.000427
76	47	49	0.000565
77	47	69	0.000438
78	48	49	0.000438
79	49	50	0.000582
80	49	51	0.000376
81	49	54	0.000445
82	49	54	0.000548
83	49	66	0.000434
84	49	66	0.00175
85	49	69	0.00041
86	50	57	0.000388
87	51	52	0.001317
88	51	58	0.000342
89	52	53	0.000502

90	53	54	0.000502
91	54	55	0.00175
92	54	56	0.00175
93	54	59	0.00175
94	55	56	0.00175
95	55	59	0.000502
96	56	57	0.000489
97	56	58	0.000502
98	56	59	0.000652
99	56	59	0.000615
100	59	60	0.000477
101	59	61	0.000414
102	60	61	0.000514
103	60	62	0.000514
104	61	62	0.000514
105	62	66	0.000439
106	62	67	0.000427
107	63	59	0.000402
108	63	64	0.000678
109	64	61	0.000439
110	64	65	0.000439
111	65	66	0.000477
112	65	68	0.000477
113	66	67	0.000427
114	68	69	0.000427
115	68	81	0.000565
116	68	116	0.000438
117	69	70	0.000438
118	69	75	0.000582
119	69	77	0.000376
120	70	71	0.000445
121	70	74	0.000548
122	70	75	0.000434
123	71	72	0.00175
124	71	73	0.00041
125	74	75	0.000388
126	75	77	0.001317
127	75	118	0.000342
128	76	77	0.000502
129	76	118	0.000502

130	77	78	0.00175
131	77	80	0.00175
132	77	80	0.00175
133	77	82	0.00175
134	78	79	0.000502
135	79	80	0.000489
136	80	96	0.000502
137	80	97	0.000652
138	80	98	0.000615
139	80	99	0.000477
140	81	80	0.000414
141	82	83	0.000514
142	82	96	0.000514
143	83	84	0.000514
144	83	85	0.000439
145	84	85	0.000427
146	85	86	0.000402
147	85	88	0.000678
148	85	89	0.000439
149	86	87	0.000439
150	88	89	0.000477
151	89	90	0.000477
152	89	91	0.000427
153	89	92	0.000427
154	90	91	0.000565
155	91	92	0.000438
156	92	93	0.000438
157	92	94	0.000582
158	92	100	0.000376
159	92	102	0.000445
160	93	94	0.000548
161	94	95	0.000434
162	94	96	0.00175
163	94	100	0.00041
164	95	96	0.000388
165	96	97	0.001317
166	98	100	0.000342
167	99	100	0.000502
168	100	101	0.000502
169	100	103	0.00175

170	100	104	0.00175
171	100	106	0.00175
172	101	102	0.00175
173	103	104	0.000502
174	103	105	0.000489
175	103	110	0.000502
176	104	105	0.000652
177	105	106	0.000615
178	105	107	0.000477
179	105	108	0.000414
180	106	107	0.000514
181	108	109	0.000514
182	109	110	0.000514
183	110	111	0.000439
184	110	112	0.000427
185	114	115	0.000402

K. Wind Data

Table 31. Real Diurnal Mean Wind Speed at Manjil Wind Farm: October 10, 2008

Hour	Real Mean Wind Speed
1	14.07
2	13.65
3	13.5
4	12.9
5	11.8
6	11.2
7	10.9
8	10.1
9	9.9
10	10.2
11	11.1
12	12.3
13	13.1
14	14.2
15	13.86
16	12.11
17	12.6
18	13.58
19	14.28
20	14.3
21	14.4
22	14.2
23	14.25
24	14.45

Table 32. Real Diurnal Wind Speed at Manjil Wind Farm Every 10 Minutes: October 10, 2008

Hour	Real Mean Wind Speed	10 min	20 min	30 min	40 min	50 min	60 min
1	14.07	14.29355	14.16434	13.81249	14.18313	13.91014	13.94656
2	13.65	13.62119	13.41486	13.65494	13.80997	13.60499	13.78573
3	13.5	13.67383	13.75962	13.05294	13.66418	13.36992	13.21222
4	12.9	12.88913	12.69042	13.02423	12.94162	12.8919	12.96749
5	11.8	11.89991	11.88906	11.80985	11.61425	11.57999	12.05952
6	11.2	11.01096	11.11978	11.40454	11.14028	11.37592	11.06868
7	10.9	10.84859	10.77306	10.60834	11.07947	10.42618	10.63778
8	10.1	10.23951	10.30823	10.42841	10.0275	9.912683	10.38186
9	9.9	9.784418	9.931995	9.840538	9.737195	10.18636	9.959824
10	10.2	10.01599	10.41334	10.17379	10.59081	10.07707	10.09082
11	11.1	11.04417	10.94012	11.4287	10.80897	11.33486	10.8741
12	12.3	12.14768	12.41249	12.25278	12.17552	11.91146	12.36897
13	13.1	12.46869	13.16547	13.28612	13.1865	12.98893	12.93171
14	14.2	14.31822	14.08438	14.55761	14.32687	14.047	14.39185
15	13.86	13.86853	13.99928	13.93803	13.35215	13.68306	14.16643
16	12.11	12.31593	12.06233	11.89525	12.22815	12.32494	12.40035
17	12.6	12.86428	12.58402	12.49105	12.48084	12.66887	12.74748
18	13.58	13.48161	13.68837	13.34926	13.61543	13.65761	13.81082
19	14.28	14.36676	14.58675	14.05175	14.49844	14.59546	14.23746
20	14.3	14.12583	14.33386	14.41772	14.36325	14.25734	14.29975
21	14.4	14.60136	14.52196	14.47149	14.16104	14.60527	14.35151
22	14.2	14.01517	14.11587	14.19028	14.1523	14.20901	14.09049
23	14.25	14.08042	14.24483	14.17416	14.06631	14.35782	14.27807
24	14.45	14.66057	14.28131	14.32492	14.50562	14.36689	14.35687

APPENDIX 4

CIRCUIT BREAKER MONITORING AND MAINTENANCE MANAGEMENT IN POWER SYSTEMS

A. Introduction

The smart grid initiative was introduced in the Energy Independence and Security (EISA) Act of 2007, which sparked the imagination and debate of what that efforts should entail [191]. The fact is that the current electric power transmission and delivery infrastructure, which is one of the most complex man-made systems, was not originally planned to meet the requirements of a smart electricity grid as defined by a NETL study, which often is considered as a major reference on the smart grid requirements [192]:

- Enabling informed participation by customers,
- Accommodating all generation and storage options,
- Enabling new products, services, and markets,
- Providing the power quality for the range of needs in the 21st century economy,
- Optimizing asset utilization and operating efficiently,
- Addressing disturbances through automated prevention, containment, and restoration,
- Operating resiliently against all types of hazards.

Circuit breakers (CBs) have a crucial role in power system operation as they are the essential switching devices responsible for interrupting the fault currents and isolating the faulted portions of the system once triggered by the protection relays. They are also

routinely used in switching in and out various power system components as they are typically, in the transmission system, available at each end of such a component. In the TLS, they are an essential part for executing the transmission line switching sequences. Hence, the reliability of their operation is of a paramount importance in practical realization of the TLS methods.

The smart grid concept has introduced quite a few interesting ideas, one of which is the extensive deployment of smart sensors and monitoring technologies. The widely deployed monitoring infrastructure could be very informative at the component level [193]-[197]. In the case of CB, data captured in real time can be translated into vital information on the component's health and reliability. The new knowledge about the component health and condition can eventually be provided to the maintenance experts and system operators. Monitoring of the protective components, including transmission CBs, supports achieving more reliable control and protection of power systems, and ensures the electric safety as well. Finally, reliable and healthy components of the power system enable successful implementation of the future smart grid applications such as power system topology control [86].

B. Circuit Breaker Roles in Electric Power Transmission Systems

In today's practice, CBs have a critical role in clearing the faults together with protective relays. As an example, the distance relays, which are mostly used for transmission system protection continuously monitor the currents and voltages, gathering the data and information from the instrument transformers (current and voltage

transformers) on transmission lines. When a fault occurs, the associated short-circuit apparent impedance is measured by the protective relays. The relays then initiate the CB operation in order to interrupt the fault current and clear the fault. The electric arc in a CB plays a key role in the interruption process and is often called a switching arc. Upon CB contact separation, the arc is extinguished in the interrupter(s) of each CB pole. Current interruption in each phase happens at the first zero crossing point. The arc voltage and the current meet the zero crossing simultaneously as the arc is of resistive nature. The arc energy is quite low around current zero, and if the CB design is in such a way that cooling or air blowing through the extinction medium is adequate, the current can be interrupted [161].

Depending on the type of the CBs considered, the device may not be successful in interrupting the current at the first zero crossing following the contact separation. It may take a certain minimum time before the CB can actually interrupt the current, because

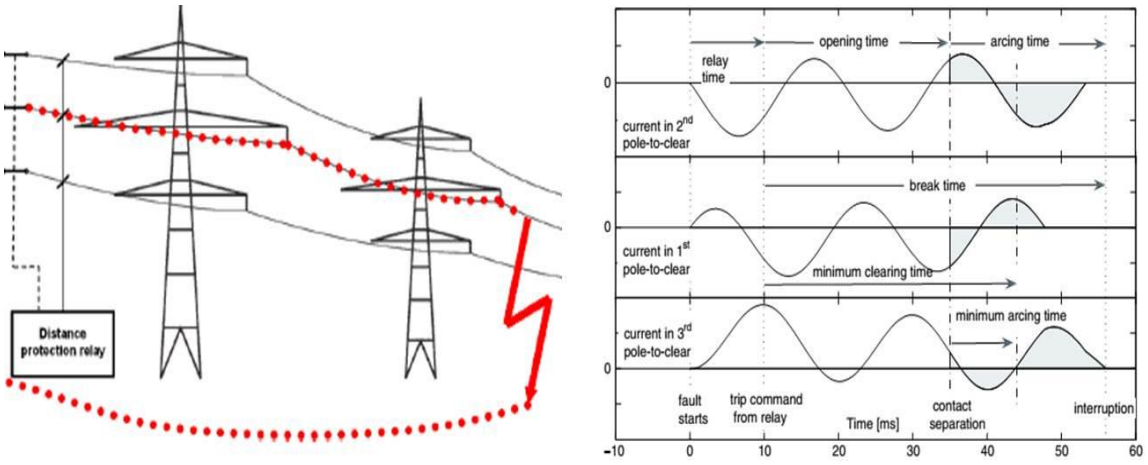

Figure 51. (a) Faults in power systems. (b) CB three-phase current waveforms in the CB opening process to isolate the fault [161].

sufficient cooling pressure/air blow of the extinction medium must be available and/or sufficient contact distance must be reached [161]. After the minimum arcing time has elapsed, the current can be interrupted at the first following current zero crossing. Crossing point takes place at the respective current zero states of each of the three phases (see Figure 51). When all the CB poles are interrupted, the fault is cleared. The time between the instant of energizing the trip coil of the CB and the current interruption in all phases is called the break time (see Figure 51) [161]. The CB technology must be able to operate reliably and withstand the high thermal energy of the arc before current zero crossing. Malfunctions in any part of the CB (mechanical, interrupter mechanism, electric circuit, etc.) may be an impediment to the successful operation of the CB when needed. CBs mal-operation in the fault clearing and isolating the faulted section may impose a significant risk to electric safety due to high fault currents, exposed faulted conductors, or other unsafe conditions due to damaged insulation. This calls for a wise and comprehensive maintenance management of CBs system-wide. This maintenance approach has also direct impact on the reliability of TLS.

The electric power grid is subject to interruptions ranging from cascading faults caused by extreme operating conditions, malicious external attacks, and intermittent electricity generation from renewable energy sources. As discussed in the earlier Section, transmission lines, although traditionally regarded as static assets in power systems, are recently approached as the flexible means of system dynamic reconfiguration and topology. In this context, transmission line switching (TLS) technology can be employed in the utility day-to-day practical operations for the sake of reliability or economic gains.

Several projects supported by the US Department of Energy (DOE) under the Green Electricity Network Integration (GENI) program have investigated the topology control solutions in power systems. An example projects is the Robust Adaptive Topology Control (RATC) for grid operation [162]. This project explored the reliability of CB operation for the TLS applications at length for the first time.

C. Monitoring CB Operations Enables Condition-Based Maintenance

C.1. CB Monitoring Importance

Reliability of CBs in the transmission system can be ensured with the timely maintenance and replacement activities. Due to a huge number of CBs in the system, with different operational characteristics, vintages, and aging mechanisms, industry experts are still discussing whether the periodic maintenance programs can be adequate as the CB annual maintenance strategy any longer [198]. The CB condition-based maintenance is desirable to meet the maintenance needs where and when necessary. This approach leads not only to a more cost-effective maintenance and asset management decisions, but could also improve CB reliability over time.

C.2. CB Monitoring Techniques

Maintenance of CBs and condition assessment have been widely researched and practiced. Research on the condition based monitoring of CBs has seen a tremendous growth during the past decade as the increasing deployment of monitoring systems and

smart sensors in substations took place worldwide. The condition based assessment approaches can be categorized into two main groups: system-oriented and component-oriented. In the former, the CBs are classified based on their role and criticality in the system overall performance. The CBs with major impacts on system reliability targets are identified in [199] as the most critical for frequent maintenance. Likewise, CB criticality from the system overall security perspectives is addressed in [200], [201]. Quantitative and qualitative system-wide prioritization analysis is pursued in [202], followed by economic analysis to find the optimal maintenance strategy of CBs in [203].

In the latter, different approaches for assessing the status of individual CBs are introduced. Depending on the type of deterioration impact, the analysis may be focused on vibration [204], [205], contact wear-and-tear [206], [207], digital modeling for sensor techniques [208], or gas pressure in the operating chamber [209], [210]. Partial discharge tests are also among the other approaches mostly focused on estimating the CB dielectric properties, requiring significant expert knowledge and statistical analysis [211], [212]. Automated approaches for CB monitoring have been also broadly investigated in [182], where signal processing techniques and expert systems are employed to perform the CB fault detection. Wavelet analysis is used in [213] to extract the features and mobile agent software technology is introduced in [214] as architecture for a flexible processing of monitored signals. The use of state diagrams in deterioration, inspection, and maintenance modeling either through the Markov approaches or Monte Carlo Simulations has been explored [163]-[169]. References [173] and [174] correlated the CB monitoring signals to reliability considering the CB failure probability as an indicator of its performance but

none of the above-addressed papers have used the CB monitoring signals to distinguish the CB deterioration/recovery states as time progresses.

C.3. CB Monitoring Practice Reports

According to the recent failure surveys conducted by a CIGRE Working Group, CB major failures are mostly found to be related to the malfunction of operating mechanism (43%) and control circuit (29%), and in that order compared to other CB subassemblies (see Figure 52) [175]. According to this international survey and as can be seen in Figure 53, malfunctions in the CB operation mechanism takes the lead when it comes to CB minor failures (44%) following by the high voltage sub-assemblies (31%) such as arching chambers, auxiliary interrupters/resistors, and insulations. Aging, wear, and corrosion are also reported as the most common (almost 50%) causes of the major failures in CBs, followed by the design faults, manufacturing faults, and incorrect maintenance (15%). As illustrated in Figure 54, the recognized CB major failures according to the internationally conducted surveys are found to be: the CB does not close on command (28.2%), locked CB in open or close operation (25.1%), and CB does not open on command (16.4%), respectively [175], [176]. This further highlights the necessity of monitoring different parts of the CB to make sure they are available for open/close operations when needed.

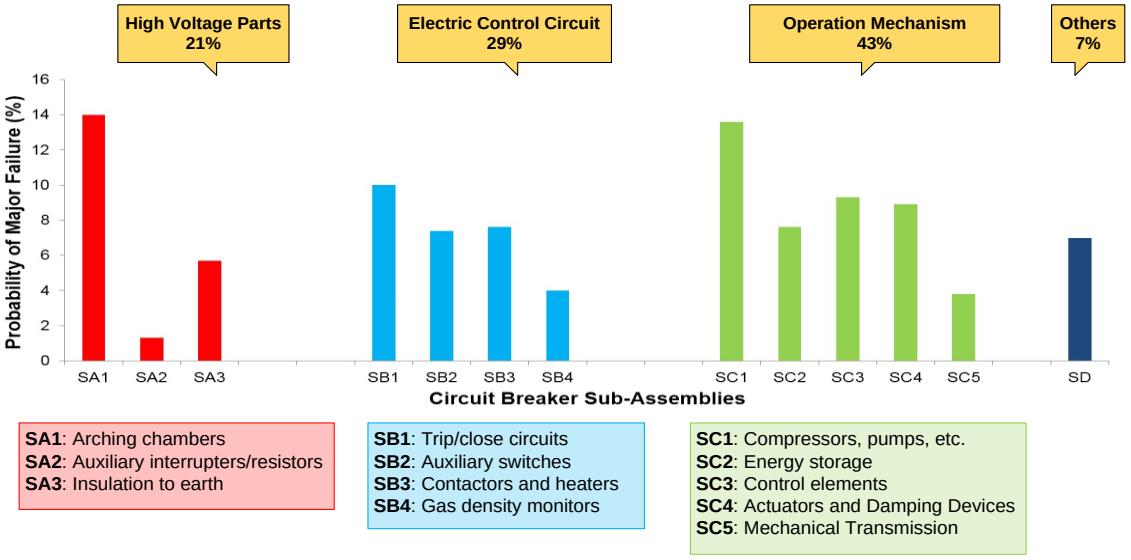

Figure 52. CIGRE International survey on the probability of *major failures* on CB sub-assemblies.

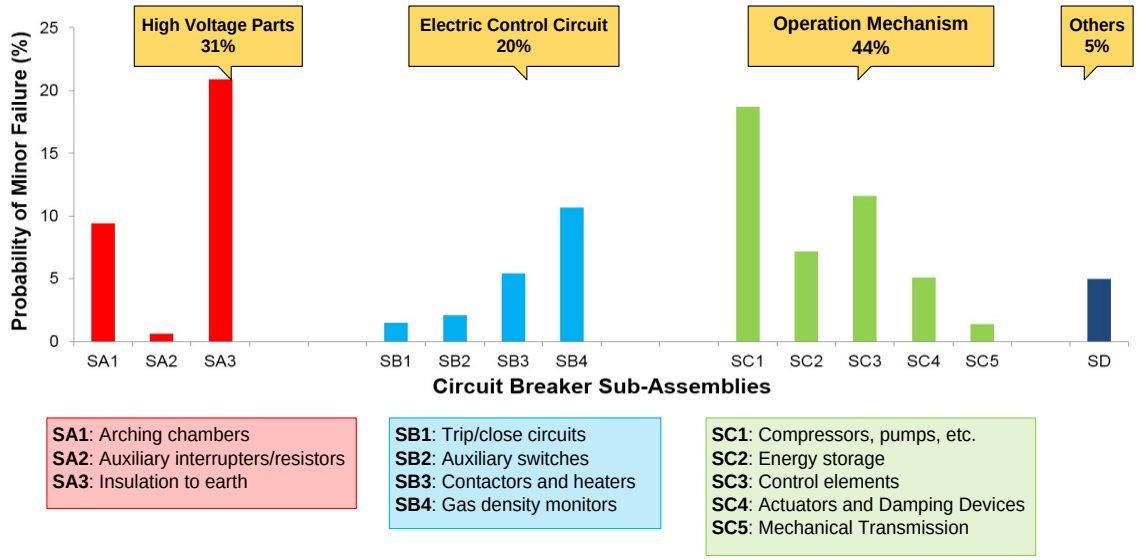

Figure 53. CIGRE International survey on the probability of *minor failures* on CB sub-assemblies.

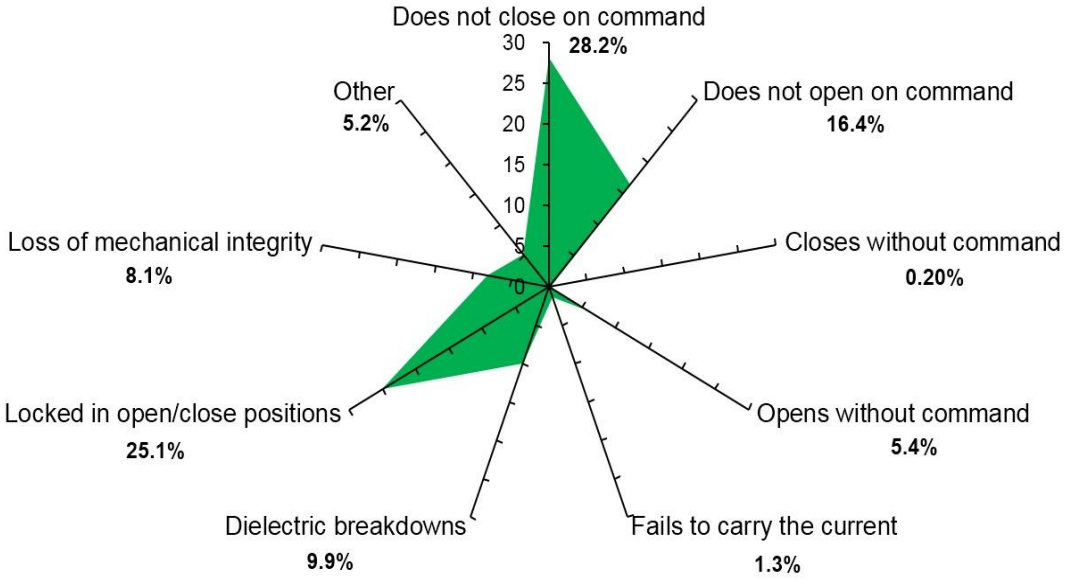

Figure 54. CIGRE International survey: critical modes (reasons) of major failures in CBs.

C.4. CB Monitoring Technology

The technology currently available in the market provides for monitoring of several critical parameters of CB operations which can be helpful in detecting potential failures. Examples of such technologies are: Alstom CBWatch-2, Siemens i-con CB monitoring, INCON Optimizer2, T-Doble software, ABB Sentinel, etc. An example of the use of such technology is the Circuit Breaker Sentinel (CBS), introduced by ABB, to implement a monitoring system for SF6 single pressure power CBs rated 38–800 kV [177]. The monitored parameters may be concerned with the interrupter wear, integrity of the gas systems, mechanical segments, electrical control circuitry and auxiliaries. There are several sensors that are used in such technology that can be mounted and used to monitor CB tank, mechanism, or control circuit. The sensors come in conjunction with a

modular microprocessor to perform the monitoring tasks. The monitoring system also keeps track of coil energization, mechanism, and reaction times, contact speed, and total travel and interrupter wear increments in every single operation of CB. The system collects monitored data over time until an alarm has happened, which is then reported to the user. The data is manually analyzed and the decision is made to either change the alarm settings or initiate thorough maintenance investigation.